United States
Environmental Protection
Agency

Industrial Environmental Research
Laboratory
Research Triangle Park NC 27711

EPA-600/7-79-031
January 1979

EPA

Filtration Parameters for Dust Cleaning Fabrics

Interagency Energy/Environment R&D Program Report

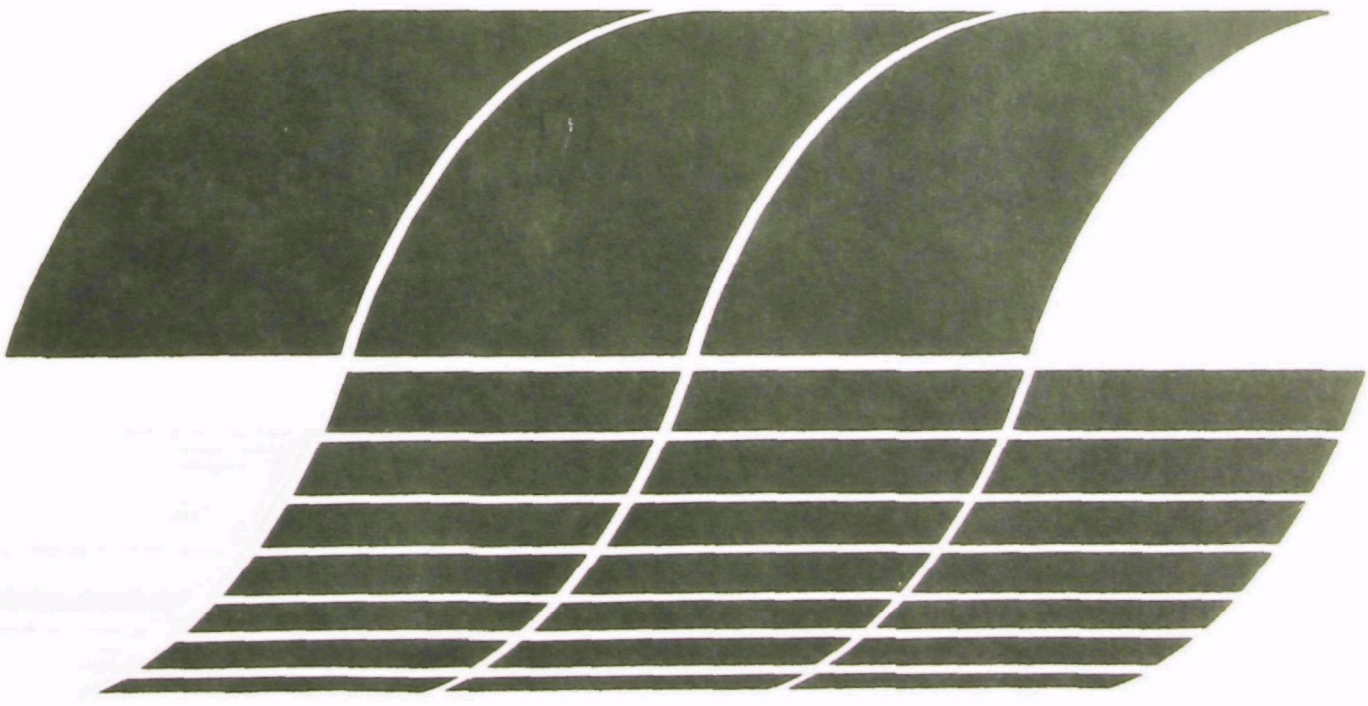

RESEARCH REPORTING SERIES

Research reports of the Office of Research and Development, U.S. Environmental Protection Agency, have been grouped into nine series. These nine broad categories were established to facilitate further development and application of environmental technology. Elimination of traditional grouping was consciously planned to foster technology transfer and a maximum interface in related fields. The nine series are:

1. Environmental Health Effects Research
2. Environmental Protection Technology
3. Ecological Research
4. Environmental Monitoring
5. Socioeconomic Environmental Studies
6. Scientific and Technical Assessment Reports (STAR)
7. Interagency Energy-Environment Research and Development
8. "Special" Reports
9. Miscellaneous Reports

This report has been assigned to the INTERAGENCY ENERGY-ENVIRONMENT RESEARCH AND DEVELOPMENT series. Reports in this series result from the effort funded under the 17-agency Federal Energy/Environment Research and Development Program. These studies relate to EPA's mission to protect the public health and welfare from adverse effects of pollutants associated with energy systems. The goal of the Program is to assure the rapid development of domestic energy supplies in an environmentally-compatible manner by providing the necessary environmental data and control technology. Investigations include analyses of the transport of energy-related pollutants and their health and ecological effects; assessments of, and development of, control technologies for energy systems; and integrated assessments of a wide range of energy-related environmental issues.

EPA REVIEW NOTICE

This report has been reviewed by the participating Federal Agencies, and approved for publication. Approval does not signify that the contents necessarily reflect the views and policies of the Government, nor does mention of trade names or commercial products constitute endorsement or recommendation for use.

This document is available to the public through the National Technical Information Service, Springfield, Virginia 22161.

EPA-600/7-79-031

January 1979

Filtration Parameters for Dust Cleaning Fabrics

by

J.R. Koscianowski, Lidia Koscianowska,
and Eugeniusz Szczepankiewicz

Institute of Industry of Cement Building Materials
45-641 Opole
Oswiecimska Str. 21, Poland

Public Law 480 (Project P-5-533-3)
Program Element No. EHE624

EPA Project Officer: James H. Turner

Industrial Environmental Research Laboratory
Office of Energy, Minerals, and Industry
Research Triangle Park, NC 27711

Prepared for

U.S. ENVIRONMENTAL PROTECTION AGENCY
Office of Research and Development
Washington, DC 20460

ABSTRACT

This report describes laboratory and pilot scale testing of bag filter fabrics. Filtration performance data and mathematical modeling parameters are given for four Polish fabrics tested with cement dust, coal dust, flyash and talc.

The following conclusions were reached:

The process of clean air flow, as well as the dust filtration process, are stochastic processes of the normal type.

For filtration Type I (laboratory scale - as defined in the report), dust collection efficiency is an exponential function depending on air-to-cloth ratio, dust covering, and type of filtration structure.

For filtration Type I, resistance increases with time or dust covering in a parabolic fashion. Outlet concentration as a function of dust covering is also a parabolic relationship. Structurally, the fabrics are heterogeneous, anisotropic media.

Free area is presently the best structural parameter for characterizing structure of staple fiber fabrics.

Electrostatic properties of dusts depend on their history; charge decays with time. Dust cake formation can be influenced by specific electrostatic properties of the fabric and dust.

CONTENTS

FIGURES

FIGURES (con.)

FIGURES (con.)

FIGURES (con.)

FIGURES (con.)

FIGURES (con.)

TABLES

TABLES (con.)

ACKNOWLEDGMENT

For their contribution and help, the authors thank each employee of the United States Environmental Protection Agency who participated in this endeavor. Special thanks for help and support throughout the program are extended to our Project Officer, Dr. James H. Turner.

SECTION I
CONCLUSIONS

The analysis and research of phase II of this project lead to the following conclusions:

- The process of clean air flow as well as the dust filtration process are stochastic processes of the normal type.
- According to Filtration Type I (laboratory scale), dust collection efficiency is an exponential function depending on the air-to-cloth ratio, the dust covering, and the type of filtration structure.
- The increase of filtration resistance with time or dust covering shows a parabolic relation on the laboratory scale.
- The variation of outlet dust concentration as a function of dust covering L_o is, on the laboratory scale, a parabolic relationship. From a structural viewpoint, the fabrics are regarded as heterogeneous anisotropic media.
- At present Free Area is the best structural parameter characterizing the structure of fabrics made of staple fibers.
- Electrostatic properties of dusts depend on their history. Dust charges are higher for fresh dusts than stored dusts.
- Specific electrostatic properties of fabrics and highly charged dusts can influence the formation of dust cake.

SECTION II

RECOMMENDATIONS

To obtain more representative statistical material for the definition of relations between large scale dust collection efficiency and filtration resistances, changes in the program for phase III (the final phase) were made. The experiments will be conducted for:

- Five levels of air-to-cloth ratio--i.e., 60, 80, 100, 120, and 160 $m^3/m^2/hr$, and
- Six levels of dust covering--i.e., L_{NK} + 100, L_{NK} + 200, L_{NK} + 300, L_{NK} + 400, L_{NK} + 600, and L_{NK} + 800 g/m^2.

This large-scale testing will be conducted according to the conditions set forth in the original detailed program statement.

Because of the enlarged experimental program, testing will be accomplished on at least two types of fabrics and one kind of dust. Similar additional experiments have been planned for the laboratory scale in order to establish correlations between Dust Filtration Type I and Type III.

The above changes in the program were discussed with and accepted by the Project Officer, Dr. J. H. Turner, during the April 1976 meeting.

SECTION III

INTRODUCTION

This report includes the results of research conducted in phase II of Project No. 5-533-3, a contract between the United States Environmental Protection Agency and IPWMB, Opole, Poland. Also, for continuity with phase I, laboratory testing of selected filtration fabrics, this report recapitulates work concerning the efficiency of Filtration Type I (characteristic of laboratory-scale filtration) conducted during the first 2 years of the project.

These results were the subject of discussions between the Project Officer, Dr. J. H. Turner, and representatives of IPWMB during their visit to the United States in April 1976. During that meeting the authors proposed modifying the detailed program and performing auxiliary work on both the laboratory scale and large scale. The proposal was accepted by the Project Officer.

The changes in the detailed program concern enlargement of some elements of the basic testing in order to obtain more empirical data and permit verification of complex empirical relations. The original fabric test plan provided a maximum of three levels of parameter variations, which is not satisfactory for adequate mathematical interpretation. Laboratory testing carried out by IPWMB before 1973 cannot be regarded as valid auxiliary statistical material because of the differences in degree of dispersion and dust concentration.

The theoretical interpretation of the conducted experiments is based on the dust filtration process rather than other filtration processes. This interpretation avoids comparisons of the dust filtration process to the air filtration process over the range of the results.

The results of phase II are very promising. Some difficulties in the correct description of the physical structure of woven materials are recognized. The structural parameters used at present do not give the specifics of the filtration structure. By considering the hydraulic properties of the fabrics, it is possible to classify the woven materials with a definite

quantitative measurement. But this measurement does not indicate the differences in the filtration properties of the fabric or its method of production. The description of the structure of a woven filtration medium will be the basic problem of phase III of the project.

RESEARCH OBJECTIVES

The basic objectives of the program financed by EPA and conducted by the Institute of Cement Building Materials in Opole were established as:

- A viable description of the effects of fabric structural parameters on the pressure drop of gas flow through a clean fabric.
- A viable description of the effects of fabric structural parameters and of the dust cake on pressure drops during the filtration process.
- A viable description of the relationship between dust collection efficiencies and the variables of the dust filtration process.
- Testing, by mathematical modeling, of those fabric structures with the best filtration properties.

Total program research will include laboratory testing, including that of the dust and the fabrics, large-scale testing, auxiliary studies, and application of mathematical methods including modeling.

GENERAL PROGRAM

Laboratory Testing

Laboratory testing was accomplished on four kinds of filtration fabrics and four types of dust. The following conditions existed at the time of measurement.

- Dust concentration in the air at the inlet of the test chamber: 10 g/m^3 + 10 percent.
- Dust covering of the filter: 100 g/m^2, 400 g/m^2, and 700 g/m^2 with ΔP < 250 mm of water.
- Air-to-cloth ratios: 60 $m^3/m^2/hr$, 80 $m^3/m^2/hr$, and 120 $m^3/m^2/hr$.
- Humidity of the dispersion medium (not adjustable): RH = 40 percent + 10.
- Temperature of the dispersion medium: 20° to 30° C.

- Dispersion medium: atmospheric air.
- Pressure: atmospheric pressure.

Large-Scale Testing

Large-scale tests were scheduled using filtration bags with an operating length of 3,000 mm and the same dusts used in the laboratory testing. Test conditions were identical to those of laboratory testing except for dust covering on the filter being tested only at 400 and 700 g/m^2 (excluding the 100 g/m^2 condition of laboratory testing) and air-to-cloth ratios of only 60 and 80 $m^3/m^2/hr$ (excluding the 120 $m^3/m^2/hr$ condition used in laboratory testing).

Definition of the Structural Parameters of a Fabric

Research leading to the identification and definition of significant structural parameters of a fabric involved analyses, measurements, and experiments.

Measurements and analyses, specifically, concerned and included the geometry of the spatial structures of fabrics, the technological parameters and production variables of fabrics and fabric structures, the technological parameters and production variables of threads and filaments, microscopic tests, etc.

The parameters defined by analyses and measurements under atmospheric air flows were then evaluated experimentally. Four types of filtration fabrics, all manufactured in Poland and each differing as to raw material, filament diameter, weave, etc., were studied. A literature search was included in this program.

Definition of the Structural Parameters of Dust Layers

Industrial polydispersed dust layers in the testing program were characterized by particular physical and chemical properties. The research program for dust layers was conducted in the same manner as that for fabrics using analyses, measurements, and experiments.

Testing of Electrostatic Properties of Dusts and Fabrics

Determination of the electrostatic properties of dusts and fabrics was accomplished using the same materials for both laboratory and large-scale testing.

Testing included measurement of dust charge by the Kunkel-Hansen method; and determinations of the influence of the gas medium on dust charge; the electrical resistance of the dust layers; the kinetics of the fabric charging process during both clean and dusty air flows; the electrical resistance of the fabrics (surface, bulk); and other electrostatic effects during the dust filtration process.

DETAILED PROGRAM FOR THE SECOND PHASE

Laboratory Tests

During laboratory tests, the following tasks were accomplished:

- Completion of the entire testing program and compilation and analysis of the results.
- Completion of the fabric auxiliary tests for definition of basic technological and production parameters.
- Completion of auxiliary tests on dusts for determination of physical and chemical properties.
- Determination of empirical relations between dust collection efficiency and air-to-cloth ratio.
- Preliminary determination of a mathematical model of dust filtration through fabrics.

Definition of the Structural Parameters of Fabrics

Defining the structural parameters of fabrics entailed examination of fabric geometry (taking under consideration the definition of the structural parameters of woven materials) and preliminary analysis of the results.

Definition of the Structural Parameters of Dust Layers

In defining the structural parameters of dust layers, determination of the influence of dust dispersion degree on the hydraulic properties of dust layers and analysis of the results (considering the definition of parameters characteristic of a dust layer) were included.

Definition of Characteristic Properties of Dusts and Fabrics

Characteristic properties of dust and fabrics were defined by determination of dust charges by the Kunkel-Hansen method and elaboration of results,

Table 1. FABRIC PARAMETERS

PARAMETER	UNIT	FABRICS							
		ET-4		ET-30		F-tor 5		PT-15	
		PS*	Measured	PS*	Measured	PS*	Measured	PS*	Measured
1	2	3	4	5	6	7	8	9	10
Width of fabric	cm	as required	36	140±4	135	140±4	140	85±1	85
Kind of yarn: warp fill		50TexZ x 2S 180Tex Z	45,21Tex x 2 178,25 Tex	21TexZ x 2S 21TexZ x 2S	22,15Tex x 2 21,99Tex x 2	Td 125/2 Td 250/1	Td 136,37 Td 253,52	Td 210/1 Td 210/1	Td 228,43 Td 233,77
Thread count in 10 cm: warp fill		180±5 126±5	180 126	477±10 276±6	488 274	540±12 376±12	528 360	564±12 360±11	545 363
Fabric weight	g / m^2	450±31	428,1	365±25	361.6	271±13	307.5	272±14	247
Thickness (pressure 100g/cm^2)	mm	-	0,92	-	0.74	-	0.50	-	0.39
Tensile strength, less than: warp fill	KG/5cm width KG/5cm width	220 260	240 310	250 130	323 182	346 276	310 225	300 200	336 233
Elongation during tension, no more than: warp fill	% %	70 50	51 35	6 50	60 48	20 30	37 15	60 40	43 28
Permeability	m^3/m^2 min at 20 mm H_2O	18-24	20.73	12-18	7.54	-	14.6	-	3.65
Weave	-	1/3 Z	1/3 Z	2/1 Z	2/1 Z	2/2 Z	2/2 Z	3/3	3/3
Finishing	-	steaming	steaming	thermal stabilization, washing	thermal stabilization, washing	crude	crude	stabilized	stabilized

*Polish standards

Table 2. PARTICLE SIZE DISTRIBUTION OF TEST DUSTS

a. Before separation

Range of Particle size in μm	Percent by weight			
	Cement	Coal	Talc	Fly Ash
1	2	3	4	5
5	12.0	9.0	23.0	19.0
5 - 10	12.0	16.0	33.0	45.5
10 - 20	16.0	24.5	30.0	15.0
20 - 30	9.5	13.0	8.5	5.0
30 - 40	10.0	7.5	2.5	3.0
40 - 50	10.0	6.5	1.2	2.0
50 - 60	7.5	4.5	0.5	1.5
60	23.0	19.0	1.3	9.0

b. After separation

Range of Particle size in μm	Percent by weight			
	Cement	Coal	Talc	Fly Ash
1	2	3	4	5
5	26.0	24.0	32.5	40.0
5 - 10	36.5	40.0	37.5	50.0
10 - 20	33.0	34.5	25.0	9.7
20	4.5	1.5	5.0	0.3

determination of the electrostatic properties of fabrics, and recapitulation and analysis of results.

FABRIC AND DUST SELECTION

Four types of filtration fabrics, differing in spatial structure, were selected for testing under Project No. 5-533-3. These selected fabrics are produced from the following raw materials:

- Polyester (staple fiber)
  - Fabric ET-30
  - Fabric ET-4
- Polyester (continuous filament)
  - Fabric F-tor 5
- Polyamide (continuous filament)
  - Fabric PT-15.

Technical characteristics of these fabrics are shown in table 1.

Also, four types of dust--cement, coal, talc, and fly ash--were tested. These industrial dusts were selected because of their chemical composition and their uniform particle size. Samples for testing were taken from appropriate points in the production processing line.

The selection of dust samples is dependent on various physical and chemical properties. Instead of testing material as sampled, testing under this project, in accordance with suggestions from Dr. James H. Turner, EPA Project Officer, was of only those dust samples containing no more than 10 percent by weight of particles with diameters greater than 20 μm. For laboratory testing, this separation was done by use of the ALPINE separator. For the large-scale tests, the dusts were preseparated and prepared by subcontractors. The characteristics of the test dusts before and after separation are shown in table 2 and figures A-1 through A-4.

SECTION IV

THEORY OF DUST FILTRATION

In the most general sense, filtration is a process for the removal of dispersed solid particles from a fluid stream (dispersion medium) by flow through a porous medium. Depending on the kind of dispersion medium and the kind of porous medium, several characteristic filtration processes differing in quantity and quality can be described. This program considers industrial aerosol filtration through woven filter fabrics.

In this program, aerosols are regarded as a two-phase system composed of a gas-dispersed phase and a solid-dispersed phase, which, under certain conditions, can be treated as quasi-stable. This definition implies a secondary classification of aerosols: atmospheric and industrial. Size distribution and concentration vary between these two types of aerosols. For both atmospheric and industrial aerosols, fractional composition depends on the absolute velocity of the gas and on thermodynamic parameters. It is a result of the terrestrial gravitational field in which the aerosol is regarded as a quasi-stable dispersion system.

This definition of an aerosol as a two-phase system is appropriate only for dry filtration. Including the third phase, fluid, of an aerosol would completely change the physics of dry filtration.

From a physical point of view, the filtration process is described by state parameters (SP), filtration parameters (FP), and structural parameters of the filtration medium (SPFM). The process is shown schematically in figure 1.

State parameters characterizing the aerosol before and after filtration are the thermodynamic and physico-chemical parameters of the gas medium, and the physico-chemical parameters of the dispersed medium (the dust).
The basic state parameters are:

The thermodynamic parameters of the dispersion medium:

- Temperature
- Humidity

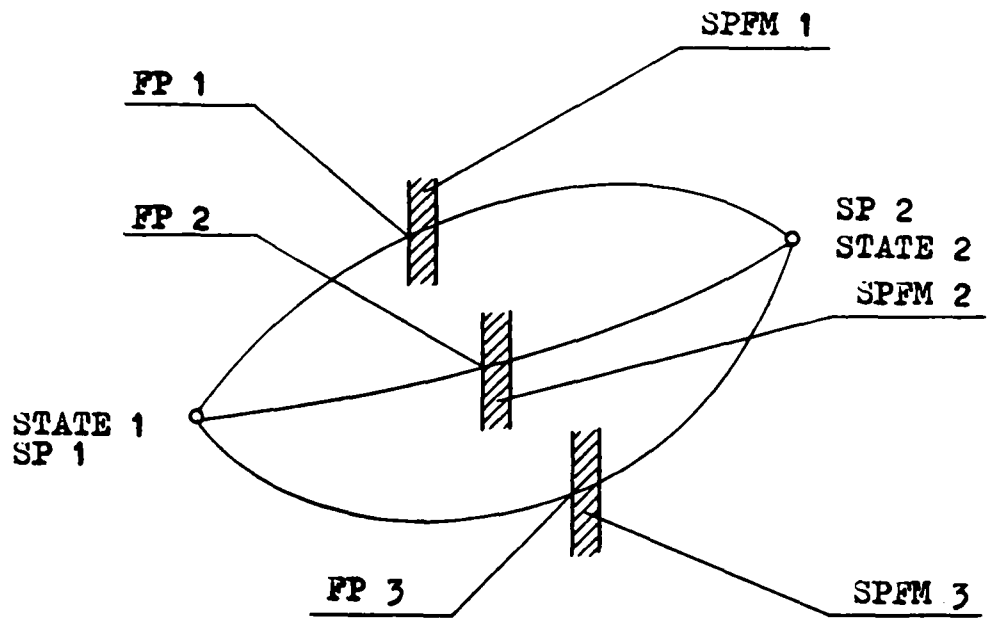

SP 1, SP 2 = State Parameters,

FP 1, FP 2, FP 3 = Filtration Parameters,

SPFM 1, SPFM 2, SPFM 3 = Structural Parameters of the Filtration Medium.

SP 1 $\neq$ SP 2

FP 1 + SPFM 1 $\neq$ FP 2 + SPFM 2 $\neq$ FP 3 + SPFM 3

E (efficiency) = constant.

Figure 1. Filtration process schematic.

Pressure, etc.

- The chemical properties of the dispersion medium:
  Chemical constitution.
- The physical parameters of the dust:
  Weight density
  Degree of pulverization
  Concentration
  Electrification, etc.
- The chemical parameters of the dust:
  Chemical constitution
  Chemical activity, etc.

Filtration parameters are the independent variables of the process: flow rate, dust loading, cleaning time, and energy, etc. The basic filtration parameters are the air-to-cloth ratio in $m^3/m^2/hr$, the normalized dust feed rate in $g/m^2/hr$, and pressure drop (filter resistivity) in mm of water.

Structural parameters of the filtration medium describe, from a physical viewpoint, the filter structure as characterized by its production, and also the physico-chemical properties of its raw materials.

For woven materials, the basic structural parameters of the filtration medium are porosity, mean pore diameter, specific surface, free area, and fiber diameter, etc.

The effectiveness of the filtration process is estimated by the filter efficiency, which is functionally correlated with the state parameters before and after filtering according to:

$$E = \left(1 - C_o/C_i\right) \times 100 \qquad (1)$$

where E = filter efficiency,
C_i = initial aerosol concentration (before filtering),
C_o = final aerosol concentration (after filtering).

As shown in figure 1, the transformation from a definite state 1 to a state 2 of an aerosol, at a given filter efficiency, does not depend on the path of transformation, but only on the initial and final concentrations (the state parameters). There are an infinite number of structural and filtration parameters by which a given filtration process effectiveness (efficiency) can be achieved.

Analyzing the above relation in equation 1, the conclusion is made that filter efficiency can be the qualitative parameter used to describe the filter structure (at a specific initial concentration, determining the physical properties of the process). And because of this, three main types of filtration processes can be selected:

1. High efficiency air filtration at an initial aerosol concentration $C_i < 1$ mg/m^3;
2. Air filtration at an initial aerosol concentration, 1 mg/m^3 < C_i < 50 mg/m^3; and
3. Dust filtration at an initial concentration, $C_i > 50$ mg/m^3.

High efficiency air filtration, as well as air filtration in general (filtration processes 1 and 2,) have their theoretical base in classical filtration theory and satisfy the assumptions required by those physical and mathematical models. In contradistinction to air filtrations, dust filtration, characteristic of industrial fabric filters, has become the subject of research only during the last few years--inspired by increased air pollution emissions from industrial plants. It has no theoretical base as yet.

Initial attempts to apply the classical filtration theory to the dust filtration process showed the wrong way to point out the differences between dust filtration and other processes of dry filtration.

Large initial concentrations of solid particles in the aerosol and regeneration phases of the filtration medium are characteristic of the dust filtration process. So, practically, the presence of a clean filtration structure and its interaction with aerosol particulates is reduced to a very short initial period, not having a major influence on the filtration process under actual industrial conditions. Figure 2 shows the actual variation of filtration resistances with time. It is clear that the state of the filtration medium can be described by definite pressure drops at a constant air-to-cloth ratio (q_g in m^3/m^2/hr) from which its degree of structural filling can be deduced.

The filtration medium exists in one of the following states:

- Pure filtration (a dust-free filter),

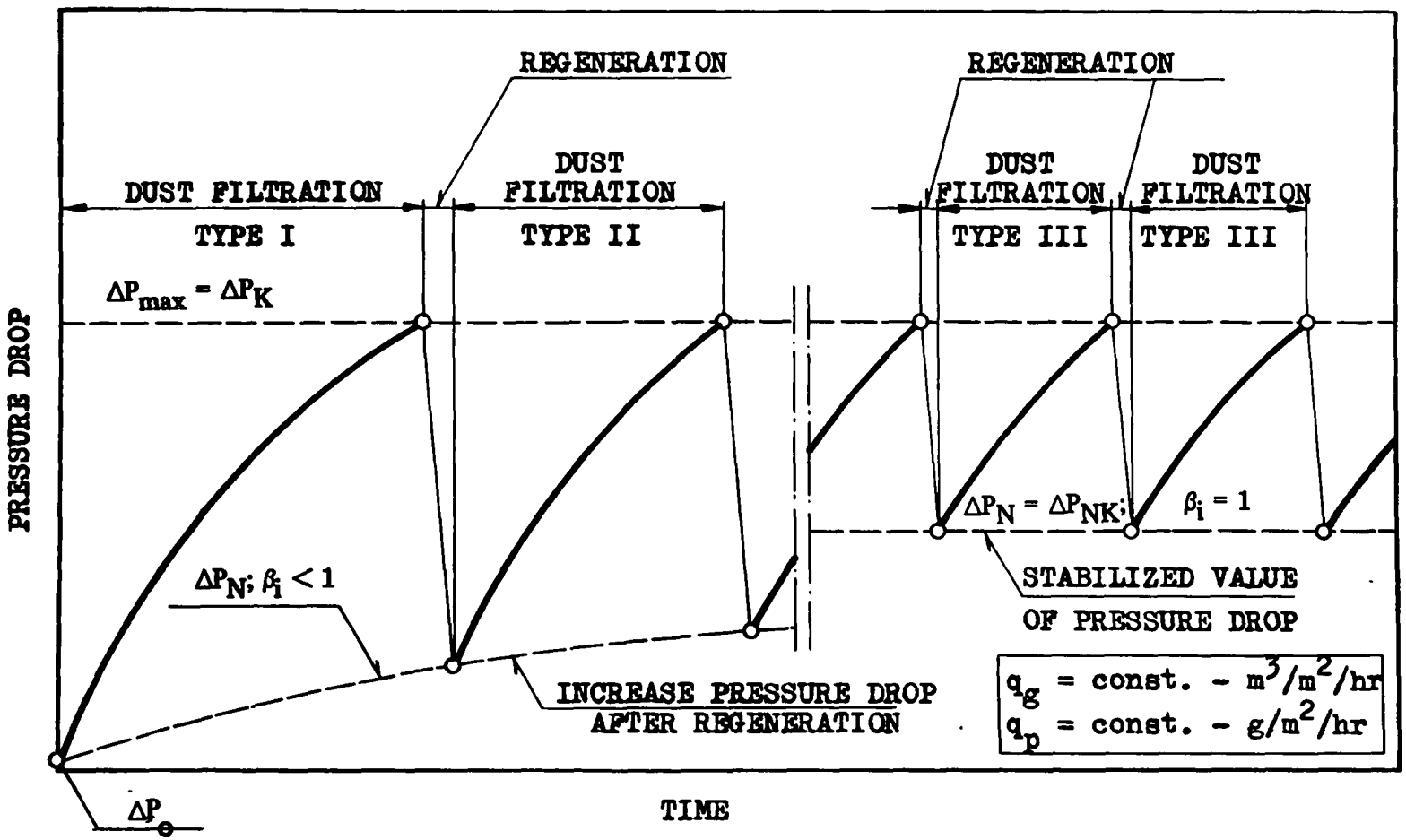

Figure 2. Types of Dust Filtration.

- Partly filled with dust,
- Filled up with dust (fully filled),
- Covered with dust (fully filled plus dust cake).

A pure (clean) filtration structure is characterized by:

$$\Delta P_o \text{ at } q_g = \text{constant}, \; q_p = 0, \text{ and } L = 0,$$

where ΔP_o is the pressure drop at a constant air-to-cloth ratio, q_g; for a zero dust feed rate, ($q_p = 0$); and with no dust load in or on the fabric (L=0).

A filter partly filled with dust for a specific regeneration system is characterized by the successive values ΔP_N tending towards ΔP_{NK} at q_p = constant. During this time period the fabric is filling with dust as described by $L=L_i$ (where i = N1 ... NK). A filter fully filled with dust for a specific regeneration system is characterized by ΔP_{NK} at q_g = constant, q_p = constant, and $L = L_{NK}$, meaning a certain amount of dust is present in the fabric structure after the regeneration cycle. A structure covered with dust is a filter fully filled with dust and with a dust cake on its working surface. This is characterized by ΔP_K at q_g = constant, q_p = constant, and $L = L_o - L_{NK} + L_p$ in g/m^2 where L_p is the areal mass density of the dust cake and L_{NK} = the areal mass density of dust filling a fabric for a specific regeneration system after the equilibrium state is reached, in g/m^2.

The concept of "fabric filling" (with dust) is set forth as:

$$\beta_i = L_i/L_{NK} \tag{2}$$

where L_i = the areal mass density of dust filling a fabric after the "i^{th}" regeneration cycle but before the equilibrium state is reached, in g/m^2, and

β_i = the fabric filling factor for cycle "i" (dimensionless).

To estimate the fabric filling from hydraulic pressure data, a fabric filling factor can be described as:

$$\beta_{r_i} = \Delta P_{Ni}/\Delta P_{NK} \tag{3}$$

where ΔP_{Ni} = the pressure drop for the filled fabric after the "i^{th}" regeneration cycle, but before equilibrium is reached, in mm of water,

ΔP_{NK} = the pressure drop for the filled fabric for a specific regeneration cycle after the equilibrium point is reached, in mm of water,

β_{r_i} = relative fabric filling factor, for cycle "i."

The following conclusions are based on previous and present research.

1. Dust filtration processes display cyclical filtration resistivities in time.
2. Each of the basic cycles prior to equilibrium is qualitatively different because each begins at a different fabric filling factor.
3. A stabilized presence of residual dust particles in the filtration structure (as in classical filtration theory) is impossible because the process is cyclic; particle penetration through the filter can occur.
4. Basic filtration mechanisms (interception, inertial impaction and diffusion) determine the efficiency of the process; however, their interaction with a fully filled structure is difficult to model, both physically and mathematically.
5. Dust cake formation is accompanied by compression effects related to the increase of pressure differences, and structural defects depending on the fabric structural composition and the physicochemical properties of the dust.

Based on these conclusions, three main types of dust filtration were identified for true dry dust filtration. They were defined as Filtration Types I, II, and III (see figure 2).

Dust Filtration Type I is the initial phase of the complete process, when the fabric first begins to operate as a filtration medium. This phase ends when the pressure drop reaches a predetermined level. This phase includes:

- Stationary filtration during the initial capture of dust particles (corresponding to classical filtration theory),

- Nonstationary filtration as the fabric structure fills with dust, and
- "Ductive" (canal) filtration as the dust cake forms and filters successively impinging dust particles.

Dust Filtration Type II is characteristic of the next filtration cycles or until the fabric is fully filled with dust, i.e., a stabilized quantity of residual dust remains in the fabric structure after its regeneration. Characteristics of this phase are $\beta_i < 1$ and $\beta_{r_i} < 1$. Dust cake formation depends on the properties of both the dust and the fabric, and also on the intensity of regeneration. This phase includes:

- Nonstationary filtration, and
- "Ductive" filtration.

Dust Filtration Type III occurs when the equilibrium point of filling the fabric by dust has been reached and when the pressure drop measured after regeneration is a stable value during successive regeneration cycles. As for Dust Filtration Type II, this phase includes:

- Nonstationary filtration, and
- "Ductive" filtration.

For this phase $\beta_i = 1$ and $\beta_{r_i} = 1$.

Specific types and phases of the dust filtration process, occurring at definite conditions (q_g = constant and q_p = constant), correspond to predetermined values of pressure drop, ΔP, quantity of dust, L, and describe the momentary states of the filtration structure.

The three types of filtration specified above describe all possible variants of dust filtration occurring in fabric filters. The differences in filling the filtration structure by dust, characterized by definite values of L in g/m^2, lead to the conclusion that individual types of dust filtration represent noncomparative physical processes. Therefore, the efficiencies of Dust Filtration Type I and Dust Filtration Type III (for the same initial state parameters, filtration parameters, and filtration medium) are not the same:

$$E_I \neq E_{III} \quad . \tag{4}$$

A correlation function, R_E, is defined as:

$$E_I = R_E E_{III} \quad . \tag{5}$$

Nonequivalence of efficiency of types I and III dust filtration, according to equation 4, shows that there is no base by which filtration efficiency in the laboratory can be compared with industrial scale filtration efficiency. Similar relations can be written for pressure drops. which also depend on the state of the filtration structure.

In spite of much experimental work, the form of the correlation function R_E has not yet been worked out, because there is no mathematical model of the filtration process itself.

F. H. H. Valentin, testing the filtration efficiency of 24 kinds of fabrics, has given the general form of the functional dependence of the laboratory filtration efficiency as follows:

$$E = 100 \times \exp(-bL_o^n) \tag{6}$$

where E = filtration efficiency in percent,

L_o = the areal mass density of the dust in or on a dust covered filter, and

b,n = constants.

Equation 6 plotted on Rosin-Rammler Paper (log log reciprocal efficiency vs. log weight of dust on the fabric) yields a straight line from the equation:

$$\log \log \frac{100}{E} = n \log L_o + c \tag{7}$$

where $c = \log b + \log \log e$.

Determining the coefficients b and n from such a plot (figure 3) enables one to compare different kinds of fabrics. However, the relationship between the above dependencies and the structural properties of the fabrics and the properties of the dust have not been determined.

By analyzing the Valentin dependence, the following conclusions are made:

1. Filtration efficiency increases with increasing thickness of dust cake.

2. The coefficient n, being the slope of the E-L_o line on Rosin-Rammler Paper, is different for different kinds of fabrics. It depends on the mechanism of dust cake formation, and hence on the structural parameters of the fabrics, the dust properties, and the filtration parameters.
3. For fixed process parameters, the value of the coefficient b is constant.
4. If the value of L_o approaches zero, the filtration efficiency reaches its minimum and is the initial efficiency, depending mainly on the structural parameters of the filtration medium and on the filtration parameters.
5. The value of initial filtration efficiency can be extrapolated from the Rosin-Rammler equation (eq. 7):

$$n \log L_o = 0, \text{ i.e., } L_o = 1 \text{ (see figure 3).}$$

Consequently:

$$\log \log \frac{100}{E_o} = c = \log e + \log b$$

so

$$\frac{100}{E_o} = e^b$$

and

$$E_o = 100 \exp(-b). \tag{8}$$

From the above, the following relations can be hypothesized:

- The initial efficiency E_o depends mainly on the structural parameters of the filtration medium and on the filtration parameters, but also on the air-to-cloth ratio, q_g. Because q_g is a function of the structural parameters:

$$E_o = 100F_1 = f\left[q_g\left(SPFM\right),\ldots\right] . \tag{9}$$

- The slope, n, in the Rosin-Rammler equation is also a function of the air-to-cloth ratio and the structural parameters of the filtration medium, so:

$$n = F_2 = f\left[q_g\left(SPFM\right),\ldots\right] . \tag{10}$$

Using the above relations and equation 8, the Valentin formula can be rewritten:

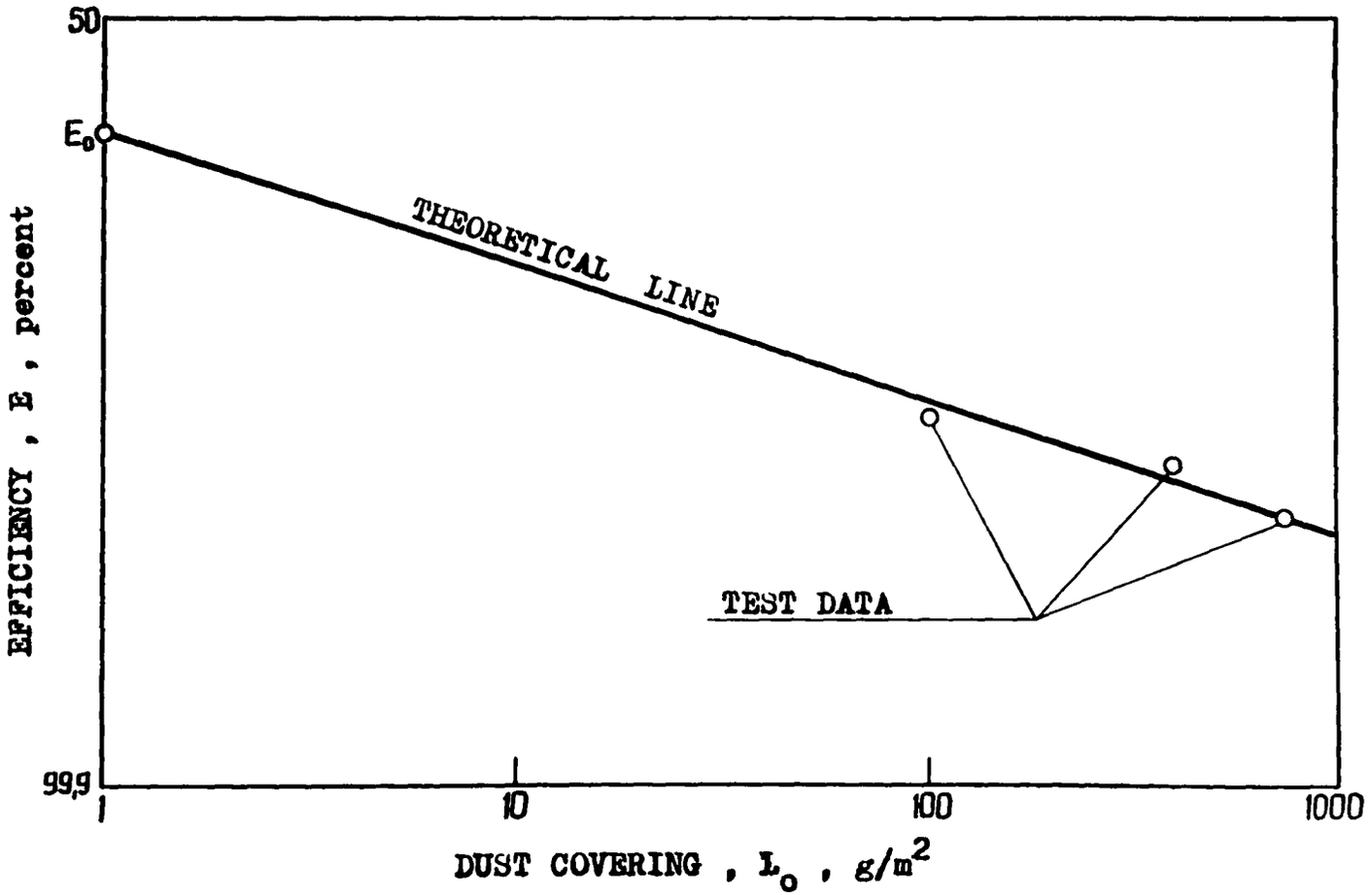

Figure 3. Efficiency as a function of dust covering.

$$E = 100 \left(\frac{E_o}{100}\right)^{L_o^n} \tag{11}$$

or

$$E = 100 \left(F_1\right)^{L_o^{F_2}} . \tag{11a}$$

The dependence given in equation 11 is valid only on the laboratory scale (and for $L_o > 0$ because equation 11 is of the functional form, $y = a^{-x}$).

In the case of Dust Filtration Type III (characteristic of industrial scale operations), where regeneration of the filtration medium occurs, filtration efficiency is greater than for Dust Filtration Type I. Higher efficiency results because of the filling dust remaining between the elemental fibers after regeneration. This value is constant for specific filter structures, types of dust, and parameters of filtration and regeneration. Based on studies conducted by M. W. First, it can be presumed that dust does penetrate the structure of the fabric; however, this does not negate the specific properties of the fabric manifested by the state-filling constant, L_N, for a definite set of operating conditions.

Introducing to the Valentin formula the additional function:

$$F_3 = f\left[L_{NK}\left(SPFM\right), \ldots\right] \tag{12}$$

where L_{NK} = the areal mass density of the filtration structure filled with dust for specific process conditions, g/m^2, we obtain an equation for Dust Filtration Type III:

$$E_{III} = 100F_3 \left(F_1\right)^{-L_o^{F_4}} . \tag{13}$$

The above equation is also a straight line on Rosin-Rammler Paper, but its position depends on the degree of structure filled with dust, L_{NK}. The initial efficiency, being a hypothetical value calculated from an extrapolation of equation 13, is higher than the initial efficiency calculated for type I filtration. Introduced as an exponent for the dust-covered structure, F_4 is not equivalent to the function F_2. F_4 represents another mechanism of dust cake formation on the filled structure:

$$F_4 = f\left[q_g\left(L_{NK},\ SPFM\right),\ \ldots\right]. \tag{14}$$

The process of filtration is accompanied by an increase in static pressure drop proportional to the increase in dust cake thickness. According to Stephan, Walsh, and Berrick, filtration drag is the ratio of pressure drop to the air-to-cloth ratio:

$$S = \Delta P/q_g. \tag{15}$$

Assuming a linear dependence of drag with time (or a linear dependence of S with L_o), it is possible to express equation 15 as:

$$S = L_o/K \tag{16}$$

where L_o = the areal mass density of the dust on a filter covered with dust in g/m^2, and

K = dust cake permeability in $\frac{g/m^2}{mmH_2O/m/hr}$.

The above dependence was regarded as suitable for the filtration range, including dust cake formation on a fabric surface. When dust cake forms, the depedence $S = F(L_o)$ is actually curvilinear. Assuming a linear dependence for this range, and calculating the initial drag from extrapolation of equation 16, a practical formula for filtration drag is:

$$S = S_R' + L_o/K \tag{17}$$

where K is designated from empirical data according to:

$K = L_o/S$, and

S_R' = projected residual drag.

This dependence is shown in figure 4. To make filtration drag depend upon time, the following simplified relation is used:

$$dL_o/dt = q_g c_o$$

so

$$L_o = \int_{t_o}^{t} q_g \cdot c \cdot dt$$

and

$$S = S_R + q_g \cdot c_o \cdot t/k. \tag{18}$$

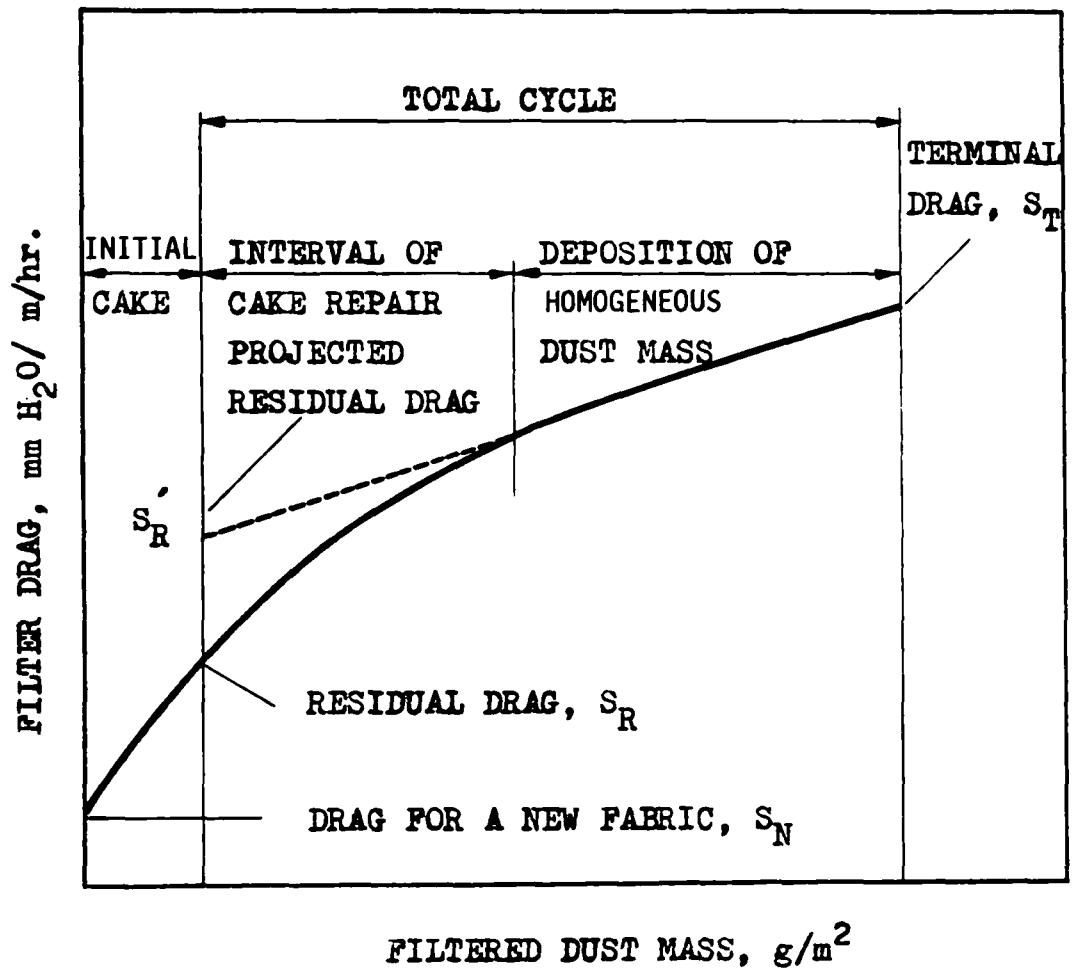

Figure 4. Schematic representation of basic performance parameters for fabric filters.

In reality, in many cases the dust concentration after the filter is too high for the above relation to be right. Accordingly:

$$L_o = \left(c_i - c_o\right) q_g \Delta t. \tag{19}$$

Based on our own research and on that published by R. Dennis the outlet concentration varies with dust cake during type I, as well as during type III dust filtration. Dennis, examining the effect of different filtration parameters on Dust Filtration Type III (industrial scale), found the following dependence for fly ash at L_o = 50-500 gr/ft^2 (35-348 g/m^2) and q_g = 3 ft/min (55 m/hr):

$$c_o = 0.65 \exp\left(- 0.0476 L_o\right) . \tag{20}$$

Substituting the above dependence into equation 19 we obtain:

$$L_o = \left[c_i - 0.65 \exp\left(-0.0476 L_o\right)\right] q_g \Delta t. \tag{21}$$

Our own research indicates a parabolic dependence of outlet concentration upon L_o.

Not discussing at this time the form of the functional dependence $c_o = f(L_o)$, it is sure that the assumption of a linear dependence of drag increasing with time needs revision. The development of the right relationship seems to be essential, especially for submicron particle penetration in the dust filtration process.

Because of the empirical character of the dependencies occurring in the dust filtration process, their verification is possible only by collecting a large amount of statistical data.

The problem directly connected with the previous deliberations is that of defining the necessary physical parameters of the fabric and of the dust cake formed during the filtration process.

The fabric, because of its very complicated geometrical composition, is very difficult to describe physically using only one parameter. Periodicity of structure does not resolve this problem because of the many variations in fibers and weave, making it impossible to model elemental surfaces or volumes. The extra condition accounting for the structural parameters of the filtration medium is its functional connection with its technological parameters of production. The present use of the parameter Free Area (FA) gives a connection to the technological parameters, but it seems too "weak" because it

does not take several fabric properties into consideration. Over the range of values FA = 0 (or negative values, where FA is reqarded as FA = 0), it does not describe the structure. The problem of finding a good structural parameter has been the subject of much prior research.

The physical parameters of a porous layer composed of elemental particles are comparatively well studied. However, according to dust cake formation on the filtration fabric, the hydraulic and qualitative effects resulting from its structural parameters cannot be predicted from knowledge of the aerosol state parameters before filtration alone. Dust cake structure does not depend only on degree of pulverization, geometry of grains, and surface properties of grains; but also on conditions of dust cake formation and on the structural properties of the fabric. However, observation of the external effects of dust cake formation is comparatively easy and leads to practical dependencies being applied in dust control technology, e.g., dust cake permeability, K = f (type of dust, kind of fabric, filtration parameters). Not enough such dependencies are yet known to be able to optimize research and take specific measures towards improvement of dust filtration process efficiency.

SECTION V
LABORATORY TESTING

EQUIPMENT AND PROCEDURES

Laboratory testing was conducted on a test stand, as illustrated in figure A-71. This apparatus was specially designed by the IPWMB and adopted for the testing of flat fabric specimens at unregulated temperature and humidity of the dispersion medium. A detailed description of the laboratory stand was included in the report on the first phase the work conducted in this project.

Average dust collection efficiency was determined by the weighing method. This method requires weighing the dust covered fabric and the control filter, and then applying the following relation:

$$\frac{E_I\ (\%)}{100} = \frac{G_z}{G_c} = \frac{G_c - G_o}{G_c} = \frac{G_z}{G_z \quad G_o}$$

where G_z = weight (grams) of dust collected on the fabric,
G_o = weight (grams) of dust collected on the control filter, and
G_c = weight (grams) of dust fed into the test chamber.

Using criteria given in the assumptions of the detailed program (Section III), laboratory testing was conducted on four kinds of Polish fabrics and four types of separated dusts. Previous test results by the IPWMB on unseparated cement and coal dusts were also added to the empirical data base.

RESULTS

Laboratory testing consisted of the following:

- A determination of the permeability of the filtration fabrics,
- A determination of the average laboratory dust collection efficiency of the tested fabrics, and

- A determination of the increase of filtration resistances as a function of time with the dust cover in or on the filter.

This section of the report includes the results of all testing carried out during both the first and the second phase of the project. Relevant test results previously obtained by the IPWMB on unseparated dusts are also included in this section.

In table 3, the results of permeability testing (a very important technological parameter) are shown. These values of permeability are based on averages of 20 to 50 measurements made on the same fabric but in different places. The complete set of measurements will be enclosed in the final report.

Table 3. PERMEABILITY OF FILTRATION FABRICS
(in $m^3/m^2/min$ at ΔP = 20 mm of water)

ET - 4	ET - 30	F-tor 5	PT - 15
20.70	7.54	14.60	3.65

Tables 4-7 show the results of testing certain filter fabrics with separated dusts of cement, coal, talc, and fly ash. The tables include the means from five measurements carried out over the range of test variables previously agreed upon. All data will be enclosed in the final report.

In tables 8-11, the archival results, obtained previously for the same kinds of fabrics but for unseparated cement and coal dusts, are shown. These data also represent the means of five measurements conducted under specific test conditions.

Tables 12-15 and 16-19 include the results of recording the final resistances (means from five measurements) obtained for different values of air-to-cloth ratio q_g and dust covering L_o. These results are from the testing of this program and from the archival data obtained from the testing of filtration fabrics with unseparated dusts.

The increase of resistances during filtration and as a function of dust covering L_o is shown in figures A-5 through A-28. Source materials (measurement reports) will be enclosed in the final report.

Table 4. LABORATORY EFFICIENCY (in percent) OF POLYESTER STYLE ET-4 (c_i = 10 g/m^3)

Air-to-Cloth Ratio q_g, in $m^3/m^2/h$	Dust covering in/on the filter L_o, in g/m^2	Kind of dust			
		Separated Cement Dust	Separated Coal Dust	Separated Talc Dust	Separated Fly Ash Dust
1	2	3	4	5	6
60	100	99.72	99.63	99.71	99·48
	400	99.93	99.85	99.95	99·82
	700	99.97	98.62	99.975	99·91
80	100	99.86	98.45	99.48	99·62
	400	99.96	97.66	99.66	99·91
	700	99.94	96.47	99.80	99·94
120	100	99.12	96.01	97.94[x]	99·23
	400	99.44[x]	96.03	96.98[x]	99.82
	700	99.17[x]	87.53	97.34[x]	99·79[x]

x Ducts/Canals present

Table 5. LABORATORY EFFICIENCY (in percent) OF POLYESTER STYLE ET-30 (c_i = 10g/m^3)

Air-to-Cloth Ratio q_g, in $m^3/m^2/h$	Dust covering in L_o, in g/m^3	Kind of dust			
		Separated Cement Dust	Separated Coal Dust	Separated Talc Dust	Separated Fly Ash Dust
1	2	3	4	5	6
60	100	99.78	99.82	99.93	99.54
	400	99.92	99.96	99.97	99.91
	700	99.96	99.96	99.98	99.98
80	100	99.81	99.74	99.71	99.74
	400	99.96	99.96	99.89	99.90
	700	99.98	99.97	99.95	99.95
120	100	99.89	99.50	99.82	99.66
	400	99.95	99.93	99.92	99.90
	700	99.97	99.97	99.95	99.94

Table 6. LABORATORY EFFICIENCY (in percent) OF POLYESTER STYLE F-tor 5 (c_i=10g/m^3)

Air-to-Cloth Ratio q_g, in $m^3/m^2/h$	Dust Covering in/on the filter L_o, in g/m^2	Kind of dust			
		Separated Cement Dust	Separated Coal Dust	Separated Talc Dust	Separated Fly Ash Dust
1	2	3	4	5	6
60	100	99.65	98.41	99.53	99.62
	400	99.90	99.65	99.47	99.91
	700	99.93	99.93	99.81	99.94
80	100	97.72	94.50	98.80	99.55
	400	99.48	99.81	99.70	99.85
	700	99.65	99.91	99.80	99.90
120	100	93.18	98.46	94.51[x]	99.18
	400	99.47	98.15	98.82[x]	99.74
	700	99.38[x]	98.64	96.94[x]	99.79

x Ducts/Canals present

Table 7. LABORATORY EFFICIENCY (in percent) OF POLYAMIDE STYLE PT-15 (c_1 =10g/m^3)

Air-to-Cloth Ratio q_g, in $m^3/m^2/h$	Dust covering in/on the filter L_o, in g/m^2	Kind of dust			
		Separated Cement Dust	Separated Coal Dust	Separated Talc Dust	Separated Fly Ash Dust
1	2	3	4	5	6
60	100	99,80	99.85	99.91	99.93
	400	99.96	99,96	99.986	99.97
	700	99.98	99,98	99.946	99,97
80	100	99.84	99.89	99.80	99.70
	400	99.98	99,98	99.98	99.93
	700	99.98	99.99	99.98	99.96
120	100	99.90	99.94	99.82	99.83
	400	99.98	99.96	99.92	99.94
	700	99.98	99.98	99.95	99.96

Table 8. LABORATORY EFFICIENCY (in percent) OF POLYESTER STYLE ET-4 (unseparated dust) (c_i = 30 g/m^3).

Air-to-Cloth Ratio q_g, in $m^3/m^2/h$	Dust Covering in/on the filter L_o, in g/m^2	Kind of dust	
		Non-separated Cement Dust	Non-separated Coal Dust
1	2	3	4
60	100	99.84	99.65
	400	99.96	99.84
	700	99.93	99.93
80	100	99.27	99.58
	400	99.88	99.91
	700	99.94	99.94
120	100	99.28	99.54
	400	99.82	99.73
	700	99.88	99.76

Table 9. LABORATORY EFFICIENCY (in percent) OF POLYESTER STYLE EI 30 (unseparated dust) (c_i = 30 g/m^3)

Air-to-Cloth Ratio q_g, in $m^3/m^2/h$	Dust Covering in/on the filter L_o, in g/m^2	Kind of dust	
		Non-separated Cement Dust	Non-separated Coal Dust
1	2	3	4
60	100	99.79	99.88
	400	99.97	99.97
	700	99.98	99.98
80	100	99.63	99.88
	400	99.91	99.96
	700	99.95	99.98
120	100	99.82	99.72
	400	99.93	99.91
	700	99.93	99.94

Table 10. LABORATORY EFFICIENCY (in percent) OF POLYESTER STYLE F-tor 5 (unseparated dust) (c_i = 30 g/m^3)

Air-to-Cloth Ratio q_g, in $m^3/m^2/h$	Dust Covering in/on the filter L_o, in g/m^2	Kind of dust	
		Non-separated Cement Dust	Non-separated Coal Dust
1	2	3	4
60	100	99.82	99.85
	400	99.87	99.95
	700	99.95	99,90
80	100	98.49	98.56
	400	99.88	98.68
	700	99.95	99.67
120	100	96.23	94.49
	400	99.89	98.47
	700	99.70	99.73

Table 11. LABORATORY EFFICIENCY (in percent) OF POLYAMIDE STYLE PT-15 (unseparated dust) (c_i = 30 g/m^3)

Air-to-Cloth Ratio q_g, in m^3/m^2/h	Dust Covering in/on the filter L_o, g/m^2	Kind of dust	
		Non-separated Cement Dust	Non-separated Coal Dust
1	2	3	4
60	100	99.88	99.92
	400	99.99	99.96
	700	99.99	99.97
80	100	98.59	99.77
	400	99.90	99.92
	700	99.99	98.99
120	100	99.89	99.93
	400	99.93	99.94
	700	99.95	99.97

Table 12. FINAL PRESSURE DROP IN LABORATORY TESTING (in mm of water) FOR POLYESTER STYLE ET-4 (c_i = 10 g/m^3)

Air-to-Cloth Ratio q_g, in $m^3/m^2/h$	Dust Covering in/on the filter L_o, in g/m^3	Kind of dust			
		Separated Cement Dust	Separated Coal Dust	Separated Talc Dust	Separated Fly Ash Dust
1	2	3	4	5	6
60	100	8,06	6,10	5,89	5,55
	400	28,50	39,10	32,71	14,20
	700	63,50	81,40	65,09	28,09
80	100	13,60	14,60	10,71	9,86
	400	48,50	67,30	55,30	29,36
	700	99,50	128,00	132,25	60,12
120	100	28,50	27,80	22,04	19,84
	400	118,30	122,20	119,59	69,76
	700	212,80	190,00	221,80	125,45

Table 13. FINAL PRESSURE DROP IN LABORATORY TESTING (in mm of water) FOR POLYESTER STYLE ET-30 (c_i = 10 g/m^3)

Air-to-Cloth Ratio q_g, in $m^3/m^2/h$	Dust Covering in/on the filter L_o, in g/m^2	Kind of dust			
		Separated Cement Dust	Separated Coal Dust	Separated Talc Dust	Separated Fly Ash Dust
1	2	3	4	5	6
60	100	16.88	15.30	10.24	9.10
	400	46.25	48.10	45.11	17.41
	700	77.13	87.20	85.64	30.18
80	100	28.24	27,00	20.03	19.05
	400	67.90	80,20	71.41	41.16
	700	123.06	149,20	115.81	68.45
120	100	54.80	55.50	44.95	41.06
	400	130.00	174.70	156.58	89.82
	700	229.00	340.30	281.80	159.53

Table 14. FINAL PRESSURE DROP IN LABORATORY TESTING (in mm of water) FOR POLYESTER STYLE F-tor 5 (c_i = 10 g/m^3)

Air-to-Cloth Ration q_g, in $m^3/m^2/h$	Dust Covering in/on the filter L_o, in g/m^2	Kind of dust			
		Separated Cement Dust	Separated Coal Dust	Separated Talc Dust	Separated Fly Ash Dust
1	2	3	4	5	6
60	100	18.64	19.10	14.41	11,50
	400	41.23	49,90	45.82	22,50
	700	70.00	102,40	89.90	39.34
80	100	25.59	27.06	25.40	23.00
	400	73.71	94.60	77,88	43.53
	700	122.40	166.00	134.81	67.78
120	100	60.72	76.60	46,57	42.34
	400	163.00	199.70	173,74	88,32
	700	269.00	331.00	319,00	150.42

Table 15. FINAL PRESSURE DROP IN LABORATORY TESTING (in mm of water) FOR POLYAMIDE STYLE PT-15 (c_i = 10 g/m^3)

Air-to-Cloth Ratio q_g, in $m^3/m^2/h$	Dust Covering in/on the filter g/m^2	Kind of dust			
		Separated Cement Dust	Separated Coal Dust	Separated Talc Dust	Separated Fly Ash Dust
1	2	3	4	5	6
60	100	32.20	28.40	19.24	16.65
	400	53.40	67.10	45.98	27.21
	700	79.50	110.30	85.16	42.24
80	100	48.40	53.50	53.00	33.34
	400	79.30	111.40	87.22	51.27
	700	150.40	183.20	155.95	83.27
120	100	110.70	111.40	79.47	77.73
	400	219.80	256.20	192.60	128.45
	700	290.00	408.00	312.20	206.80

Table 16. FINAL PRESSURE DROP IN LABORATORY TESTING (in mm of water) FOR POLYESTER STYLE ET-4 (unseparated dust) (c_i = 30 g/m^3)

Air-to-Cloth Ratio q_g, in $m^3/m^2/h$	Dust Covering in/on the filter L_o, in g/m^2	Kind of dust	
		Non-separated Cement Dust	Non-separated Coal Dust
1	2	3	4
60	100	5.40	4.15
	400	15.20	16.80
	700	25.30	20.40
80	100	8.60	7.20
	400	33,12	27,04
	700	49.50	41,90
120	100	17,20	14.30
	400	57.50	47.80
	700	92.30	68,40

Table 17. FINAL PRESSURE DROP IN LABORATORY TESTING (in mm of water) FOR POLYESTER STYLE ET-30 (unseparated dust) (c_i = 30 g/m^3)

Air-to-Cloth Ratio q_g, in $m^3/m^2/h$	Dust Covering in/on the filter L_o, in g/m^2	Kind of dust	
		Non-separated Cement Dust	Non-separated Coal Dust
1	2	3	4
60	100	13.60	6.20
	400	23.70	21.00
	700	38,80	24.50
80	100	23.40	12.40
	400	51.00	34.20
	700	71.70	51.40
120	100	50.30	37.20
	400	104.00	84.40
	700	121.00	94.00

Table 18. FINAL PRESSURE DROP IN LABORATORY TESTING (in mm of water) FOR POLYESTER STYLE F-tor 5 (unseparated dust) (c_i = 30 g/m^3)

Air-to-Cloth Ratio q_g, in $m^3/m^2/h$	Dust Covering in/on the filter L_o, in g/m^2	Kind of dust	
		Non-separated Cement Dust	Non-separated Coal Dust
1	2	3	4
60	100	11.80	12.45
	400	24.85	29.20
	700	36.60	33.10
80	100	21.80	19.49
	400	47.70	47,30
	700	72.00	64.06
120	100	44.20	41.08
	400	93.50	99.54
	700	128.00	135.88

Table 19. FINAL PRESSURE DROP IN LABORATORY TESTING (in mm of water) FOR POLYAMIDE STYLE PT-15 (unseparated dust) (c_i = 30 g/m^3)

Air-to-Cloth Ratio q_g, in $m^3/m^2/h$	Dust Covering in/on the filter L_o, in g/m^2	Kind of dust	
		Non-separated Cement Dust	Non-separated Coal Dust
1	2	3	4
60	100	17.80	10.90
	400	29.80	22.70
	700	46.30	30.90
80	100	32.80	35.63
	400	62.20	67.86
	700	86.10	96.54
120	100	68.80	57.50
	400	117.00	89.20
	700	156.70	124.00

The laboratory testing was conducted according to conditions previously defined in the detailed program description.

DISCUSSION OF RESULTS

In contradistinction to the discussion of results conducted in phase I of this project (based on comparative analyses rather than theoretical analysis), this phase (phase II) analyzes Dust Filtration Type I (laboratory scale) beginning with the modified Valentin relation for dust collection efficiency (eq. 11a, section IV):

$$E_I = (F_1)^{L_o F_2} \times 100(\%) \tag{23}$$

where E_I = laboratory dust collection efficiency in percent,

L_o = the areal mass density of the dust in or on the dusty filter (the dust load), g/m^2,

$$F_1 = \frac{E_o}{100} = f\left[q_g(\text{SPFM}), \ldots.\right], \text{ and}$$

$$F_2 = n = f\left[q_g(\text{SPFM}), \ldots\right].$$

According to equation 23, L_o and E_I should plot as straight lines on Rosin-Rammler Paper (at constant q_g). Most of the empirical data confirm this assumption. However, for some kinds of fabrics, discrepancies characterized by a large dispersion of points exist.

To fit a linear relation to a specific set of empirical data, regression lines were determined, after eliminating outlying data points--those that deviated widely from the average or were not consistent with the theoretical predictions.

The calculation was conducted for:

$$y = a + bx$$

$$\text{where } y = \log \log \frac{100}{E} \tag{24}$$

$$x = \log L_o \text{ at } q_g = \text{constant}.$$

The coefficients of the regression equation (a and b) are empirically determined and are calculated from the following relations:

$$a = \log \log \frac{100}{E_o} = \frac{(\Sigma y)\ (\Sigma x^2) - (\Sigma x)\ (\Sigma xy)}{n(\Sigma x^2) - (\Sigma x)^2} \tag{25}$$

and

$$b = n = \frac{n(\Sigma xy) - (\Sigma x)\ (\Sigma y)}{n(\Sigma x^2) - (\Sigma x)^2} \tag{26}$$

where n in the numerator and denominator of the right hand side of the equation is the number of points through which the regression line was fitted.

The plots of the empirical data and the corresponding regression lines on Rosin-Rammler Paper are shown in figures A-29 through A-52.

Calculated values of $a = \log \log \frac{100}{E_o} = f(q_g)$ and $b = n = f(q_g)$ are shown in tables 20 and 21. Values of n and E_o as a function of air-to-cloth ratio q_g are shown in figures A-53 through A-62.

The data collected in tables 20 and 21 show that for individual groups of dusts of the same kind and for specific fabrics, F_1 and F_2 are not linear:

$$F_1 = \frac{E_o}{100} = f(q_g) \tag{27}$$

and

$$F_2 = n = f(q_g). \tag{28}$$

The hypothesis was presented that the relations in equations 27 and 28 would be at least quadratic, so the empirical data should be better approximated by a parabola. Applying the least squares method to determine the coefficients a, b, and c of the parabolic equation:

$$y = ax^2 + bx + c, \tag{29}$$

the following sets of equations should be solved:

$$\begin{aligned} cn + b\Sigma x + a\Sigma x^2 &= \Sigma y \\ c\Sigma x + b\Sigma x^2 + a\Sigma x^3 &= \Sigma xy \\ c\Sigma x^2 + b\Sigma x^3 + a\Sigma x^4 &= \Sigma x^2 y \end{aligned} \tag{30}$$

where $x = q_{g1}, q_{g2}, \cdots$

$y = E_{o1}, E_{o2}, \ldots$ and $y = n_1, n_2, \ldots,$

and n in the first equation is the number of data points being fitted.

Table 20. INITIAL EFFICIENCY E_0 AS A FUNCTION OF q_g.

Type of filtration fabric	q_g in $m^3/m^2/hr$	Kind of dust					
		Sep. cement	Non-sep. cement	Sep. coal	Non-sep. coal	Sep talc	Sep. fly ash
1	2	3	4	5	6	7	8
ET-4	60	56.75	87.64	92,30	88.89	37.44	72.99
	80	85.43	12.72	-	64.47	95.24	70.72
	120	-	64,89	-	97.97	-	41.58
ET-30	60	88.97	48,85	80.32	90.25	98.55	0.11
	80	68.68	57,01	58.14	89.21	79.94	85.47
	120	97.74	98.06	9,61	90.42	96,25	83.33
F-tor 5	60	83.96	96.99	1.71	93.63	97,18	76.69
	80	12.27	0	0	76.75	69.11	83,68
	120	0	0	98.14	0	0	80,06
PT-15	60	58.89	19.23	77.52	99,25	91.16	99,45
	80	0.077	0	62.46	0.075	39.86	71,28
	120	82.71	99,34	99,07	99,75	31.66	94,97

Table 21. COEFFICIENT n AS A FUNCTION OF q_g.

Type of filtration fabric	q_g in $m^3/m^2/hr$	Kind of dust					
		Sep. cement	Non-sep. cement	Sep. coal	Non-sep. coal	Sep. talc	Sep. fly ash
1	2	3	4	5	6	7	8
ET-4	60	-1,14	-0.77	-0,66	-0,78	-1,27	-0,88
	80	-0.96	-1,24	-	-1,02	-0,47	-0.98
	120	-	-0.90	-	-0.33	-	-1,03
ET-30	60	-0,86	-1.28	-1.06	-0.97	-0,66	-1,56
	80	-1.15	-1.05	-1,17	-0,97	-0.92	-0,87
	120	-0.66	-0.53	-1,36	-0,78	-0.66	-0,87
F-tor 5	60	-0.85	-0,60	-1,49	-0,82	-0.36	-0.94
	80	-0.99	-1.90	-2,17	-0.60	-0,91	-0.79
	120	-1.77	-2.45	-0.03	-1,43	-1,13	-0,72
PT-15	60	-1.21	-1.57	-1.09	-0.49	-0,55	-0.46
	80	-1.77	-2.39	-1,30	-1,66	-1.34	-1,02
	120	-1,15	-0.39	-0.57	-0,29	-1,35	-0.74

Consequently the coefficients a, b, and c were calculated according to relations $E_o = f(q_g)$ and $n = f(q_g)$. The results are shown in tables 22 and 23.

The determination of the true values of the coefficients a, b, and c enable one to write the explicit modified form of the Valentin relation as follows:

$$E_I = \left[a_1(q_g)^2 + b_1(q_g) + c_1\right]^{-L_o \left[a_2(q_g)^2 + b_2(q_g) + c_2\right]} \tag{31}$$

where a_1, a_2, b_1, b_2, c_1, c_2 = constants depending on the kind of dust and the structural parameters of the fabric.

The first part of equation 31 corresponds to the function F_1:

$$F_1 = \left[a_1(q_g)^2 + b_1(q_g) + c_1\right]. \tag{32}$$

It is easy to notice that equation 32 has its extreme at an air-to-to cloth ratio of $q_{g\ ext}$:

$$q_{g\ ext} = -\frac{b_1}{2a_1} \tag{33}$$

The sign of the second derivative of equation 32 decides whether the extreme is a maximum or a minimum. The calculated values of $q_{g\ ext}$ for specific initial dust collection efficiency are shown in table 24.

In most cases, the extreme corresponds to a minimal initial efficiency. The filtration of fly ash is an exception--in three of four cases a maximum of initial efficiency was observed.

It is very interesting that the extreme values of the function F_1 occur over a relatively narrow range of air-to-cloth ratios, 70-100 $m^3/m^2/h$. The above regularity was also observed in other testing conducted by the IPWMB for 16 kinds of fabrics and unseparated dusts.

The parabolic dependence of initial dust collection efficiency on the air-to-cloth ratio has a very important consequence because it leads to the hypothesis that there are two separate dust penetration processes--one for low q_g values and another for high q_g values. The value of $q_{g\ ext}$ is probably that air-to-cloth ratio at which the transition from one mechanism to the other occurs. This hypothesis applies also to the function $F_2 = f(q_g)$,

Table 22. COEFFICIENTS OF THE PARABOLIC EQUATION: $F_1 = a_1(q_g)^2 + b_1 q_g + c_1$

Type of filtration fabric	Parabola coefficient	Kind of dust					
		Sep. cement	Non-sep. cement	Sep. coal	Non-sep coal	Sep. talc	Sep. fly ash
1	2	3	4	5	6	7	8
ET-4	a_1	-	0,082545	-	0.034308	-	-0.010250
	b_1	-	-15.20491	-	-6,02416	-	1.32150
	c_1	-	700,82	-	326,83	-	30.60
ET-30	a_1	0.029016	0,000262	0,001737	0.001370	0.022304	-0.069208
	b_1	-5,07683	0,37125	-0.86575	-0.24391	-4.05308	13.95716
	c_1	289,12	25,63	300.14	99,95	261.44	-588.17
F-tor 5	a_1	0.054629	0.080825	-	0,017912	-0,005404	-0.007345
	b_1	-11,23258	-16.165	-	1.66375	-0,64691	1,37616
	c_1	561.25	775.92	-	58.29	155.45	20.43
PT-15	a_1	0,083441	0,057416	0.027804	0.124177	0.039333	0.033345
	b_1	-14,60242	-8.99966	-4.64558	-22.34354	-8.07166	-6.07841
	c_1	635,85	352.52	256.16	992.825	433.86	344.02

Table 23. COEFFICIENTS OF THE PARABOLIC EQUATION: $F_2 = n = a_2(q_g)^2 + b_2 q_g + c_2$

Type of filtration fabric	Parabola coefficient	Kind of dust					
		Sep. cement	Non-sep. cement	Sep. coal	Non-sep. coal	Sep. talc	Sep. fly ash
1	2	3	4	5	6	7	8
ET-4	a_2	-	0.000567	-	0.000488	-	0,000063
	b_2	-	-0,105	-	-0.08025	-	-0.01375
	c_2	-	3.52	-	2.28	-	-0,30
ET-30	a_2	0,000445	0.000108	0,000012	0,000079	0,000325	-0,00056
	b_2	-0.07691	-0,03	-0.00725	-0.01108	-0.05850	0.115
	c_2	2.15	-2.49	-0.67	-0.59	1.68	-6.39
F-tor 5	a_2	-0.000208	-0,000045	-	-0.000529	0.000366	-0,000095
	b_2	0,02216	-0.02258	-	0.08508	-0.07883	0,02091
	c_2	-1.43	0,92	-	-4.02	3,05	-0,85
PT-15	a_2	0.000725	0,001516	0.000479	0,001545	0.000654	0.000583
	b_2	0.12950	0,25333	-0.07758	-0,27491	-0,13108	-0,10966
	c_2	3.95	8,17	1.84	10,44	4,96	4.02

Table 24. EXTREMAL AIR-TO-CLOTH RATIOS, $q_{g\ ext}$.

Type of filtration fabric	Initial efficiency*	Kind of dust					
		Sep. cement	Non-sep. cement	Sep. coal	Non-sep. coal	Sep. talc	Sep. fly ash
1	2	3	4	5	6	7	8
ET-4	$E_{o\ min}$	-	92.10	-	87.80	-	-
	$E_{o\ max}$	-	-	-	-	-	64.46
ET-30	$E_{o\ min}$	87.48	-708.49	249.21	89.02	90.86	-
	$E_{o\ max}$	-	-	-	-	-	100.83
F-tor 5	$E_{o\ min}$	102.81	100.00	-	-46.44	-	-
	$E_{o\ max}$	-	-	-	-	-59.85	93.68
PT-15	$E_{o\ min}$	87.62	78.37	83.54	89.97	102.61	91.14
	$E_{o\ max}$	-	-	-	-	-	-

*Listing $q_{g\ ext}$ as corresponding to $E_{o_{min}}$ or $E_{o_{max}}$ depends on the sign of the coefficient a_1 (Table 22); i.e. positive a_1 implies a minimum value of E_o; negative a_1, a maximum.

which mainly describes the filtration properties of the dust cake, taking under consideration the conditions of its formation. F_2 functions for various dust-fabric combinations are shown in figures A-53 through A-62.

Considering the fact that the analyses of the dust filtration process include only a comparatively narrow statistical range, it is necessary to verify them, based on data obtained from additional individual tests conducted both in the laboratory and on large scale.

The increase of pressure drops accompanying dust filtration results from thickening of the dust cake formed on the fabric surface. The analysis of results obtained at laboratory scale for separated cement and coal dusts was carried out according to the previously presented theoretical aspects of the dust filtration process (section IV), where nonlinear behavior of filtration resistance as a function of time (or as a function of dust load, L_o) was confirmed.

For specific dust-fabric combinations and values of air-to-cloth ratio, q_g, the outlet dust concentrations (C_o) corresponding to definite dust loadings L_o, were calculated consecutively. The results of these calculations are shown in tables 25 and 26 and figures A-63 through A-70.

Applying the least squares method, the forms of the functions $c_o = f(L_o)$ were determined, assuming a parabolic relationship as the first approximation. The following equations were developed:

For separated cement dust and fabrics as indicated:

ET-4

$$q_g = 60;\quad c_o = 1.0 \times 10^{6} (L_o)^2 \quad 12.3 \times 10^{-4} (L_o) + 0.403$$

$$q_g = 80;\ c_o = 0.066 \times 10^{-6}(L_o)^2 - 0.66 \times 10^{-4}(L_o) + 0.01994$$

$$q_g = 120;\ c_o = 0.338 \times 10^{-6}(L_o)^2 - 2.76 \times 10^{-4}(L_o) + 0.11422$$

ET-30

$$q_g = 60;\ c_o = 0.627 \times 10^{-7}(L_o)^2 - 0.796 \times 10^{-4}(L_o) + 0.02934$$

$$q_g = 80;\ c_o = 0.7 \times 10^{-7}(L_o)^2 - 0.8472 \times 10^{-4}(L_o) + 0.0265$$

$$q_g = 120;\ c_o = 0.33 \times 10^{-7}(L_o)^2 - 0.412 \times 10^{-4}(L_o) + 0.015734$$

Table 25. OUTLET CONCENTRATION, c_o in g/m^3 , IN LABORATORY TESTING OF CEMENT DUST.

Type of filtration fabric	Air-to-Cloth Ratio in $m^3/m^2/h$	Dust loading, g/m^2		
		L_o = 100	L_o = 400	L_o = 700
1	2	3	4	5
ET-4	60	0.29	0.07	0.03
	80	0.014	0.0041	0.0061
	120	0.09	0.058	0.087
ET-30	60	0.022	0.0075	0.00429
	80	0.01875	0.00388	0.001667
	120	0.012	0.00475	0.003428
F-tor 5	60	0.035	0.009	0.007
	80	0.22782	0.05129	0.03417
	120	0.73	0.0555	0.06129
PT-15	60	0.021	0.00425	0.001857
	80	0.01594	0.001935	0.001667
	120	0.01	0.00225	0.001714

Table 26. OUTLET CONCENTRATION C_o IN g/m^3, IN LABORATORY TESTING OF COAL DUST

Type of filtration fabric	Air-to-Cloth Ratio in $m^3/m^2/h$	Dust Loading, g/m^2		
		L_o = 100	L_o = 400	L_o = 700
1	2	3	4	5
ET-4	60	0.037	0.0145	0.117
	80	(0,1528)	(0.2327)	(0,3622)
	120	(0.375)	(0.401)	(1.3753)
ET-30	60	0.016	0.0035	0.003571
	80	0.02438	0.003629	0.0025
	120	0.046	0.006	0.003
F-tor 5	60	0.16	0.03375	0.007
	80	0.5653	0.01839	0.0094
	120	(0,165)	(0.18075)	(0.1324)
PT-15	60	0.016	0.00475	0.001857
	80	0.01125	0.001694	0.0011
	120	0.006	0.004	0.002714

F-tor 5

$q_g = 60;\ c_o = 0.133 \times 10^{-6}(L_o)^2 - 0.78 \times 10^{-3}(L_o) + 0.06766$

$q_g = 80;\ c_o = 2.405 \times 10^{-6}(L_o)^2 - 1.037 \times 10^{-3}(L_o) + 0.32207$

$q_g = 120;\ c_o = 3.676 \times 10^{-6}(L_o)^2 - 4.138 \times 10^{-3}(L_o) + 1.1060$

PT-15

$q_g = 60;\ c_o = 7.976 \times 10^{-8}(L_o)^2 - 9.57 \times 10^{-5}(L_o) + 0.02977$

$q_g = 80;\ c_o = 7.63 \times 10^{-8}(L_o)^2 - 8.48 \times 10^{-5}(L_o) + 0.023435$

$q_g = 120;\ c_o = 4.0 \times 10^{-8}(L_o)^2 - 4.58 \times 10^{-5}(L_o) + 0.014864.$

For separated coal dust and fabrics as indicated:

ET-4

$q_g = 60;\ c_o = 9.361 \times 10^{-7}(L_o)^2 - 4.22 \times 10^{-4}(L_o) - 0.04613$

ET-30

$q_g = 60;\ c_o = 6.983 \times 10^{-8}(L_o)^2 - 7.6583 \times 10^{-5}(L_o) + 0.023198$

$q_g = 80;\ c_o = 10.9 \times 10^{-8}(L_o)^2 - 12.36 \times 10^{-5}(L_o) + 0.034547$

$q_g = 120;\ c_o = 20.55 \times 10^{-8}(L_o)^2 - 23.611 \times 10^{-5}(L_o) + 0.0676$

F-tor 5

$q_g = 60;\ c_o = 5.527 \times 10^{-7}(L_o)^2 - 6.922 \times 10^{-4}(L_o) + 0.224194$

$q_g = 80;\ c_o = 21.838 \times 10^{-7}(L_o)^2 + 8.206 \times 10^{-4}(L_o) + 0.5055$

PT-15

$q_g = 60;\ c_o = 4.652 \times 10^{-8}(L_o)^2 - 6.076 \times 10^{-5}(L_o) + 0.021611$

$q_g = 80;\ c_o = 5.0288 \times 10^{-8}(L_o)^2 - 5.6744 \times 10^{-5}(L_o) + 0.016426$

$q_g = 120;\ c_o = 0.4 \times 10^{-8}(L_o)^2 - 0.8655 \times 10^{-5}(L_o) + 0.006825.$

The time and initial concentration (c_i) dependence of the dust covering L_o is described by the equation:

$$L_o = (c_i - c_o)\, q_g \Delta t \qquad (34)$$

where c_o corresponds to the functions of L_o just presented.

Based on the dust cake equation:

$$S = L_o/K \tag{35}$$

which, according to experimental data given by many authors, describes a straight line in the S-L_o coordinate system (with slope 1/K, where K is the permeability of the dust cake and fabric). The obtained results show that the coefficient K cannot be a constant dependent only on the specific dust and fabric. Intuitively, the above statement is also ascertained.

The permeability coefficient of a porous layer in the Darcy Formula assumes a stationary spatial system of layered elements, while in a dust filtration process displacement and compression effects appear. First's experiments, conducted using trace elements, confirm this statement.

During our testing, a nonlinear dependence of filtration resistivities upon dust cover was recorded. The complete analysis of the empirical data will be included in the final report.

CONCLUSIONS

Based on the results of fabric testing on a laboratory scale, a modified form of the Valetin equation for dust collection efficiency as a function of dust cover L_o and air-to-cloth ratio q_g was developed. Also, the experiments performed confirmed the appearance of defects in the dust cake structure, in the form of canals (ducts), considerably reducing the dust collection efficiency. And finally, nonlinear variation of filtration resistances with time (dust cover), which results from differences between the theoretical and the real models of dust cake formation, were found.

SECTION VI

PRELIMINARY MATHEMATICAL MODEL OF DUST FILTRATION*

The problem of inferring fabric properties has all the characteristics needed for applying the methods of statistical inference. The characteristics of a population are inferred from the behavior of a sample. Thus, a specific fabric can be considered a population whose characteristics we wish to describe. The sample is a piece of that fabric on which measurements are made of certain specific characteristics, either in the laboratory or on a large scale. The parameter examined most often is fabric permeability to the flow of air or clean or dirty gas. The basic problem from a statistical point of view is that of the existence and interpretation of a random variable representing a specific characteristic. The random variable can be introduced in many ways depending on the questions to be answered.

Fibers from which a fabric is built are not heterogeneous but they do differ in shape and in such properties as elasticity or thickness. This element of heterogeneity comes about because of random variations in the production process. In the case of fabric production from synthetic materials, just a little temperature variation causes the fibers to vary in thickness and other properties. With natural fabrics, variations in the fiber properties cause the fabric to be heterogeneous. The variables influencing the above processes have random character. So each of the examined fabric parameters related to the above heterogeneity is a random variable. Thus we have, by the nature of the manufacturing processes, a probability space in which random variables are situated.

More practical is the random variable introduced in another way. Let the probability space (E, A, P) be given. As random variables, we consider the univariate real functions making up a set of elementary events E (a Borel field of sets) in IR^n (a Borel field of sets in IR^n). As an elemen-

*Section VI was written by Dr. Eugeniusz Szczepankiewicz, Institute of Mathematics of WSP, Opole.

tary event in the set IR^n, we consider an arbitrary open rectangle. As an elementary event on the fabric, we consider an arbitrary rectangle cut out from the fabric bale. As a set of elementary events we consider all the rectangles covering the fabric bale. Circles can be used as easily as rectangles. This definition of a random variable is very useful in applying statistics to fabrics and especially in studying those fabric characteristics related to filtration.

It is important to notice that fabric properties related to filtration are random variables having finite expected values and variances. Since the filtration process acts in time, it is a stochastic process. If we want to make this process dependent upon geometrical parameters (which is advisable in many cases) we develop a random field. This random field has finite expected value and variance. Thus it is a stationary random field in the broad sense, but if it depends on the distance between points, it is an isotropic random field.

Let f(p) be the examined characteristic of the fabric filtration process--a stationary random field in the broad sense. The properties of the random field can be described as

$$E\left[f(p)\right] = m = \text{const. at} \quad \left|E\left[f(p)\right]\right| < \infty \tag{36}$$

$$D^2\left[f(p)\right] = \sigma^2 < \infty. \tag{37}$$

The correlation function depends only on the distance between points p and q:

$$R\left[f(p), f(q)\right] = R(|\overrightarrow{pq}|). \tag{38}$$

Since the fabric filtration process involves many characteristics of the fabric, many parameters of this process can be examined. Each characteristic, and the parameter which represents it, can be described by a stationary random field in the broad sense, which is also isotropic. Thus the problem is the formation of a stochastic filtration model that includes all dependencies existing between the parameters of the fabric filtration process.

Let us consider parameters described by the random fields $f_1(p),\ldots,$ $f_n(p)$ that makeup the filtration process. Parameters are intercorrelated.

The relation between arbitrary parameters is expressed by the correlation function describing the stochastic connection of these parameters. This correlation function can be written:

$$R\left[f_i(p),\ f_j(q)\right] = R_{ij}\left(|\overrightarrow{pq}|\right),\ (i \neq j;\ i,j = 1,\ \ldots,\ n). \quad (39)$$

We have assumed that the connections between parameters are stationary. The relation between all parameters is expressed by a multiple correlation function:

$$R\left[f_1(p),\ \ldots,\ f_n(q)\right] = R_{1,\ \ldots,\ n}\left(|\overrightarrow{pq}|\right). \quad (40)$$

In dependence (40) we have assumed stationary relations between all parameters of the fabric filtration process.

Functions (38), (39), and (40) should be chosen from classes of functions which could be correlation functions of stationary, isotropic, and stationary-related random fields. Optimal selection of these functions will be discussed in a later part of this section.

Thus far the random field has been described taking into consideration only one bale of fabric. Now we are interested in the problem in a wider sense. We want to look at the filtration problem for more than one bale of material (the same kind of fabric). The random field defined for one bale of material can be extended to all bales of the same fabric. For this purpose, we introduce the following expression:

$$M(D) = \frac{1}{|D|}\int_D f(p)dp \quad (41)$$

which we call the mean of the random field f(p) over the range D, where $|D|$ is a field of range D, and dp is a differential of measurement in D.

The expression (41) is considered the mean of one bale of fabric and is estimated from the mean of a sample. The limits are 1 and m M(D), where D increases without limit (the problem needs definition but here this definition is omitted) and is the expected value of the random field. So it is a natural extension of the mean of one fabric bale to all bales of a specific fabric. This definition is compatible with the generally accepted definition of a random field. Because we cannot find the expected value of the

random field in the sense mentioned above, we will estimate it from the mean of a sample. In classical statistics such estimates are based on the arithmetic mean of the random sample. Random values (individual measurements) are taken on the sample in order to achieve independence. In the case of the random field this choice is usually impossible. We can obtain dependent random variables but the samples from which we estimate are not random samples. They (random samples) do not guarantee that all parts of D will be represented. Consequently, systematic samples are used. The problem of optimal sampling will be discussed later in this paper. We will be interested in those samples which best represent the parameters of fabric filtration. Now we will deal with the problem of estimating the mean (41) with the help of measurements of values of the random field at points in D.

Let $f_1 = f(p_1)$, ..., $f_m = f(p_m)$ be values of the random field f(p) at points p_1, ..., p_m in D. M(D) in (41) will be estimated by the linear estimators given below. It is shown that the best estimator is included among these estimators.

Estimator 1

$$m_1(D) = c_o + c_1 f_1 + \ldots + c_m f_m \tag{42}$$

where $c_i \geq 0$ $(i = 0, 1, \ldots, m)$

and $c_o + c_1 + \ldots + c_m = 1$.

The error of this estimator is s_1, given by

$$s_1^2 = \min_{c_o, c_1, \ldots, c_m} E[m_1(D) - M(D)]^2. \tag{43}$$

Estimator 2.

$$m_2(D) = c_1 f_1 + \ldots + c_m f_m \tag{44}$$

where $c_i \geq 0$ $(i = 1, \ldots, m)$

and $c_1 + \ldots + c_m = 1$.

The error of this estimator is s_2, given by

$$s_2^2 = \min_{c_1, \ldots, c_m} E[m_2(D) - M(D)]^2. \tag{45}$$

Estimator 3

$$m_3(D) = c_1 f_1 + \ldots + c_m f_m$$

where $c_i \geq 0$ $(i = 1, \ldots, m)$

and $c_1 + \ldots + c_m = 1$.

and the constants are selected so that

$$S_3^2 = \min_{c_1, \ldots, c_m} E[m_3(D) - M(D)]^2 \tag{47}$$

and $E[m_3(D)] = M(D)$.

The error of this estimator is calculated from formula (47).

Estimator 4.

$$m_4(D) = c(f_1 + \ldots + f_m) \tag{49}$$

where $c = 1/m$, (50)

$$E[m_4(D)] = M(D), \tag{51}$$

and constant c is selected so that

$$S_4^2 = \min_{c} E\,[m_4(D) - M(D)]^2. \tag{52}$$

The error of this estimator is calculated from formula (52).

In all estimators, E represents the expected value operator.

It is shown that the constants $c_o, \ldots, c_m$ appearing in the estimators are solutions of a set of specific linear equations of the Cramer type. For estimator 1 we have the equation system:

$$\left.\begin{aligned} \alpha(f_1, f_1)c_1 + \ldots + \alpha(f_1, f_m)c_m &= \alpha(f_1, M(D)) \\ \vdots \qquad\qquad\qquad \vdots \qquad\qquad &\vdots \\ \alpha(f_m, f_1)c_1 + \ldots + \alpha(f_m, f_m)c_m &= \alpha(f_m, M(D)) \\ c_o + E(f_1)c_1 + \ldots + E(f_m)c_m &= M(D) \end{aligned}\right\} \tag{53}$$

where $\alpha(f_i, f_j)$ $(i, j = 1, \ldots, m)$ represents the covariance of the random variables f_i, f_j; $\alpha(f_i, M(D))$ is the covariance of the random variables f_i and M(D), and $E(f_i)$ is the expected value of the random variable f_i.

Constants appearing in estimator 2 are calculated from the equation system:

$$\left.\begin{aligned} E(f_1 f_1)c_1 + \ldots + E(f_1 f_m)c_m &= E(f_1, M(D)) \\ \vdots \qquad\qquad\qquad \vdots \qquad\qquad &\vdots \\ E(f_m f_1)c_1 + \ldots + E(f_m f_m)c_m &= E(f_m M(D)) \end{aligned}\right\} \tag{54}$$

where $E(xy) = \alpha(x,y) + E(x)E(y)$.

Constants appearing in estimator 3 are calculated from the equation system:

$$\left.\begin{array}{l} \alpha(f_1,f_1)c_1 + \ldots + \alpha(f_1,f_m)c_m + \lambda = \alpha(f_1,M(D)) \\ \vdots \qquad\qquad\qquad \vdots \qquad\qquad \vdots \\ \alpha(f_m,f_1)c_1 + \ldots + \alpha(f_m,f_m)c_m + \lambda = \alpha(f_m,M(D)) \\ c_1 + \ldots + c_m = 1 \end{array}\right\} \tag{55}$$

where λ is an indeterminate Lagrange factor.

Errors of the estimators 1, 2, 3, and 4 are calculated from the following equations:

$$s_1^2 = \begin{vmatrix} \alpha(f_1,f_1) & \ldots & \alpha(f_1,f_m) & \alpha(f_1,M(D)) \\ \vdots & & \vdots & \vdots \\ \alpha(f_m,f_1) & \ldots & \alpha(f_m,f_m) & \alpha(f_m,M(D)) \\ \alpha(f_1,M(D)) & \ldots & \alpha(f_m,M(D)) & \alpha(M(D),M(D)) \end{vmatrix} \cdot \cdot \begin{vmatrix} \alpha(f_1,f_1) & \ldots & \alpha(f_1,f_m) \\ \vdots & & \vdots \\ \alpha(f_m,f_1) & \ldots & \alpha(f_m,f_m) \end{vmatrix} \tag{56}$$

$$s_2^2 = \begin{vmatrix} E(f_1f_1) & \ldots & E(f_1f_m) & E(f_1M(D)) \\ \vdots & & \vdots & \vdots \\ E(f_mf_1) & \ldots & E(F_mf_m) & E(f_mM(D)) \\ E(f_1M(D)) & \ldots & E(f_mM(D)) & E(M(D)M(D)) \end{vmatrix} \cdot \cdot \begin{vmatrix} E(f_1f_1) & \ldots & E(f_1f_m) \\ \vdots & & \vdots \\ E(f_mf_1) & \ldots & E(f_mf_m) \end{vmatrix} \tag{57}$$

$$\begin{aligned} s_3^2 = \; & c_1 \{c_1\alpha(f_1,f_1) + \ldots + c_m\alpha(f_1,f_m) - \alpha(f_1,M(D))\} \\ & + c_m \{c_1\alpha(f_m,f_1) + \ldots + c_m\alpha(f_m,f_m) - \alpha(f_m,M(D))\} \\ & - \{\alpha(f_1,M(D)) + \ldots + \alpha(f_m,M(D)) - \alpha(M(D),M(D))\} \end{aligned} \tag{58}$$

$$s_4^2 = \left\{ \frac{1}{m^2} m\sigma^2 + 2\sum_{i<j} \alpha(f_i, f_j) - 2m\sum_{i=i}^{m} \alpha(f_i, M(D)) + m^2 \alpha(M(D), M(D)) \right\} \quad (59)$$

where σ^2 is a variance of the random field f(p).

To calculate the constants $c_o, \ldots, c_m$, in estimator 1, it is sufficient to know the correlation function of the random field and its expected value $E(f_i)(i = 1, \ldots, m)$. For $c_1, \ldots, c_m$, in estimator 2, it is sufficient to know the correlation function of the random field and the ratio M/σ. For $c_1, \ldots, c_m$, in estimator 3, it is sufficient to know only the correlation function of the random field. The errors of the estimators 1,2,3, and 4 are also based on the correlation functions of the random field.

It is shown that the worst of the linear estimators are estimators 1 and 2, and that the best of all estimators are estimators 3 and 4. For calculation of the mean (41) we recommend first of all the use of estimator 4, which will be called the arithmetic mean. Its calculation is very simple, as is the calculation of the error of this estimator.

Note the important role of correlation functions in these calculations. Correlation functions can also be used to measure the variation in the parameter of fabric filtration being studied. The correlation function is calculated from empirical data. Let $f_1, \ldots, f_m$ be measurements of the random field at points $p_1, \ldots, p_m$ belonging to set D. Let t be a parameter of the random field, i.e. an argument of the correlation function R(pq) = R(t). Let us assume that values of the parameter t, namely $t_1 < t_2 < \ldots < t_s$, are known. Let us group the measurement set $f_1, \ldots, f_m$ into subsets of $(f_{i1}, f_{j1}), \ldots, (f_{is}, f_{js})$ pairs. We will calculate the correlation coefficient of the random variables f_{ik}, f_{jk}, obtaining $\rho_k = \rho(t_k)$ $(k = 1, \ldots, s)$. Values $\rho_1, \ldots, \rho_s$ are equated with the help of known functions of correlation of a random field. It can be shown that the following classes of functions:

$$R(t) = \exp\left(- A\, t^{2^{-k+1}}\right) \quad (60)$$

and

$$R(t) = \frac{1}{1 + At^{2^{-k+1}}} \tag{61}$$

where $A > 0$; $k = 0, 1, \ldots$ are correlation functions of stationary random fields and, in the broad sense, isotropic. From the classes of these functions, the correlation function that best describes the parameters of the filtration process will be chosen by the Gauss least squares method. Q is minimized in the formula:

$$Q = \frac{1}{s} \sum_{\substack{r=1 \\ (i=1,2)}}^{s} [\rho_r - R_i(t_r)]^2 \tag{62}$$

From the classes of functions (60) and (61) we should choose the best one. The function that best matches the empirical data (the best correlation function of the random field) $\rho_1, \ldots, \rho_s$ is the function for which Q in formula (62) is the smallest.

In the classical minimization problem, analogous to (62), the two sides of the formula are partially differentiated with respect to A and k and the derivatives are equated to zero. This yields a set of two linear equations with two unknowns. In our case this method of proceeding is impossible. We will minimize formula (62) by trial and error.

Let us pick an arbitrary k value. We calculate values of the constant A for $t_1, \ldots, t_s$ from equation (60). The minimization of function (61) is analogous to the one described below.

From all values $A_1, \ldots, A_s$ obtained for $t_1, \ldots, t_s$ from function (60) pick the smallest value and the largest value. Denote the smallest value by a and the largest by b. Now, the interval [a,b] will be subdivided and ordered by values $a_1 < a_2 < \ldots < a_m$. Using formula (62) we calculate the Q corresponding to each a_i, using the same arbitrary k for all calculations. Among the set of Q values corresponding to $a_1, \ldots, a_m$, there is a smallest value. Let that value be a_{min}. The value a_{min} belongs to the interval $[a_{-1}, a_{+1}]$. Now, this interval will be divided into m parts and formula (62) will be used to calculate Q for these m points. We choose the smallest Q value from this set. Repeating the operation as long as it is necessary, we

obtain the value $A_0(k)$ for which Q in formula (62) is the smallest for that specific k. Repeating the procedure for all k = 0,1,... we choose the pair A_0 and k_0 from the value $A_0(k)$ for which Q in formula (62) is the smallest. In this way we calculate the best correlation of the random field. It appears that this calculation method is more precise than verification criteria of probability distributions.

Now, we will discuss the problem of sampling. Random field theory sampling theory is different than sampling according to classical statistics. It is more complete and precise than in classical statistics. In classical statistics there is no problem of the optimum sample. Here this problem can solved. In classical statistics, the sample is a random sample so the measurements are chosen to be independent. Generally it is recommended that the distributions of these random variables be equal and normal. So we do recognize a probability distribution that is approximately normal. In random field theory, it is possible to distinguish an approximately-normal distribution.

Below we formulate the problem of the optimum sample. It has already been ascertained that the arithmetic mean is a "good" one. The random sample is assigned as follows. Set D is established on the unfolded fabric. From this set we choose randomly (that is, with the same probability, according to a monotonic probability distribution) m independent points, obtaining $p_1, \ldots, p_m$. At these points we measure the values of the random field, f(p). The set of values $f(p_1), \ldots, f(p_m)$ constitutes the random sample.

The stratified sample is obtained as follows. The set D is divided into congruent subsets $\Delta_1, \ldots, \Delta_m$ called strata. From each stratum we choose a point at random, obtaining $p_1, \ldots, p_m$. At each point p_i, we measure the value of the random field f(p), obtaining values $f(p_1), \ldots, f(p_m)$, which constitute the stratified sample.

Let the interval $\Delta_1, \ldots, \Delta_m$ from set D be given and the sets $\Delta_1, \ldots, \Delta_m$ be congruent. From set Δ_1 we choose at random one point p_1. From set Δ_i we choose the point p_i, so sets Δ_1 and Δ_i, after displacement of the vector p_1p_i, will overlap. At points p_i (i = 1, ..., m) we measure values of the random field f(p) obtaining $f(p_i), \ldots, f(p_m)$ as the systematic sample.

We have described above the ways of obtaining the three basic samples used in experimentation. The statistical data collected and verified in this project were obtained using these samples and especially the optimal samples.

Let

$$M_1 = \frac{1}{m} \sum_{j=1}^{m} f(p_j) \tag{63}$$

be the arithmetic mean obtained using random samples;

$$M_2 = \frac{1}{m} \sum_{j=1}^{m} f(p_j) \tag{64}$$

be the arithmetic mean obtained using stratified samples, and

$$M_3 = \frac{1}{m} \sum_{j=1}^{m} f(p_j) \tag{65}$$

be the arithmetic mean obtained using systematic samples. Let us call

$$s_1^2 = E[M(D) - M_1]^2 \tag{66}$$

the variance of the mean estimator (41), using the arithmetic mean M_1 obtained from the random sample;

$$s_2^2 = E[M(D) - M_2]^2 \tag{67}$$

the variance of the mean estimator (41) using the arithmetic mean M_2 obtained from the stratified sample; and

$$s_3^2 = E[M(D) - M_3]^2 \tag{68}$$

the variance of the mean estimator (41) using the arithmetic mean M_3 obtained from the systematic sample.

The above theorems are proven below.

1. Equality

$$s_1^2 = \frac{1}{m} [\sigma^2 - D^2 (M(D))] \tag{69}$$

occurs in the arbitrary set D.

2. If set D can be divided into separable congruent subsets $\Delta_1, \ldots, \Delta_m$ or if the random field f(p) is stationary and in the broad sense isotropic, and set D can be divided into separable similar subsets $\Delta_1, \ldots, \Delta_m$, then

$$s_2^2 = \frac{1}{m}\left[\sigma^2 - D^2(M(\Delta_1))\right]. \tag{70}$$

3. If set D is a sum of separable congruent subsets $\Delta_1, \ldots, \Delta_m$, then

$$s_3^2 = \frac{\sigma}{m^2} \sum_{i=1}^{m} \sum_{j-1}^{m} R(\overrightarrow{p_i p_j}) - D^2(M(D)) \tag{71}$$

where p_i is a center of gravity of the subset Δ_i ($i = 1, \ldots, m$).

In formulas (69), (70), and (71), σ^2 represents the variance of the random field f(p); $D^2(M(D))$ is the variance of the mean (41) in set D; $D^2(M(\Delta_1))$ is the variance of the mean (41) in set Δ_1; and $R(\overrightarrow{p_i p_j})$ is the correlation coefficient of the random variables $f(p_i)$, $f(p_j)$ (values of the correlation function).

The formulas (69), (70), and (71) give us errors of estimation of the mean (41) with the help of the arithmetic mean obtained using random, stratified and systematic samples. Notice that for solution of the problem of optimal sampling, it is sufficient to compare the variances (69), (70), and (71). The theorems below give this comparison.

4. If set D is a sum of separable congruent subsets $\Delta_1, \ldots, \Delta_m$, or if the random field f(p) is stationary and in the broad sense isotropic, and subsets $\Delta_1, \ldots, \Delta_m$ are similar, then

$$s_2^2 \leq s_1^2 \quad . \tag{72}$$

5. If set D is a sum of separable congruent subsets $\Delta_1, \ldots, \Delta_m$, then the condition

$$s_3^2 \leq s_2^2 \tag{73}$$

for each i and j leads to the inequality:

$$R(\overrightarrow{p_i p_j}) \leq \frac{1}{|\Delta_1|^2} \int_{\Delta_1} \left\{ \int_{\Delta_1} R(\overrightarrow{pq})\,dq \right\} dp \tag{74}$$

where p_i is the centroid of the subset Δ_1 and p_j is the centroid of the subset Δ_j. If relation (74) occurs in each set $\Delta' = \Delta_i \cup \Delta_j$ ($i \neq j$; $i, j = 1, \ldots, m$), then inequality (74) results.

Theorems 4 and 5 are the criteria making it possible to choose the best sample. From theorem 4 it follows that the worst sample is the random sample. From theorem 5 it follows that under known specific conditions, the best sample is the systematic sample. This theorem makes it possible to solve the problem of optimality of both the stratified and systematic samples. The problem of sample optimality can be solved quite easily when we deal with a random field that is stationary and isotropic. These kinds of fields describe fabric filtration. In this case it is sufficient to examine the correlation function of this field $R(\vec{pq})$ and to find the diameter of the set in which $R(\vec{pq})$ is underdamped so as to ascertain that, for a set of this specific diameter, the stratified sample is worse than the systematic one. If the correlation function is underdamped, the stratified sample is worse than the systematic one. If the correlation function is overdamped the stratified sample is better than the systematic one.

It also appears that the stratified sample is the best for sets D of small diameters. The term "small diameter" is not the same for each parameter or for each fabric. It depends on the correlation function of the random field. But it can be proven that when the area of the fabric is not bigger than 2 m^2 and the set D is not a zone of diameter smaller than 10 cm, the diameter of this set is small. A set has big diameter when it is bigger than 10 m^2. But if its zone is smaller than 10 cm its area can be smaller. In the last case the systematic sample is better than the stratified one. These values of diameter were obtained from correlations between the velocity and pressure drop of clean air flow through fabrics.

We examined 16 kinds of fabrics of different raw materials and structure. We formed the correlation function for these two parameters

$$R(\vec{x}) = \exp[- A|\vec{x}|] \qquad (75)$$

where $\vec{x} = \sqrt{x^2 + y^2}$, $A > 0$ and is different for each fabric.

The other parameters influencing the filtration process should also be examined and incorporated into the correlation function. We have reason to suppose that the correlation functions will be similar to (75).

This model of fabric filtration has a descriptive character and should be considered preliminary. The statisitical methods used in the analyses of the empirical data also have a descriptive character. In the final report we will give the full mathematical-statistical description of this model and also the mathematical-statistical and literature background.

SECTION VII

STUDY OF FILTER MEDIUM PARAMETERS

INTRODUCTION

As proven in section IV, obtaining a specific collection efficiency from a specific initial aerosol state is possible only by selection of suitable filtration parameters or filtration medium structure parameters. Differences in the spatial composition of the filtration medium cause definite performance differences in the filtration process. They influence the dust collection efficiency, filtration resistance and also the ease of regeneration, the degree of filling the filtration medium with dust, etc.

For a long time, the description of nonwoven textile materials, assuming their homogeneity and isotropy, consisted of the following parameters:

- Elemental fiber diameter,
- Filtration layer thickness, and
- Porosity or packing (bulk) density.

These structural parameters of nonwoven materials have technological as well as physical character. Once they are specified a definite fabric structure is produced, but the filtration performance parameters of the fabric (dust collection efficiency and filtration resistance) are often independent of them.

Although the qualitative differences between fabrics (woven materials) have been studied and the effects of various technological parameters on their formation are known, the spatial structure of a fabric cannot be described in a physical sense. It is a result of the much more complicated spatial structure of woven materials as compared to nonwoven ones.

In woven materials, elemental fibers are not the only elements of the structure, although they do make up the structural units of the warps and fills, which are spatially arranged. In the case of double fabrics the spatial structure is even more complicated. Because of the heterogeneity of the yarn used for fabric production and also because of technological condi-

tions of production, woven filtration materials cannot be regarded as homogeneous and isotropic, but as heterogeneous and anisotropic.

According to the above statement, characterizing the structure of woven materials by porosity, diameter of pore and density of packing is not consistent with the basic assumptions of the DARCY equation; thus the applicability of the Darcy equation in its unmodified form is limited. Although specific values of porosity can be ascribed to individual elements of the structure of woven materials, structural variations do not allow such values to apply to the entire volume.

If the heterogeneity of fabrics is not taken into consideration, the analytical determination of porosity based on fabric thickness is subject to considerable error because of the voids between weave elements protruding above or below the bulk structure. This problem is illustrated in figure 4a.

Assuming that woven and non-woven materials are characterized by the same thickness, b, by the same weight per square meter, G, and the same specific gravity of materials, $\rho_{m1} = \rho_{m2}$, the packing density of the structure will be

$$\rho_{b1} = \rho_{b2} = G/b \quad (g/m^3). \tag{76}$$

Calculating the fraction of solids in the filter and the porosity, we have:

$$\alpha = \rho_b/\rho_m \tag{77}$$

and

$$\varepsilon = 1 - \alpha. \tag{78}$$

Denoting the true thickness of the woven material by b' (fabric thickness does not include the voids between weave elements), we have

$$\rho_{b'} = G/b' > \rho_{b1} = \rho_{b2}, \tag{79}$$

and the true mean porosity of the woven material is

$$\varepsilon' < \varepsilon. \tag{80}$$

The errors illustrated by this calculation depend on yarn thickness and type of weave.

The determination of the porosity of woven materials by using measuring methods needs additional definition of the kinds of pores that are important in the filtration process. An appropriate measuring method should be determined in advance. In some cases a description of woven materials by measure-

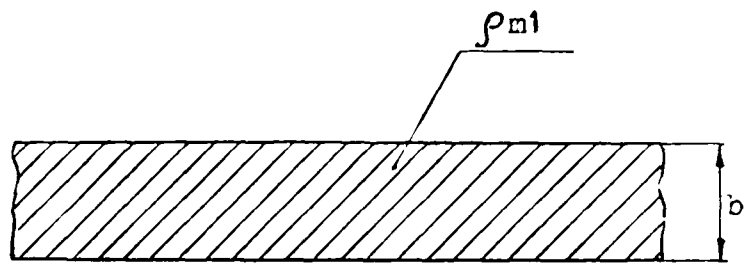

a. Non-woven material

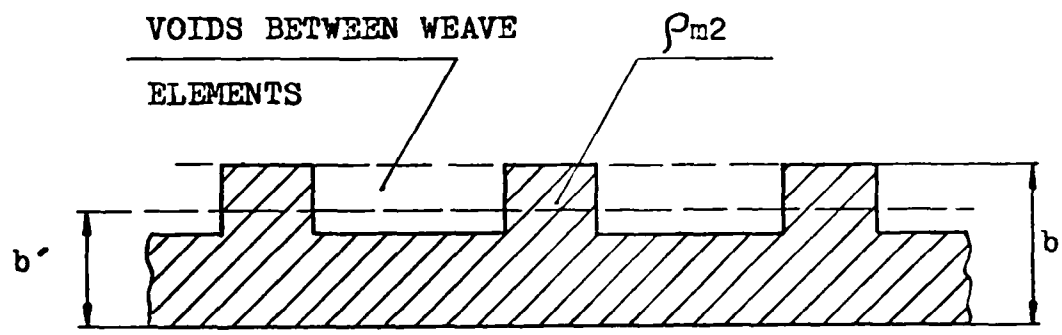

b. Woven material

Figure 4a. Geometrical Considerations Attributed to Fabric Structures.

ment of porosity or fraction of solids is valid, but these parameters are not analytically related to the technological parameters, which greatly limits their usefulness. Any parameter characterizing the structure of woven filtration materials should be related to the technological parameters of production.

To obtain adequate data, testing was conducted on 16 kinds of Polish fabrics instead of just 4 fabrics as originally planned. Fabric characteristics were included in the phase I report of this project. The testing included:

- Examination of hydraulic properties during clean air flow (laboratory experiments).
- Application of mathematical methods for estimating similarities or differences between materials on the basis of test results and technological parameters.
- Description of fabric geometric structure as a function of technological parameters.

CLEAN AIR FLOW THROUGH FILTRATION STRUCTURES

The phase I report of this project includes the results of fabric testing with clean air flow at two values of air-to-cloth ratio and the corresponding ranges of pressure drop:

- Low values of flow: $\Delta P = 0 - 10$ mm of water, and
- High values of flow: $\Delta P > 10$ mm of water.

Each flow and pressure drop was measured 30 times, so each reported value (phase I report) was the mean of 30 measurements. Mean values of air-to-cloth ratio for specific values of pressure drop are shown in table 27.

The mean and the standard deviation were estimated using the following relations:

$$q_{gm} = \frac{1}{n} \sum_{i=1}^{n} q_{g(i)} \tag{81}$$

$$\sigma = \frac{1}{n} \sqrt{\sum_{i=1}^{n} (q_{g(i)} - q_{gm})^2} \, . \tag{82}$$

The calculated values of the standard deviation are given in table 28. To verify the hypothesis of the normality of the q_g distribution, the Kolmo-

Table 27. CLEAN AIR FLOW THROUGH FABRICS

ΔP in mm H_2O	Air-to-Cloth Ratio q_{cm} in $m^3/m^2/min$ for fabric							
	ET-1	ET-2	ET-3	ET-4	ET-30	BT-57	WBT-208	WBT-210
1	2	3	4	5	6	7	8	9
5	5.09	7.98	3.01	5.79	2.25	3.17	6.50	6.65
10	9.39	13.66	7.02	10.83	4.35	6.87	12.85	13.18
20	16.66	23.60	13.08	19.33	8.10	13.04	23.77	23.52
30	21,56	32.16	19,31	26.04	10,92	18,09	34.42	33.32
40	29.44	38,55	23,72	33.51	13.70	22,94	42,59	41.01
50	35.32	45.83	29,39	39.80	16.69	29,04	51,54	49.41
60	40,56	60,41	35,03	48,59	19.62	34.61	63.70	60.40
70	45.99	54.16	39.61	53,08	22,19	38.41	71.22	68,47
80	52.47		43.74	55.20	24,38	42.97	79.23	74,86
90	58.15		49,39	58,67	26,35	47.57	86.84	81,97
100	59.09		52.63		30.13	50.51	94.85	88.58
110			55.78		32.22	53,11	102.58	94.77
120					34,01		112.58	103.29
130					36,24		118.19	110.10
140					39.37			115.92
150					40.53			
160					42,50			

Table 27 (continued)

1	2	3	4	5	6	7	8	9
170					42.50			
180					45.58			
190					47.80			
200					48.82			
	ST-41	ST-1	ST-13	BWA-1539	WT-201	WT-203	WT-204	WT-207
5	4.96	12.23	9.44	4.07	14.22	10.90	19.28	6.94
10	8.80	19.89	14.44	8.24	26.80	19.89	35.11	13.34
20	14.77	31.81	22.58	15.31	49.53	36.70	64.90	24.78
30	20.09	39.53	29.10	21.89	71.48	51.64	88.55	36.10
40	23.35	46.54	33.19	28.84	84.15	65.43	108.16	44.86
50	27.72	53.44	39.90	35.33	103.28	77.88	127.12	55.78
60	31.66	52.98	44.00	41.29	117.48	89.83		67.06
70	35.17		48.10	46.29		103.80		75.72
80	37.91		52.24	51.89		119.38		83.99
90	40.95		53.05	55.69				92.69
100	43.64		54.24					102.80
110	46.23							110.63
120	49.03							117.07

Table 27 (continued)

1	2	3	4	5	6	7	8	9
130	50.15							
140	51.13							
150	52.49							
160	52.24							
170	53,60							

Table 28. STANDARD DEVIATION IN THE AIR-TO-CLOTH RATIO (in $m^3/m^2/min$)

ΔP in mm H_2O	Kind of fabrics							
	ET-1	ET-2	ET-3	ET-4	ET-30	BT-57	WBT-208	WBT-210
1	2	3	4	5	6	7	8	9
5	0.28	1.04	0.59	1.21	0.39	0.84	0.54	0.31
10	0.99	0.75	0.99	2.29	0.82	1.04	0.61	1.13
20	1.21	0.53	1.71	3.12	1.07	1.98	1.81	0.80
30	0.96	0.42	2.58	2.82	1.45	2.25	1.65	1.31
40	2.56	0.40	2.84	5.24	1.84	2.29	1.85	2.07
50	1.74	0.39	3.53	5.32	2.05	2.54	2.63	1.65
60	2.47	0.48	3.71	6.53	2.57	1.95	2.68	2.74
70	2.61	0.27	3.82	8.20	2.69	2.80	2.39	1.85
80	4.11		4.75	5.28	3.06	3.29	2.91	2.21
90	4.20		4.80	3.73	2.30	3.97	2.99	3.24
100	3.18		4.34		3.76	4.31	3.59	2.56
110			4.54		4.30	2.96	4.08	4.46
120					4.94		5.75	3.44
130					4.82		4.06	3.94
140					3.96			2.09
150					2.00			
160					3.78			

Table 28 (continued)

1	2	3	4	5	6	7	8	9
170					2.46			
180					2,12			
190					3,74			
200					3.59			
	ST-41	ST-1	ST-13	BWA-1539	WT-201	WT-203	WT-204	WT-207
5	0,86	1.36	1,49	0.67	1,86	0.80	2.37	0.45
10	1,08	2,33	1,60	1.03	2,40	1,13	3,08	0,71
20	1,83	2,73	2.04	1,36	3,09	1,90	5.65	1.14
30	2,70	3.65	3,72	3.19	4.59	3.17	6,65	1.73
40	2,78	4.78	4,07	4.53	4.91	3,20	9.55	1,87
50	3.86	4.81	3.39	4.21	7,59	3.02	8.67	3.42
60	3.83	3.20	4.45	4,57	4.80	3.69		3.85
70	3.67		4,59	3,94		5,91		3,13
80	3.80		4.89	3.72		4.66		3.11
90	4,32		3.57	2,70				4.09
100	4.77		4.69					4.68
110	5.19							4.62
120	5,20							4.27

Table 28 (continued)

1	2	3	4	5	6	7	8	9
130	5.13							
140	4.63							
150	4.19							
160	3.90							
170	4.05							

gorov test was applied (small sample size, n = 30) at the probability level u = 0.2. The results of this test are shown in table 29. For all probability distributions except those at $\Delta P = 5$ no basis is found for rejecting the hypothesis of a normal distribution for q_g. Notice that $\Delta P = 5$, $\Delta P = 10$, ..., $\Delta P = 200$ are states of a stochastic process. The probability distribution defines the type of stochastic process. For individual fabrics, these processes are normal because their probability distributions are normal. It should also be noticed that q_{gm} and σ vary with ΔP, so we obtain a stochastic process with a density function as follows:

$$g\,[m(\Delta P)] = \frac{1}{\sigma(\Delta P)\,\sqrt{2\pi}} \exp \left\{ -\frac{[\lambda - m(\Delta p)]^2}{2[\sigma(\Delta P]^2} \right\} . \tag{83}$$

To determine the mathematical form of the relation $\Delta P = f(q_g)$, the fabric testing data at high values of flow were used. Using the method of least squares, it was found that a polynomial function of the second degree gave the best fit. The following expression was minimized:

$$Q = \frac{1}{n} \sum_{i=1}^{n} [y_i - f(x_i)]^2 \tag{84}$$

where y_i = empirical values of the variable ΔP, and

$f(x_i)$ = value of the function $f(q_g)$, the specific form of which depends on the number of parameters.

It was assumed that the functional relationship between $\Delta P = y$ and $q_g = x$ is a polynomial function of degree n in x. The possible specific forms were:

$$\begin{aligned} f(x) &= a_0 + a_1 x \\ f(x) &= a_0 + a_1 x + a_2 x^2 \\ f(x) &= a_0 + a_1 x + a_2 x^2 + a_3 x^3 \\ &\vdots \\ f(x) &= a_0 + a_1 x + \ldots + a_n x^n \end{aligned} \tag{85}$$

for $n \leq 21$ (because the number of measurements did not exceed 22).

Equation (84) was successively minimized for each f(x) in (85). By differentiation of equation 84, we obtained the sets of equations from

Table 29. RESULTS OF λ KOLMOGOROV TEST

Range of ΔP	Fabric															
	ET-1	ET-2	ET-3	ET-4	ET-30	BT-57	WBT-208	WBT-210	ST-41	ST-1	ST-13	BWA-1539	WT-201	WT-203	WT-204	WT-207
1	2	3	4	5	6	7	8	9	10	11	12	13	14	15	16	17
5	1	1	0	1	1	1	1	1	0	1	0	1	1	1	1	1
10	0	1	1	1	1	1	1	0	1	1	1	0	1	0	1	1
20	1	1	1	1	0	1	1	1	1	1	1	1	1	1	1	1
30	0	1	1	0	0	1	1	1	1	1	1	0	1	0	1	1
40	1	1	1	1	0	1	1	1	1	1	1	1	1	1	1	1
50	1	1	1	1	1	1	1	0	0	1	1	0	1	1	1	0
60	1	1	0	0	0	1	0	0	1	1	1	1	1	0		1
70	1	1	1	1	1	1	1	1	1		1	1		1		1
80	1		1	1	0	1	1	0	1		1	1		1		1
90	1		1	1	1	1	1	1	1		1	1				1
100	1		1		1	1	1	1	1		1					1
110			1		1	1	1	1	1							1
120					1		1	1	1							1
130					1		1	0	1							
140					0			1	1							
150					1				1							

Table 29 (continued)

1	2	3	4	5	6	7	8	9	10	11	12	13	14	15	16	17
160					1				1							
170					1				1							
180					1											
190					1											

1 - normal distribution

0 - non-normal distribution

which to estimate the parameters a_0, a_1, ..., a_n which minimize Q in equation 84. The total set of equations is:

$$\frac{\partial Q}{\partial a_0} = 0, \quad \frac{\partial Q}{\partial a_1} = 0, \ \ldots, \ \frac{\partial Q}{\partial a_n} = 0.$$

The parameters a_0 and a_1 for the first polynomial; a_0, a_1, and a_2, for the second polynomial, and so on were thus estimated and the corresponding sequence of values Q_0, Q_1, Q_2, ..., Q_n was obtained. According to the least squares method (the polynomial that best fits the empirical data is that for which the value of Q is the smallest), it was found that, for high velocity of flow, the best-fitting relationship was:

$$\Delta P = aq_g^2 + bq_g + c \tag{86}$$

where ΔP = pressure drop in mm of water,

q_g = air-to-cloth ratio in $m^3/m^2/hr$, and

a,b,c, = estimates of the parameters a_2, a_1, and a_0 respectively.

Using the relationship (86), it is possible to compare the functions and to group the fabrics into pairs with the most similar hydraulic properties. The quantity used to make this comparison is:

$$n_{ij} = \frac{1}{|x_n - x_o|} \sup F_{ij} \tag{87}$$

where $F_{ij} = y_i - y_j \quad i, j = 1 \ldots\ldots 16$

x_o = the smallest common value of the argument x,

x_n = the largest value of this argument for curves i and j.

The smallest values of n_{ij} define the fabrics that are most similar. The obtained pairs of most similar fabrics are shown in table 30.

The testing of fabrics at low velocity flow in the range $\Delta P < 10$ mm of water (see table 31) showed a linear relationship between velocity and ΔP (phase I report), which can be depicted analytically as:

$$\Delta P = aq_g + b, \tag{88}$$

where ΔP = pressure drop,

q_g = air-to-cloth ratio,

a,b = constants.

Table 30. SIMILARITY OF TESTED FABRICS

Range of η_{ij}	Pairs of most similar fabrics	
1	2	
0 - 5	ET-1 and ET-4	WBT-210 and WT-207
	BWA-1539 and ET-1	WBT-210 and WBT-208
	BWA-1539 and ET-4	ST-41 and ET-3
	BT-57 and ET-3	ST-41 and BT-57
	WBT-208 and WT-207	ST-13 and ET-4
5 - 10	ET-1 and ET-3	WBT-210 and ET-4
	ET-2 and ET-4	WBT-210 and ST-1
	BWA-1539 and ET-3	WBT-210 and WT-207
	ST-1 and ET-2	ST-41 and ET-1
	BT-57 and ET-1	ST-41 and BWA-1539
	BT-57 and ET-4	ST-41 and ET-30
	BT-57 and BWA-1539	ST-13 and ET-1
	WT-207 and ET-2	ST-13 and ET-2
	WT-207 and ST-1	ST-13 and BWA-1539
	WBT-208 and ET-2	ST-13 and WBT-210
	WBT-208 and ST-1	ST-13 and ST-41
10 - 15	ET-1 and ET-2	ET-30 and ET-3
	ET-3 and ET-4	ET-30 and BT-57
	BWA-1539 and ET-2	ST-41 and ET-4
	ST-1 and ET-4	ST-13 and ET-3
	WBT-208 and ET-4	ST-13 and ST-1
	WBT-210 and ET-1	ST-13 and BT-57
	WBT-210 and BWA-1539	ST-13 and WBT-208

Table 31. CLEAN AIR FLOW THROUGH FABRICS AT LOW VALUES OF PRESSURE DROP.

Type of filtration fabric	Air-to-Cloth Ratio, q_g in $m^3/m^2/min$, for pressure drop in mm of water								
	0.5	1.0	2.0	3.0	4.0	5.0	6.0	7.0	10.0
1	2	3	4	5	6	7	8	9	10
ET-1	0.436	1.00	2.37	3.47	4.78	5.94	6.88	8.00	10.89
ET-2	0.80	1.54	3.185	4.74	6.23	7.51	8.74	9.397	13.07
ET-3	0.42	0.74	1.38	2.27	3.03	3.74	4.693	5.50	7.396
ET-4	0.68	1.52	3.37	4.73	6.17	7.77	9.04	10.38	13.19
ET-30	0.218	0.42	0.76	1.07	1.54	2.01	2.44	2.81	3.97
BT-57	0.36	0.69	1.22	1.99	2.70	3.31	3.96	4.63	6.30
BWA-1539	0.32	0.56	0.95	1.61	2.14	2.68	3,12	3.68	5.41
WT-201	1.49	2.89	5.30	7.68	9.99	12.17	14.39	16.84	23.29
WT-202	0.70	1.08	2.15	3.10	4.04	5.08	6.13	7.049	9.89
WT-203	0.81	1.65	3.38	5.30	6.89	8.60	10.16	11.73	16.54
WBT-210	0.62	1.05	2.25	3.25	4.39	5.57	6.59	7.56	10.59
ST-13	1.61	2.84	4.98	6.57	8.03	9.30	10.48	11.55	12.25
ST-1	1.56	2.67	4.96	6.93	8.80	10.38	11.88	13.36	17.30
ST-41	0.44	0.81	1.62	2.55	3.25	4.02	4.82	5.61	7.49

The coefficients a and b are shown in table 32.

The quantity by which similarity of linear characteristics is determined is the slope of the straight lines, which over this particular range of pressure drop, can group the fabrics according to similar hydraulic properties. As can be seen from tables 30 and 32, fabrics that are similar at low flow velocity did not always show the same similarity at higher flow velocities. This behavior of fabrics leads to the conclusion that at higher flows and pressure drops there are structural changes influencing the values of permeability. The values of the standard deviation for selected ranges of pressure drop ΔP (see table 28) also show this effect of increasing q_g and ΔP.

The peculiarities of clean air flow through the test fabrics lead to the conclusion that the fabrics must be regarded not as stiff bodies but as elastic media. Mechanical properties such as elongation under the influences of force (elasticity) can play an important role in determining flow. Full confirmation of this statement requires further research.

Recapitulating the conducted experiments and theoretical studies, it can be concluded that:

- For clean air flow through woven filtration materials the functional relation $\Delta P = f(q_g)$ appears to be parabolic except for the initial flow range in which it appears to be linear.
- The flow of clean air through a woven structure is a stochastic process of the normal type. The change in functional form of $\Delta P = f(q_g)$, from linear to parabolic, is indicative of changing flow mechanisms (variation of flow type) at specific values of ΔP and q_g.
- The increasing σ values of the variable q_g accompanying the increase of ΔP indicate heterogeneity of structure, i.e., the increase of its deformation with increase in flow velocity is not uniform over the whole structure.
- From a physical viewpoint, woven filtration structures cannot be modeled as stiff bodies because of the observed structural variations.

Table 32. VALUES OF COEFFICIENT a and b FOR EQUATION 88

Type of filtration fabric.	Range of coefficient "a"	Value of coefficients	
		"a"	"b"
1	2	3	4
WT-201	0 - 0,5	0,44	-0,29
ET-1	0,5 - 1,0	0,89	-0,07
ET-2		0,76	-0,40
ET-4		0,73	-0,34
WT-203		0,60	-0,07
WBT-210		0,94	-0,08
ST-1		0,59	-0,84
ST-13		0,77	-1,53
ET-3	1,0 - 1,5	1,32	0,01
WT-202		1,02	-0,18
ST-41		1,32	-0,23
BT-57	1,5 - 2,0	1,57	-0,10
BWA-1539		1,87	0,03
ET-30	2,0	2,49	0,06

ESTIMATION AND COMPARISON OF SOME FABRIC PARAMETERS

The purpose of the following analysis is to find the common properties among (or the the differences between) the structures of the test fabrics based on their technological parameters and the use of statistical methods.

Based on 40 measurements of the metric number of the yarn of the fill and warp and of the number of threads in 10 cm, the following set of derivative parameters (based on known technological relations) was estimated:

- Dimension of inside FA between threads along warp, ko,
- Dimension of inside FA between threads along fill, kw,
- Diameter of warp, do,
- Diameter of fill, dw,
- Superficial packing with yarn, Zt,
- Relative warp packing, Zo,
- Relative fill packing, Zw,
- Complete packing of yarn in fabric along warp, Eo,
- Complete packing of yarn in fabric along fill, Ew,
- Free area, P,
- Free area per 100 cm^2, FA.

In the first phase of the statistical analysis, based on the χ^2 test, failure to reject the hypothesis of a normal probability distribution for the individual parameters of all fabrics was shown.

The next phase was the analysis of differences between, or common properties of, the test structures. Because of the large number of parameters analyzed, comparative analysis was judged to be of little value, and the Student t-test was applied, using the following formulas:

$$t_{ij} = \frac{m_i - m_j}{S_{ij}} \tag{89}$$

where

$$S_{ij} = \sqrt{\frac{n_i + n_j}{n_i n_j}} \sqrt{\frac{n_i \sigma^2 + n_j \sigma^2}{n_i + n_j - 2}} \tag{90}$$

where m_i, m_j = the average of the individual parameters in fabrics i and j ($i \neq j$; i,j = 1, 2, 3, ...),

n_i, n_j = sample sizes,

σ_i, σ_j = standard deviations.

From these calculations, t-Student statistics for the individual parameters were obtained. Because n > 30, the following interpretation of the t-Student criterion was used:

when t < 4, the fabrics do not differ significantly with respect to the test parameter,

when t > 4, the fabrics differ significantly with respect to the test parameter.

Based on the indicated values of t, we drew the following conclusions:

1. According to kw, the following fabrics are similar:
   - ET-3 and WT-203 (t = 1.016)
   - ET-1 and WBT-208 (t = 0.208)
   - WT-207 and WT-203 (t = 3.382)
   - all others differ significantly.
2. According to ko, the following fabrics are similar:
   - ET-30 and WT-203 (t = 1.766)
   - ET-3 and BWA-1539 (t = 3.236)
   - ET-4 and ST-41 (t = 0.095)
   - all others differ significantly.
3. According to dw, the following fabrics are similar:
   - ET-1 and ET-2 (t = 3.196)
   - ET-1 and ET-4 (t = 3.329)
   - ET-2 and ET-4 (t = 1.065)
   - ST-1 and ST-13 (t 2.163)
   - ST-1 and ST-41 (t = 0.363)
   - ST-13 and ST-41 (t = 3.247)
   - all others differ significantly.
4. According to do, the following fabrics are similar:
   - ET-3 and ET-1 (t = 1.187)
   - ET-2 and WT-203 (t = 1.838)
   - ST-1 and ST-41 (t = 2.997)
   - all others differ significantly.

5. According to Zt, the following fabrics are similar:
   ET-30 and WT-203 (t = 1.541)
   BWA-1539 and ET-4 (t = 0.696)
   ET-2 and WBT-208 (t = 0.505)
   all others differ significantly.
6. According to Zw, the following fabrics are similar:
   ET-30 and WBT-208 (t = 2.727)
   BT-57 and WT-201 (t = 2.209)
   ET-4 and WT-203 (t = 2.435)
   all others differ significantly.
7. According to Zo, the following fabrics are similar:
   ET-1 and BWA-1539 (t = 1.617)
   BT-57 and ST-41 (t = 1.344)
   WBT-208 and WBT-210 (t = 0.550)
   ST-1 and ST-41 (t = 2.683)
   all others differ significantly.
8. According to Ew, the following fabrics are similar:
   ET-30 and ET-3 (t = 3.957)
   ET-30 and WT-203 (t = 1.145)
   ET-3 and WT-203 (t - 1.225)
   ET-1 and WT-207 (t = 2.427)
   ET-4 and WBT-208 (t = 1.239)
   all others differ significantly.
9. According to Eo, the following fabrics are similar:
   ET-1 and ST-13 (t = 0.257)
   BT-57 and ST-1 (t = 0.791)
   BWA-1539 and WT-203 (t = 0.062)
   all others differ significantly.
10. According to P, the following fabrics are similar:
   ET-30 and ET-3 (t = 3.261)
   ET-30 and ET-1 (t = 3.886)
   ET-3 and ST-13 (t = 0.583)
   ET-1 and BWA-1539 (t = 0.390)
   ET-1 and WT-207 (t = 3.051)
   ET-2 and ST-41 (t = 0.172)
   all others differ significantly.

11. According to FA, the following fabrics are similar:

ET-30 and WT-203 (t = 1.477)

ET-3 and ET-1 (t = 1.707)

BWA-1539 and ET-2 (t = 2.950)

WBT-208 and WT-201 (t = 0.610)

WBT-208 and ST-13 (t = 3.356)

all others differ significantly.

Assuming the equivalence of all test parameters, the hypothesis can be made that those fabrics showing the largest number of common properties are the most similar. By this criterion the following classification, at different levels of similarity, was obtained

First Level of Similarity

ET-30 and WT-203

Second Level of Similarity

ST-1 and ST-41

Third Level of Similarity

ET-30 and ET-3

ET-3 and ET-1

ET-3 and WT-203

ET-1 and ET-30

ET-1 and WT-207.

Analyzing the influence of the measured parameters of filtration structure on the levels of similarity, it was shown that FA (Free Area) showed the best correlation. The values of FA for the indicated levels of similarity are as follows:

First Level of Similarity	
ET-30 and WT-203	FA = 6.07 and FA = 6.44
Second Level of Similarity	
ST-1 and ST-41	FA=28.02 and FA = 23.58
Third Level of Similarity	
ET-30 and ET-3	FA = 6.07 and FA = 1.86
ET-3 and ET-1	FA = 1.86 and FA = 2.79

ET-3 and WT-203	FA = 1.86 and FA = 6.44
ET-1 and BWA-1539	FA = 2.79 and FA = 8.29
ET-1 and WT-207	FA = 2.79 and FA = 3.37

Statistical analysis of the technological structural parameters leads to the conclusions that from a statistical point of view, the best parameter for characterizing the effect of technological parameters on fabric structure is FA (Free Area). Also, further research should be performed to explain the nonrepresentative values of FA characterizing clean air flow through continuous filament fabrics. (These values were measured during the testing of U.S. fabrics during phase I of project 5-533-4.)

TESTING OF FABRIC GEOMETRY

The above results of the statistical analysis of the effects of technological parameters on fabric structure served as the inspiration for developing measurements research capable of reconstructing the geometry of fabrics. This research will be finished in 1977 and the results will be included in the final report.

CONCLUSIONS

- Filtration fabrics can be regarded as porous, heterogeneous anisotropic media.
- Because of the mechanical properties of the material (e.g., fiber, yarn) the physical model cannot be approximated by a stiff body.
- The process of clean air flow through fabrics is stochastically normal.
- From a statistical viewpoint FA (Free Area) is at present the best physical parameter for incorporating the technological parameters which determine the spatial geometry of fabrics.
- Continuous filament fabrics display a different functional form of $\Delta P = f(FA)$ than staple fiber fabrics.

SECTION VIII

STUDY OF DUST PARAMETERS

INTRODUCTION

Fabric filters, tested with similar fractions of different kinds of dust, show differences in filtration resistances and efficiencies. It can be presumed that the kind of dust (the type of raw material making up the dust), its aerosol state, and the specific filtration parameters determine the forces between the particles and the filtration structure and also between individual particles. In our research, we point out the dominant character of electrostatic forces.

Our observations lead to the conclusion that while dust layers are usually regarded as heterogeneous, quasi-isotropic media, the dust cake formed on the filtration structure is an anisotropic medium. The anisotropy of the dust cake is caused by the presence of local variations in gas velocity in front of the filtration surface. These local variations contribute to the separation effects and give rise to dust layers with unidirectional isotropy.

Consequently, the development of theoretical expressions based on geometrical models that are multidirectionally symmetrical, result in descriptions which are not confirmed by experiment.

The dust cake problem is complicated because of the absence of practical methods for observing and measuring the structure of the dust cake. Attempts to prepare cross-sections of dust cakes formed during laboratory tests invariably suffer from displacement of dust particles during the preparation or handling of the cross-section. Random microscopic examination confirms the presence of dust particle separation caused by the effects of a specific fabric surface.

The work conducted under this project was originally concentrated on defining the relation between the degree of dispersion of the dust in the aerosol stream and the properties of the dust layer formed by this dust.

The degree of dispersion was described by the fraction less than an arbitrary value of diameter, d_{lim}, and MMD (d_{50}). Dust samples from a specific separation were fractionally analyzed and the corresponding surfaces measured. All empirical data obtained in phase I and phase II of the project were analyzed.

EQUIPMENT AND PROCEDURES

Two kinds of dust, cement and coal, were studied. Particle size distribution of the tested dusts was measured by use of the Bahco centrifugal separator and on the Sartorious sedimentation balance ($d < 5$ μm).

Identification of the stationary specific surface was done by the Establishment of Catalysis and Physics of Surfaces of the Polish Academy of Sciences in Cracow, using the BET apparatus and argon or krypton (for hydrated lime) as an adsorbent. Identification of the kinetic specific surface was done by IPWMB using LEA-NURSEA apparatus.

RESULTS AND DISCUSSION

Based on the test results shown in table 33, plots of the functions $S = f(M_d)$ and $S = f(d_{50})$ were made. They are shown in figures 5 and 6.

Measurements of the degree of dispersion were made from diagrams of the particle size distribution of the test dusts and by assumption of specific values. Particle size distributions are shown in figures 7 and 8.

Tests lead to the following statements:

- The stationary specific surface, being the total area of the dust sample covered by a monomolecular layer of adsorbent, is for all kinds of dusts and for all degrees of dispersion higher than the kinetic specific surface. The stationary specific surface depends on the kind of dust (raw material), and therefore on the surface structure of the dust particles (porosity of particles).
- The kinetic specific surface, being the total external surface without taking the pores of individual particles under consideration, is a value varying proportionally to the degree of dispersion of the particles in a suspended state.

From the above statements and applying statistical methods in interpreting the empirical data, the preliminary functional relation S = f(degree of

Table 33. COMPARISION OF DUST PARAMETERS.

Kind of dust and fraction	Average value of static specific surface in cm^2/g	Average value of kinetic specific surface in cm^2/g	MMD in μm	Part of fraction less than $d_{lim}=20\mu m$ in percent.
1	2	3	4	5
Cement:				
nonfractionated	-	7 082	22.00	48.0
fraction <5 μm	-	27 556	2.25	-
fraction<10 μm	-	19 429	4.80	100.0
fraction<20 μm	36 390 ± 1 280	11 952	6.50	99.7
fraction>20 μm	-	1 467	48.00	15.0
Coal:				
nonfractionated	-	7 423	30.00	40.0
fraction<10 μm	-	24 775	5.20	100.0
fraction<20 μm	63 950 ± 2 400	15 775	7.00	98.0
fraction<30 μm	-	11 007	10.00	78.0
fraction>30 μm	-	1 539	80.00	6.0

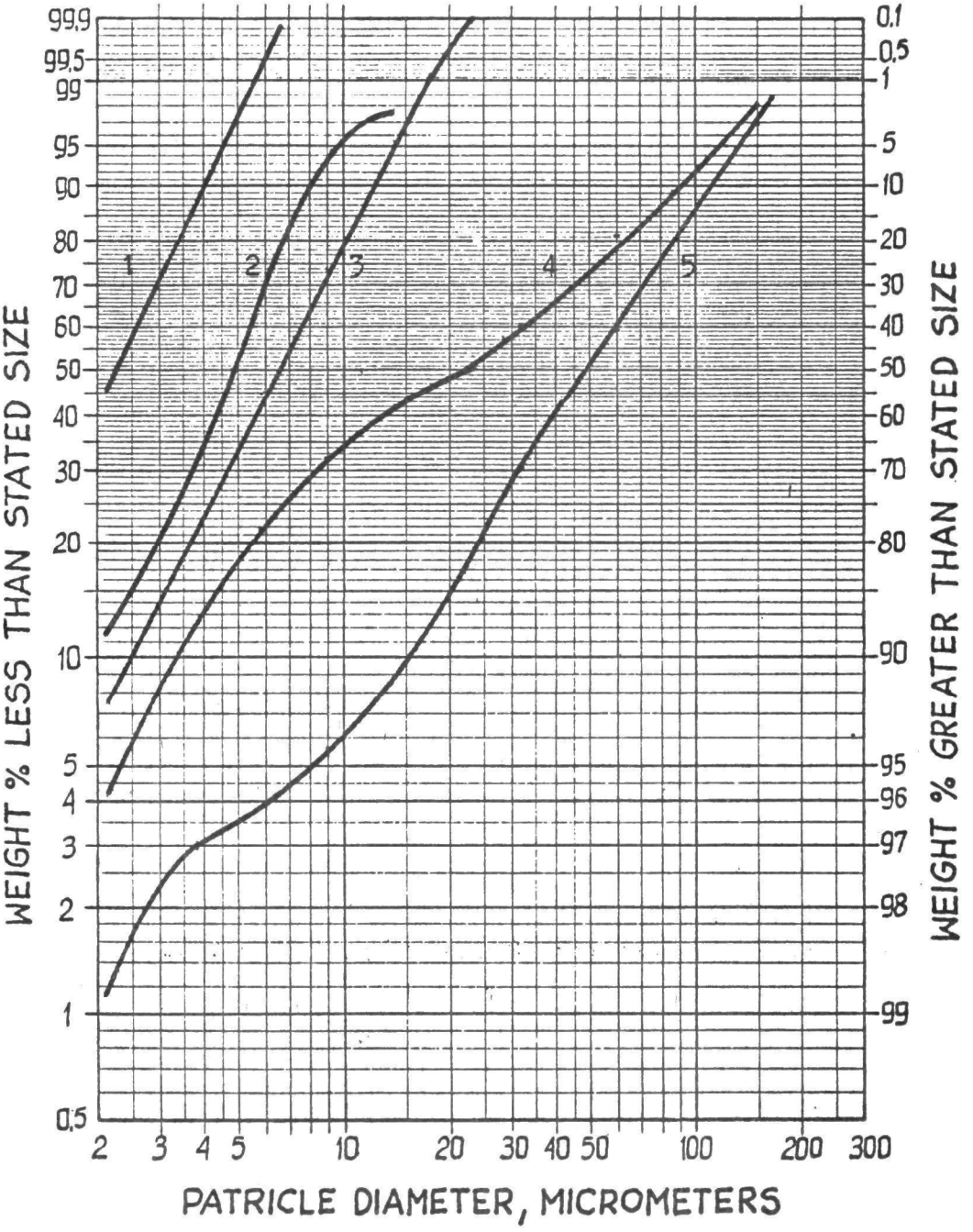

1 - Fraction $d_{lim} < 5\ \mu m$

2 - Fraction $d_{lim} < 10\ \mu m$

3 - Fraction $d_{lim} < 20\ \mu m$

4 - Nonfractionated

5 - Fraction $d_{lim} > 20\ \mu m$

Figure 5. Particle Size Distribution for Cement Dust.

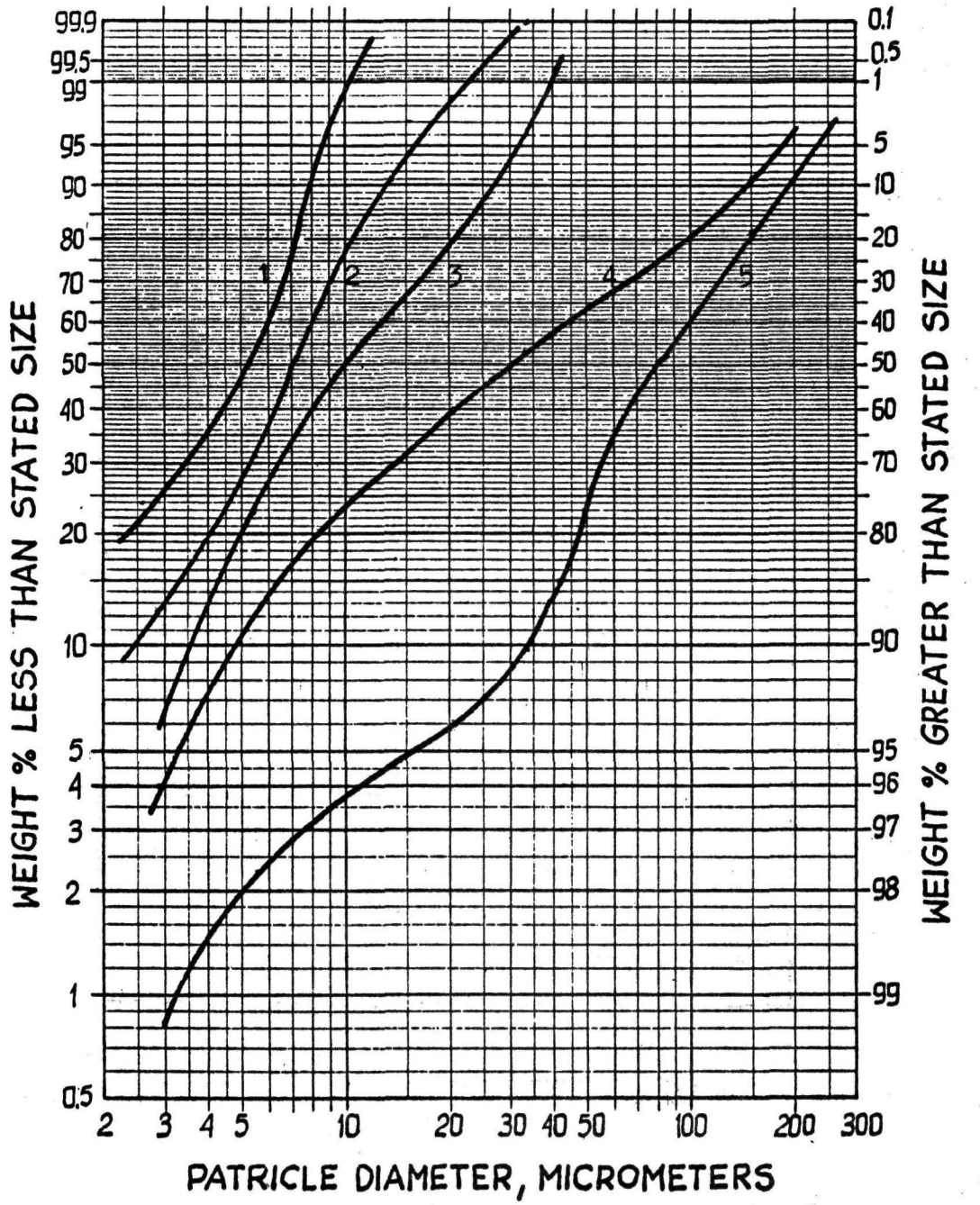

1 - Fraction $d_{lim} < 10$ μm

2 - Fraction $d_{lim} < 20$ μm

3 - Fraction $d_{lim} < 30$ μm

4 - Nonfractionated

5 - Fraction $d_{lim} > 30$ μm

Figure 6. Particle Size Distribution for Coal Dust.

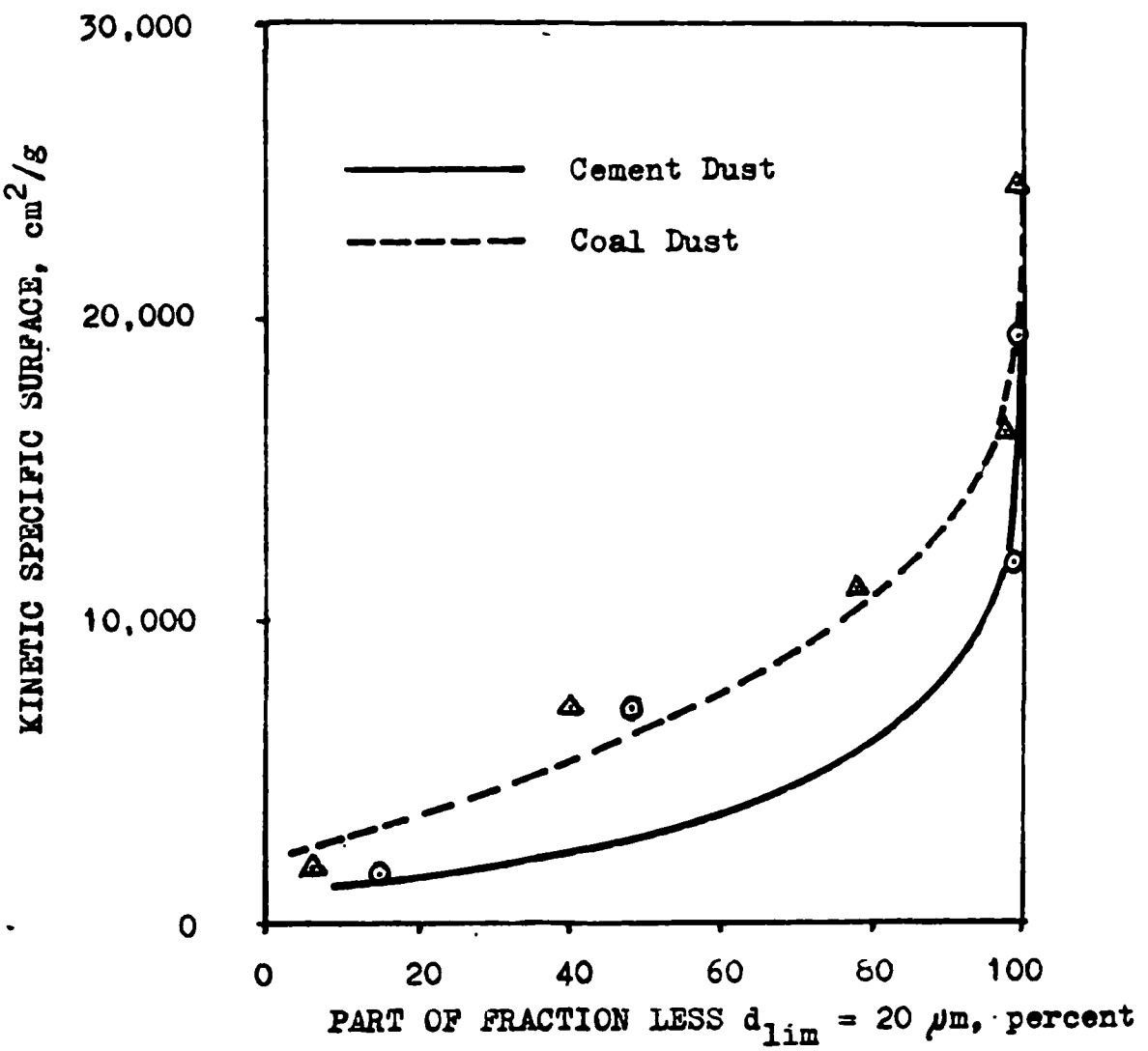

Figure 7. Dependence of Kinetic Specific Surface On Degree of Dispersion Measurement M_d.

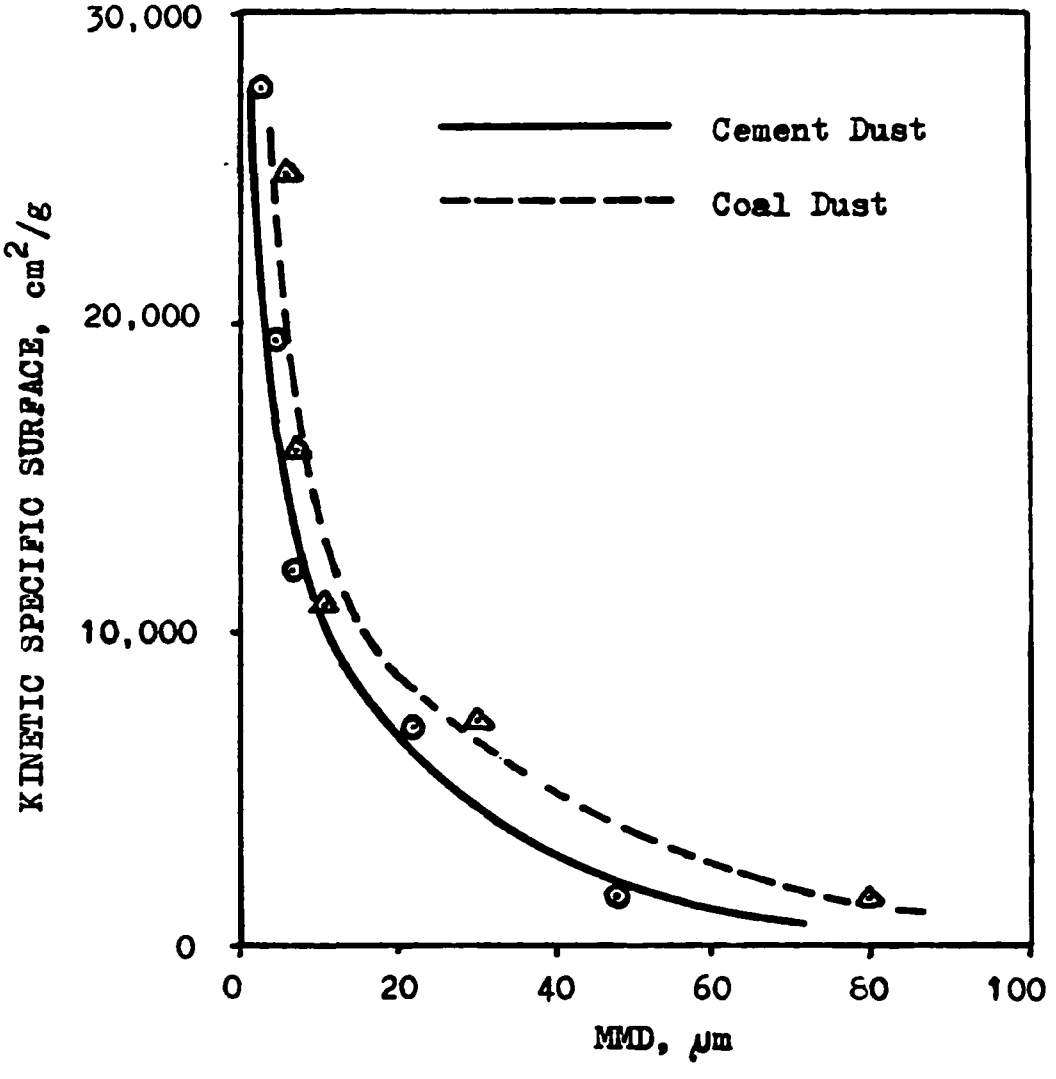

Figure 8. Dependence of Kinetic Specific Surface On Degree of Dispersion Measurement MMD.

dispersion) was developed. The degree of dispersion measurement, M_d (part of fraction less than d_{lim}, in percent), was obtained from the following type of dependence:

$$S = a\,(M_d)^b \tag{91}$$

where a, b = constants. The degree of dispersion measurement, d_{50} (MMD), was obtained from the following type of dependence:

$$S = a\,(d_{50})^{-b} \tag{92}$$

where a, b = constants.

The functions $S = f(M_d)$ and $S = f(d_{50})$ are similar for different kinds of dust; however, they have different values that exist probably because of differences in grain shapes. The testing of cement and coal dust conducted in this phase confirmed this supposition.

The ultimate verification of the hypothesis and the verification of the empirical relations will be done in phase III of this project using microscopic research.

CONCLUSIONS

- The best parameter for assessing degree of dust dispersion, according to these tests to characterize dust in a suspended state, is d_{50} (MMD).
- The dust layer parameter most closely related to the MMD of the dust sample in the suspended state is the kinetic specific surface.
- Development of the functional relation $S = f(d_{50})$ makes it possible to estimate the hydraulic properties of the dust layer from the degree of dust dispersion in the suspended state, defined by d_{50} (MMD).

SECTION IX

ELECTROSTATIC PROPERTIES OF DUSTS AND FABRICS

INTRODUCTION

Generation and concentration of electric charge are observed in many industrial processes in which contact, friction, milling, mixing, etc. occur in the flow of gas, liquid, or solid streams.

In most cases, the electrostatic phenomena accompanying industrial processes are not desirable, because they complicate the process operation, decrease the efficiency, or create the danger of explosion. Commonly recognized production problems exist in textile technology, cosmetics production, food-processing, and petrochemistry. One such problem is the electrification of parts of machines and devices that can lead to the concentration of electric charge, producing electric potentials of tens or hundreds of kilovolts. Although electrostatic phenomena have been known for hundreds of years, many peculiarities connected with static electrification are not yet explained.

The effect of electrostatic phenomena on the filtration process is pointed out in many scientific publications, but no complete description of it exists yet for the dust filtration process.

Based on the many years of experience of the Institute of Physics of Wroclaw Polytechnic on research into dust charging mechanisms, a cooperative project was established to determine the influence of electrostatic phenomena on the dust filtration process.

The research concentrated on the following problems:

- Determination of the natural charges on industrial dusts,
- Determination of the resistivity of dust layers,
- Determination of the electrostatic properties of fabrics,
- Determination of the kinetics of fabric charging during the flow of both clean and dusty air of specific properties, and
- Development of a preliminary physical model of the dust filtration process, including the effect of electrostatic phenomena.

The solutions to these problems required the development of suitable methods and programs. The basic experiments were conducted by the Institute of Physics of Wroclaw Polytechnic, managed by Dr. Anna Szaynok; also, other experiments of a statistical character were conducted by IPWMB.

EQUIPMENT AND PROCEDURES

Measurement of Dust Charges

Dust charges were measured by photographing the paths of dust particles falling between two vertical, charged capacitor plates. This method was first used by HOPPER and LABY to measure the charge of the elementary electron, and was next applied by KUNKEL and HANSEN to measure the electric charges of dust. The diagram of the apparatus is shown in figure 9. This apparatus includes a thermally isolated column, 1; parallel plate capacitor, 2; optical system, 3; Illumination system, 4; and a photographic camera, 5.

Dust particles are fed to the upper part of the column and then fall through the space between the vertically placed capacitor plates. The particles move under the influence of gravity, electric forces, and drag forces. Some of the particles pass through the d.c. electric field of the capacitor and are mapped onto the film of the photographic camera by the optical system. A diaphragm permits the use of dark field illumination. Illumination is chopped by a rotating disk containing small holes.

The images of the falling particles are registered in the form of consecutive light points on a dark background. The frequency of disk rotation is held constant for each measurement series, but it can be adjusted as desired. The apparatus is equiped with an extra optical system to obtain reference mapping on each negative, which is especially important in calculating the path deviation of the falling particles. For precise determination by enlargement, a glass scale is placed in the visual field before each measurement. After the scale is photographed, the capacitor is placed in the visual field, without changing the placement of the elements of the optical system. The resultant negatives are copied with the help of an enlarger so as to facilitate the measurement of particle path coordinates.

The diameter d_i and quantity of charge q_i of the i-dust particle are calculated from Stokes Law assuming a spherical particle:

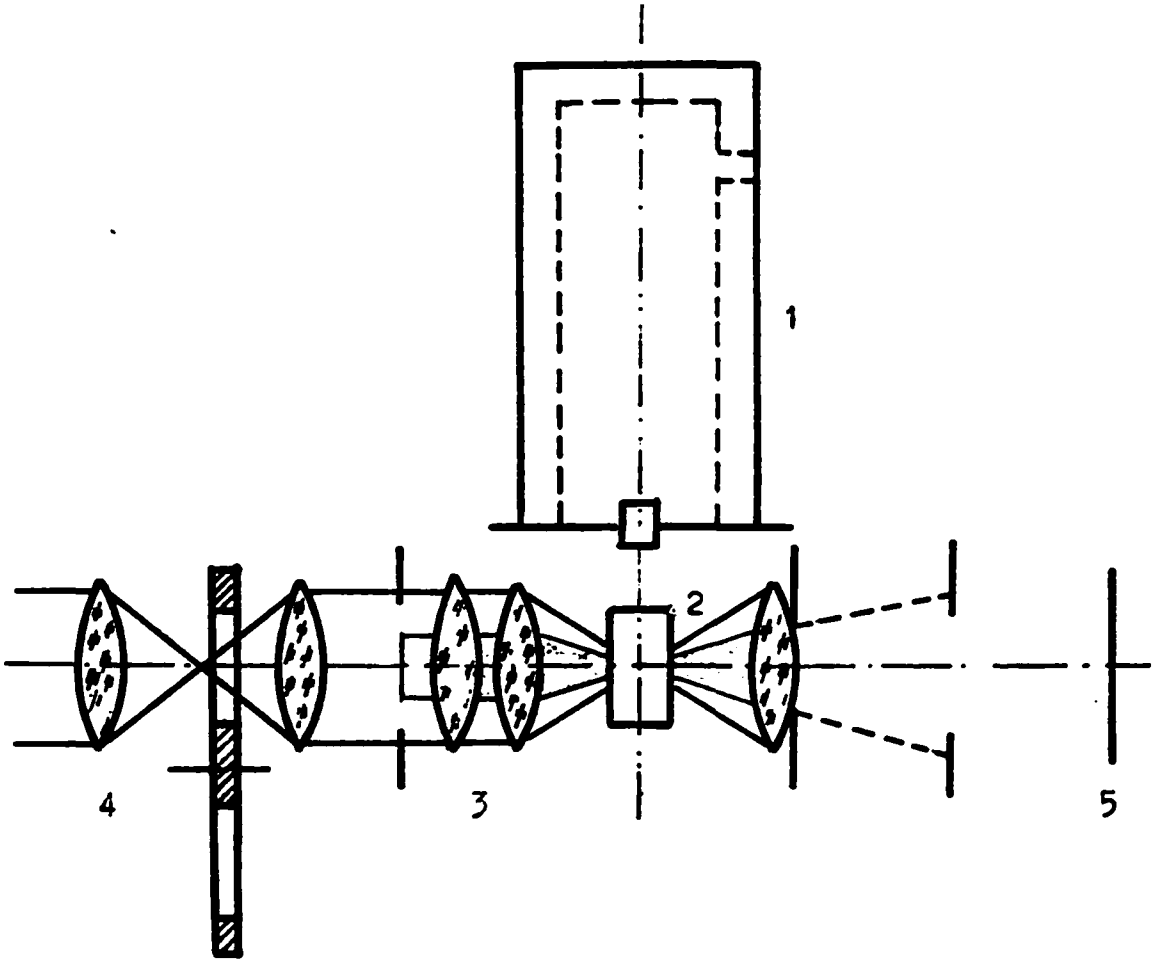

Figure 9. Diagram of Dust Charge Measurement.

$$d = \left[\frac{18\eta\ v_y}{(\rho_1 - \rho_2)\ g}\right]^{1/2} \tag{93}$$

$$q = \left[\frac{3\pi\eta\ v_x}{E}\right] d \tag{94}$$

where η = kinematic viscosity of air,

g = acceleration of gravity,

ρ_1 = density of dust material,

ρ_2 = air density,

E = intensity of electric field,

v_y = vertical component of particle velocity, and

v_x = horizontal component of particle velocity.

Components of particle velocity are calculated from the measurement of the distance between adjacent particle images on the photographs:

$$v_x = \frac{\upsilon}{p} X \tag{95}$$

$$v_y = \frac{\upsilon}{p} Y \tag{96}$$

where X = horizontal component of distance,

Y = vertical component of distance,

υ = illumination frequency,

p = enlargement.

To obtain reliable data, it is necessary to make the measurements on at least 1,000 dust particles. From measured values of charge it is possible to deduce a statistical charge distribution in the dust cloud and to calculate the average charge and standard deviation. The statistical charge distributions in the dust clouds are similar-normal distributions.

Study of Filter Fabric Electrical Resistivity

The measurements of filter fabric electrical resistivity were conducted using the ring-dot set of electrodes shown in figure 10.

The three measuring electrodes are: (1) the upper protected (the dot); (2) the lower; and (3) the protective ring. They are made of brass. The protective ring provides the required field homogeneity for measuring the bulk resistivity of the fabric and is also an outer electrode for measuring the surface resistivity.

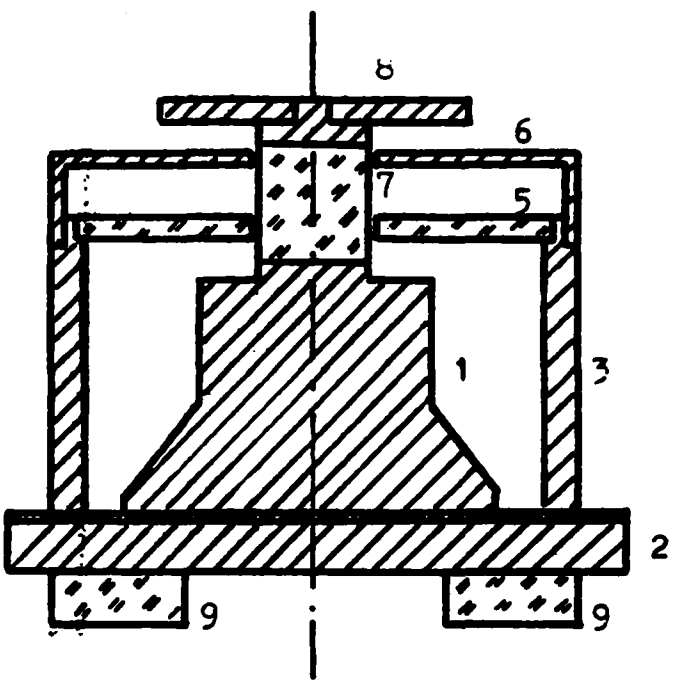

Figure 10. Electrodes for Measurement of Fabric Resistivity.

Elements (5), (7), and (9) of the electrode set are made of Teflon, a material characterized by very high electrical resistivity and by surface hydrophobicity, quaranteeing stable measuring conditions even under variable air humidity.

Weights of 1 to 10 kg of mass were placed on the weigh pan (8) in order to examine the effect of pressure on resistivity.

The measurement schemes for bulk and surface resistivity are shown in figure 11.

Both types of resistivities were measured with a type 219A electrometer produced by ZRK Unitra. It has a current range of 10^{-5} to 10^{-12} A and a measuring accuracy of 5 percent.

Bulk resistivity ρ_v and surface resistivity ρ_s were calculated from the relations:

$$\rho_v = R_v \frac{s}{d} \tag{97}$$

where ρ_v = bulk resistivity,
R_v = bulk resistance,
s = area of the protected electrode, and
d = thickness of the test fabric.

and $$\rho_s = R_s \frac{2\pi}{\ln r_1/r_2} \tag{98}$$

where ρ_s = surface resistivity,
R_s = surface resistance,
r_1 = inner radius of the ring electrode (protective ring), and
r_2 = radius of the dot electrode (the protected electrode).

Study of Dust Resistivity

Dust resistivity was measured in a chamber designed by the Institute of Physics of Wroclaw Polytechnic. The chamber permits measurement at a stable value of dust compression K.

$$K = 100\ \Delta V/V\ (\%) \tag{99}$$

where K = the compression ratio of the dust in percent,

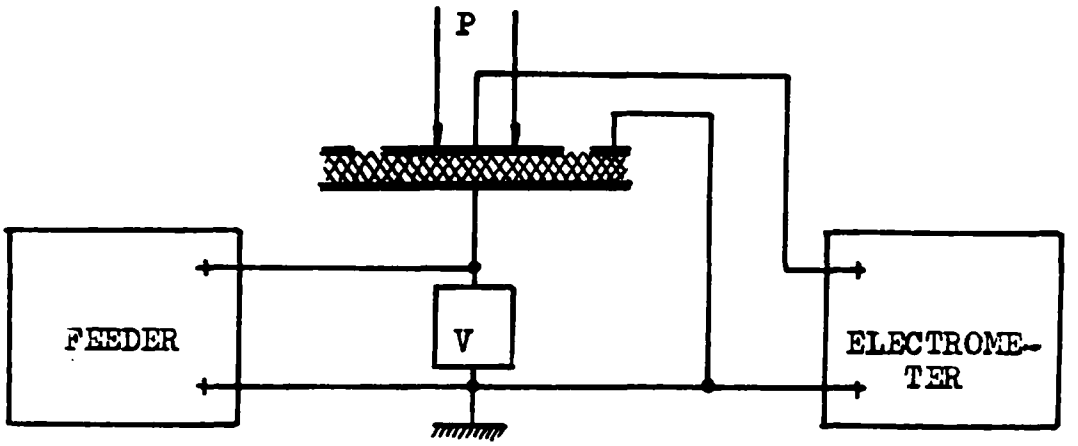

a. Measurement of Bulk Electrical Resistivity.

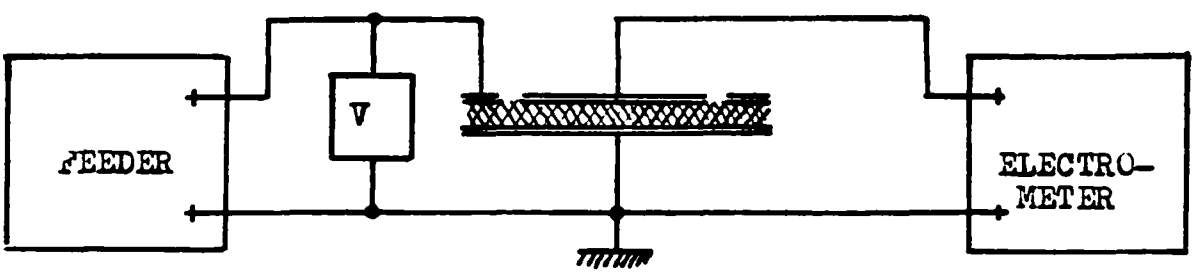

b. Measurement of Surface Resistivity.

Figure 11. Measurement Schematics for Fabric Electrical Properties.

ΔV = volume loss resulting from compression,

V = volume of the layer after compression.

Resistivity of the dust layer is evaluated by the formula:

$$\rho = R \frac{2\pi\ell}{\ln r_1/r_2} = RA \qquad (100)$$

where ρ= dust layer resistivity,

R = measured resistance of layer,

ℓ = length of dust layer,

r_1 = inner radius of ring electrode,

r_2 = radius of internal electrode (the dot), and

A = constant of the chamber.

A TO-2 megohm meter of Russian manufacture, with a range to 10^7 MΩ, was used for the measurements.

Study of Electric Charge Leakage From Fabrics

The system schematic is shown in figure 12. In the figure it is shown that a dc voltage, U = 100 V, from a constant-voltage supply, was connected to the protected electrode of the measuring capacitor K by turning on the switch W_1. The voltage was measured by the electrometer E. The electrometer was connected to the system through a coupling capacitor, C_o, which, together with the inlet capacity of the electrometer and the lead cable capacity, formed a capacitor voltage divider, dividing the voltage U into the ratio 1:33.3. The fabric was charged by the 100-V supply for 1 minute, and then the switch W_1 was turned off. From this moment on the capacitor K discharged through the fabric resistance.

The function U(t), describing the decrease of electrode voltage with time, was traced out on recorder R (type eKB produced in East Germany), which was connected to the outlet drive of the electrometer E. From the function U(t), a charge function Q(t) describing the time changes of charge on the fabric can be deduced from the relation Q = CU (where Q is charge and C is capacity).

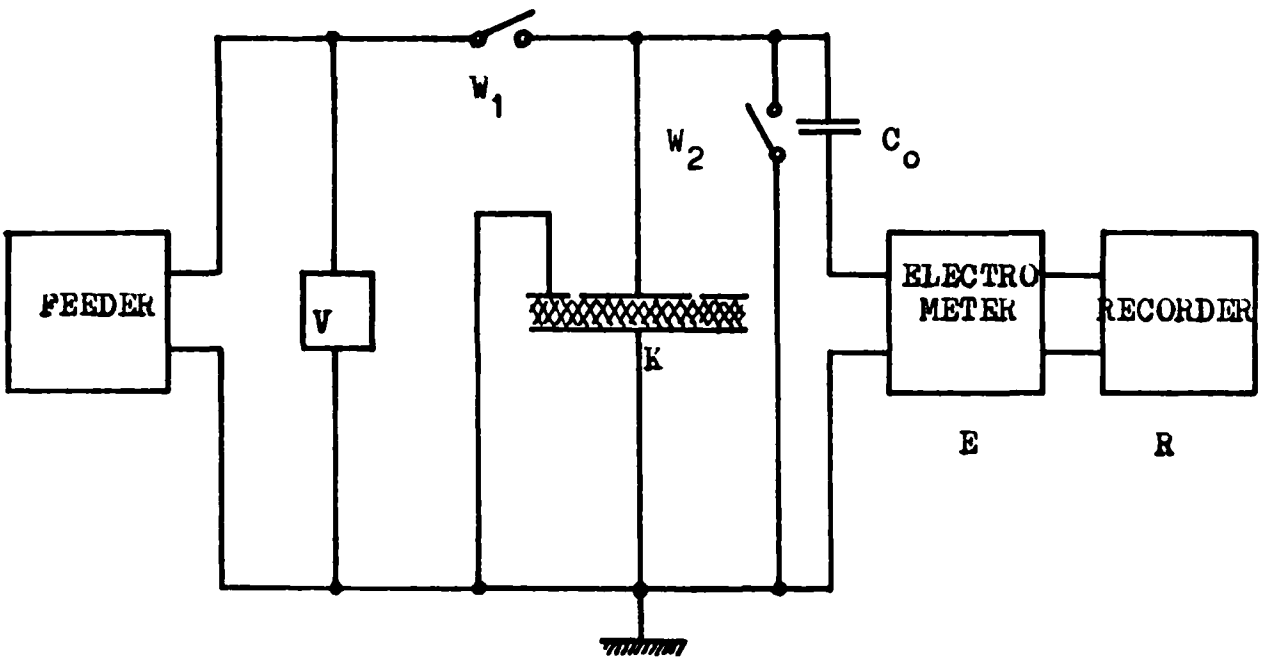

Figure 12. Measurement of Charge Decay Time.

From the Q(t) curves, it is possible to define a time, $t_{1/2}$, at which the charge on the fabric has decreased to half its initial value--the half decay time. Half decay time is a parameter describing the charge decay process. It is also used when the functions Q(t) or U(t) are not exponential.

For these measurements, a lamp electrometer of 10^{14} Ω input impedance (type 219A, produced by ZRK Unitra Poland) was used. A vibrating reed electrometer of input impedance greater than 10^{15} Ω (type VA-I-51 produced in East Germany) was also used.

RESULTS AND DISCUSSION

Dust Electrical Charge

Investigation of dust electrical charge was conducted by the Institute of Physics of Wroclaw Polytechnic using cement and coal industrial dusts.

The electrical charges on the non-fractionated dusts and also those on the following fractions of dusts were determined:

Cement dust 0 - 1.70 μm fraction I
1.70 - 2.94 μm fraction II
2.94 - 5.95 μm fraction III

Coal dust 0 - 2.46 μm fraction I
2.46 - 4.40 μm fraction II

Fractionation of the dust was done by the BAHCO centrifugal device. The results of charge measurements on non-fractionated cement dust are shown in table 34.

Table 34. CHARGES ON NONFRACTIONATED CEMENT DUST

Range of particle size in μm	d in μm	σ in e	q in e
1	2	3	4
4.80 - 8.40	6.31	72.5	-22
4.80 - 5.70	5.43	63.4	-20
5.70 - 6.70	6.12	70.1	-24
6.70 - 8.40	7.53	81.5	-27

The measurement includes dust particles in the range of diameter 4.80 - 8.40 μm. The standard deviation and average charge were calculated for the mean particle diameter of the entire sample and also for the three diameter size ranges shown.

The results for fractionated cement dust are shown in table 35.

Table 35. CHARGES ON FRACTIONATED CEMENT DUST

Fractions in μm	Range of particle size μm	d in μm	σ in e	q in e
0 - 1.70	4.40 - 7.90	5.60	100.5	+2
	4.40 - 5.00	4.87	73.0	+5
	5.00 - 6.00	5.44	92.2	0
	6.00 - 7.90	6.68	154.5	+5
1.70 - 2.94	4.70 - 9.99	6.75	100.8	-17.7
	4.70 - 6.50	5.67	81.5	-17
	6.50 - 9.00	7.76	115.5	-7
2.94 - 5.95	5.60 - 7.70	6.52	93.0	-6

The calculations conducted for the first fraction include the statistical distributions for all the data and for three ranges of particle size; for the second fraction, the calculations include all measurements and two ranges of particle size. The measurements of cement dust charging of the third fraction showed the least variation of particle size, so the statistical distribution of charge was made only for the entire sample. Plots showing particle charge dependence upon diameter for both the entire lot of cement dust and for the three fractions are shown in figures 13 and 14.

Additionally, measurements of the charges on non-fractionated cement dust exposed to an electrical discharge were made. Electrodes, between which the electrical discharge occurs, were placed above the capacitor of the measuring apparatus. The dust falling down the column passed through this discharge zone just before measurement. The results of these charge measurements are shown in table 36, and the relation between charge and diameter size is shown in figure 15.

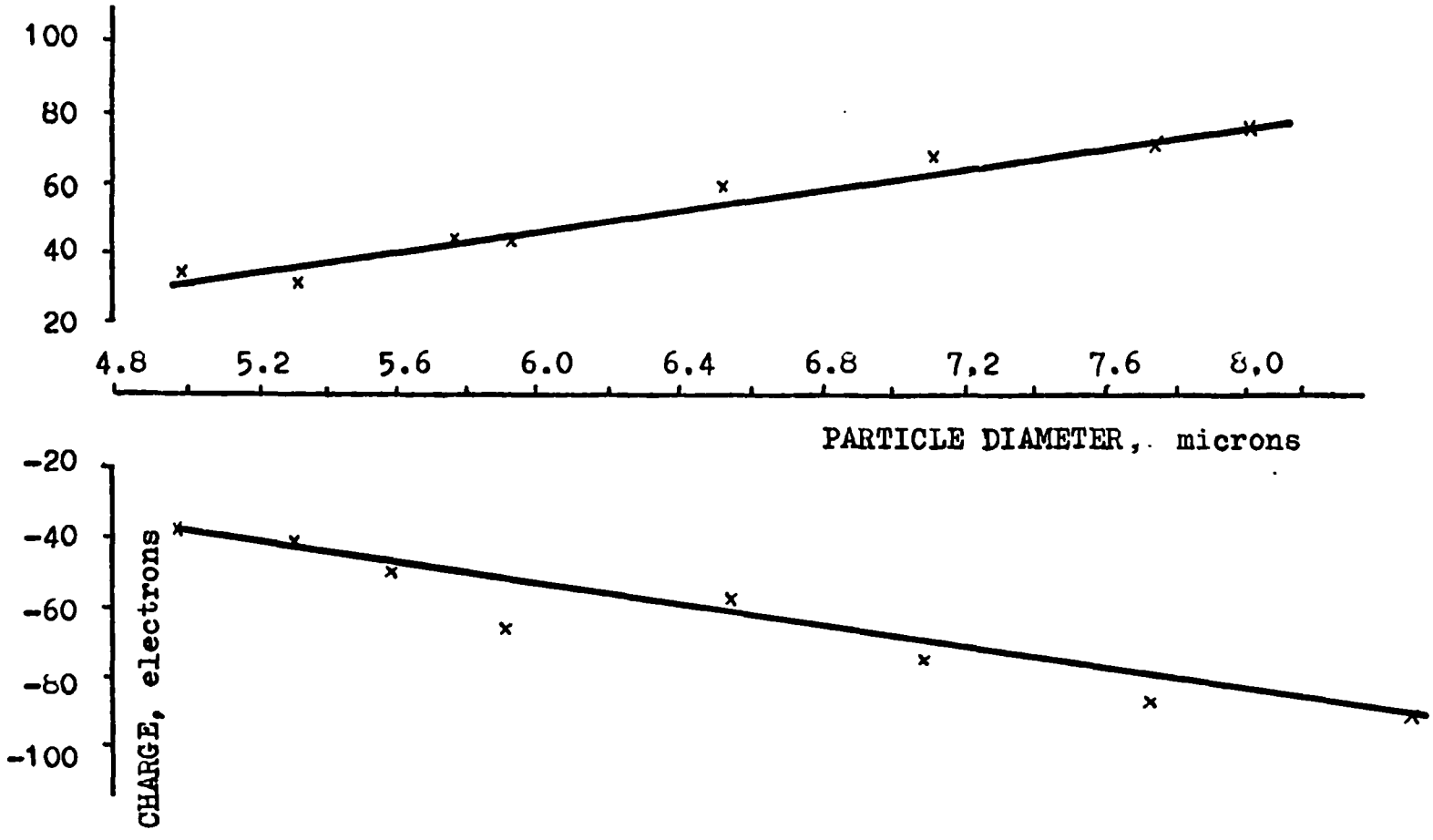

Figure 13. Particle Charge Dependence on Diameter (Non-fractionated Cement Dust).

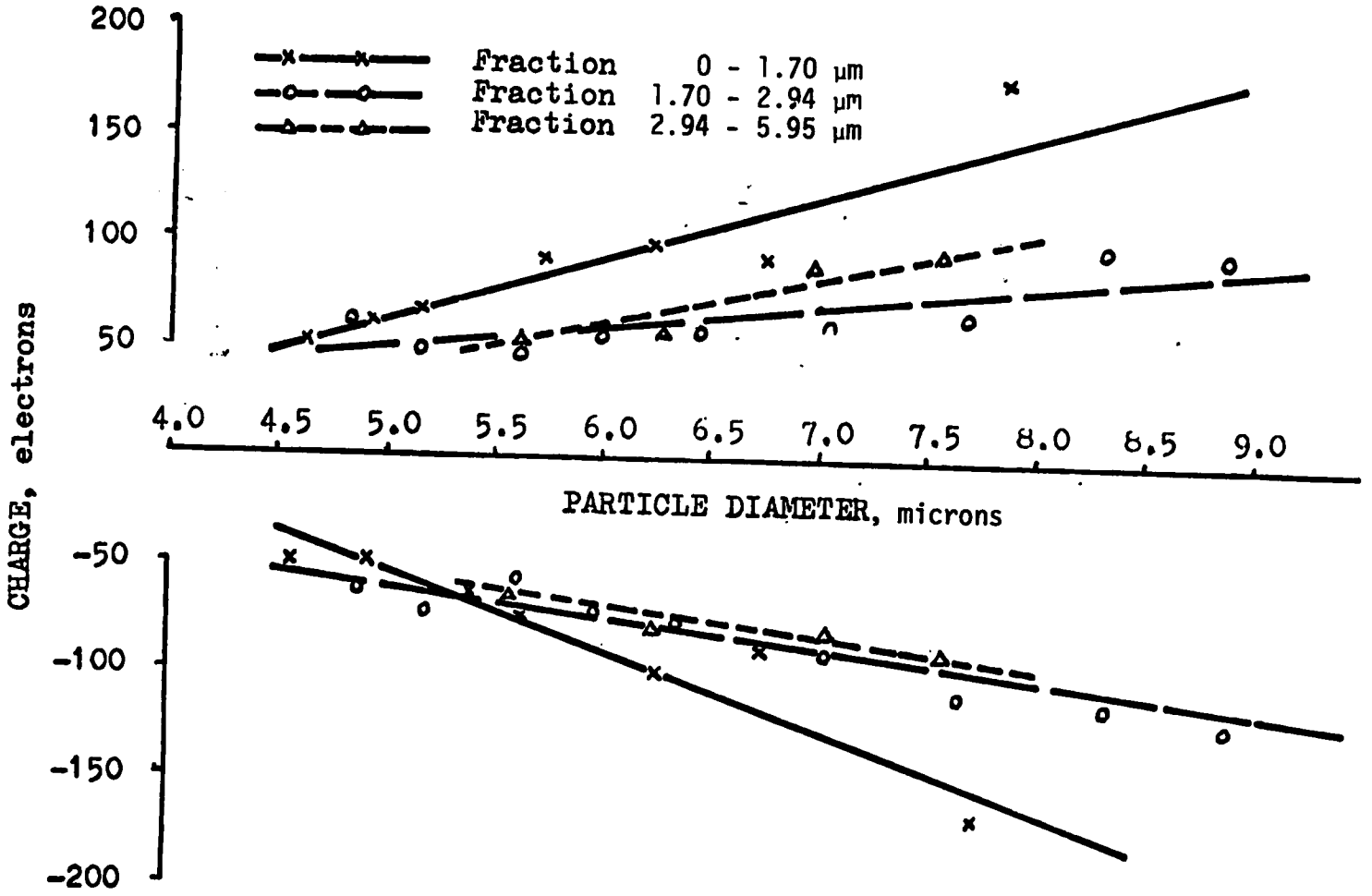

Figure 14. Particle Charge Dependence On Diameter (Fractionated Cement Dust).

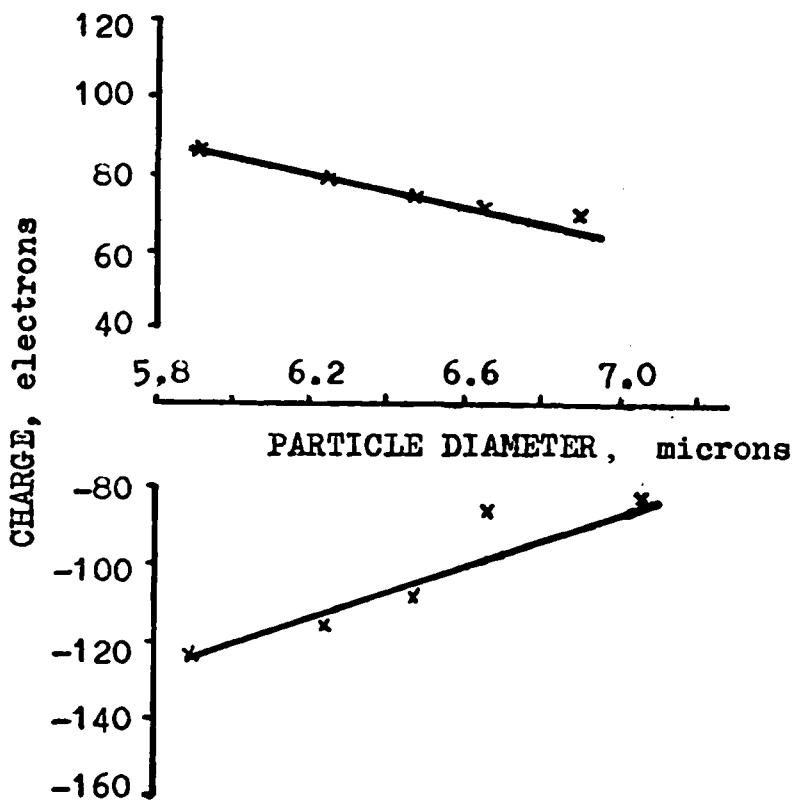

Figure 15. Particle Charge vs. Diameter for Non-fractionaed Cement Dust Passed through an Electrical Discharge.

Table 36. CHARGES ON NON-FRACTIONATED CEMENT AFTER PASSING THROUGH AN ELECTRICAL DISCHARGE

Range of particle size in μm	d in μm	σ in e	q in e
1	2	3	4
5.90 - 7.10	6.40	112.5	-25

As with the cement dust, measurements of coal dust charges were also made. The results are shown in tables 37-39 and in figures 16-18.

Table 37. CHARGES ON NON-FRACTIONATED COAL DUST

Range of particle size in μm	d in μm	σ in e	q in e
1	2	3	4
9.60 - 13.00	11.30	352	+30
9.60 - 11.50	10.53	327	+19
11.50 - 13.00	12.20	368	+31

Table 38. CHARGES ON FRACTIONATED COAL DUST

Fractions in μm	Range of particle size μm	d in μm	σ in e	q in e
0 - 2.46	6.60 - 9.15	7.64	117.5	+9
2.46 - 4.40	6.70 - 8.50	7.52	127	-10

Table 39. CHARGES ON NON-FRACTIONATED COAL DUST PASSED THROUGH AN ELECTRICAL DISCHARGE

Range of particle size in μm	d in μm	σ in 3	q in 3
1	2	3	4
7.20 - 11.80	8.68	236	+5

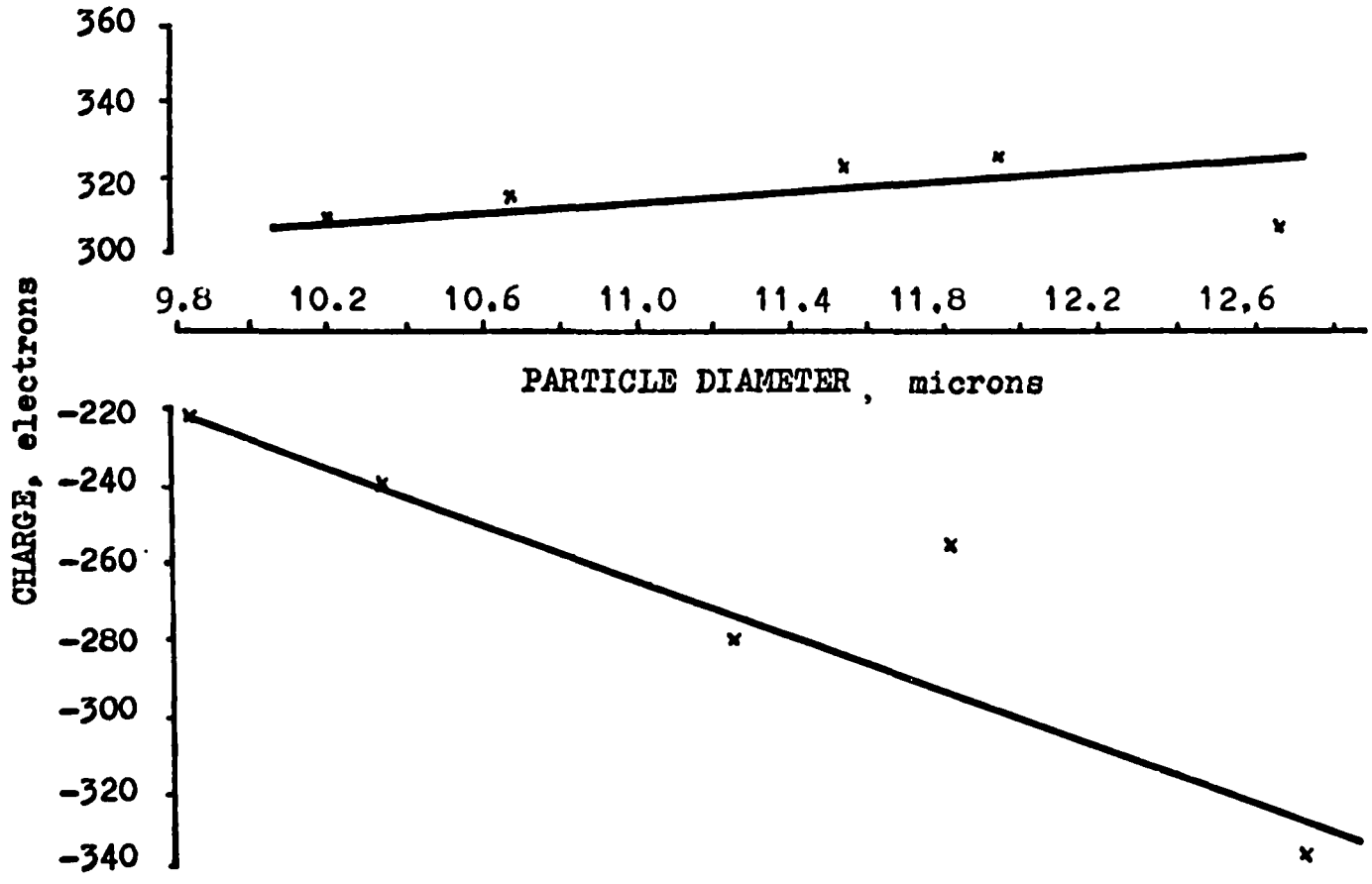

Figure 16. Particle Charge Dependence On Diameter (Non-fractionated Coal Dust).

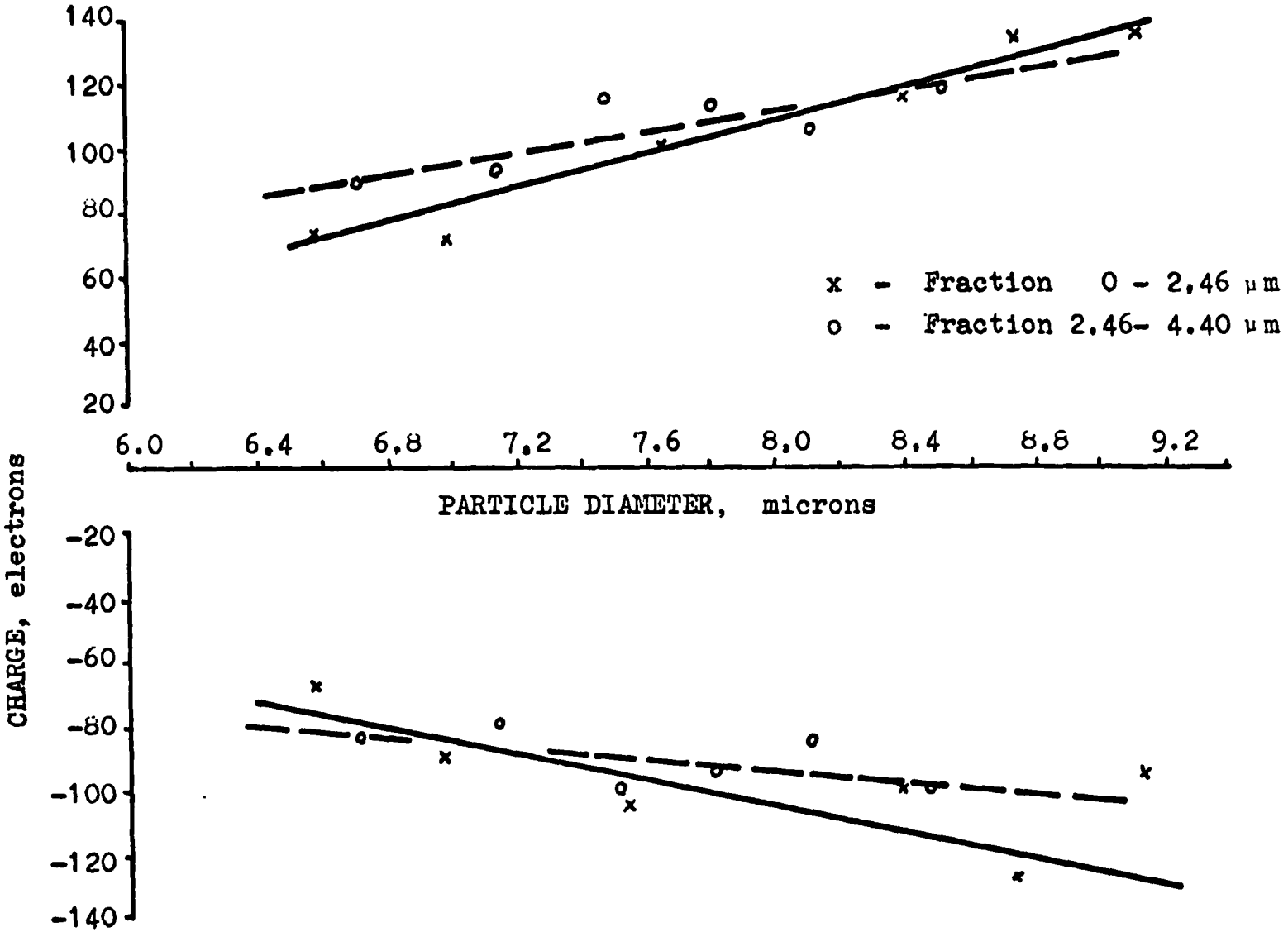

Figure 17. Particle Charge Dependence On Diameter (Fractionated Coal Dust).

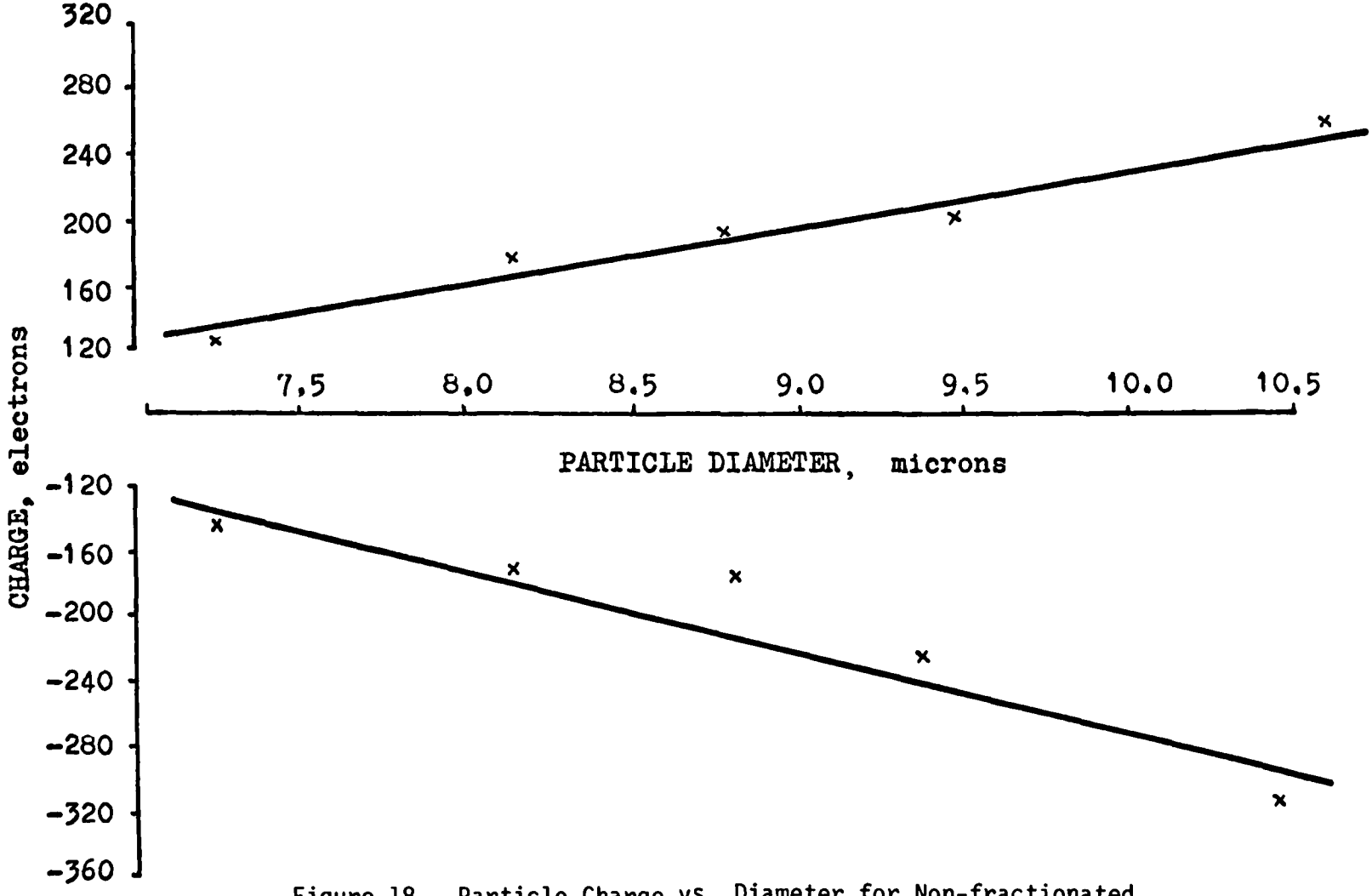

Figure 18. Particle Charge vs. Diameter for Non-fractionated Coal Dust Passed Through an Electrical Discharge.

As the measurements show, test dust particles are generally electrically charged. There are negative and positive charges and a comparatively small number of uncharged particles in the dust clouds. The average charge in a dust cloud differs from zero and indicates the sign of the dominant charge.

Analyzing the relationship between particle charge and diameter for the fractionated dusts, it is clear that the measured particle diameters are much bigger than the classified size range of the fraction. This difference between measured particle size and classified particle size is greatest for the size fraction classified to have the smallest diameter particles. Microscopic observation confirms the formation of 5 - 20 μm agglomerates, which explains the results. The formation of agglomerates is probably caused by electrostatic effects.

The preceding plots show a linear dependence between charge and particle diameter, $q = f(d)$. Based on the above we can write:

$$q^{(\pm)} = k^{(\pm)} d_m \qquad (101)$$

where k = the slope of the plotted straight line.

The values of slope are given in table 40.

Table 40. VALUES OF SLOPE k

Kind of dust	$\frac{q^+}{d_m}$ e/μm	$\frac{q^-}{d_m}$ e/μm
1	2	3
Non-fractionated cement	15.0	16.0
Cement - fraction I	22.8	30.0
Cement - fraction II	10.0	14.4
Cement - fraction III	23.4	14.4
Non-fractionated coal	8.5	36.0
Coal - fraction I	27.0	19.0
Coal - fraction II	18.0	9.0

Analyzing the data in table 40, we come to the conclusion that among the classified test dusts, the largest slopes are generally shown by the smallest dust particles.

The standard deviation, also being a measurement of the degree of dust charge as a function of diameter, can also be regarded as an approximately linear relation.

For cement dust, the strongest dependence of particle charge on diameter was observed for the smallest dust fraction; the weakest, for the non-fractionated dusts. This charging effect is probably caused by the dust fractionation process. During this process, the probability of contact between particles, between particles and the walls of the apparatus, and between particles and the atmosphere, increases. Cement dust is comparatively difficult to charge, so that increased contact can lead to increased charging. Because of the low electrical conduction of cement dust, any produced charges on the cement particles have little chance to neutralize, even during the long time of contact.

The phenomena occuring with coal dust are quite different. Nonfractionated coal dust shows many more charges than fractionated dust. Dust possessing large primary charge has a greater chance of losing that charge than of acquiring additional charge because of contact; that is why the coal dust charge decreases during the fractionation process.

Electrical discharges have a similar influence on dust charge, because they increase the ion concentration in the atmosphere. Electrical discharges cause an increase in the charge density of dusts of low primary charge. For dusts of high primary charge, electrical discharges cause a decrease in dust charge. These results are attributable to the partial neutralization of charge by air ions.

Apart from the above investigation, statistical measurements of the charges on dusts of cement, coal, talc and fly ash, for separated and non-separated samples, and according to the Detailed Program, were made. In contradistinction to the investigation conducted by Institute of Physics of Wroclaw Polytechnic, samples of fresh, nonstored dust were used (except talc). The results of all series of measurements are shown in table 41. It was found that the average particle charge as well as the amount of particle charging is much larger for fresh dusts than for stored dusts. The increase of charging during separation was also observed (except talc).

The investigation of natural charging of industrial dusts led to the following conclusions:

- Charging is closely connected with industrial dust generation and processes such as material pulverization.

Table 41. Charges on Fresh Industrial Dusts.

Kind of dust	σ in e	q in e
1	2	3
Cement - unseparated	915.00	+724.30
separated	703.00	+389.00
Coal (sample 1) - unseparated	1347.00	-82.00
separated	1083.00	+377.00
Coal (sample 2) - unseparated	1550.00	-116.90
separated	1360.00	+760.90
Talc - unseparated	820.90	-274.00
separated	863.30	+412,00
Fly Ash - unseparated	731.00	+481.00
separated	708.00	+200.10

- Charging measured by standard deviation depends on dust history.
- The average charge of a dust cloud depends on the present state of the aerosol and also on the dust history. Depending on where the sample is taken from an industrial installation, the same kind of dust can show a predominance of either negative or positive charge.
- Charges on fresh industrial dusts are very high, so their effect on dust cake formation and on dust collection efficiency in industrial fabric filtration can be considerable.

Electrical Resistivity of Fabrics

Electrical resistivity across the fabrics was measured at a different electric field intensity over the range:

$$20 \text{ V/cm} \leq E \leq 2000 \text{ V/cm}$$

and pressure, p, over the range:

$$2.5X10^3 \text{ N/m}^2 \leq p \leq 1.5X10^4 \text{ N/m}^2.$$

The measurements were conducted at an air temperature of 23 - 25° C and a relative humidity of 40-50 percent. For all fabrics, no changes in bulk resistivity were observed over this range of electric field intensity. But a dependence of bulk resistivity on the pressure is very evident (figure 19).

Measuring surface resistivity, the effects of interelectrode voltage on the results were clearly observed. We could observe the phenomena of fabric polarization by changing electrode placement or by reversing the polarity between the electrodes. Current values stabilized in some cases only after many hours. This phenomena especially characterized fabric ET-30. The results of the measurements are shown in table 42.

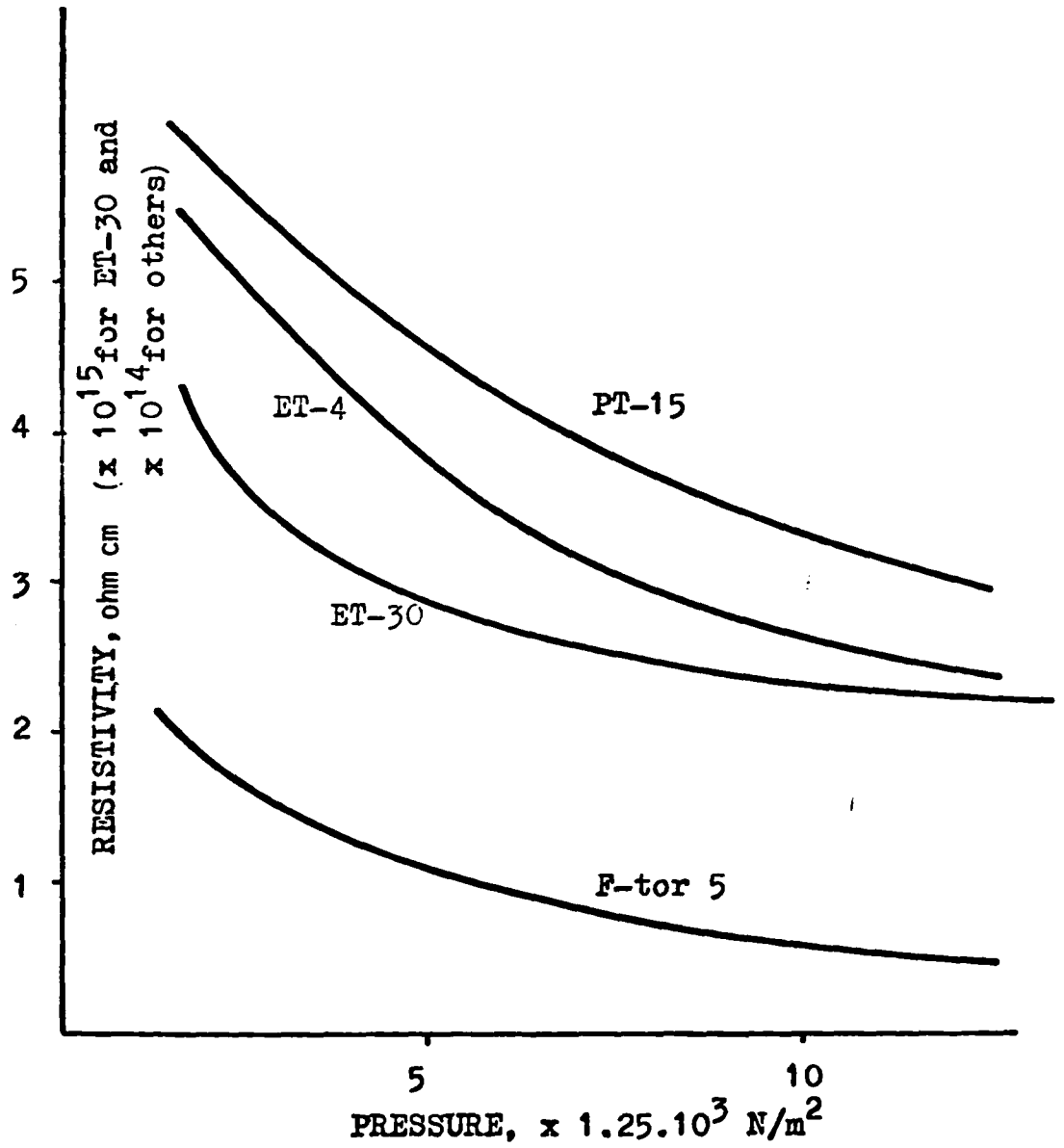

Figure 19. Dependence of Bulk Resistivity On Pressure.

Table 42. RESISTIVITY OF FABRICS

Kind of fabric	Thick-ness in mm	ρ_v in Ω cm	ρ_s in Ω/sq	R_vS in Ωcm^2
1	2	3	4	5
ET-4	0.75	$5.2X10^{14}$	$9.5X10^{14}$	$3.9X10^{13}$
ET-30	0.6	$4.3X10^{15}$	$3.3X10^{16}$	$2.6X10^{14}$
F-tor 5	0.5	$1.8X10^{14}$	$0.7\text{-}1.1X10^{14}$	$9.0X10^{12}$
PT-15	0.4	$5.8X10^{14}$	$3.0\text{-}4.5X10^{15}$	$2.3X10^{13}$

The last column of table 42 is a bulk resistance, calculated per unit of area R_vS, where S = the area of the protected electrode. According to the authors, this quantity is more suitable for estimating fabric electrical properties.

Resistivity of Dusts

The measurements of dust resistivity were made at a temperature of 23° C and a relative air humidity of 51 percent. Depending on the degree of compression, the resistivities were as follow.

Cement dust	K = 10%	$\rho = 9.5 \times 10^9$	Ωcm
	K = 20%	$\rho = 5.7 \times 10^9$	Ωcm
Talc	K = 10%	$\rho = 9.0 \times 10^{11}$	Ωcm
	K = 20%	$\rho = 6.1 \times 10^{11}$	Ωcm
Coal dust	K = 10%	$\rho = 4.5 \times 10^{13}$	Ωcm
	K = 20%	$\rho = 2.0 \times 10^{13}$	Ωcm

To examine the effect of humidity on dust resistivity, the dust samples were placed in desiccators along with specific saturated solutions to maintain the desired relative humidity. After 48 hours of acclimatization, the measurements of resistivity were made. For all dusts a decrease of resist-

ivity with increased humidity was observed as is illustrated in figure 20. The dependence of resistivity on temperature was examined after placing the measurement chamber in a thermostatically controlled enclosure. Stabilization of the measured resistivities indicated the stabilization of temperature inside the measurement chamber. The dependence of cement dust resistivity on temperature is shown in figure 21.

Electric Charge Leakage From Fabrics

In figures 22 through 25, the curves U(t) are shown describing the decrease of voltage in time for individual kinds of clean and dusty fabrics.

Little influence of the cover thickness on the curves was observed, so the measurements were done for only one thickness of dust cover (10 mg/cm^2). The presence of dust and the type of dust have considerable influence on U(t), especially for fabrics covered with talc. Different dust covers lead to increases or decreases in half decay time. Analyses of the U(t) curves show considerable departure from the exponential dependence given by the equation:

$$U(t) = U_0 \exp(-t/\varepsilon_0 \cdot \kappa \cdot \rho) \qquad (102)$$

where U_0 = initial value of voltage (100 V),

$\varepsilon_0 = 8.85 \times 10^{12}$ F/m, the permittivity of a vacuum,

κ = dielectric constant ($\equiv \frac{\varepsilon}{\varepsilon_0}$),

ρ = dielectric resistivity, and

ε = dielectric permittivity.

Equation 102 holds for dielectrics of constants κ and ρ.

Repeated measurements of the U(t) function on the same sample showed that the half decay time, $t_{1/2}$, tended to increase for all fabrics.

After a pause in measurements lasting a dozen or so hours, $t_{1/2}$ decreased to its initial value. This phenomenon, as well as the difference between the actual U(t) curve and the exponential form, can be explained by a resistivity increase in the discharging process, which is caused by the displacement of ions to the vicinity of the electrodes. In the appendix (figure A-72), a typical measurement cycle (for fabric F-tor 5) is shown.

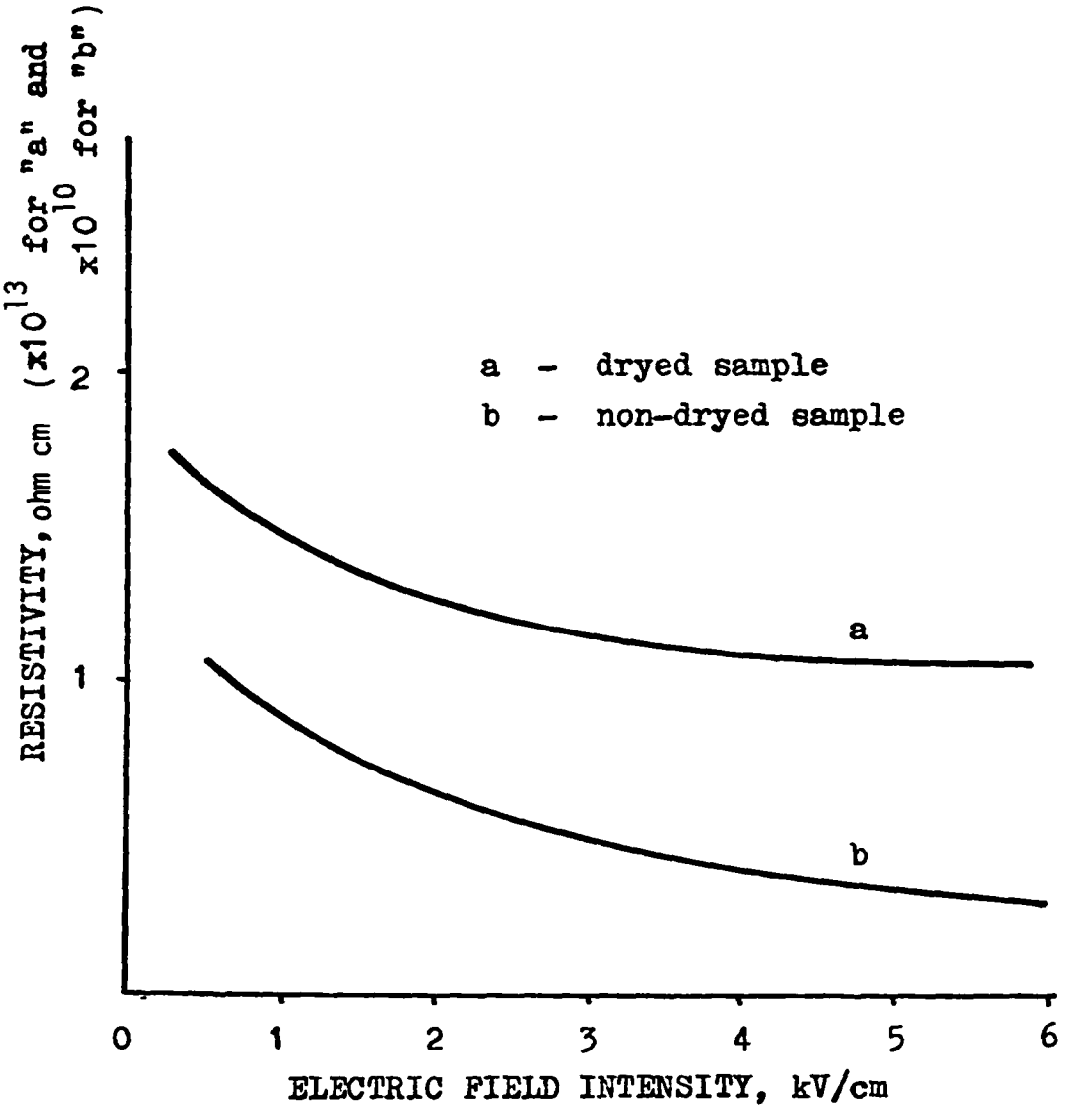

Figure 20. The Effect of Humidity Upon Cement Dust Resistivity.

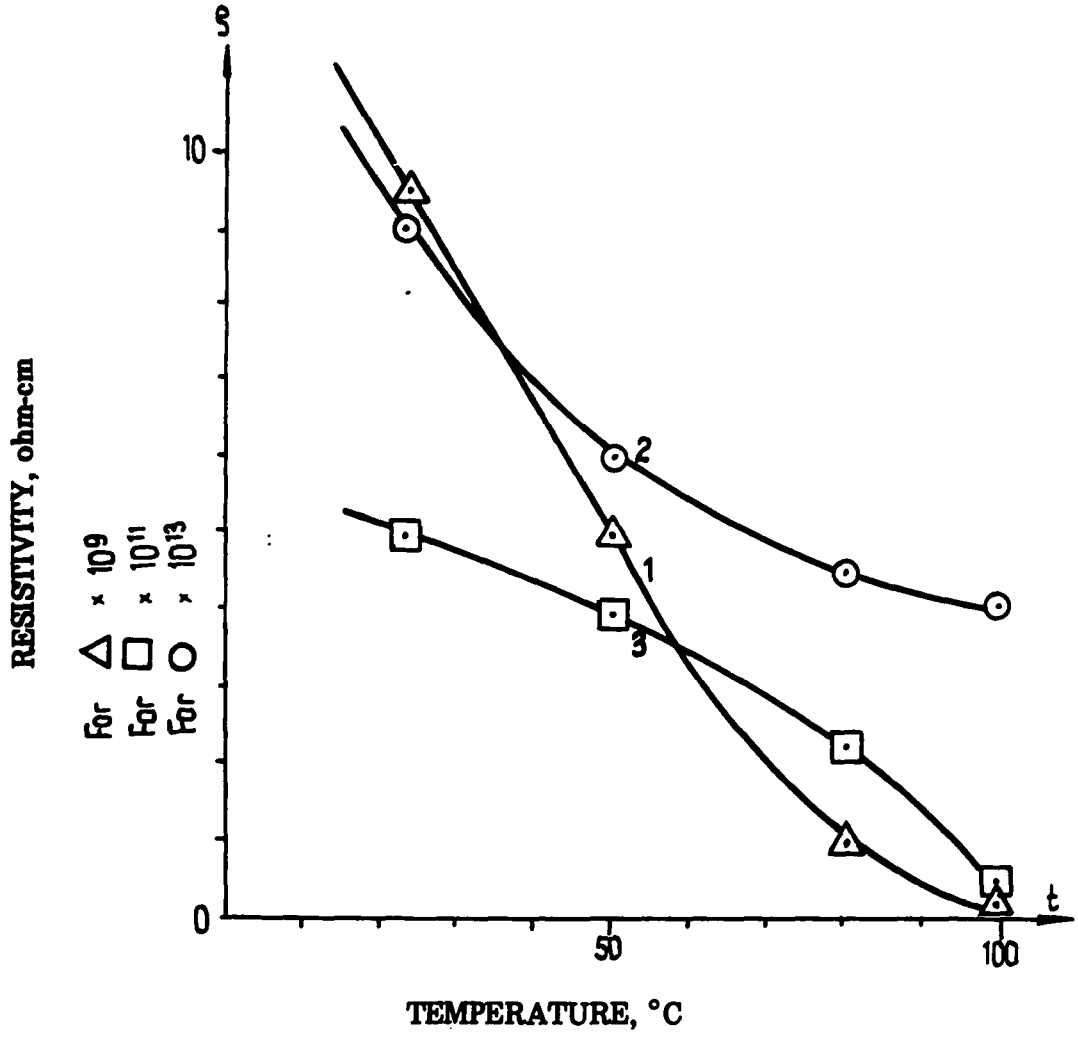

Figure 21. Dependence of Dust Resistivity Upon Temperature (K = 10%).
1. Cement, 2. Talc, 3. Coal.

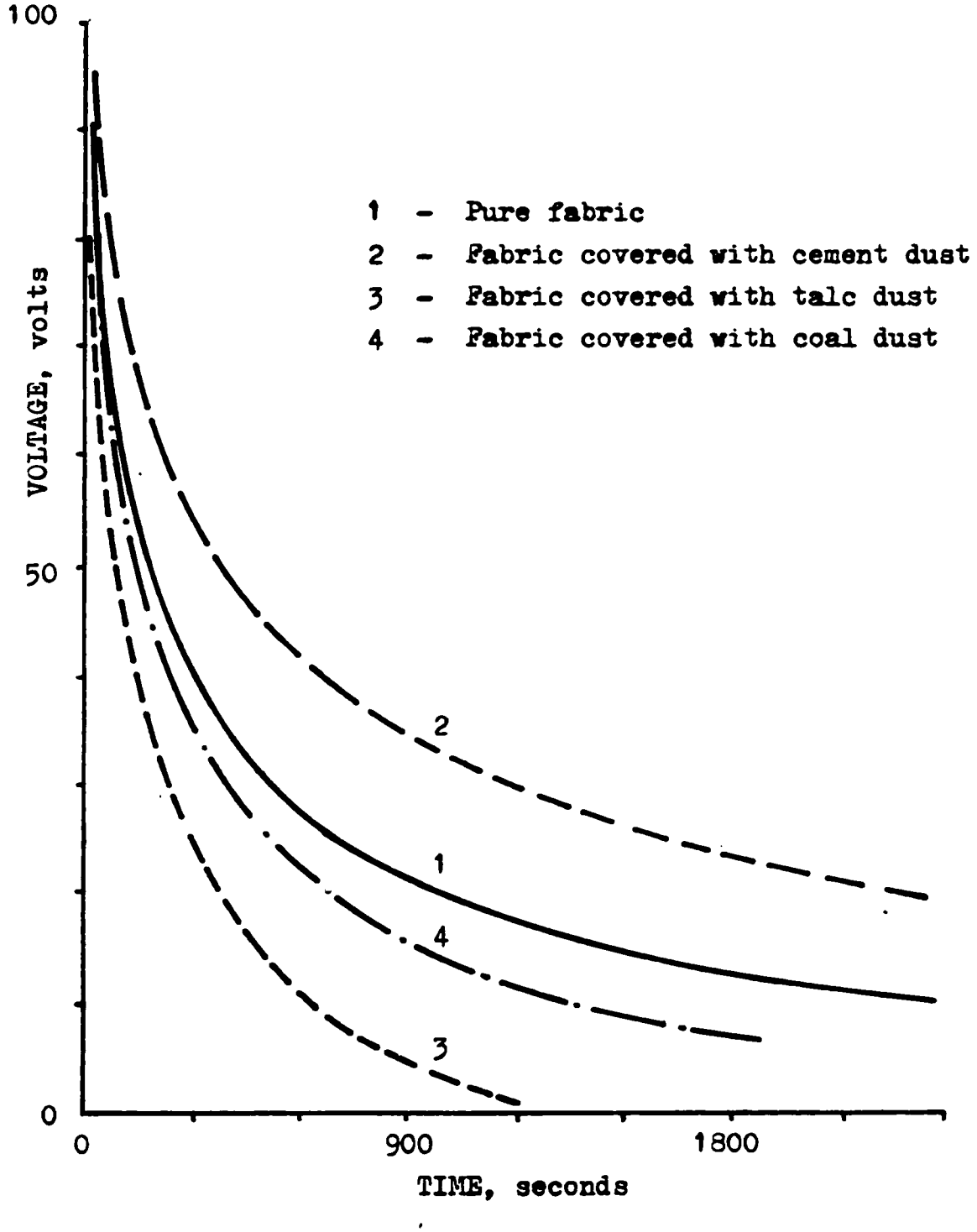

Figure 22. Function U(t) for Fabric ET-4.

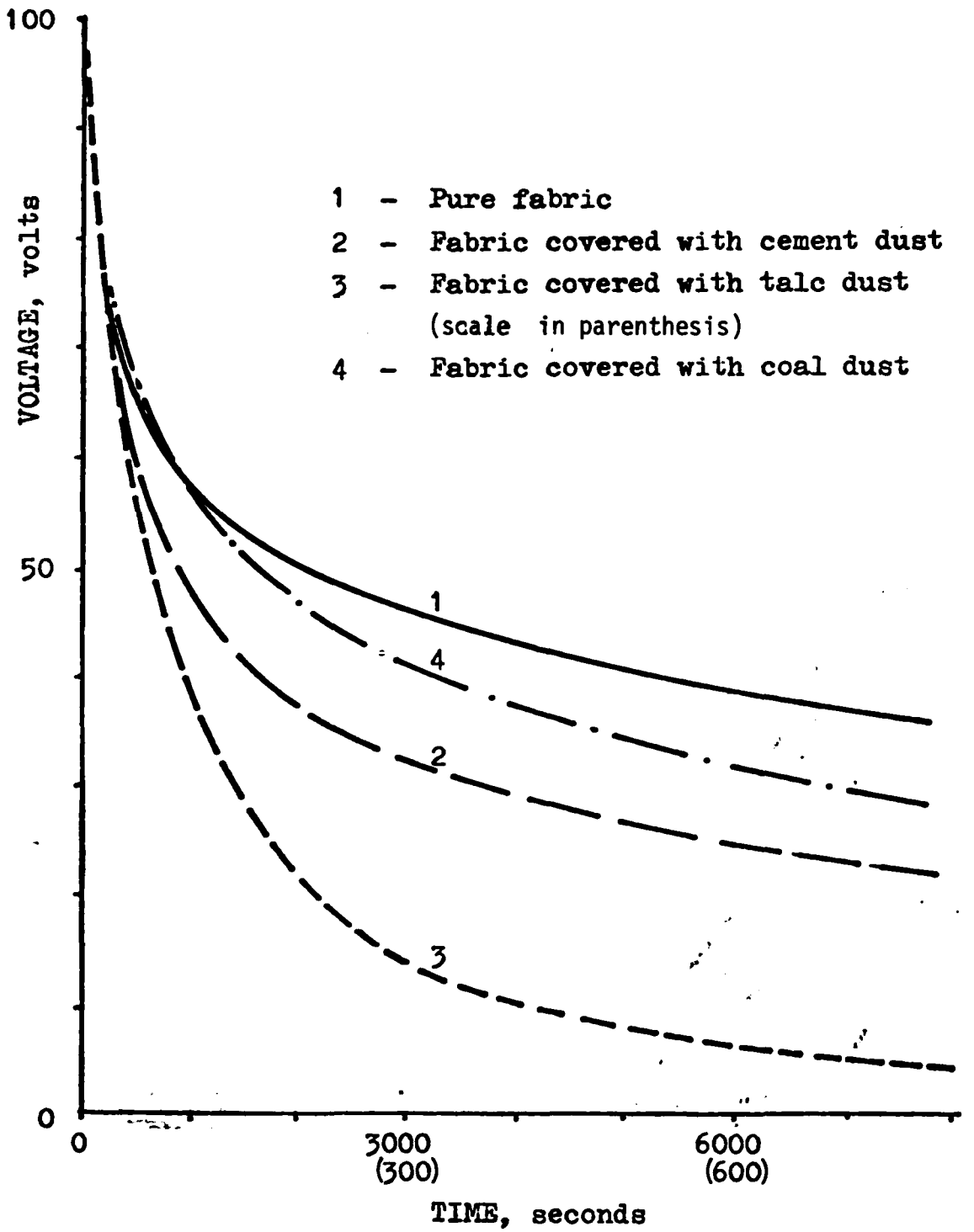

Figure 23. Function U(t) for Fabric ET-30.

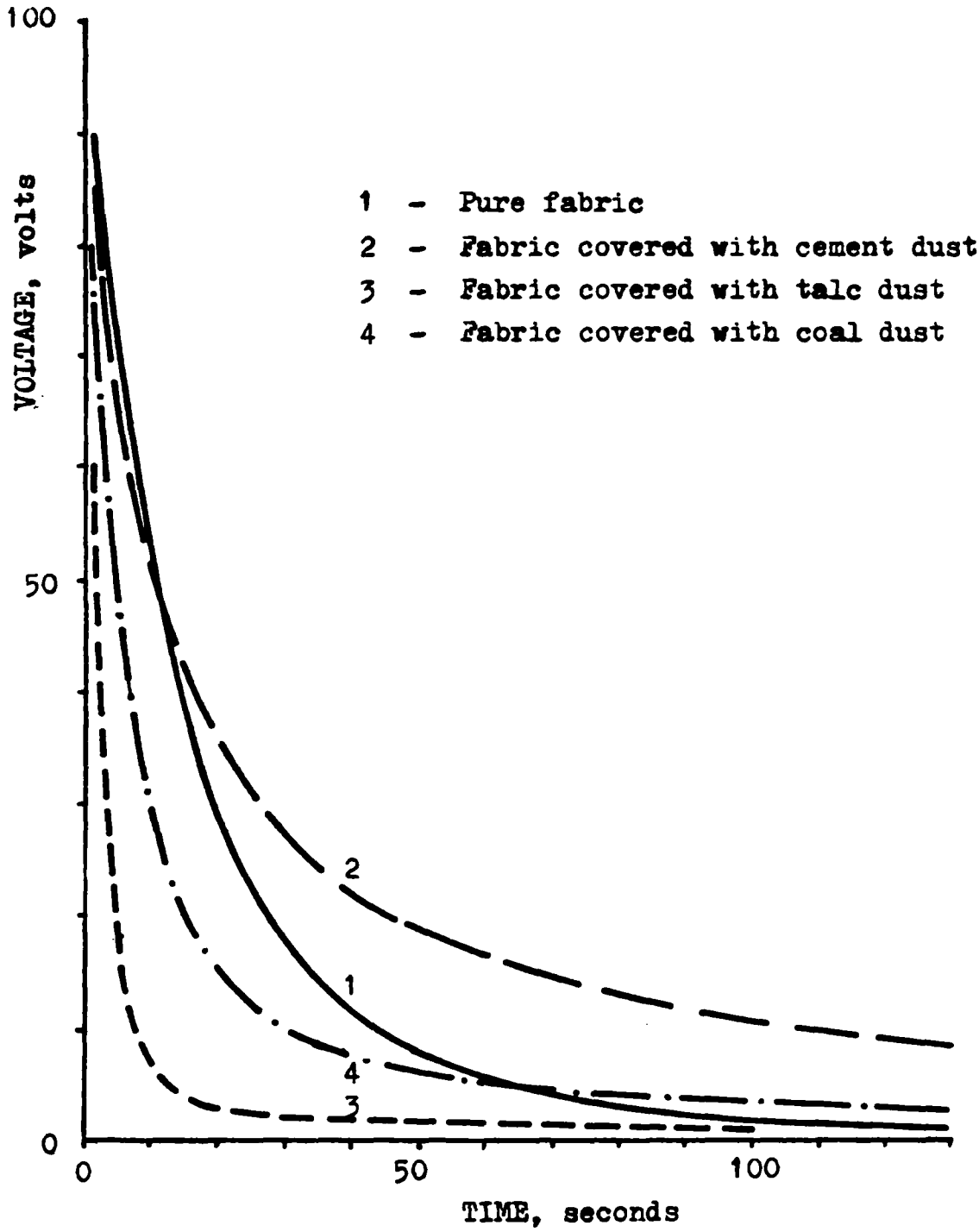

Figure 24. Function U(t) for Fabric F-tor 5.

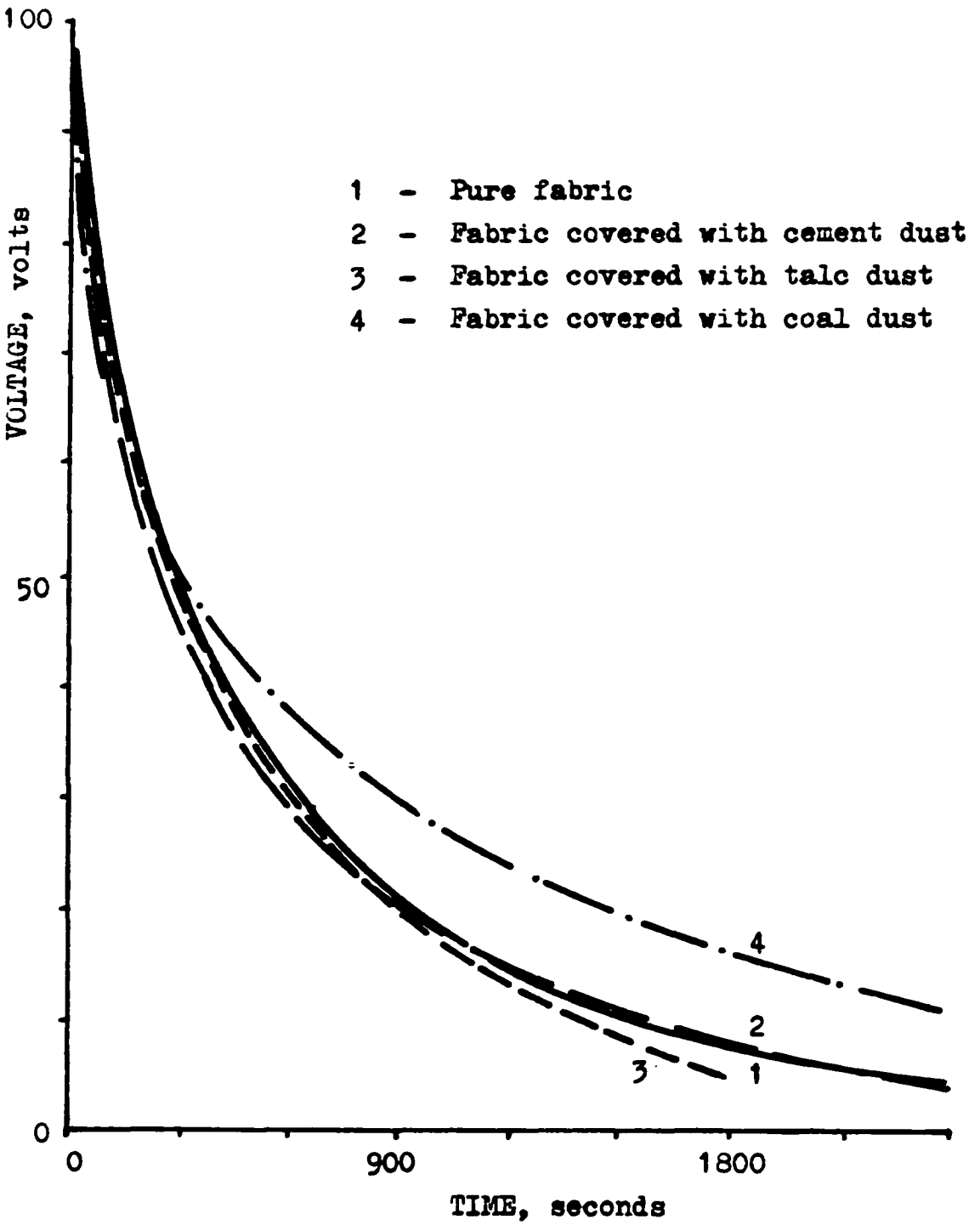

Figure 25. Function U(t) for Fabric PT-15.

CONCLUSIONS

Studies of the electrostatic properties of dusts and fabrics lead to the conclusion that electrostatic effects in specific dust-fabric systems under specific external conditions can determine, qualitatively and quantitatively, the course of the dust filtration process.

These studies are regarded as preliminary. An interpretation of the importance of these experiments upon a real dust filtration process will be presented in the final report.

SECTION X

ADDITIONAL WORK

Because of the kindness of the Project Officer, the Institute has received for the project period a Helium-Air Pycnometer Model 1302, produced by Micromeritics Instrument Corporation, Coulter Electronics Limited. The purpose of this instrument is to measure the density of dust. Previously the density was measured using a liquid pycnometer.

It is an inspiration to start the additional work (not included in the original program of the project) of comparing methods of dust density definition. The results will be included in the final report.

APPENDIX A

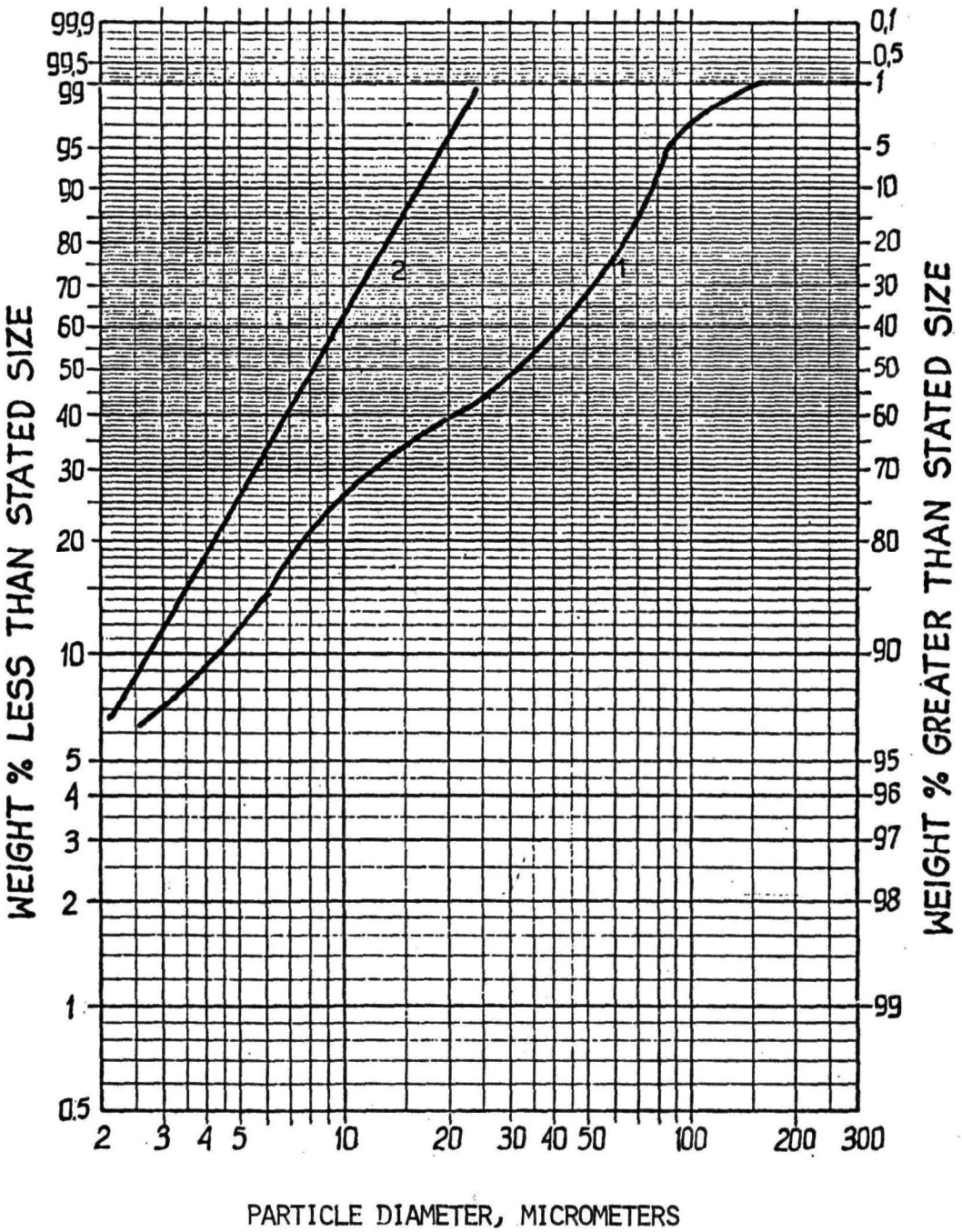

Figure A-1. Particle Size Distribution for Cement Dust (1 - before separation; 2 - after separation).

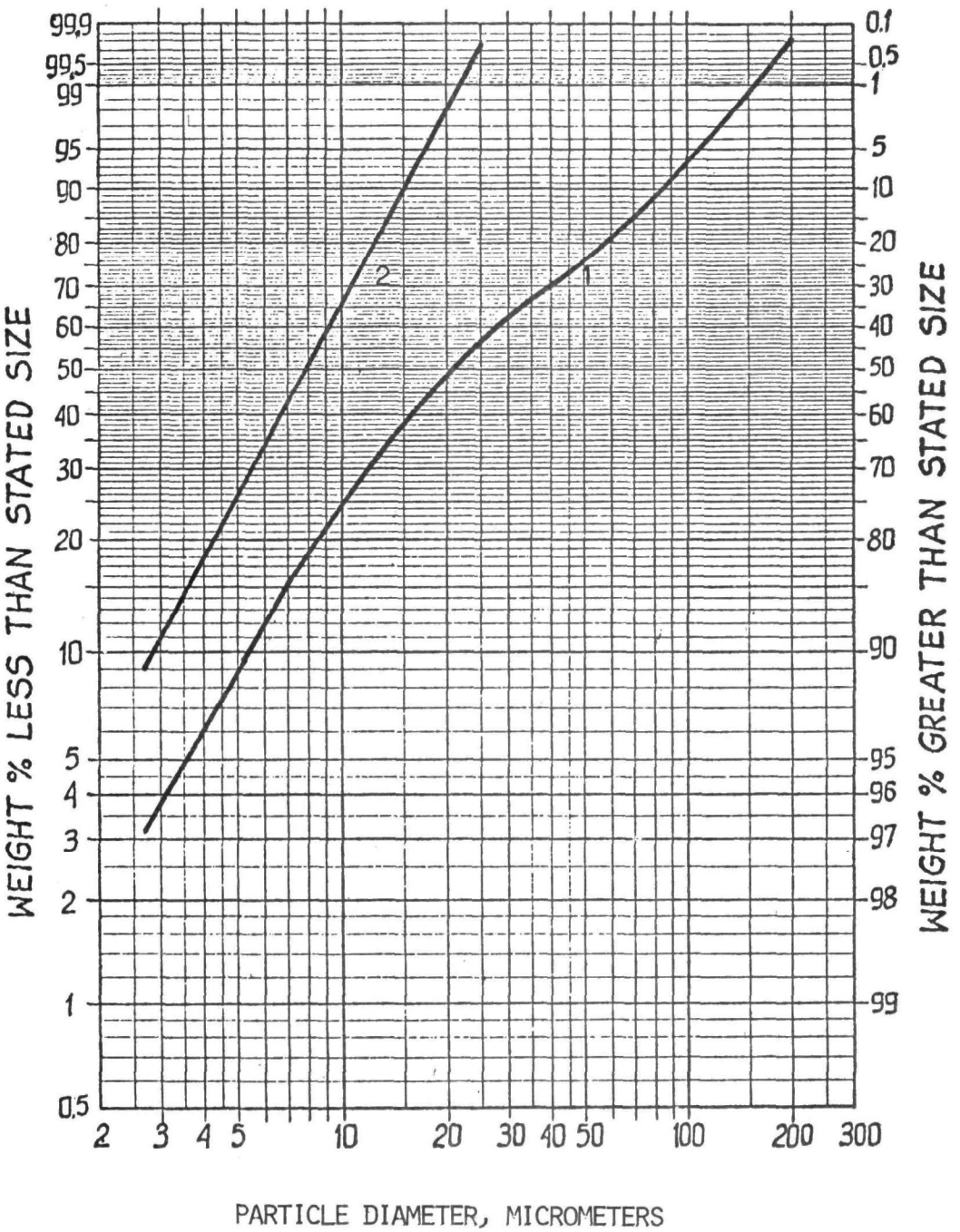

Figure A-2. Particle Size Distribution for Coal Dust (1 - before separation; 2 - after separation).

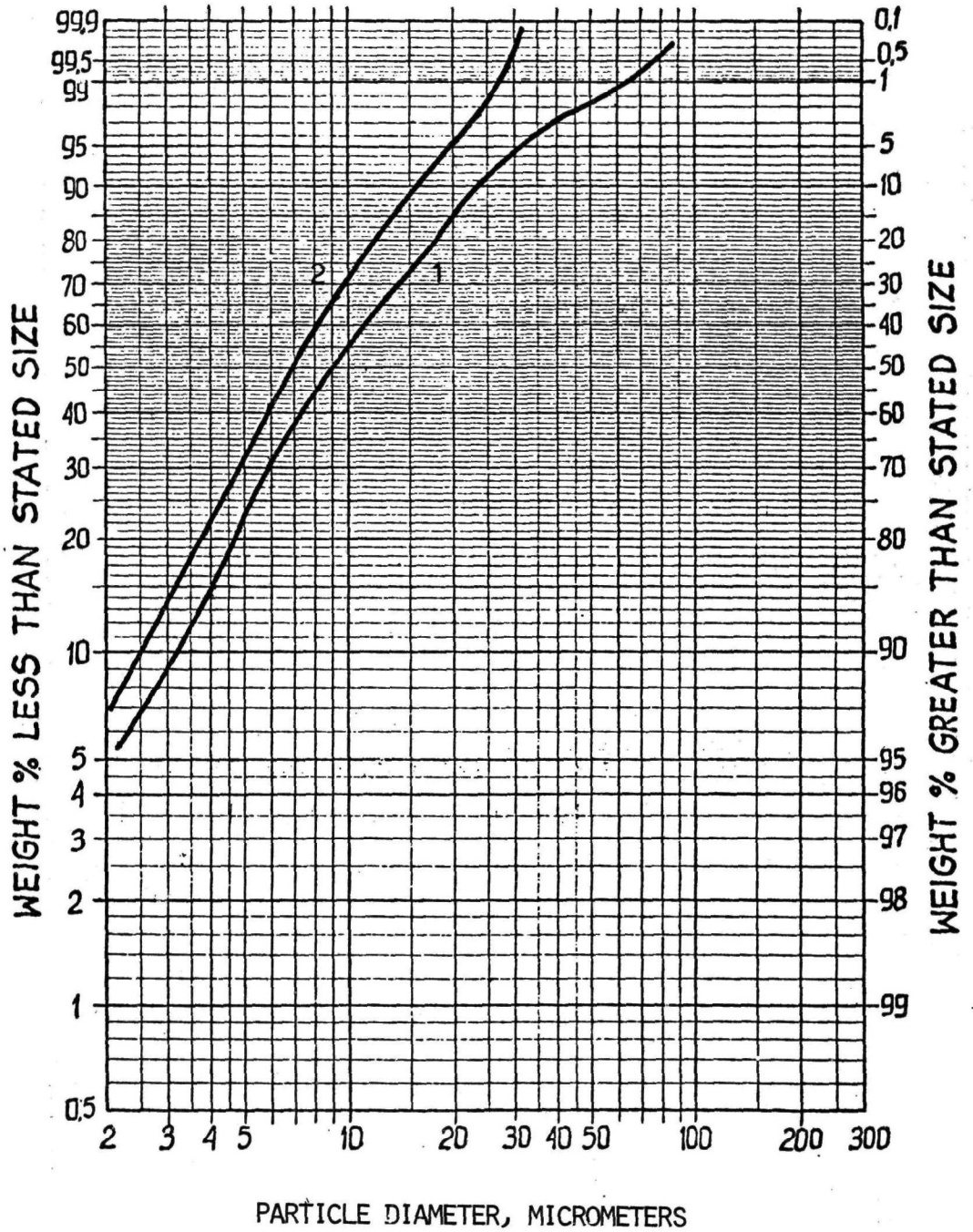

Figure A-3. Particle Size Distribution for Talc Dust (1 - before separation; 2 - after separation).

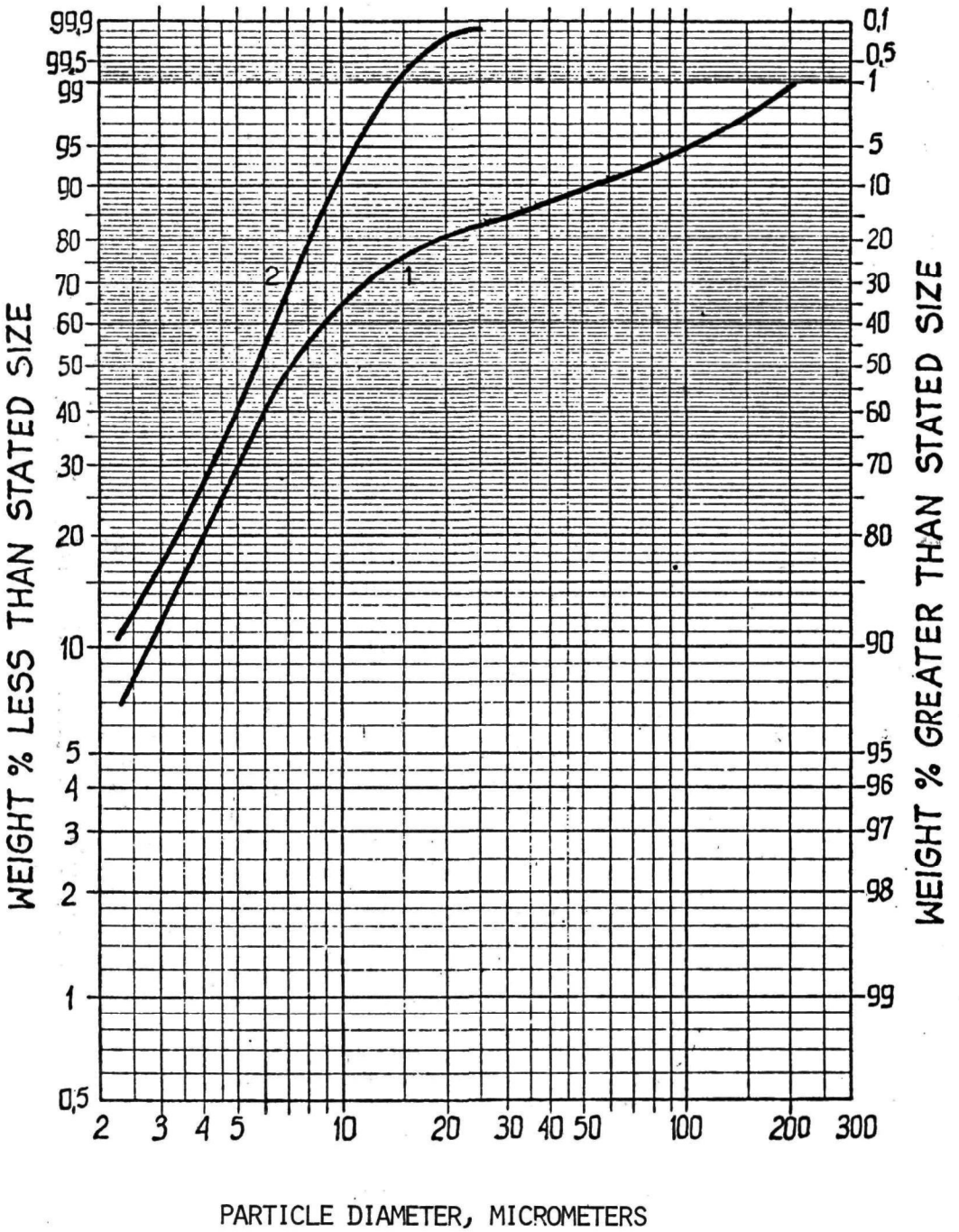

Figure A-4. Particle Size Distribution for Fly Ash Dust (1 - before separation; 2 - after separation).

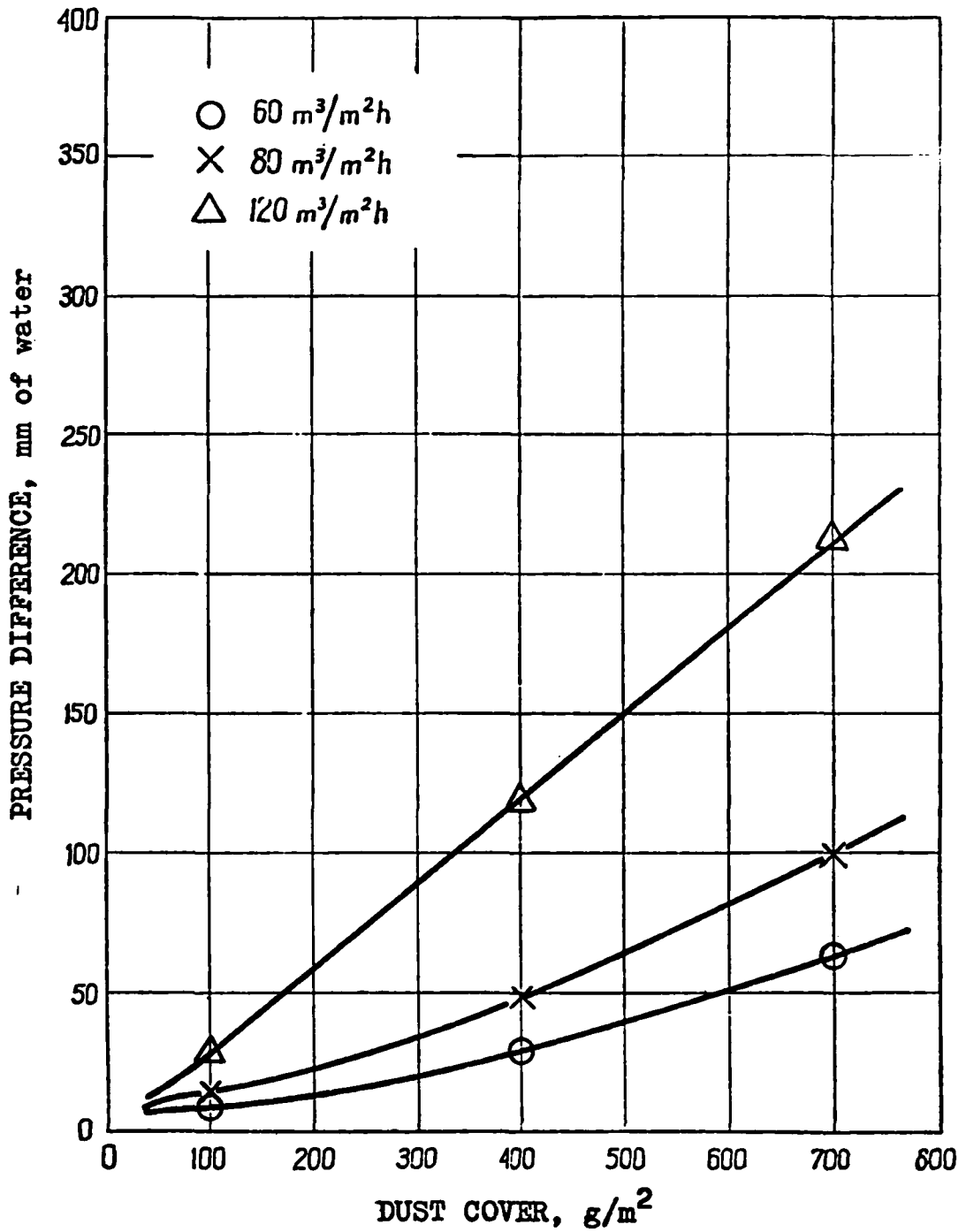

Figure A-5. Pressure Difference vs. Dust Cover for Cement Dust and Fabric ET-4 (separated dust).

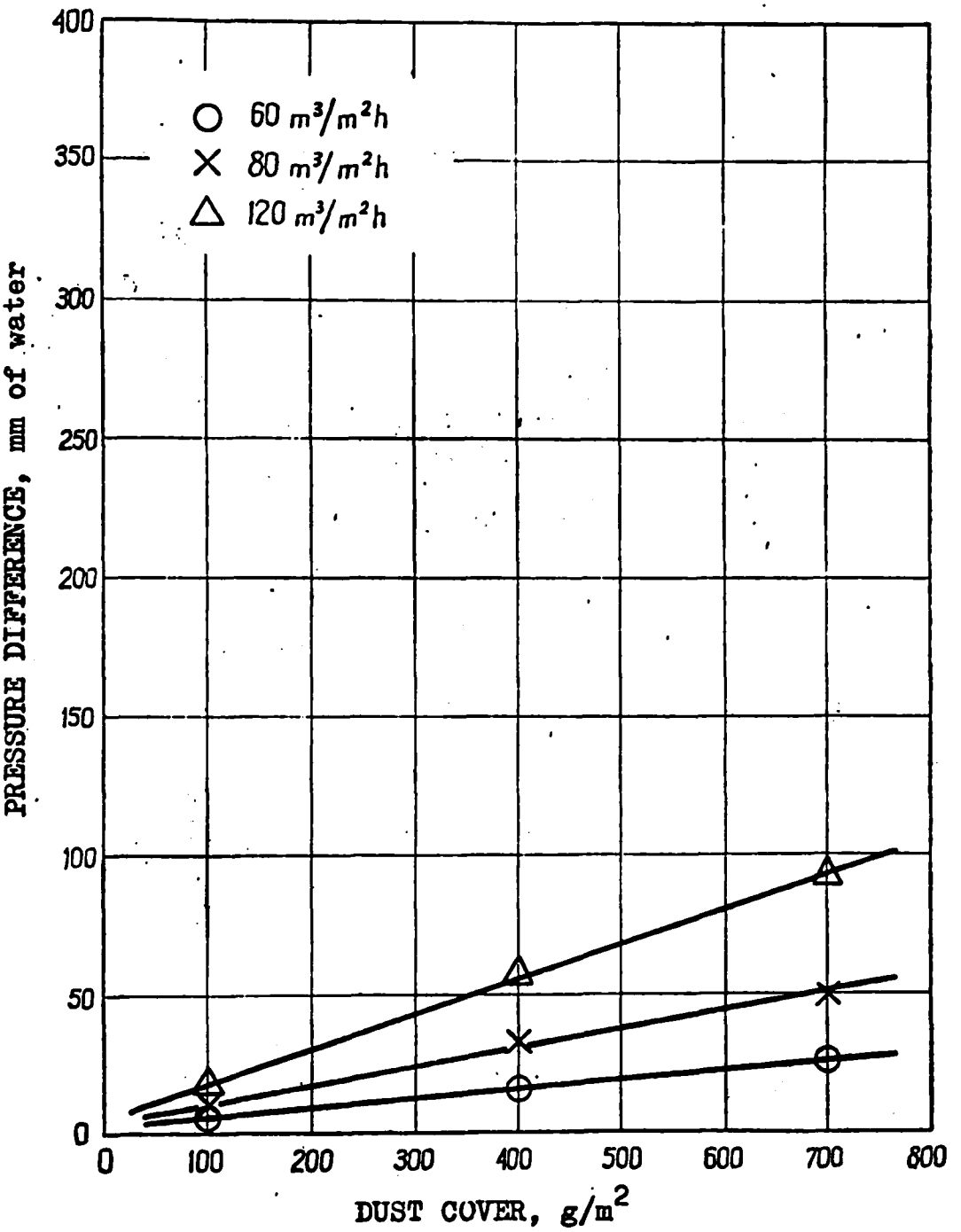

Figure A-6. Pressure Difference vs. Dust Cover for Cement Dust and Fabric ET-4 (unseparated dust).

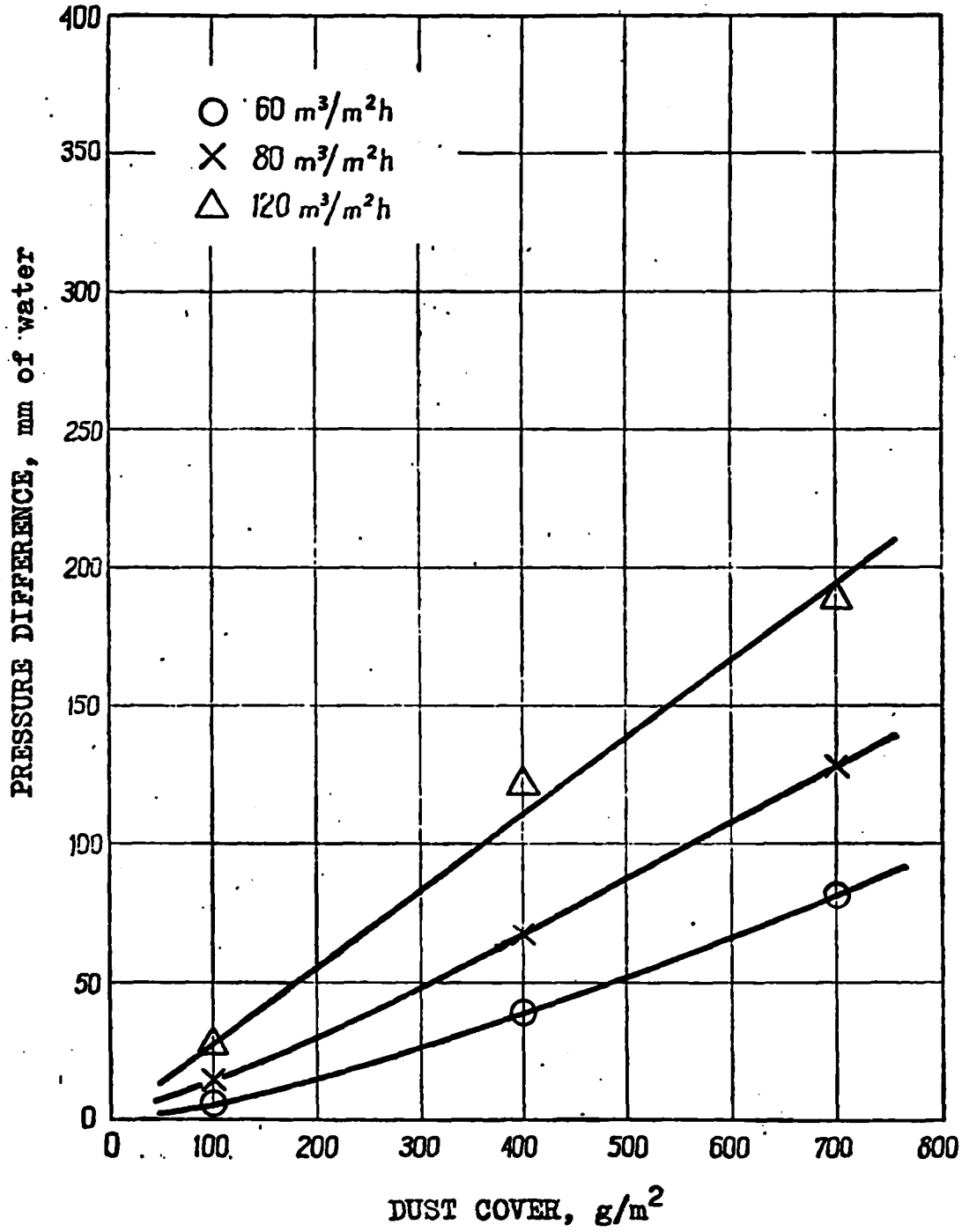

Figure A-7. Pressure Difference vs. Dust Cover for Coal Dust and Fabric ET-4 (separated dust).

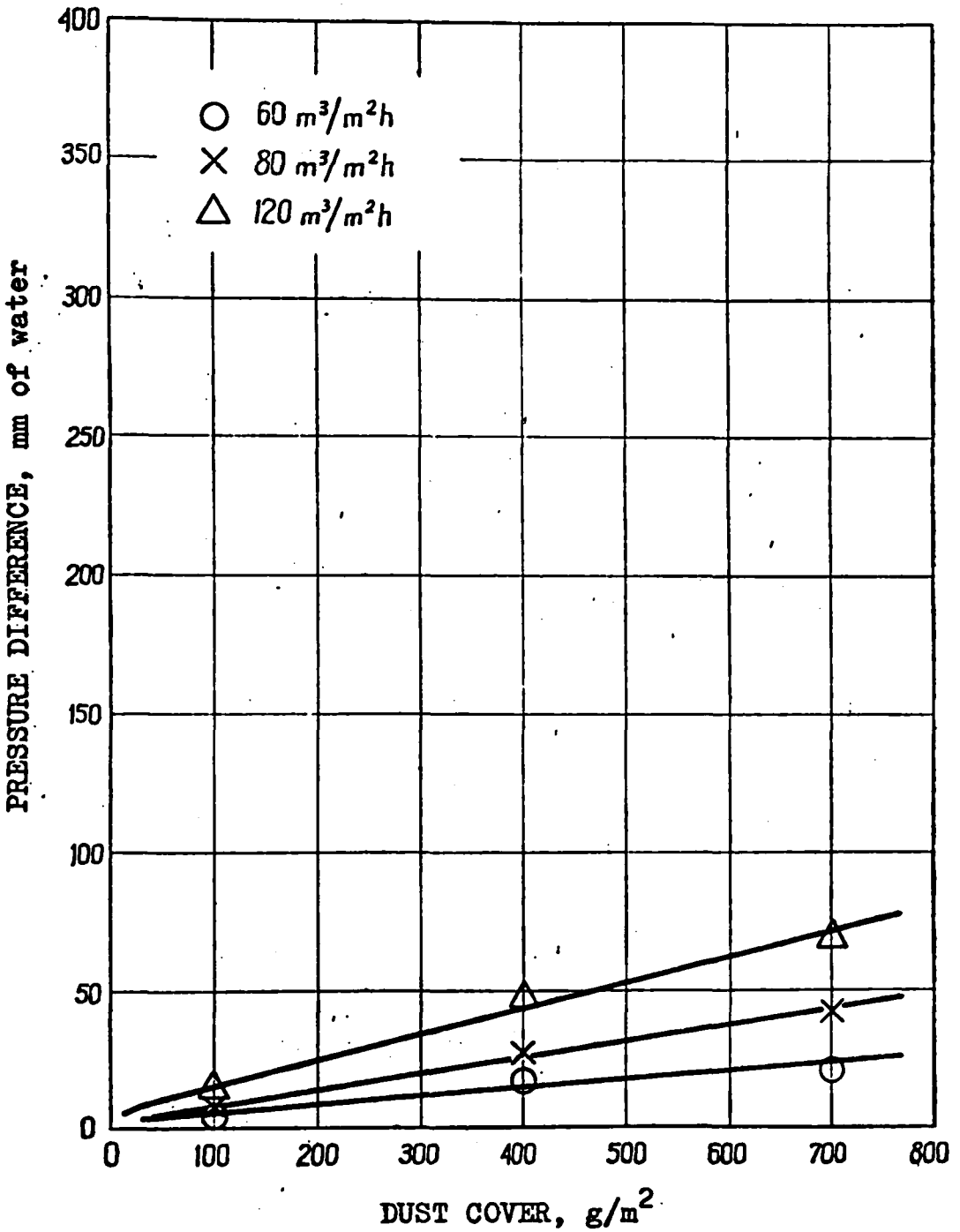

Figure A-8. Pressure Difference vs. Dust Cover for Coal Dust and Fabric ET-4 (unseparated dust).

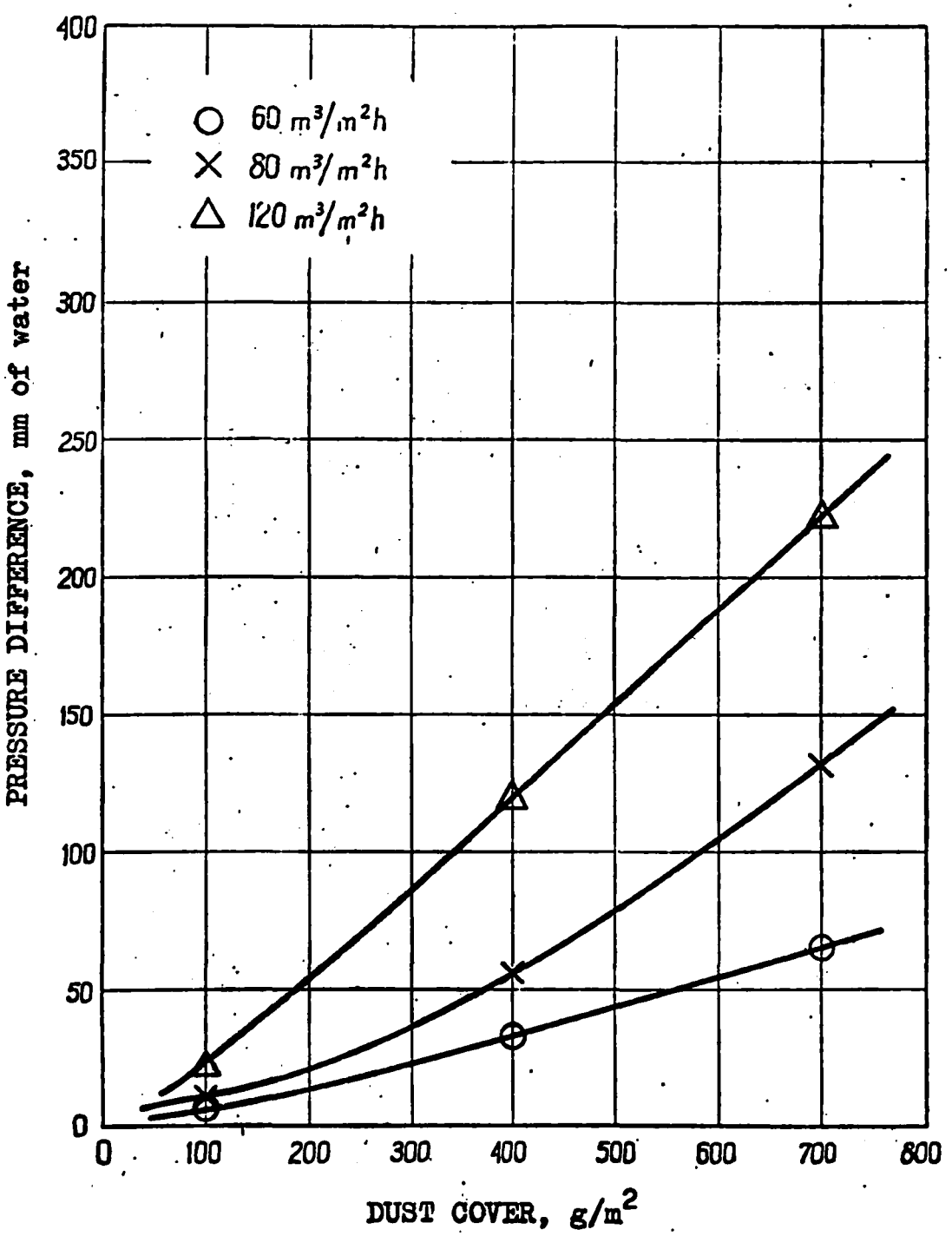

Figure A-9. Pressure Difference vs. Dust Cover for Talc Dust and Fabric ET-4 (separated dust).

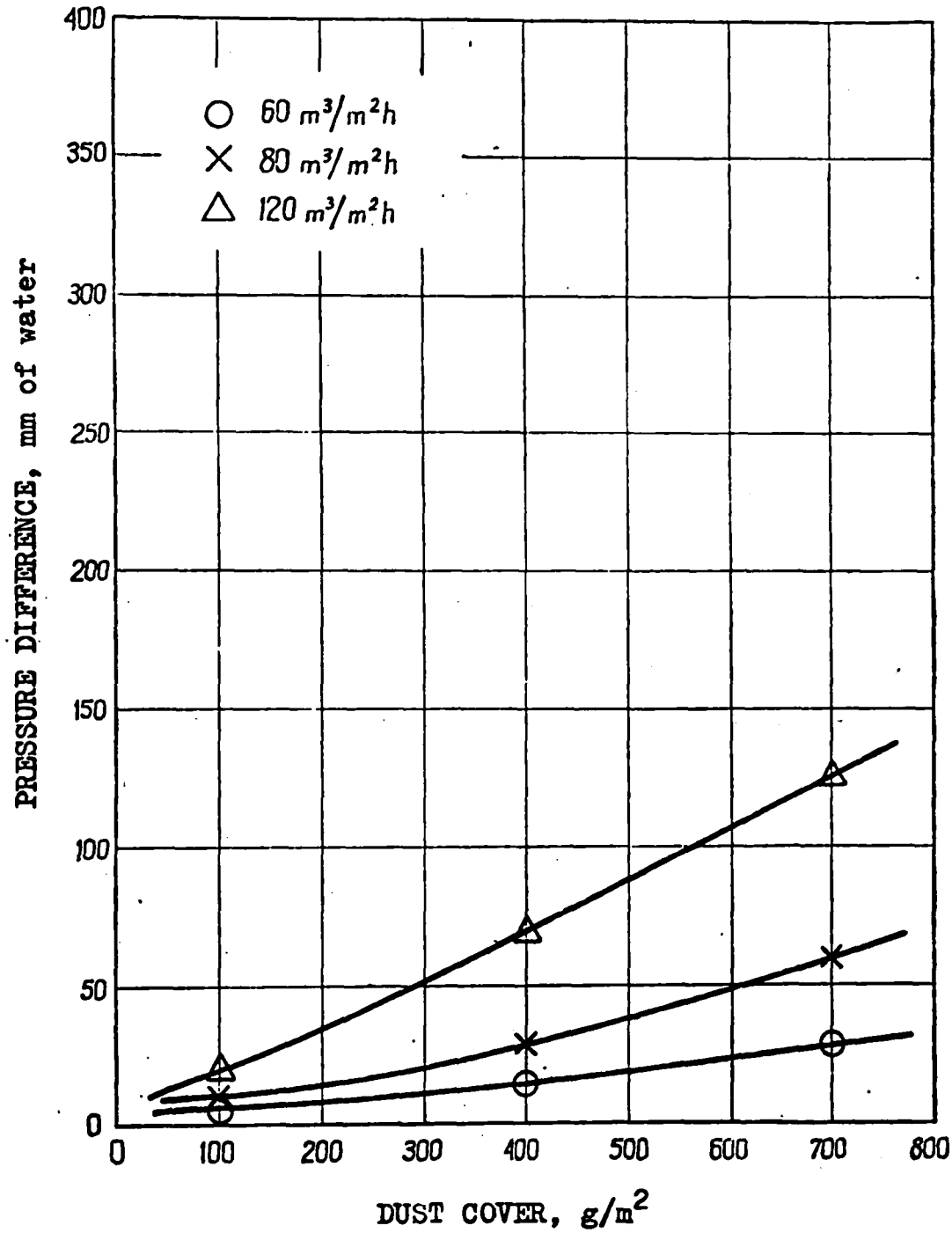

Figure A-10. Pressure Difference vs. Dust Cover for Fly Ash Dust and Fabric ET-4 (separated dust) .

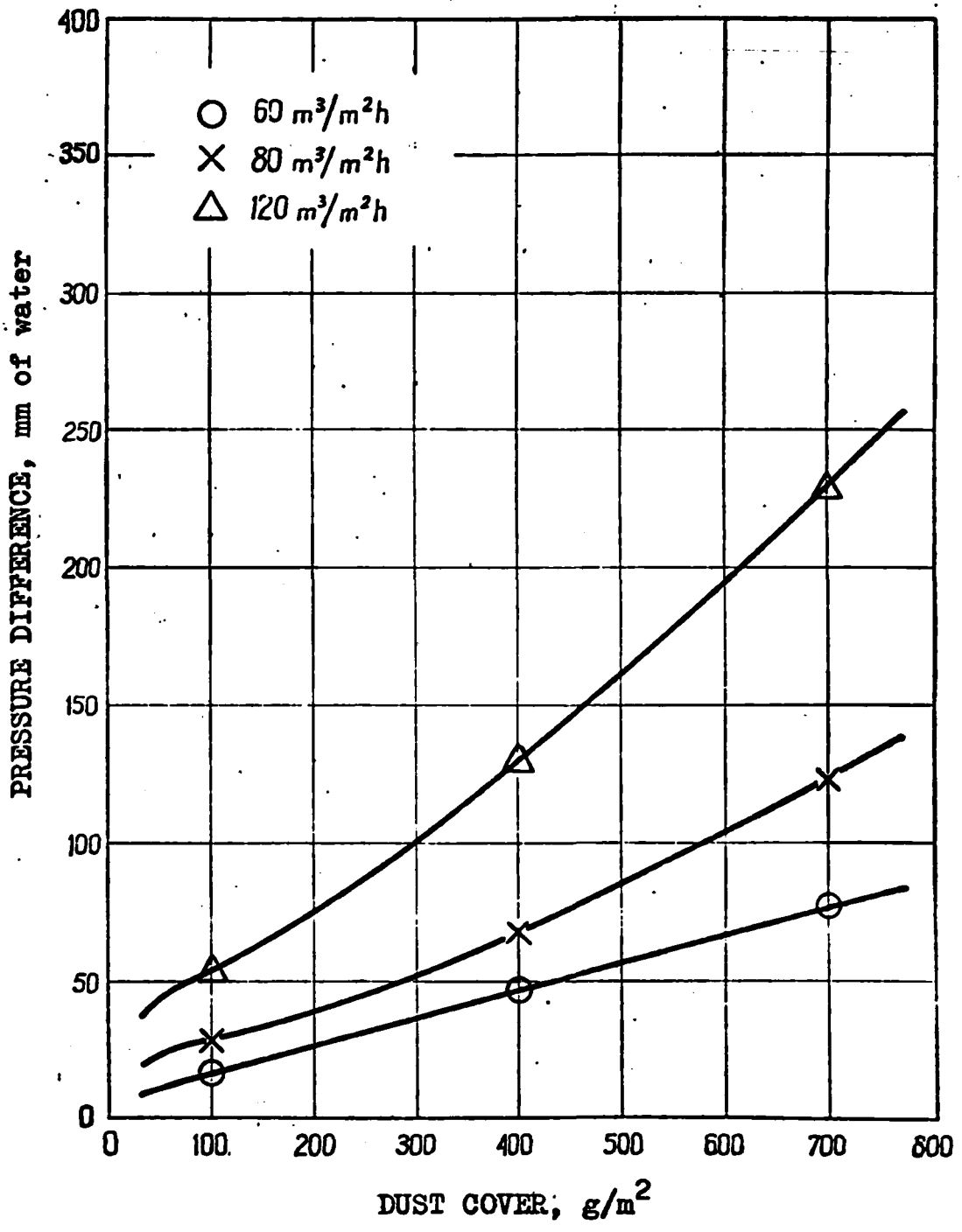

Figure A-11. Pressure Difference vs. Dust Cover for Cement Dust and Fabric ET-30 (separated dust).

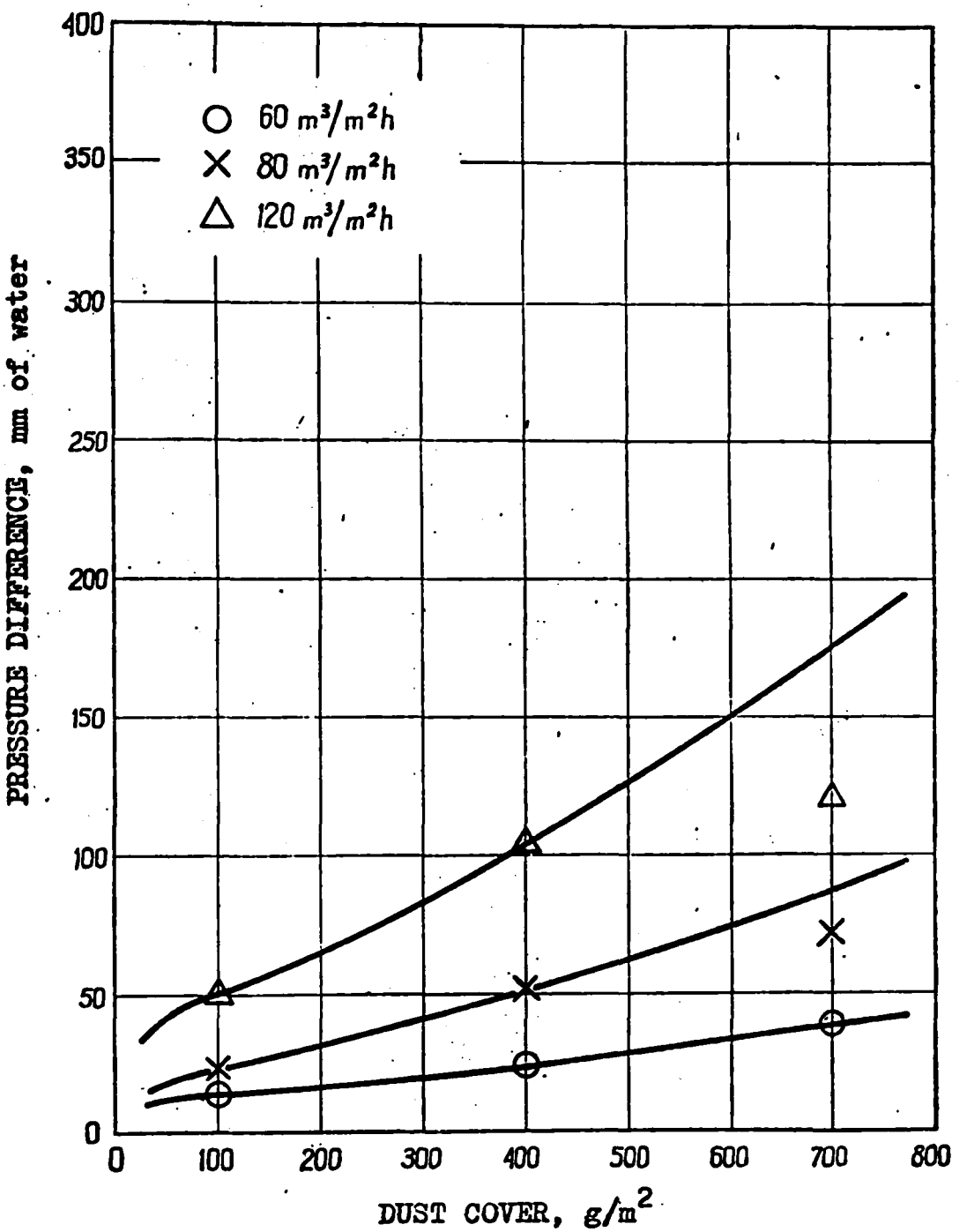

Figure A-12. Pressure Difference vs. Dust Cover for Cement Dust and Fabric ET-30 (unseparated dust).

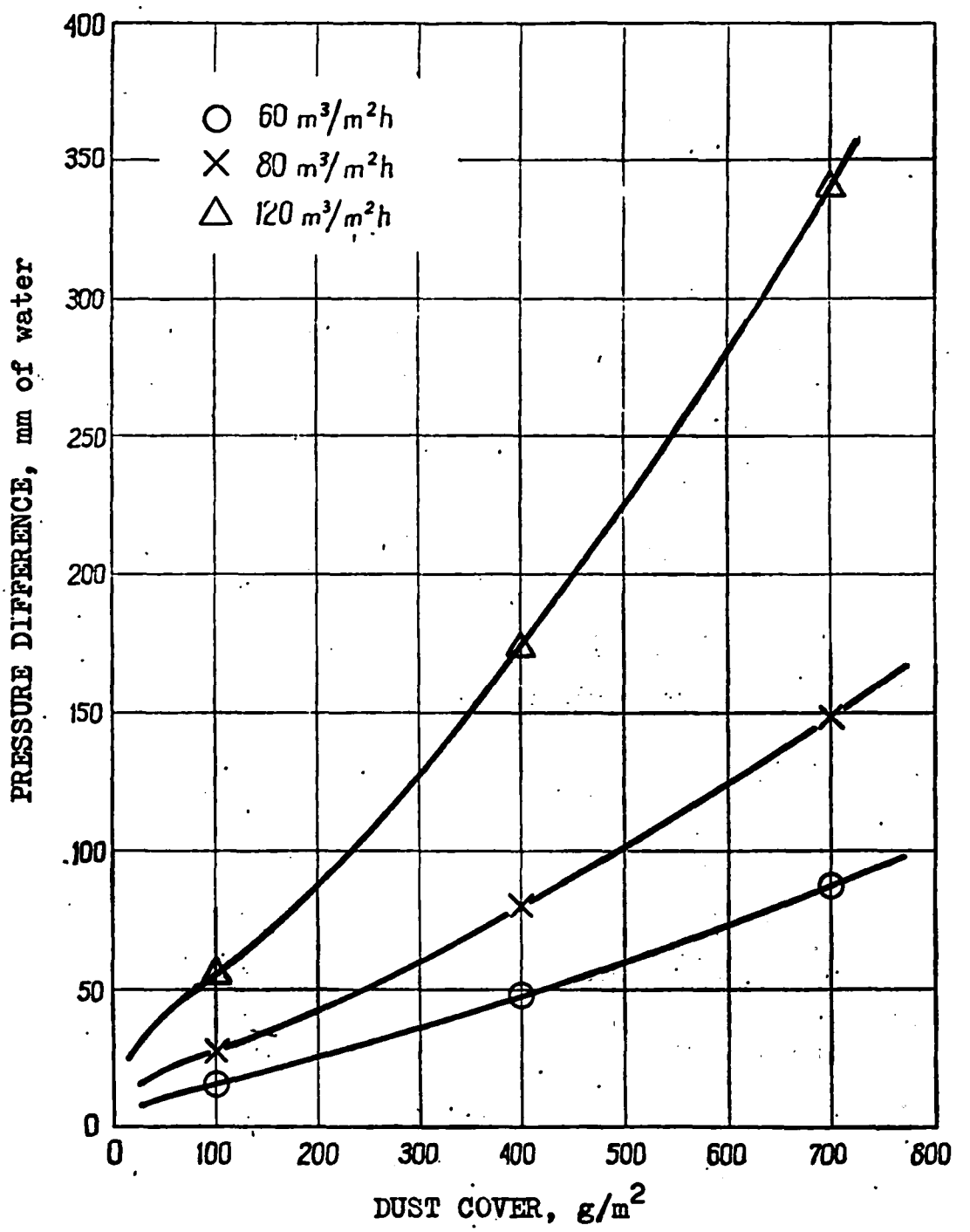

Figure A-13. Pressure Difference vs. Dust Cover for Coal Dust and Fabric ET-30 (separated dust).

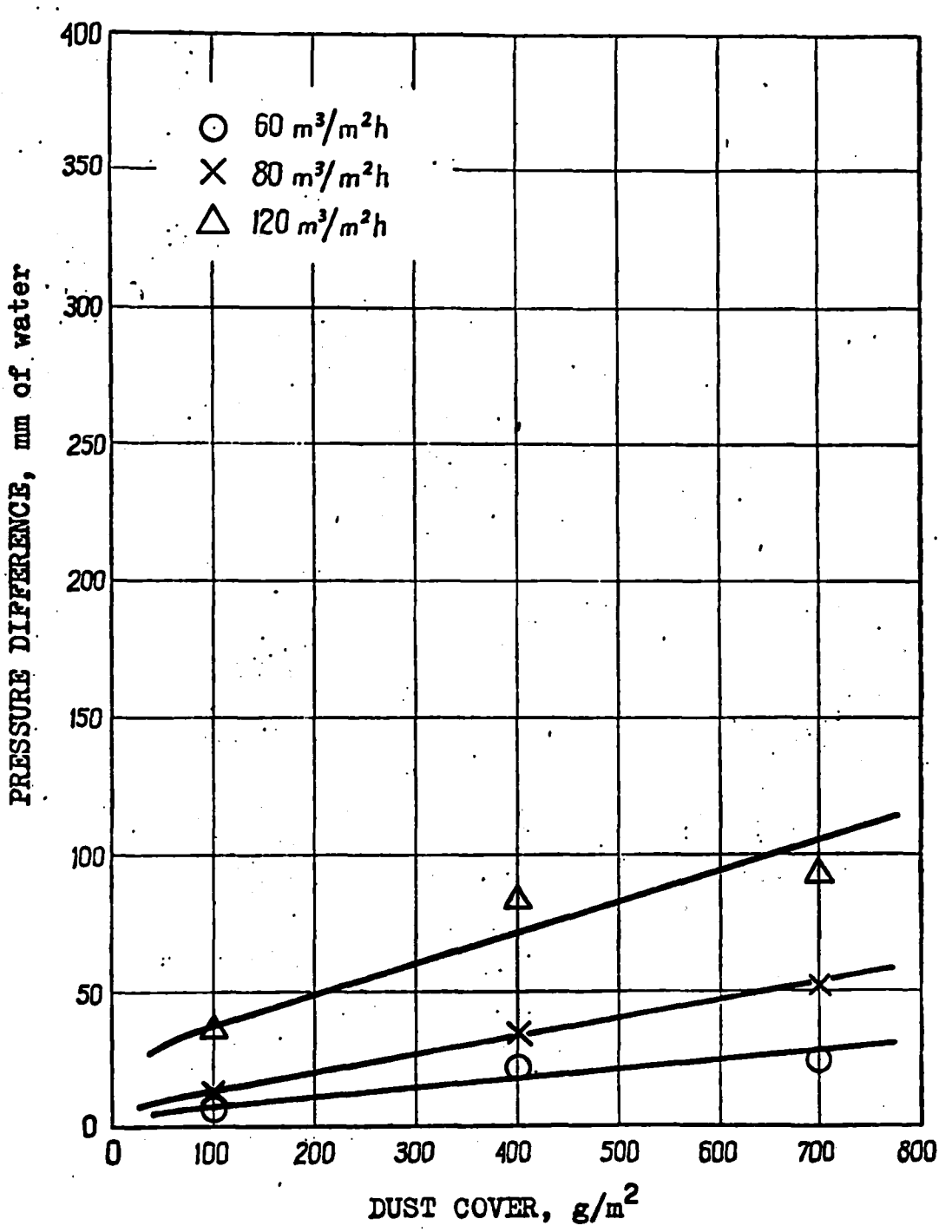

Figure A-14. Pressure Difference vs. Dust Cover for Coal Dust and Fabric ET-30 (unseparated dust).

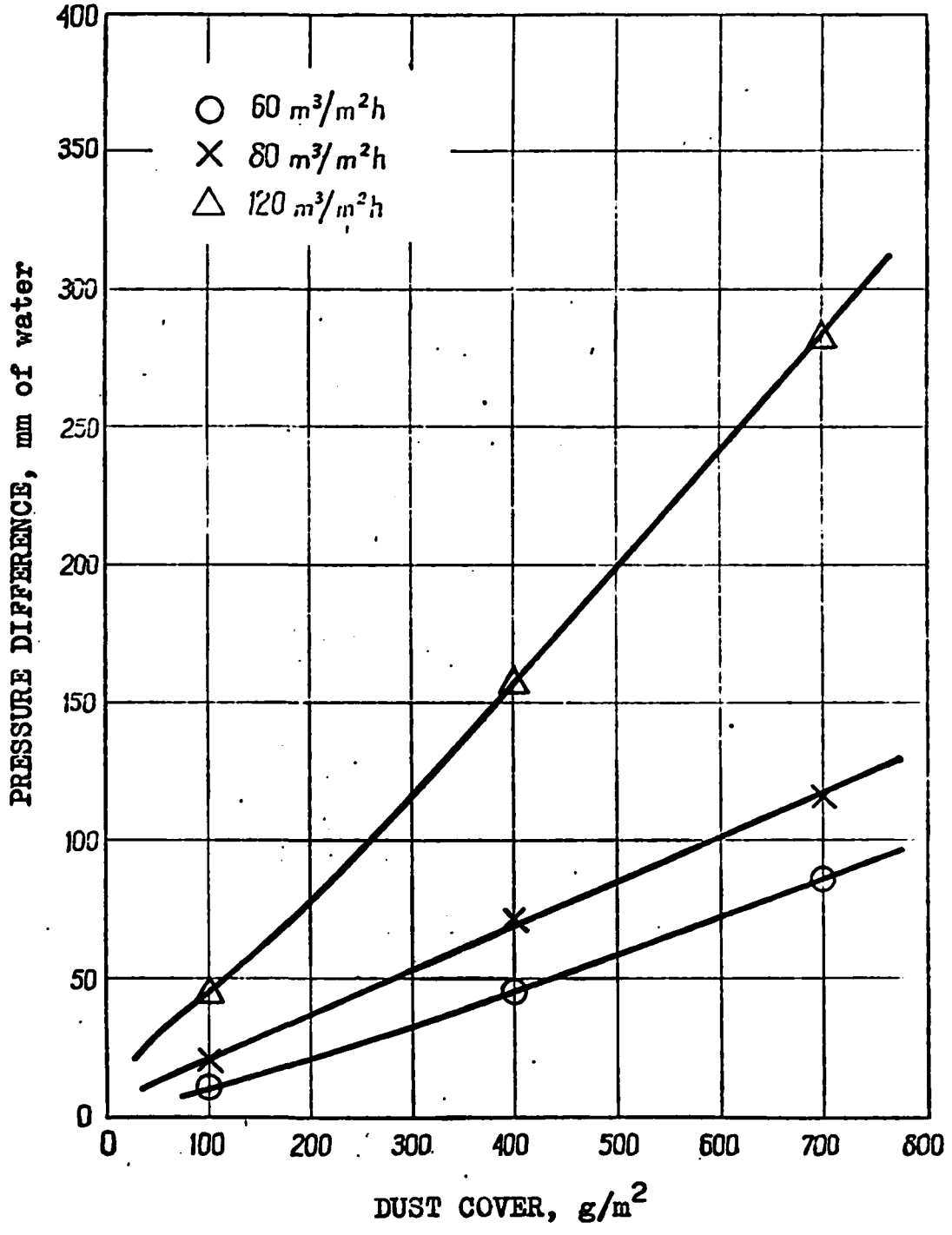

Figure A-15. Pressure Difference vs. Dust Cover for Talc Dust and Fabric ET-30 (separated dust).

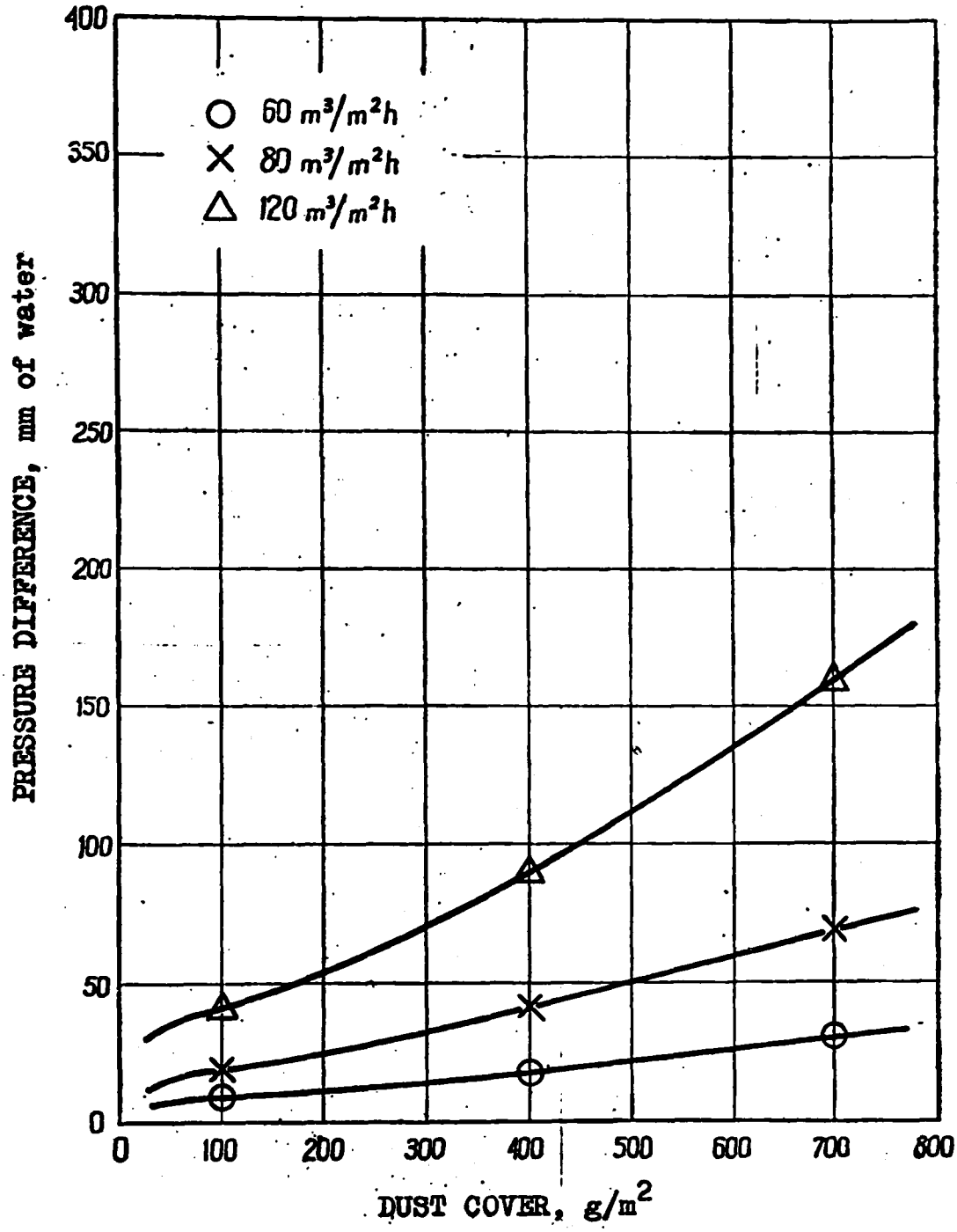

Figure A-16. Pressure Difference vs. Dust Cover for Fly Ash Dust and Fabric ET-30 (separated dust).

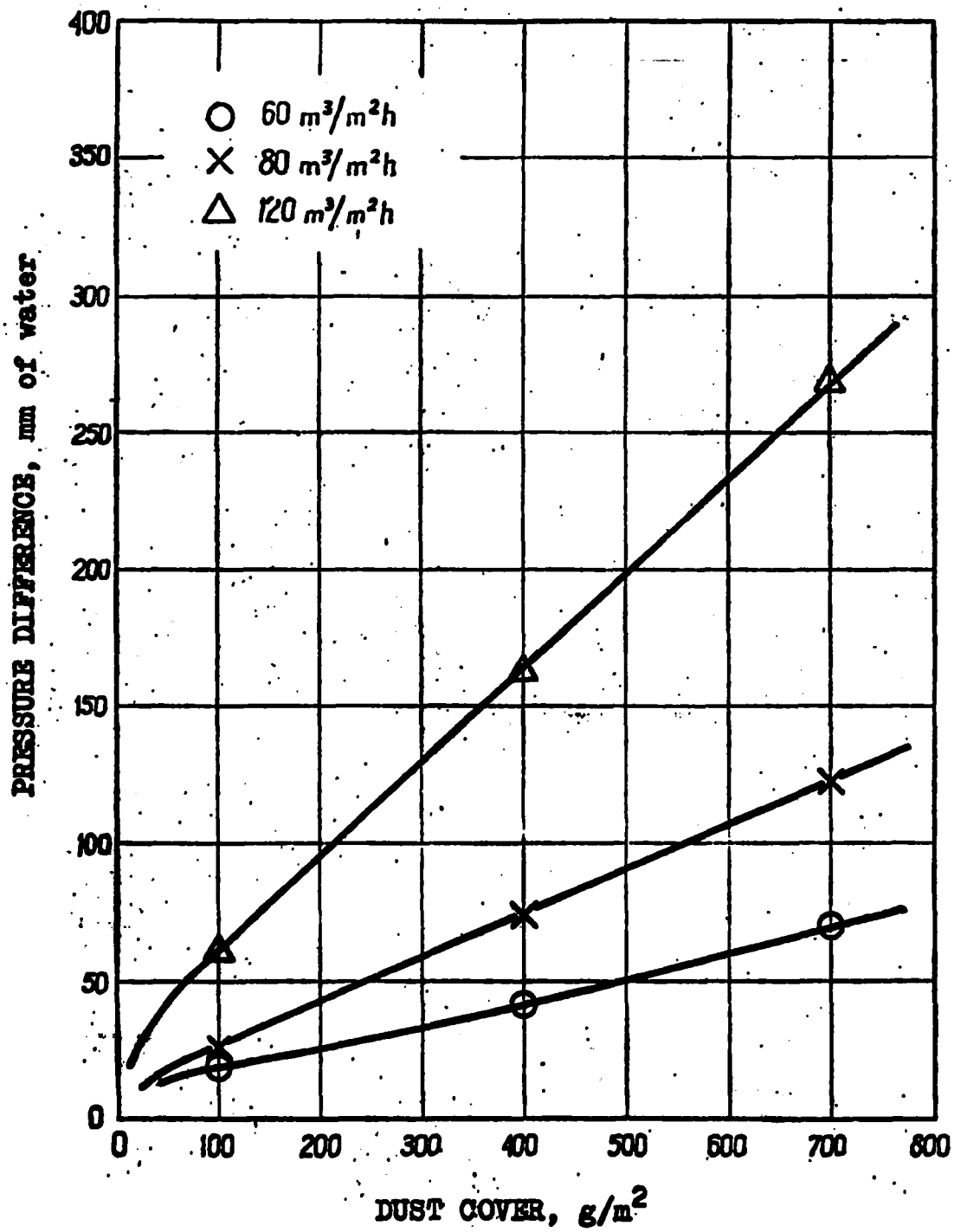

Figure A-17. Pressure Difference vs. Dust Cover for Cement Dust and Fabric F-tor 5 (separated dust).

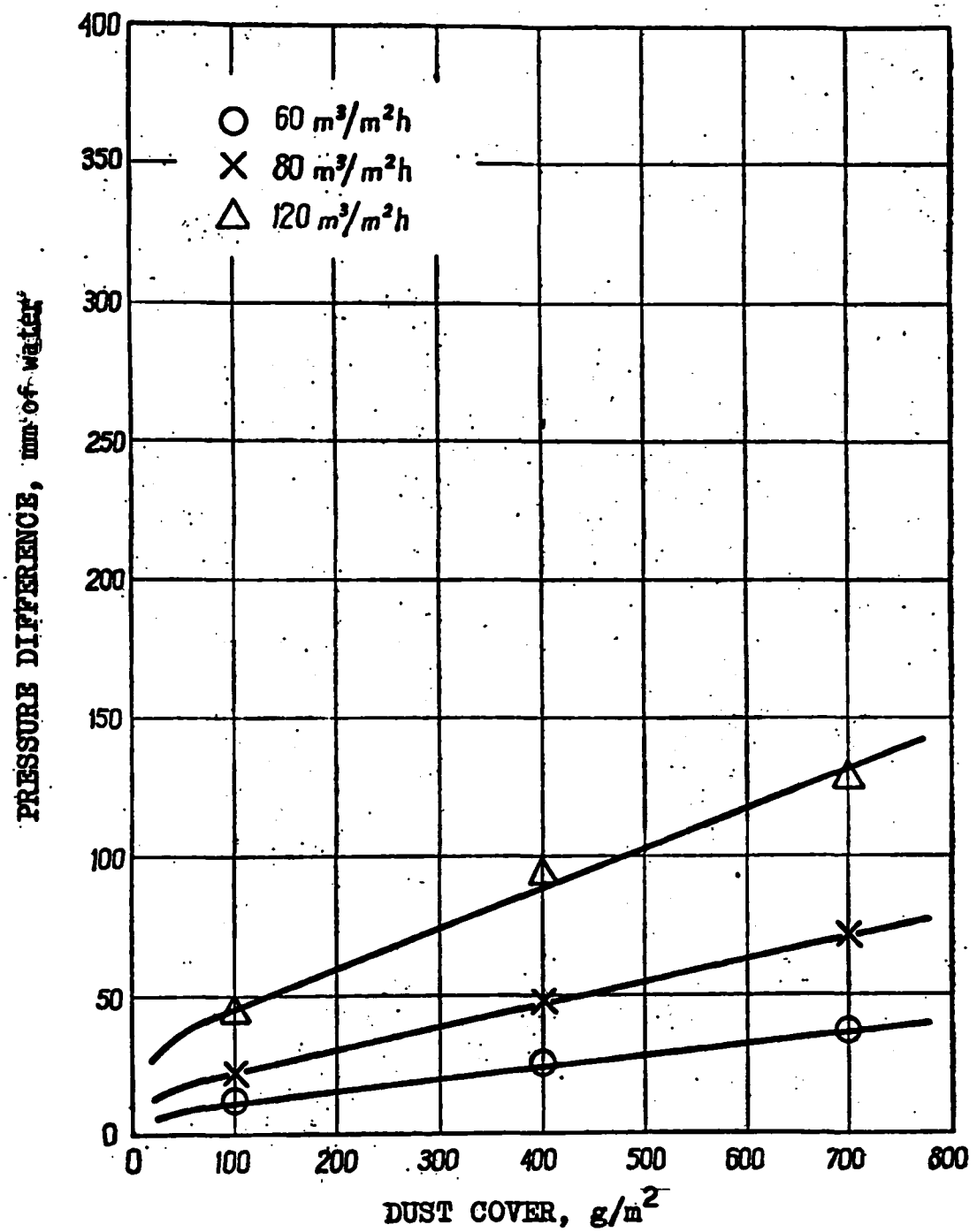

Figure A-18. Pressure Difference vs. Dust Cover for Cement Dust and Fabric F-tor 5 (unseparated dust).

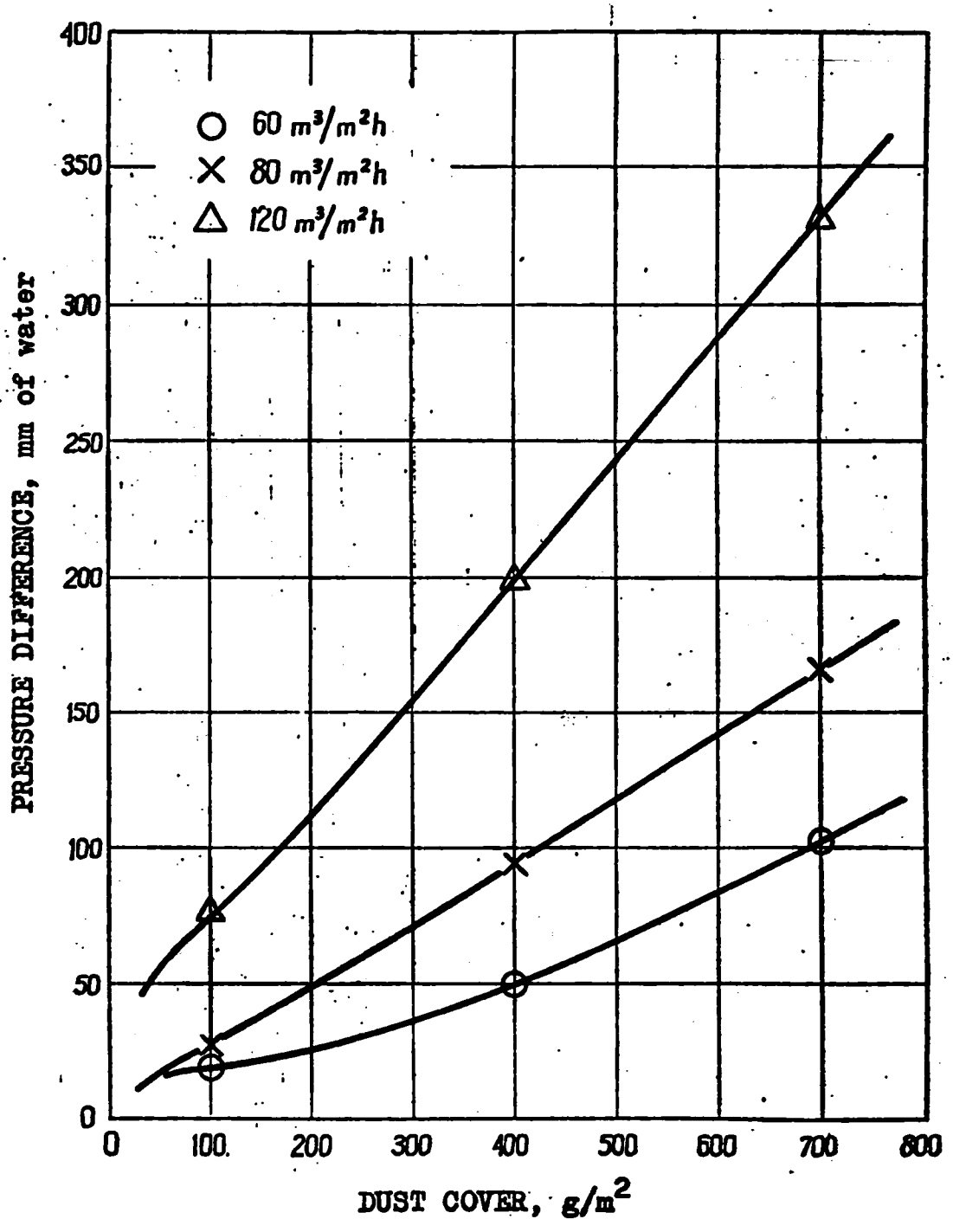

Figure A-19. Pressure Difference vs. Dust Cover for Coal Dust and Fabric F-tor 5 (separated dust).

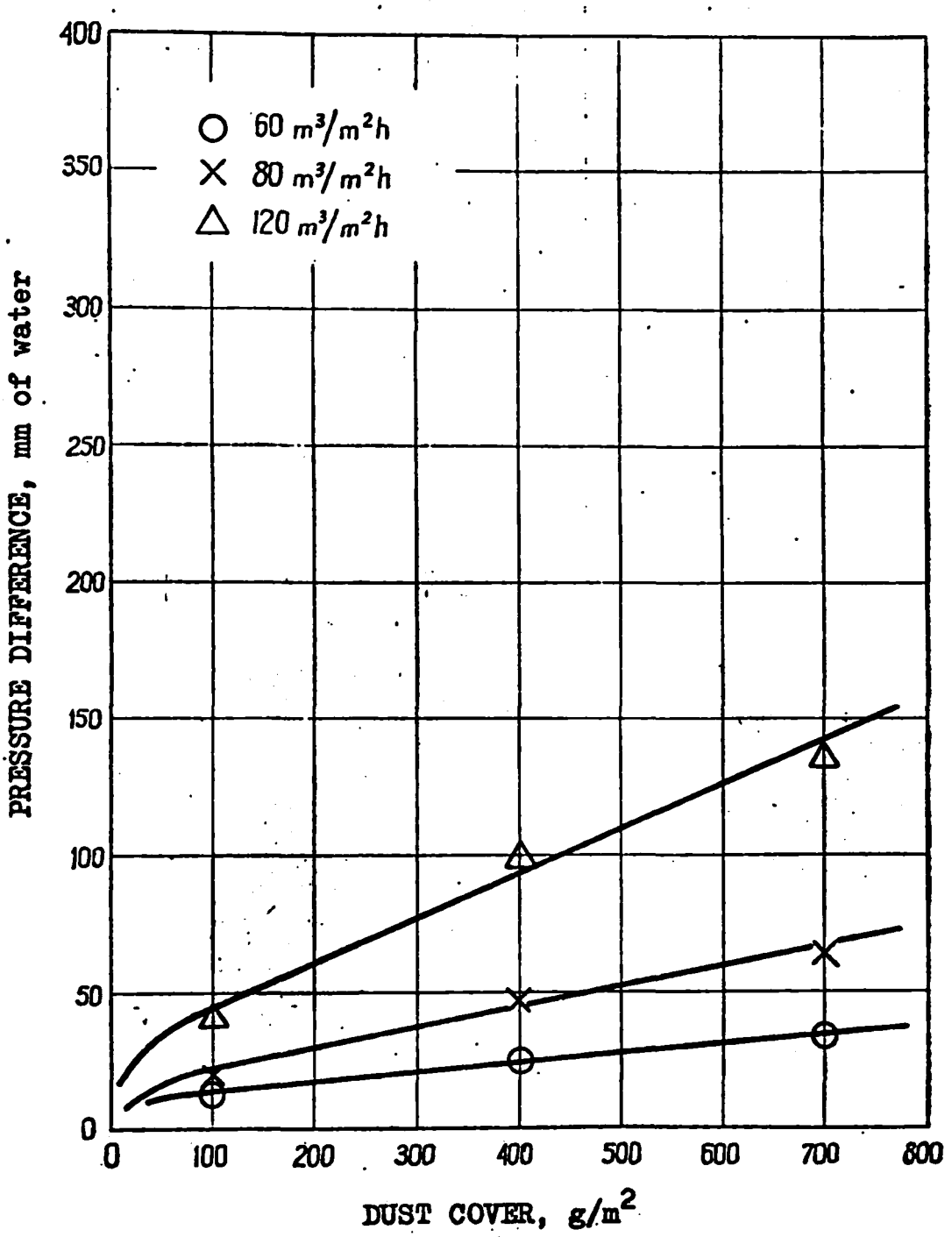

Figure A-20. Pressure Difference vs. Dust Cover for Coal Dust and Fabric F-tor 5 (unseparated dust).

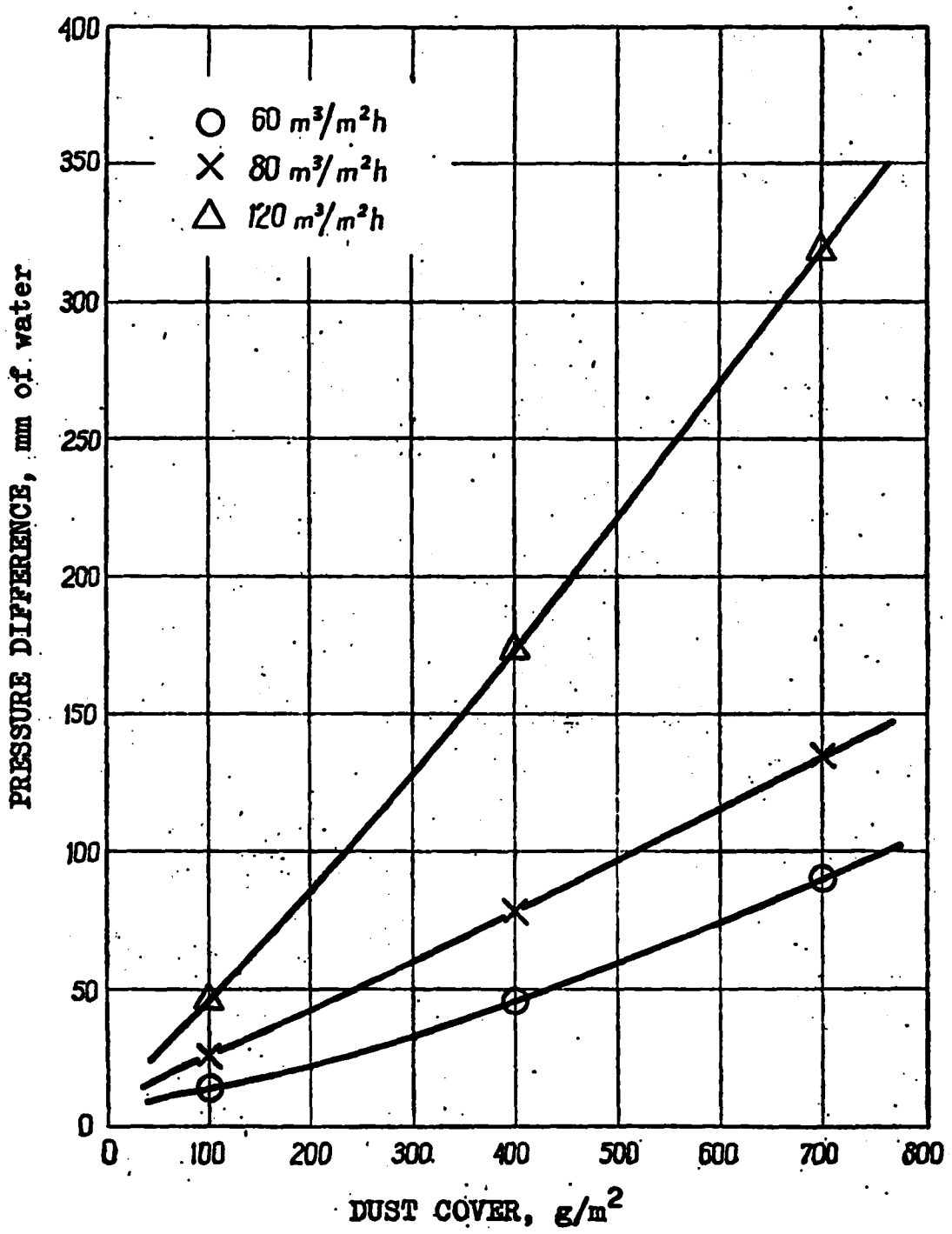

Figure A-21. Pressure Difference vs. Dust Cover for Talc Dust and Fabric F-tor 5 (separated dust).

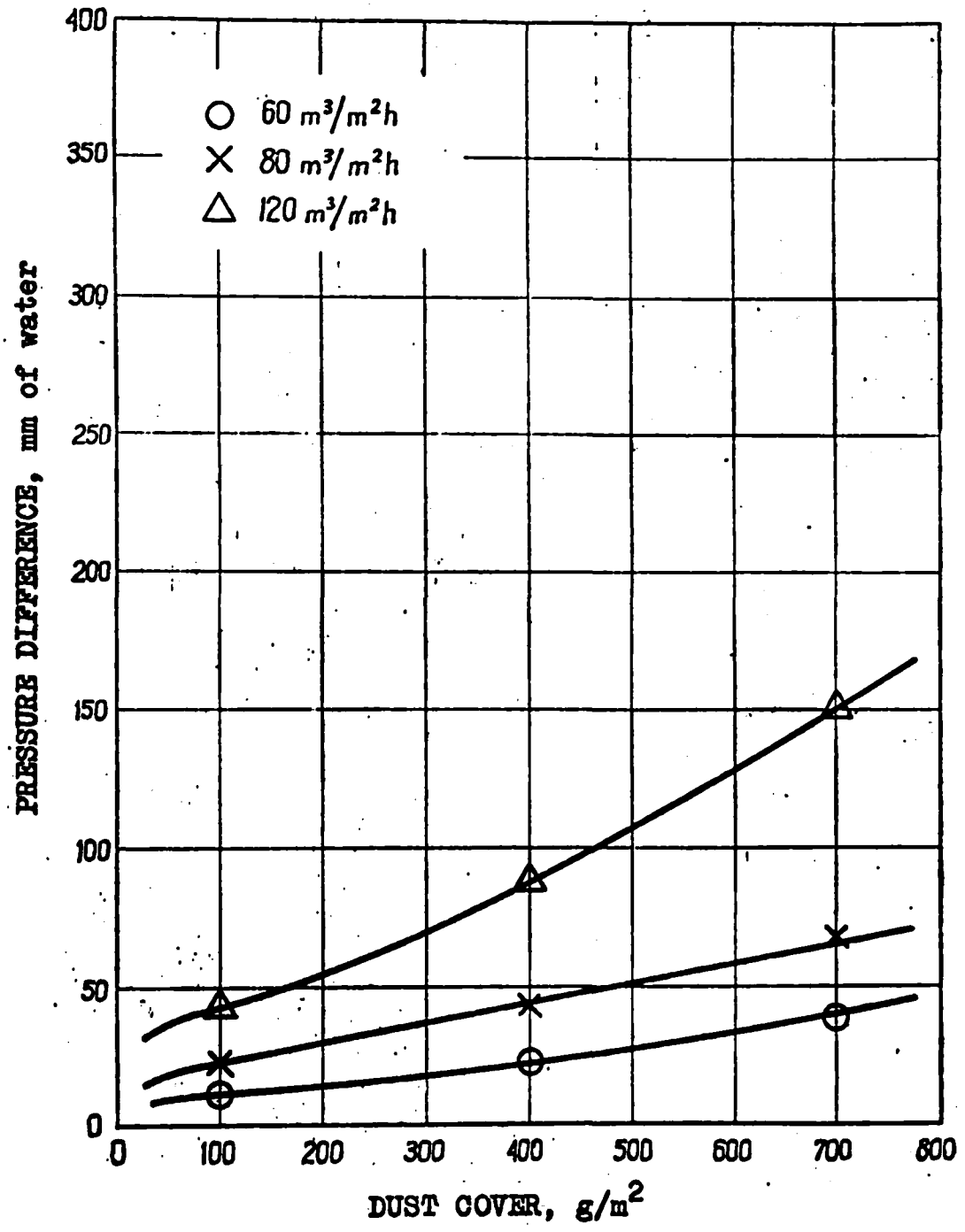

Figure A-22. Pressure Difference vs. Dust Cover for Fly Ash Dust and Fabric F-tor 5 (separated dust).

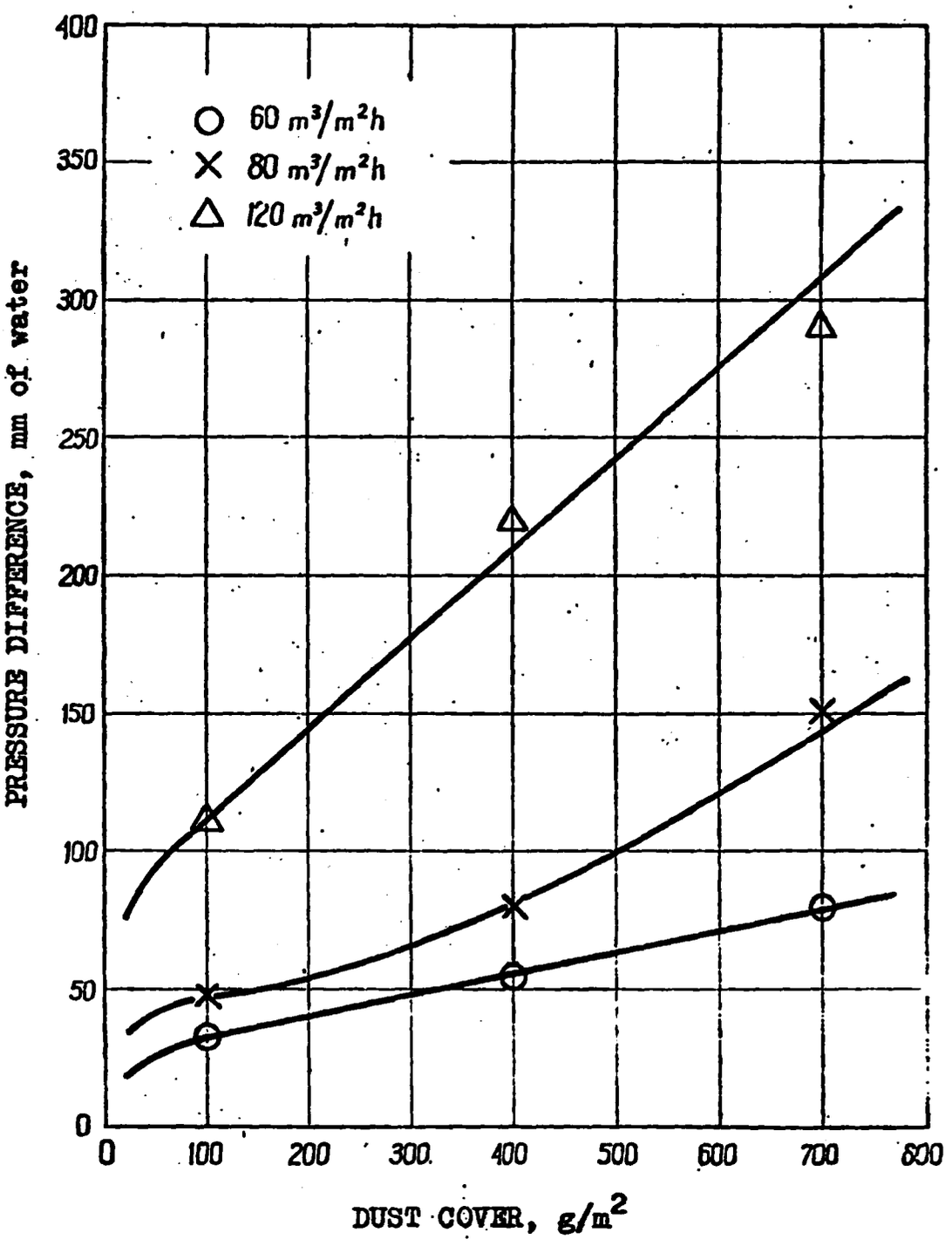

Figure A-23. Pressure Difference vs. Dust Cover for Cement Dust and Fabric PT-15 (separated dust).

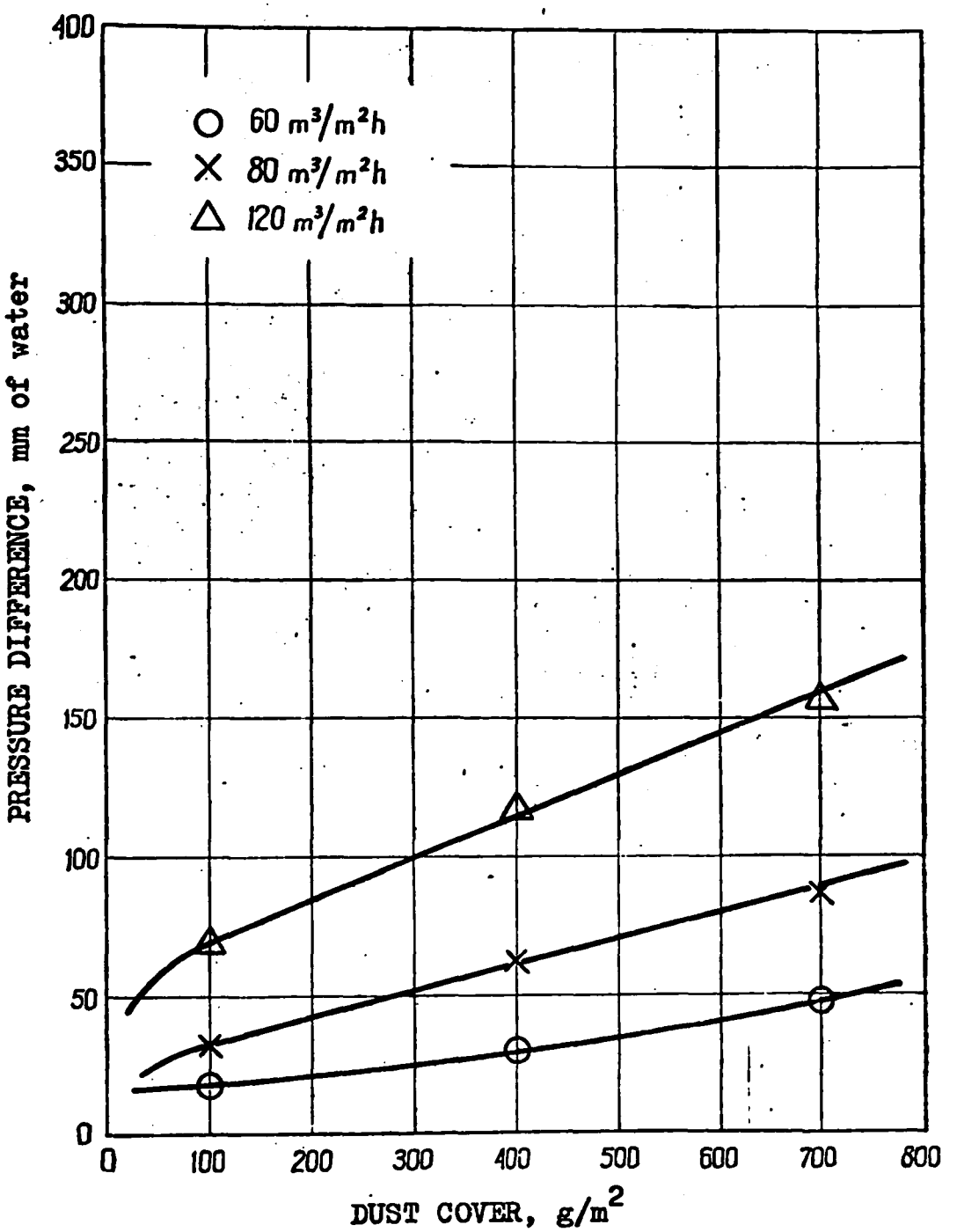

Figure A-24. Pressure Difference vs. Dust Cover for Cement Dust and Fabric PT-15 (unseparated dust).

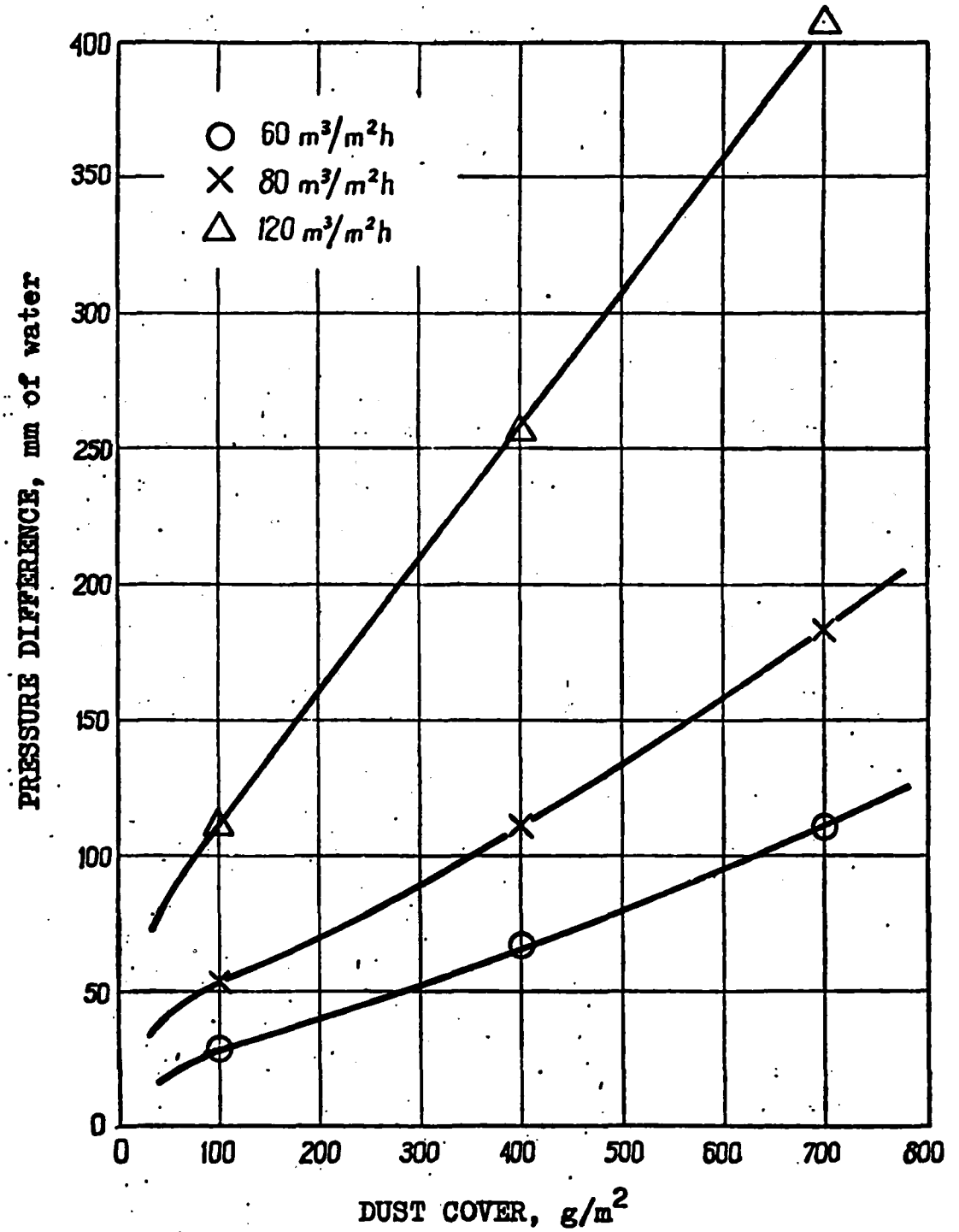

Figure A-25. Pressure Difference vs. Dust Cover for Coal Dust and Fabric PT-15 (separated dust).

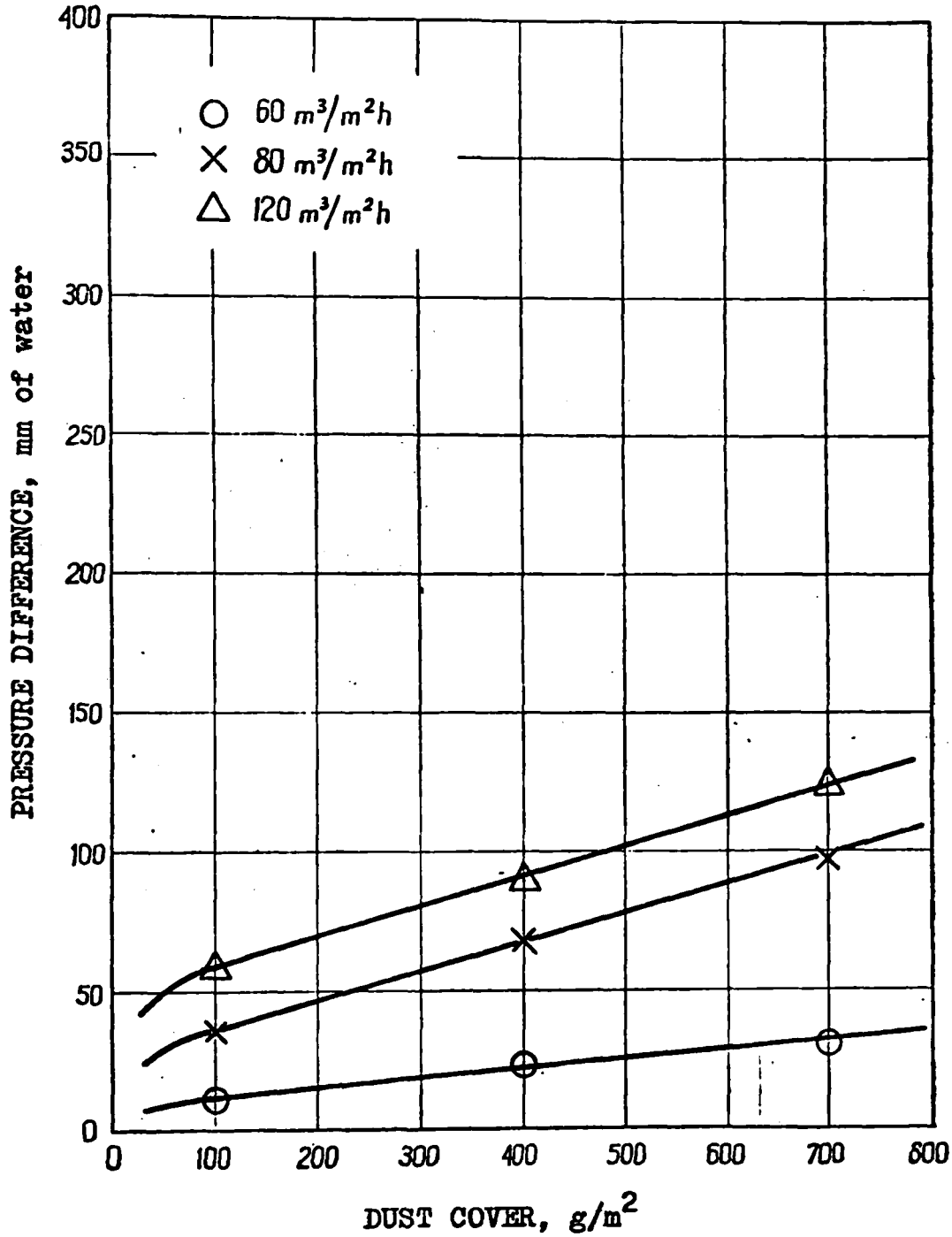

Figure A-26. Pressure Difference vs. Dust Cover for Coal Dust and Fabric PT-15 (unseparated dust)

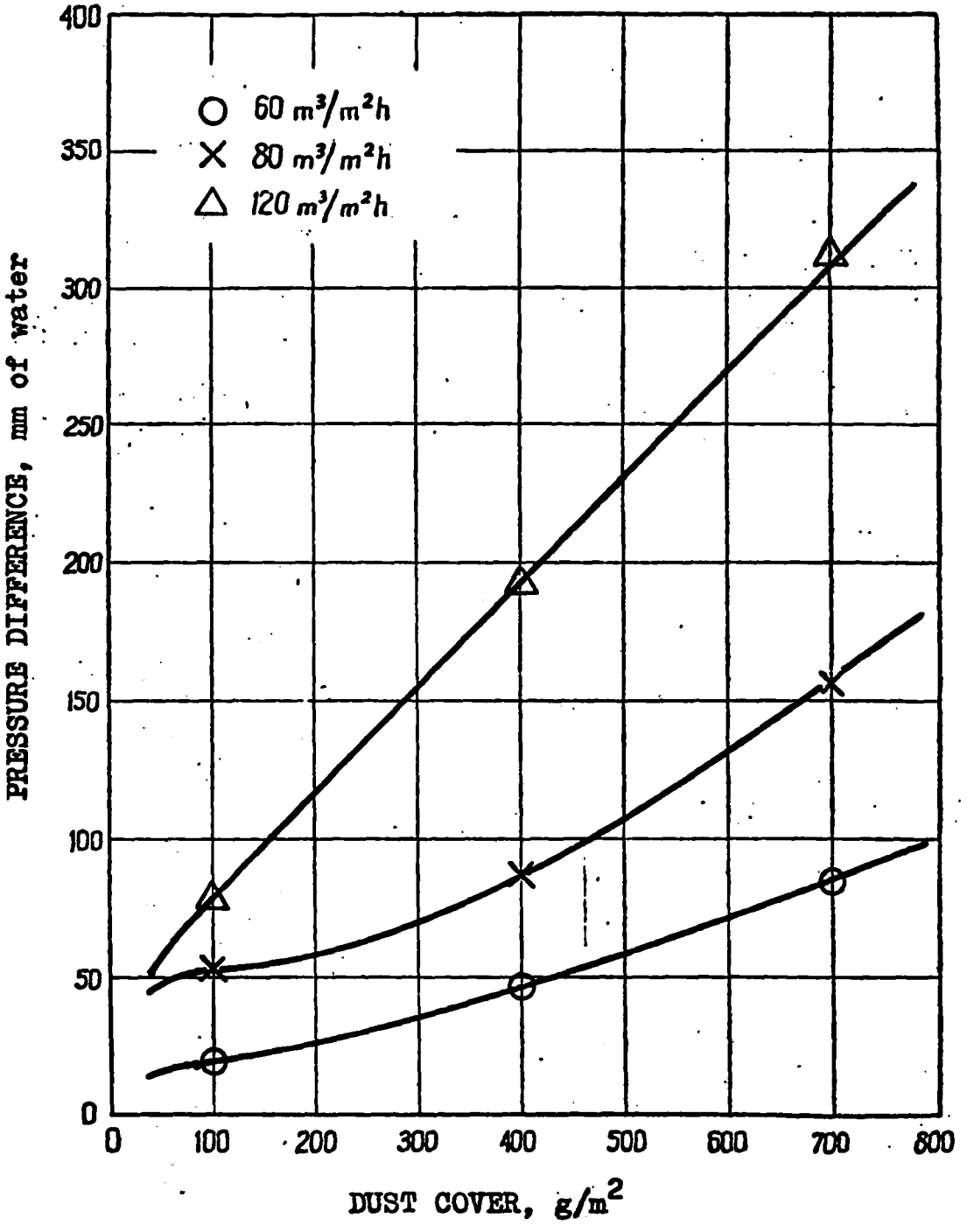

Figure A-27. Pressure Difference vs. Dust Cover for Talc Dust and Fabric PT-15 (separated dust)

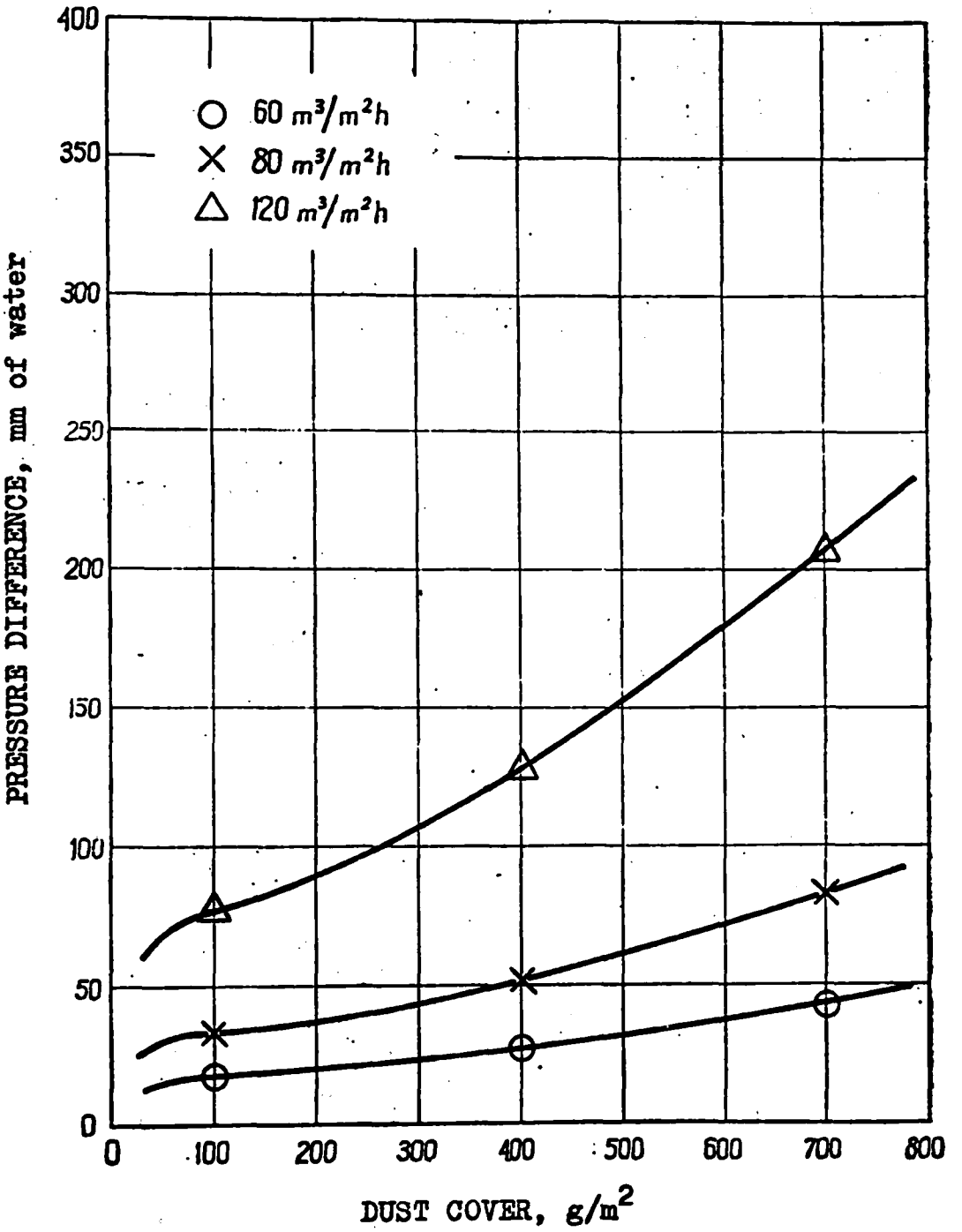

Figure A-28. Pressure Difference vs. Dust Cover for Fly Ash Dust and Fabric PT-15 (separated dust).

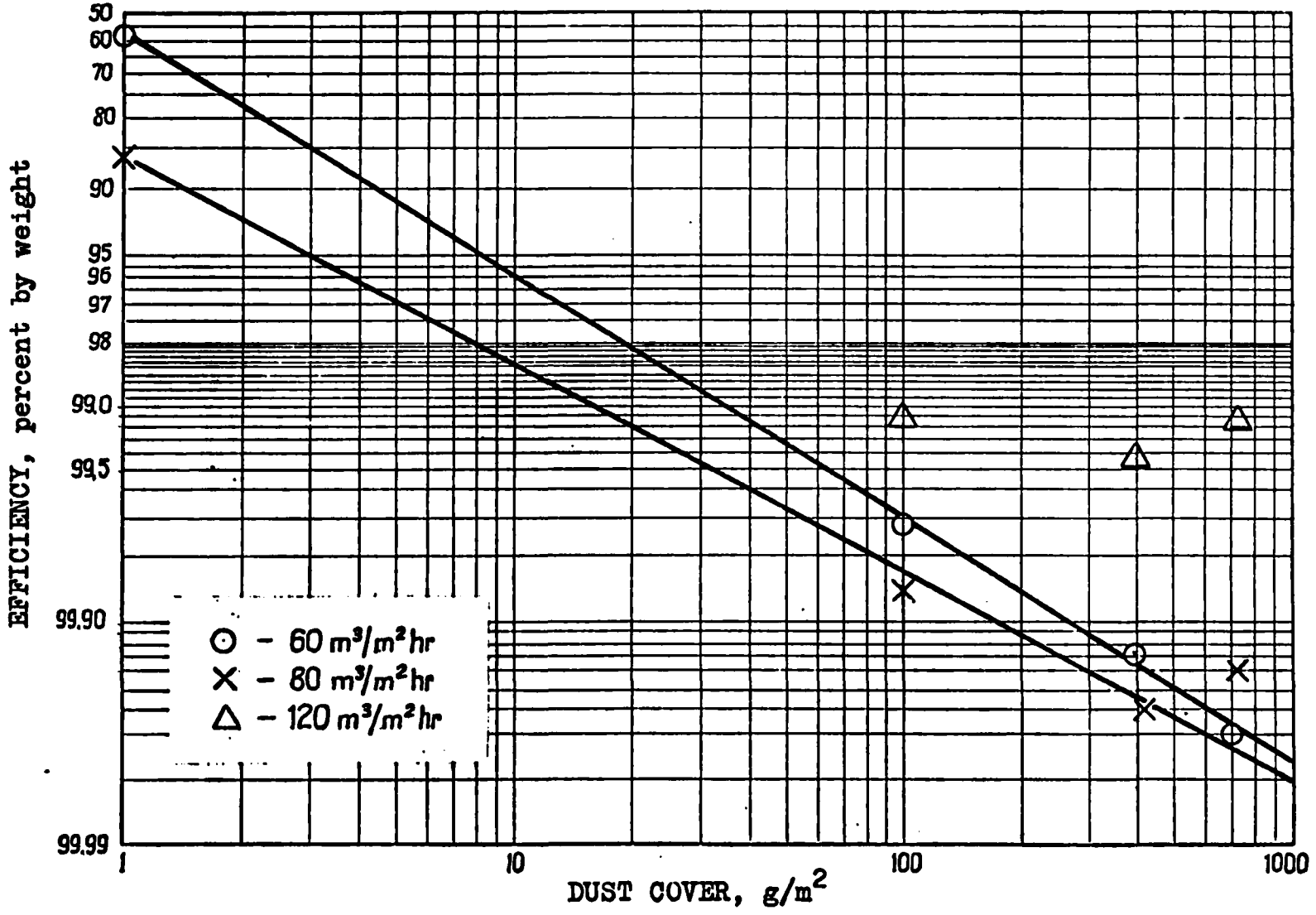

Figure A-29. Theoretical Laboratory Efficiency for Cement Dust and Fabric ET-4 (Separated dust).

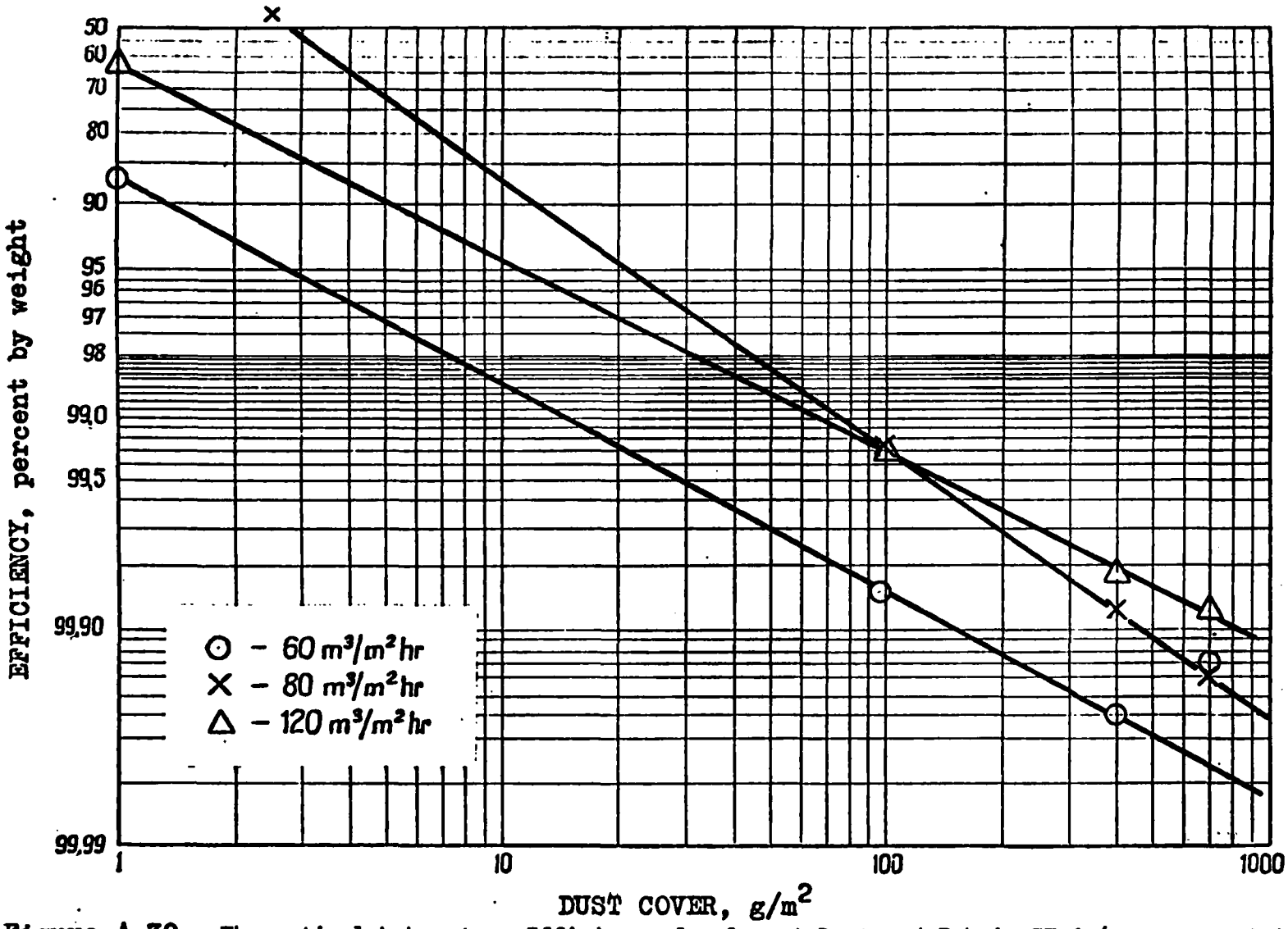

Figure A-30. Theoretical Laboratory Efficiency for Cement Dust and Fabric ET-4 (unseparated dust).

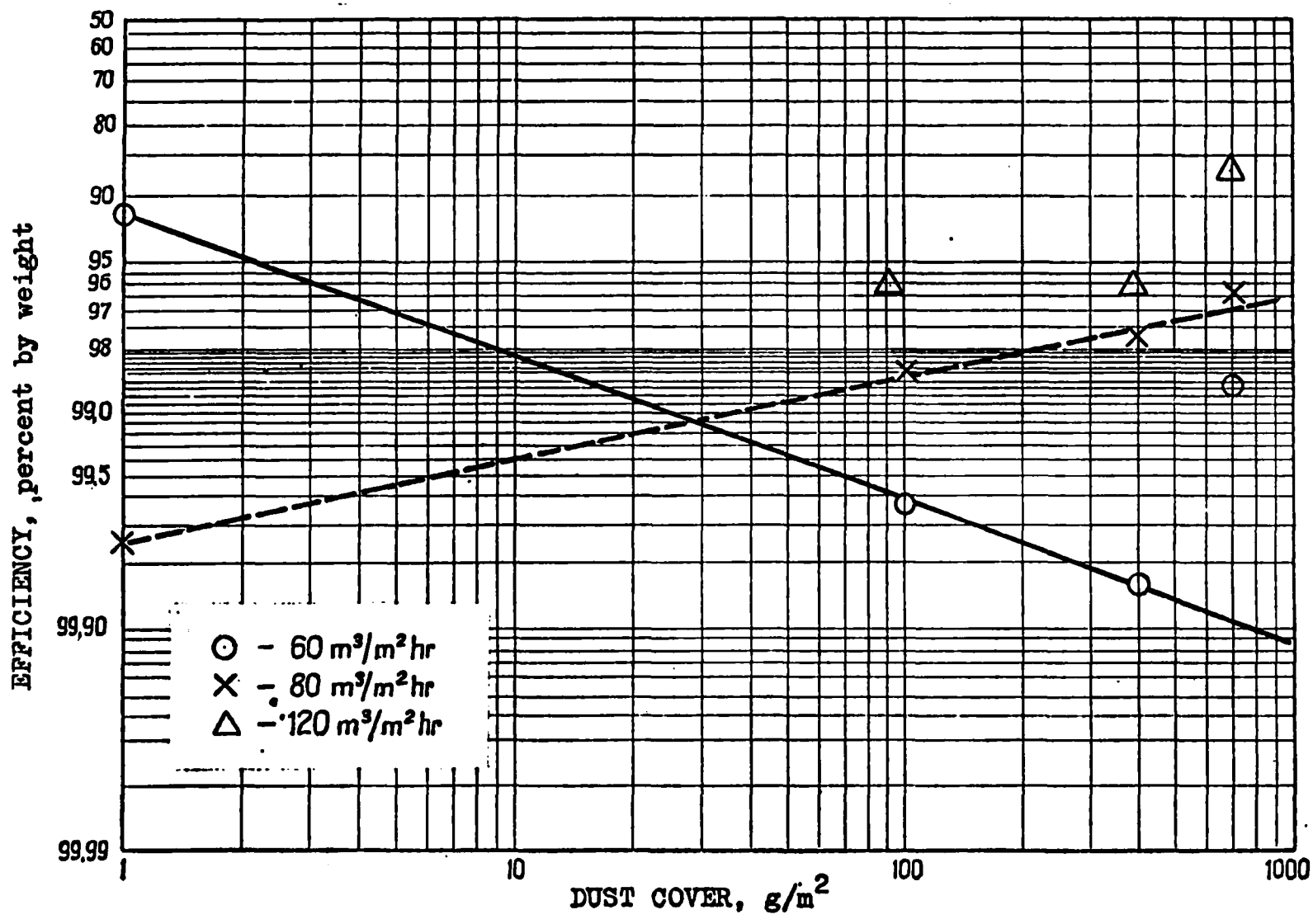

Figure A-31. Theoretical Laboratory Efficiency for Coal Dust and Fabric ET-4 (separated dust).

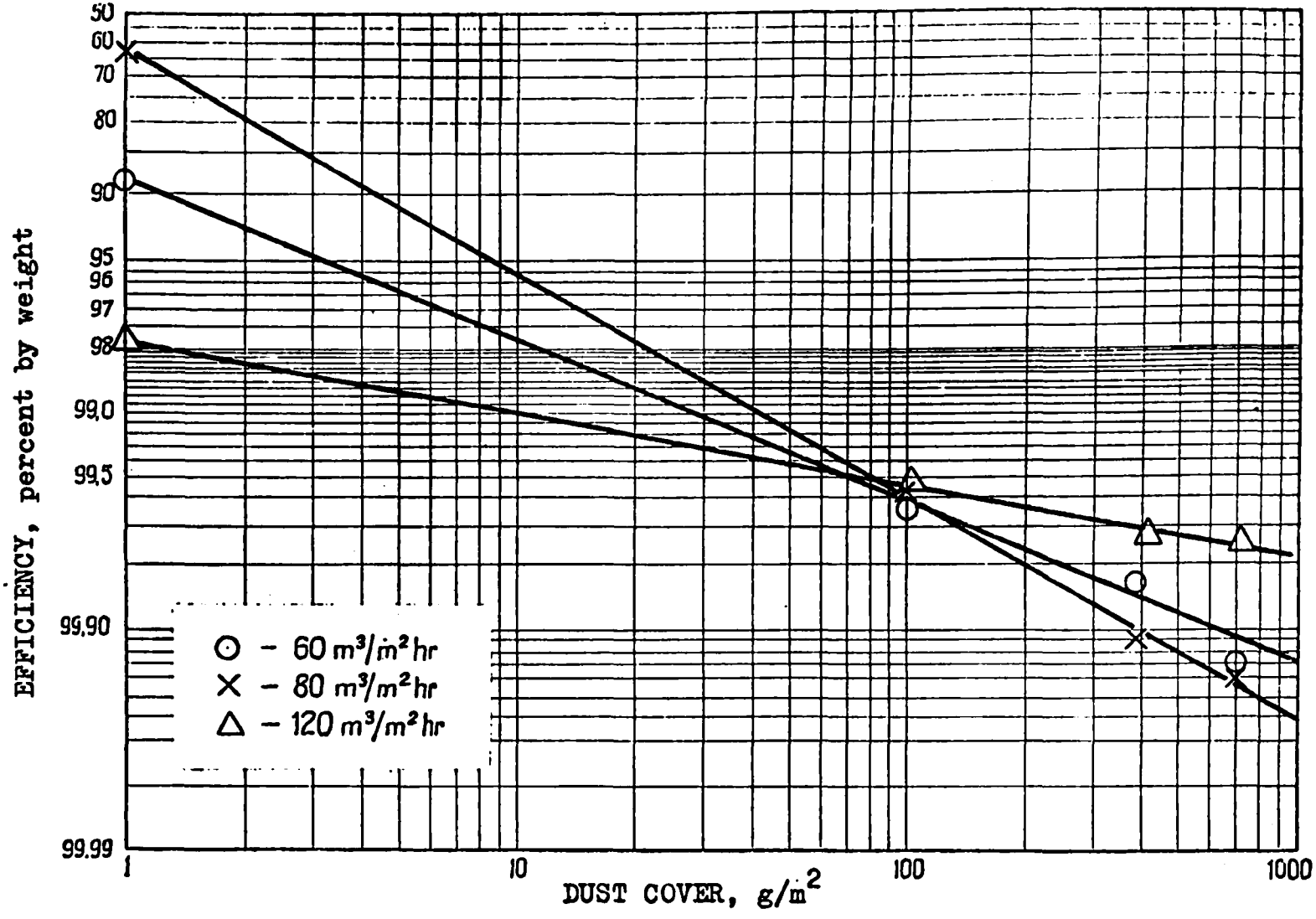

Figure A-32. Theoretical Laboratory Efficiency for Coal Dust (unseparated dust) and Fabric ET-4.

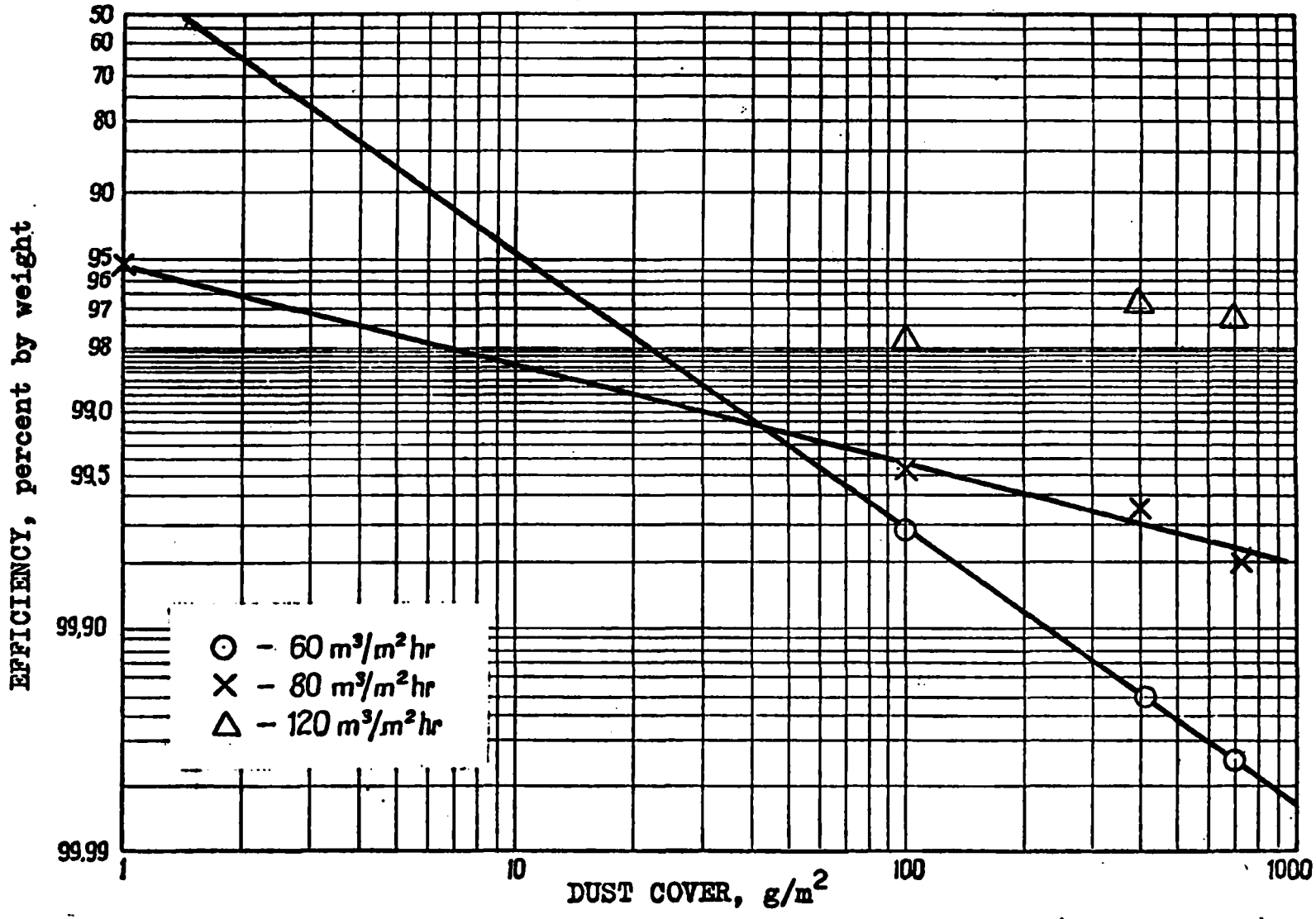

Figure A-33. Theoretical Laboratory Efficiency for Talc Dust and Fabric ET-4 (separated dust).

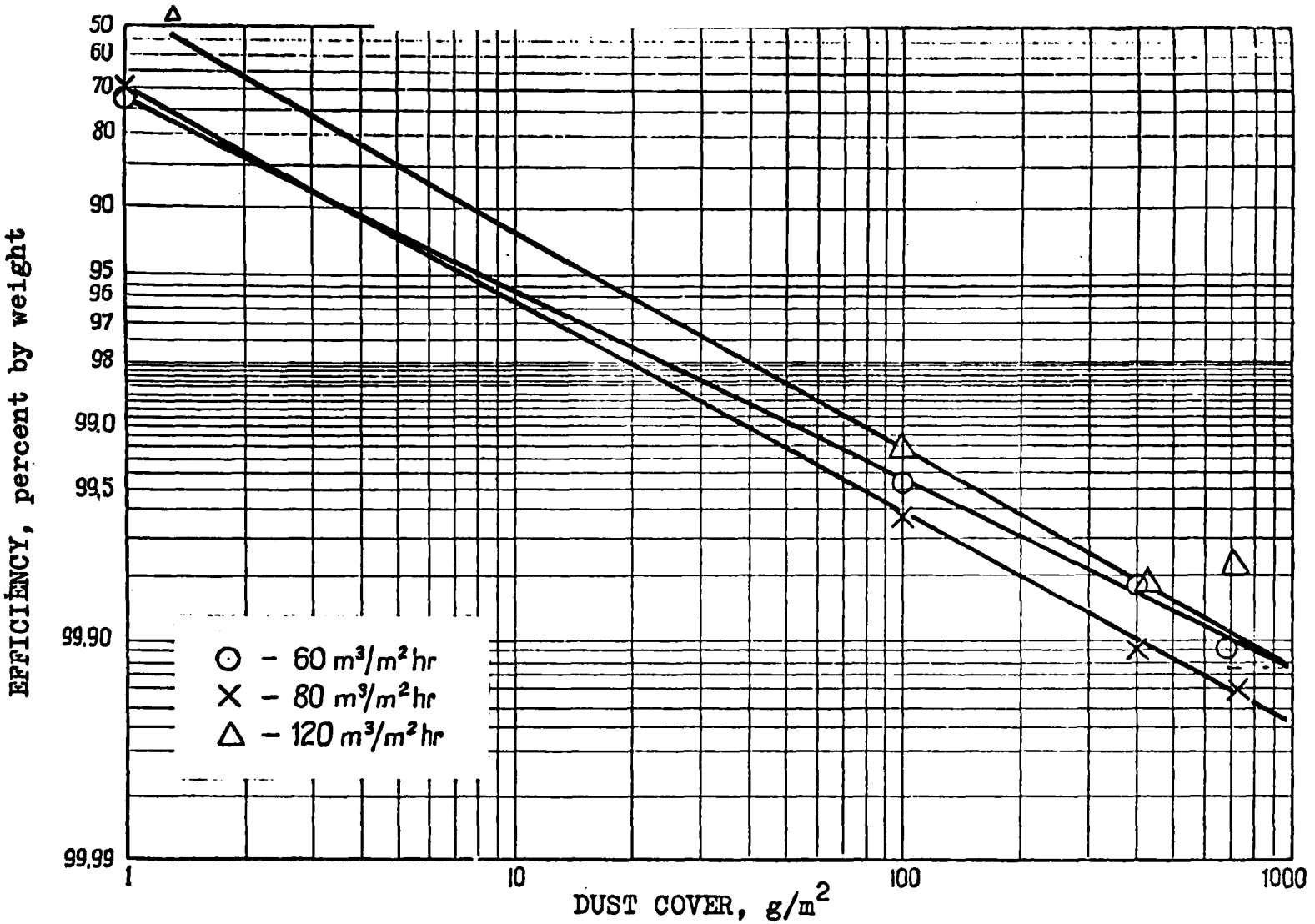

Figure A-34. Theoretical Laboratory Efficiency for Fly Ash and Fabric ET-4 (separated dust).

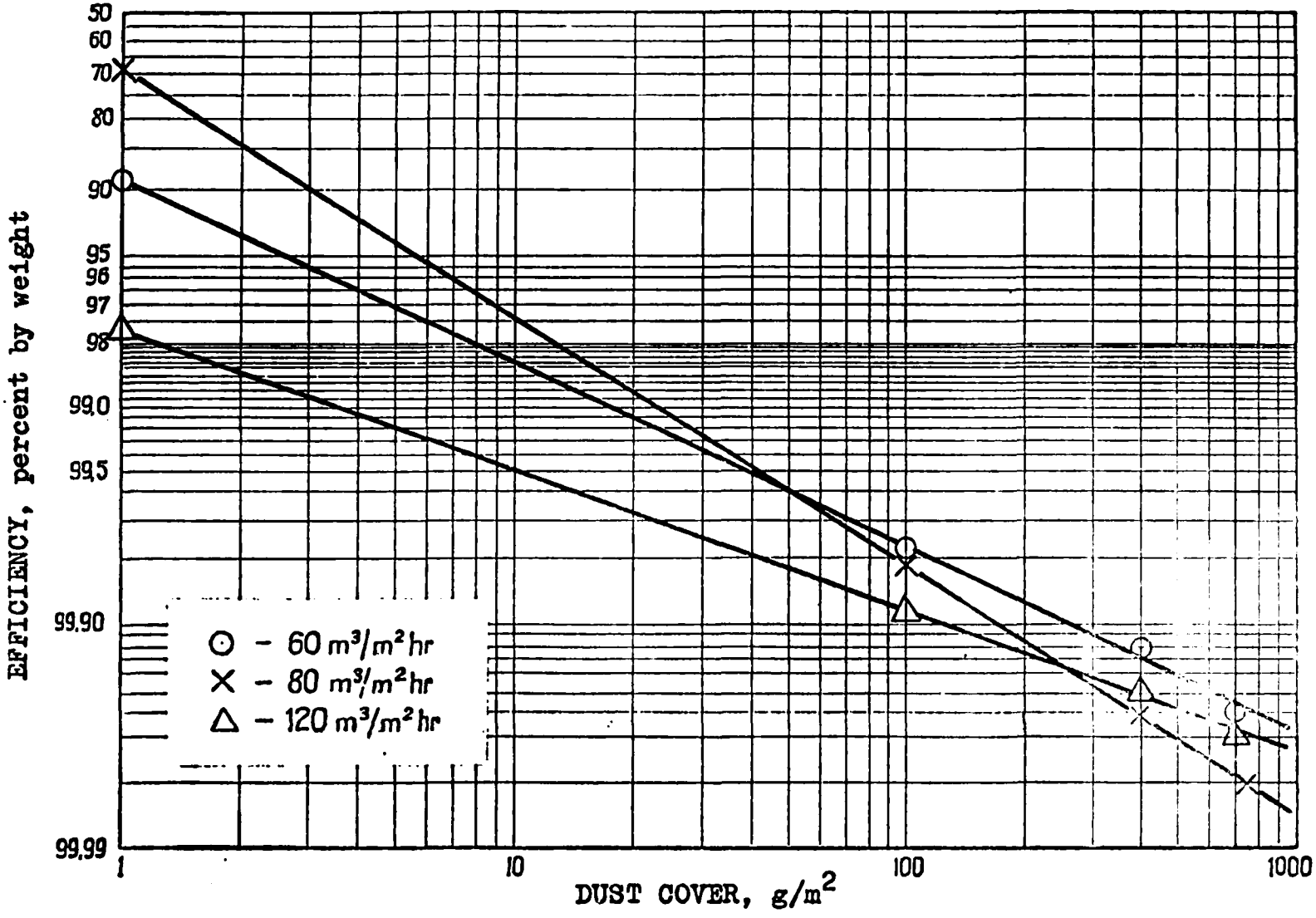

Figure A-35. Theoretical Laboratory Efficiency for Cement Dust and Fabric ET-30 (separated dust).

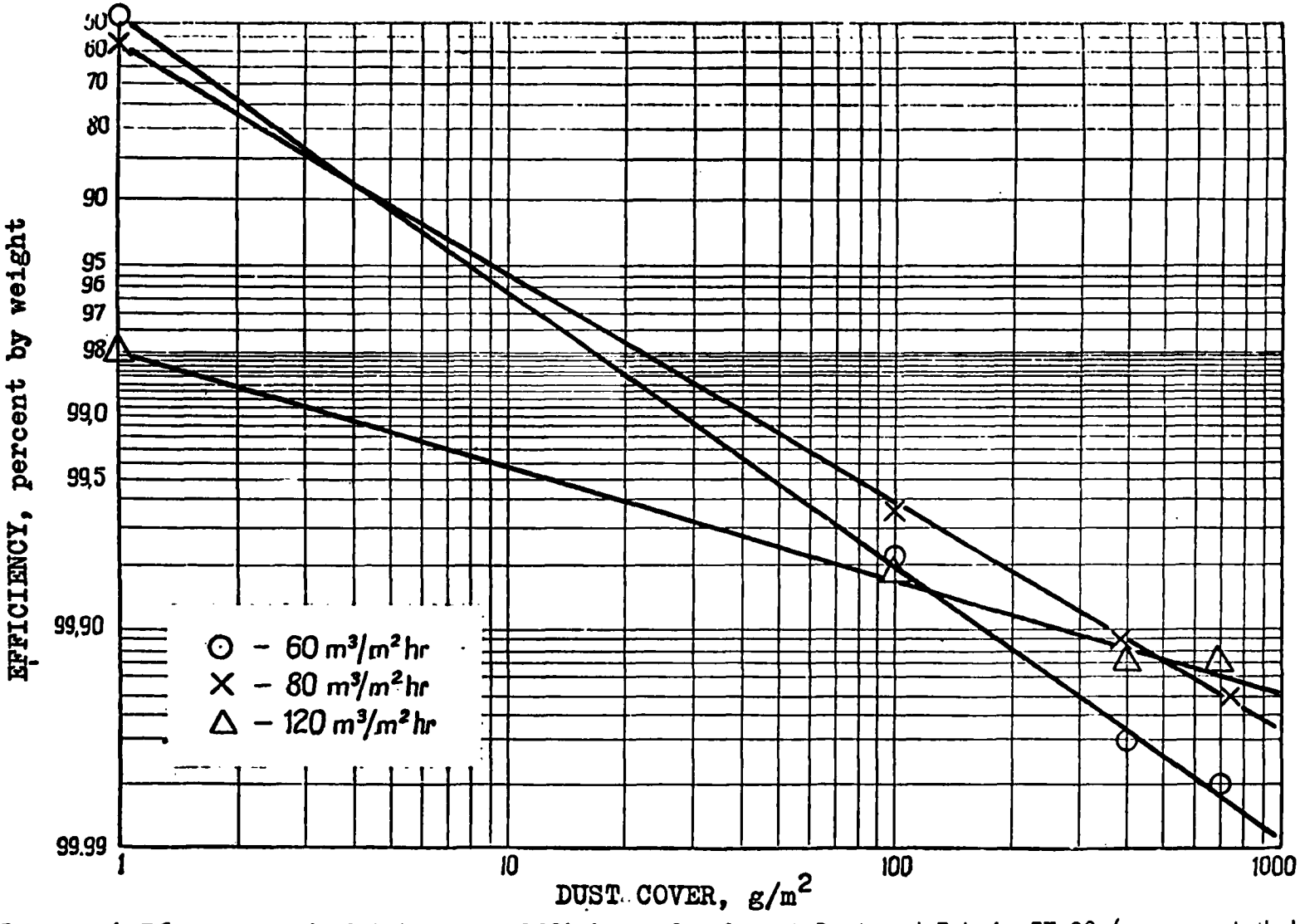

Figure A-36. Theoretical Laboratory Efficiency for Cement Dust and Fabric ET-30 (unseparated dust).

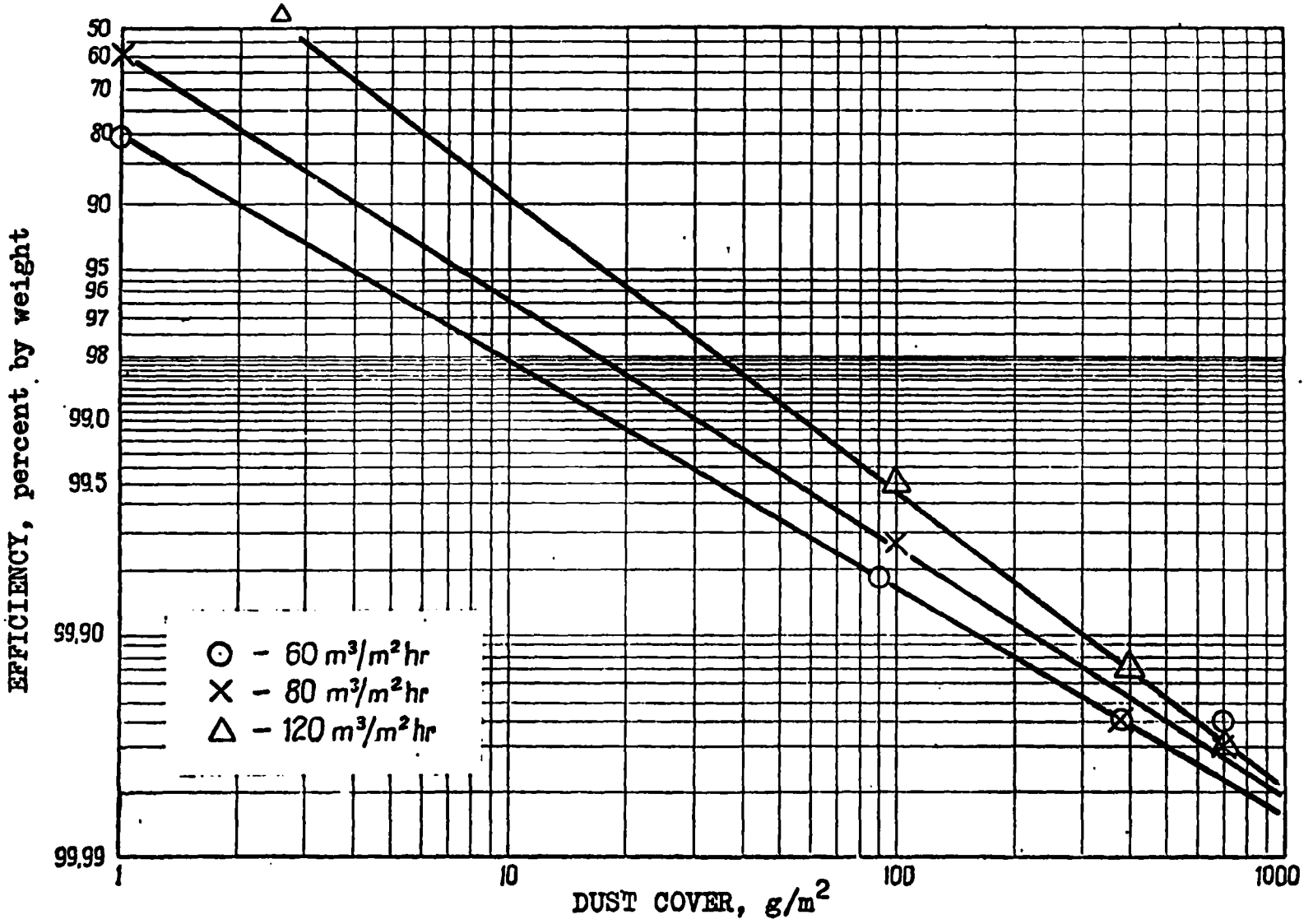

Figure A-37. Theoretical Laboratory Efficiency for Coal Dust and Fabric ET-30 (separated dust).

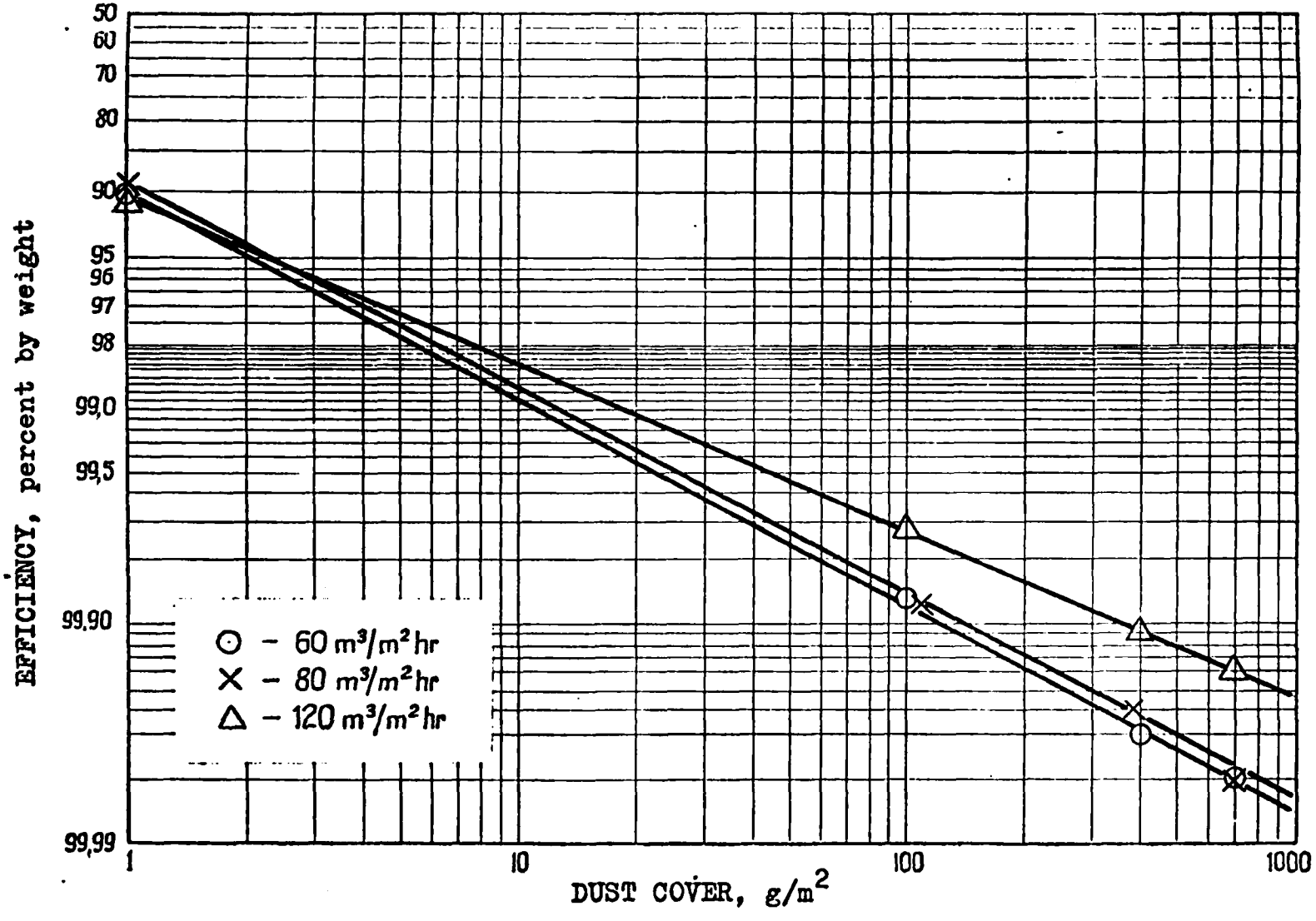

Figure A-38. Theoretical Laboratory Efficiency for Coal Dust and Fabric ET-30 (unseparated dust).

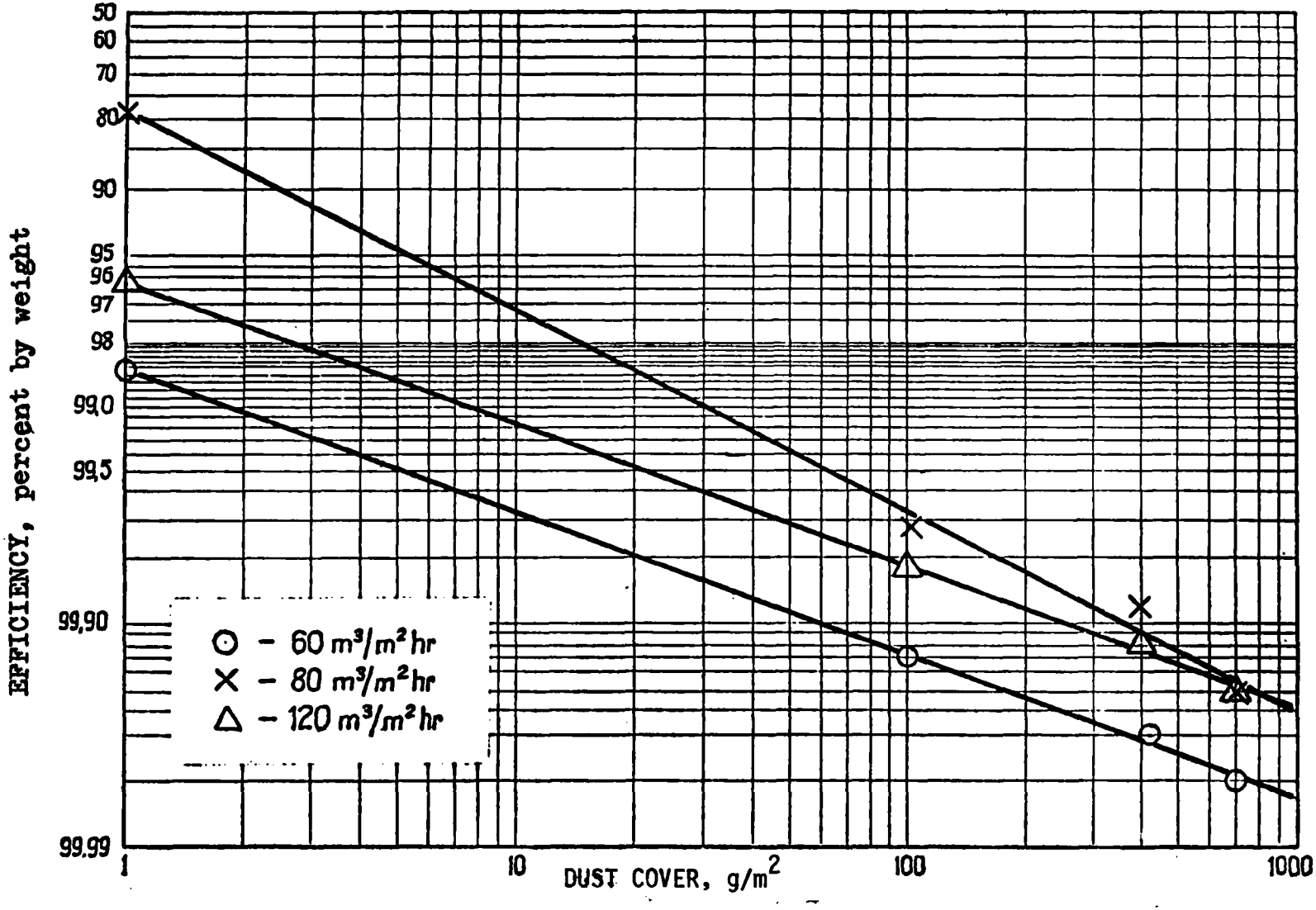

Figure A-39. Theoretical Laboratory Efficiency for Talc Dust and Fabric ET-30 (separated dust).

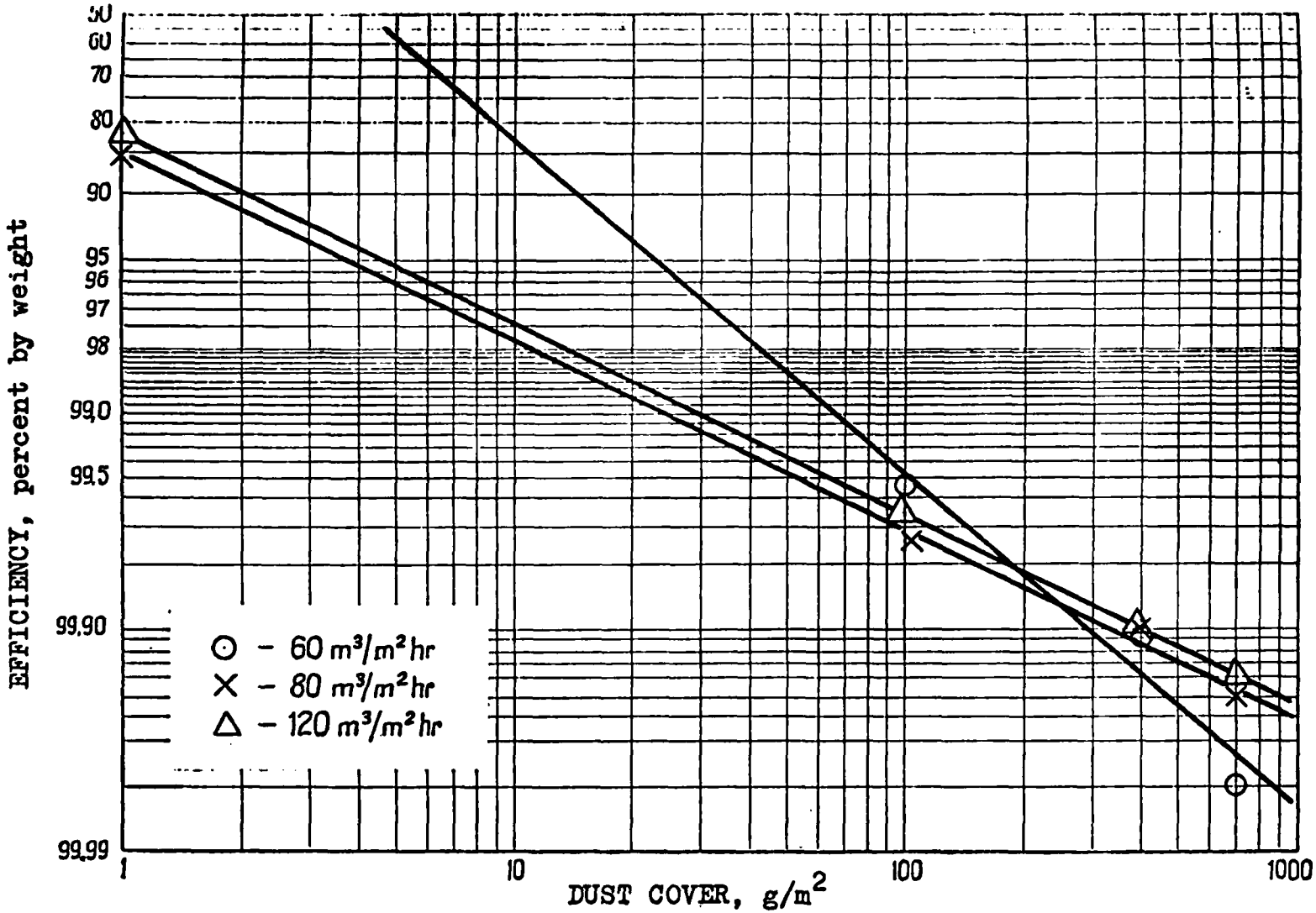

Figure A-40. Theoretical Laboratory Efficiency for Fly Ash Dust and Fabric ET-30 (separated dust).

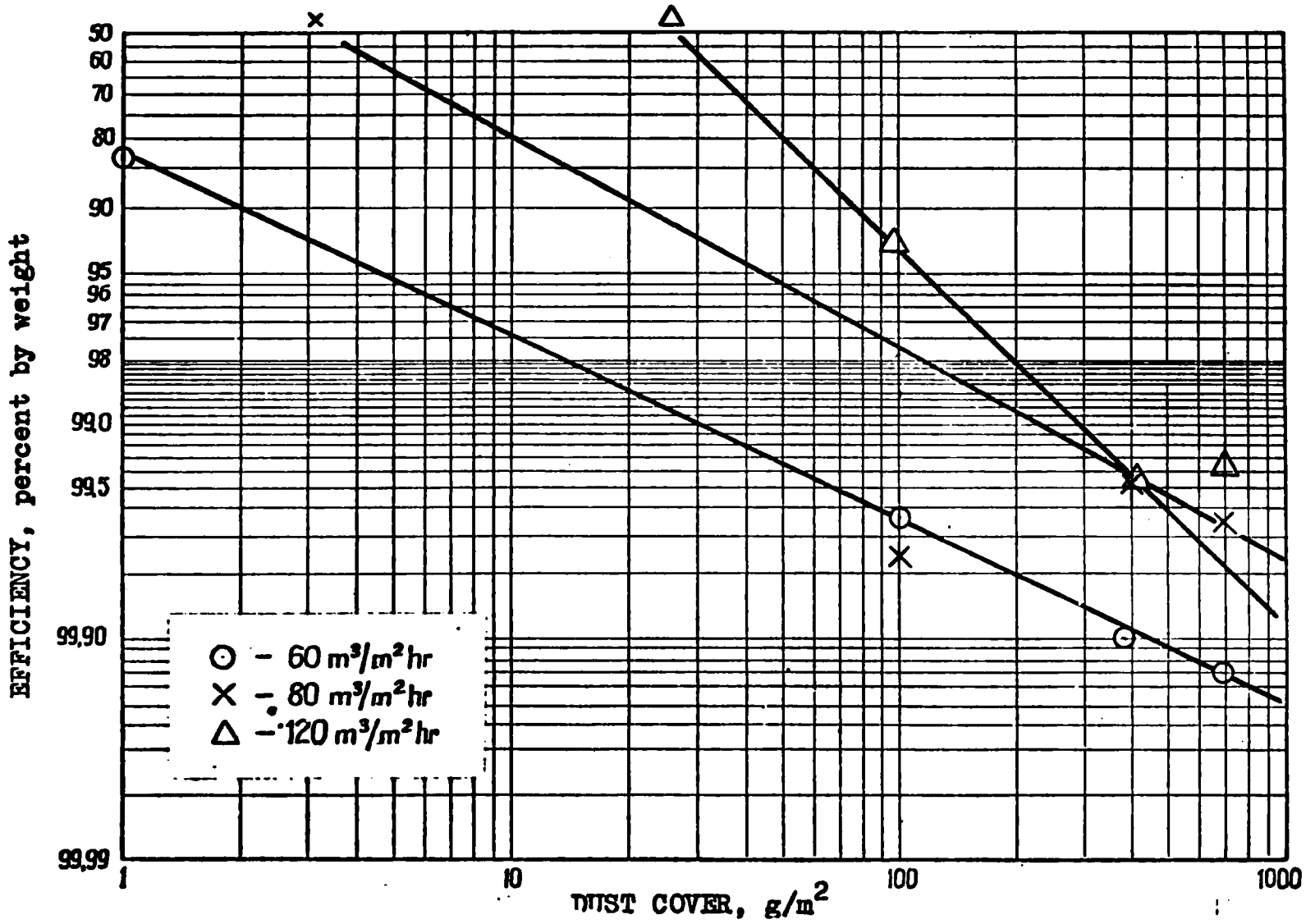

Figure A-41. Theoretical Laboratory Efficiency for Cement Dust and Fabric F-tor 5 (separated dust).

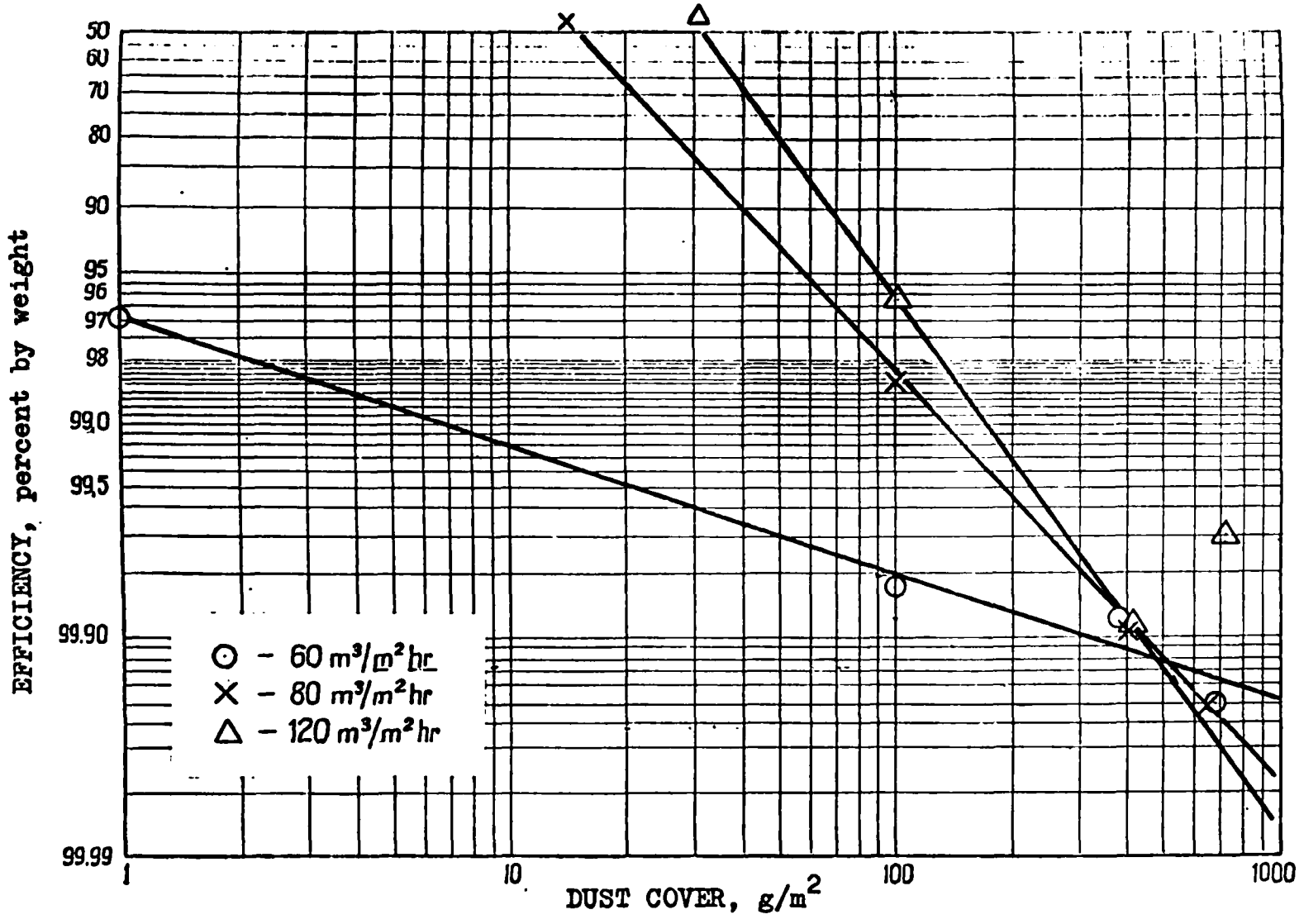

Figure A-42. Theoretical Laboratory Efficiency for Cement Dust and Fabric F-tor 5 (unseparated dust).

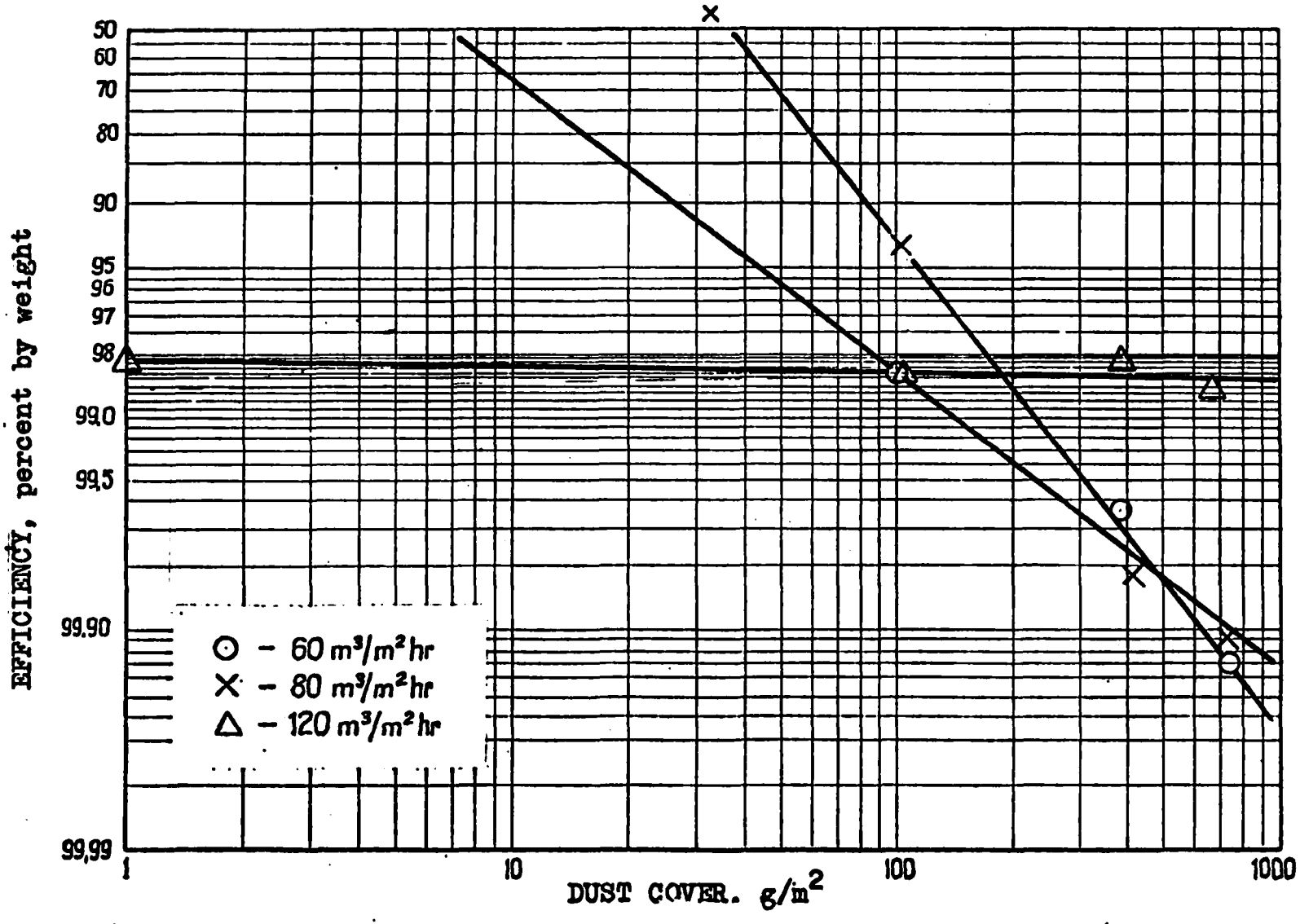

Figure A-43. Theoretical Laboratory Efficiency for Coal Dust and Fabric F-tor 5 (separated dust).

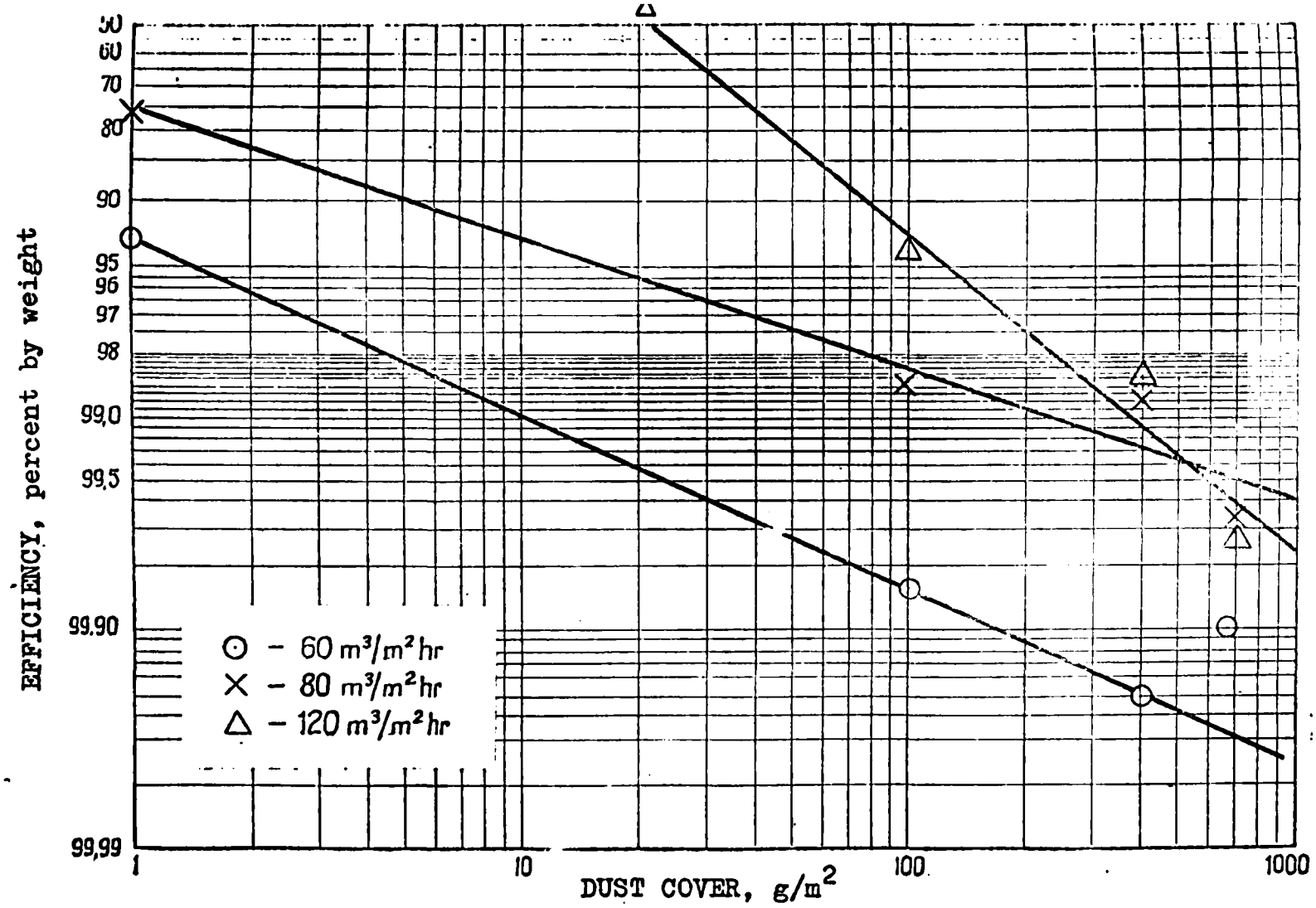

Figure A-44. Theoretical Laboratory Efficiency for Coal Dust and Fabric F-tor 5 (unseparated dust).

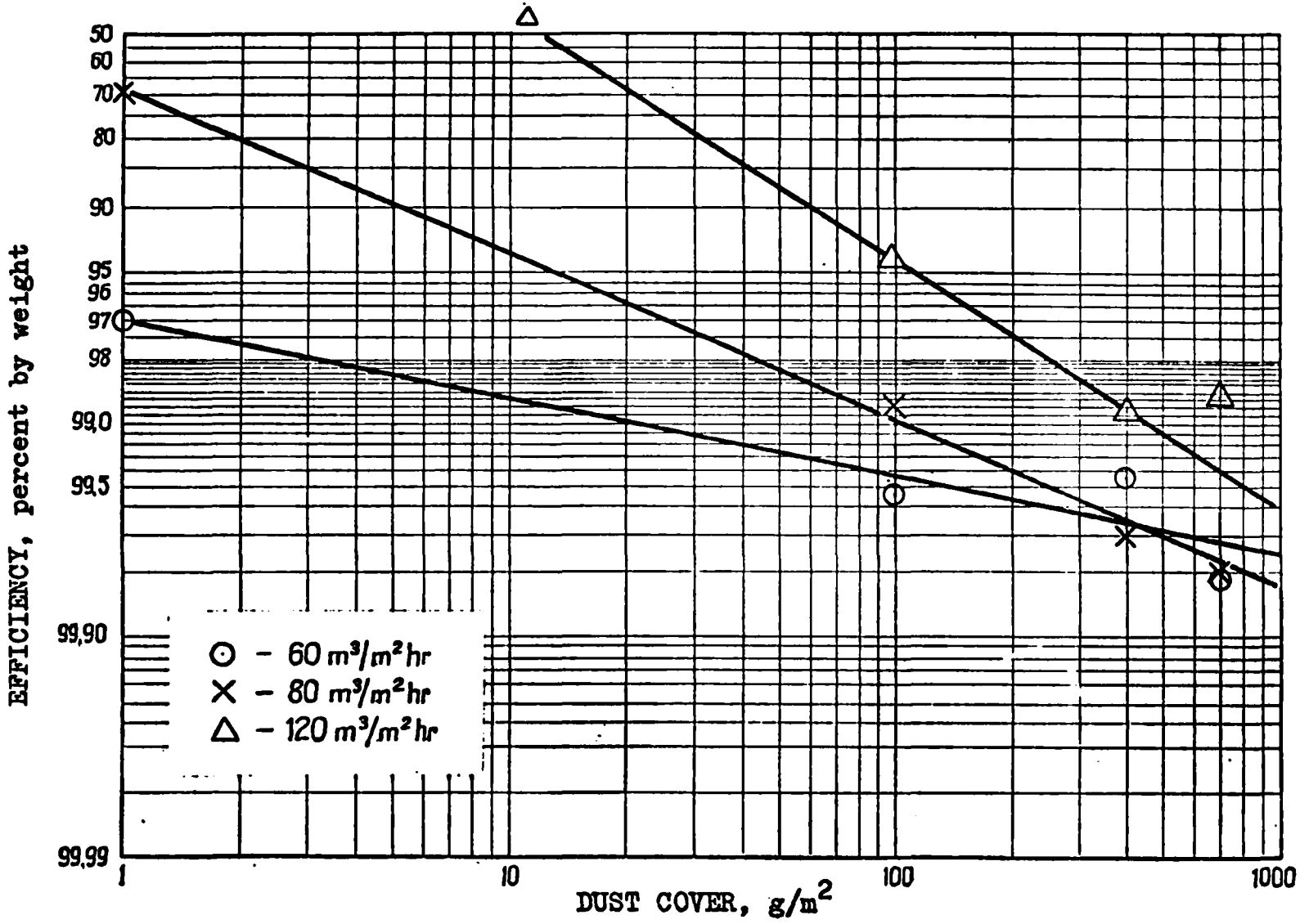

Figure A-45. Theoretical Laboratory Efficiency for Talc Dust and Fabric F-tor 5 (separated dust).

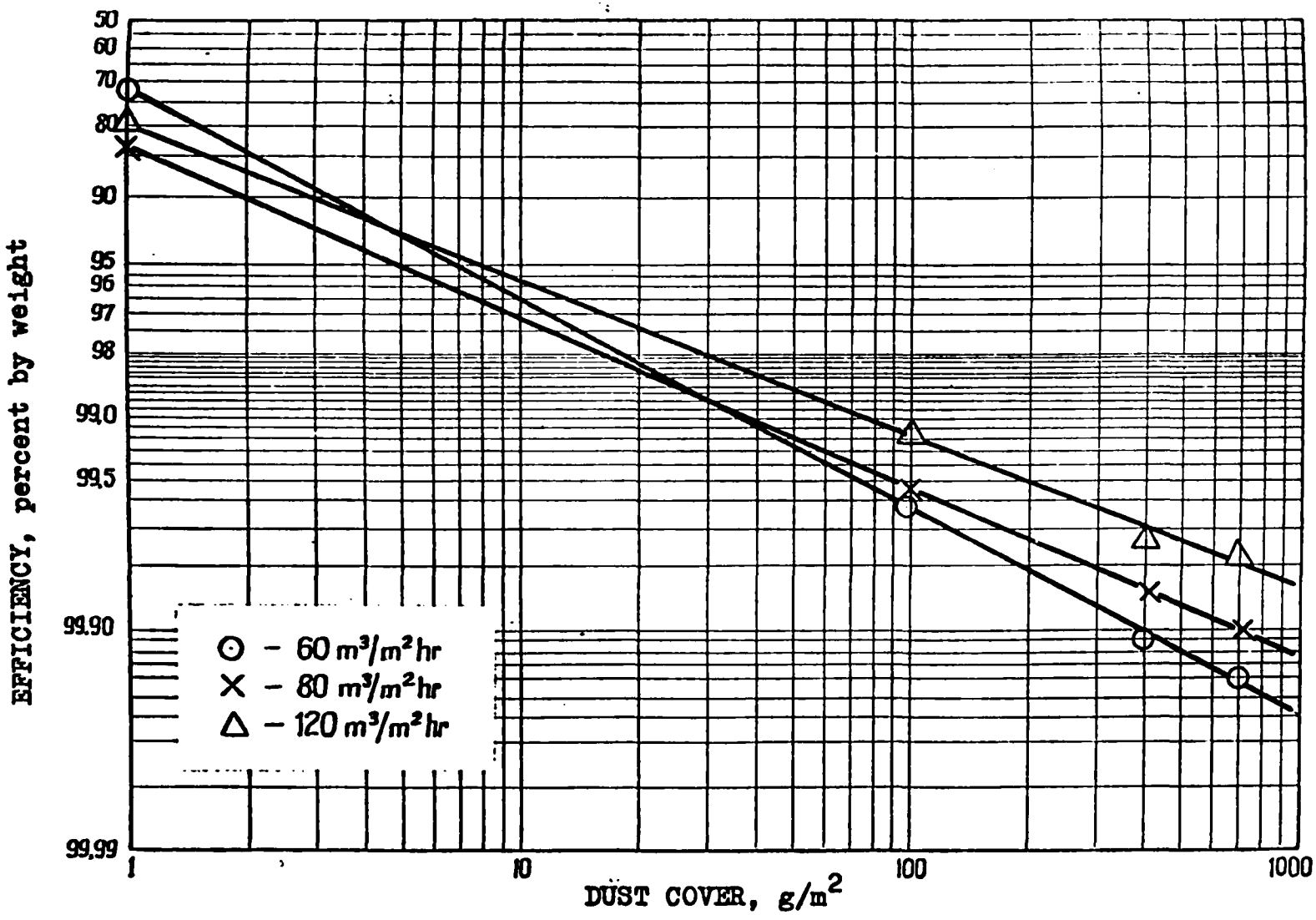

Figure A-46. Theoretical Laboratory Efficiency for Fly Ash Dust and Fabric F-tor 5 (separated dust).

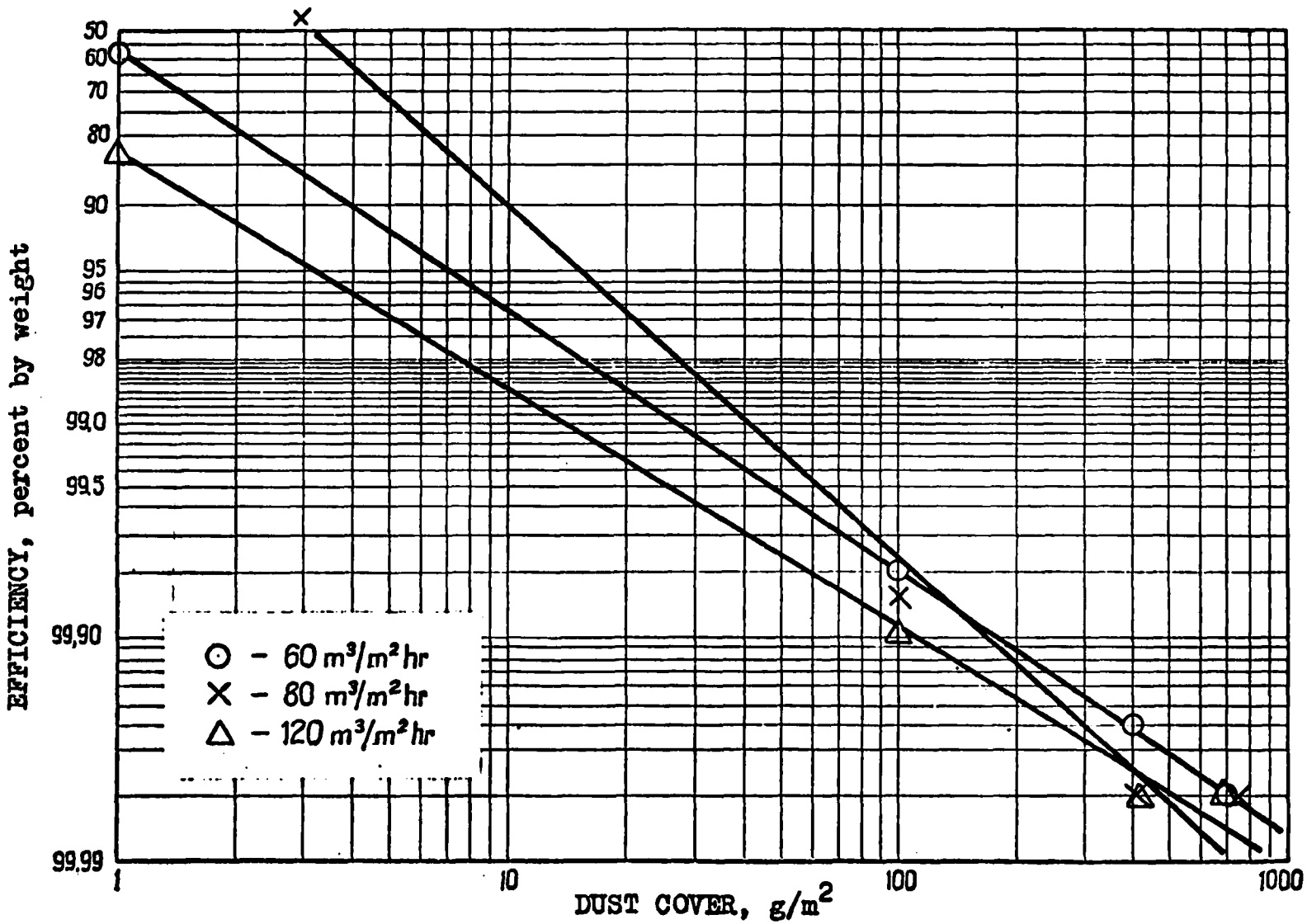

Figure A-47. Theoretical Laboratory Efficiency for Cement Dust and Fabric PT-15 (separated dust).

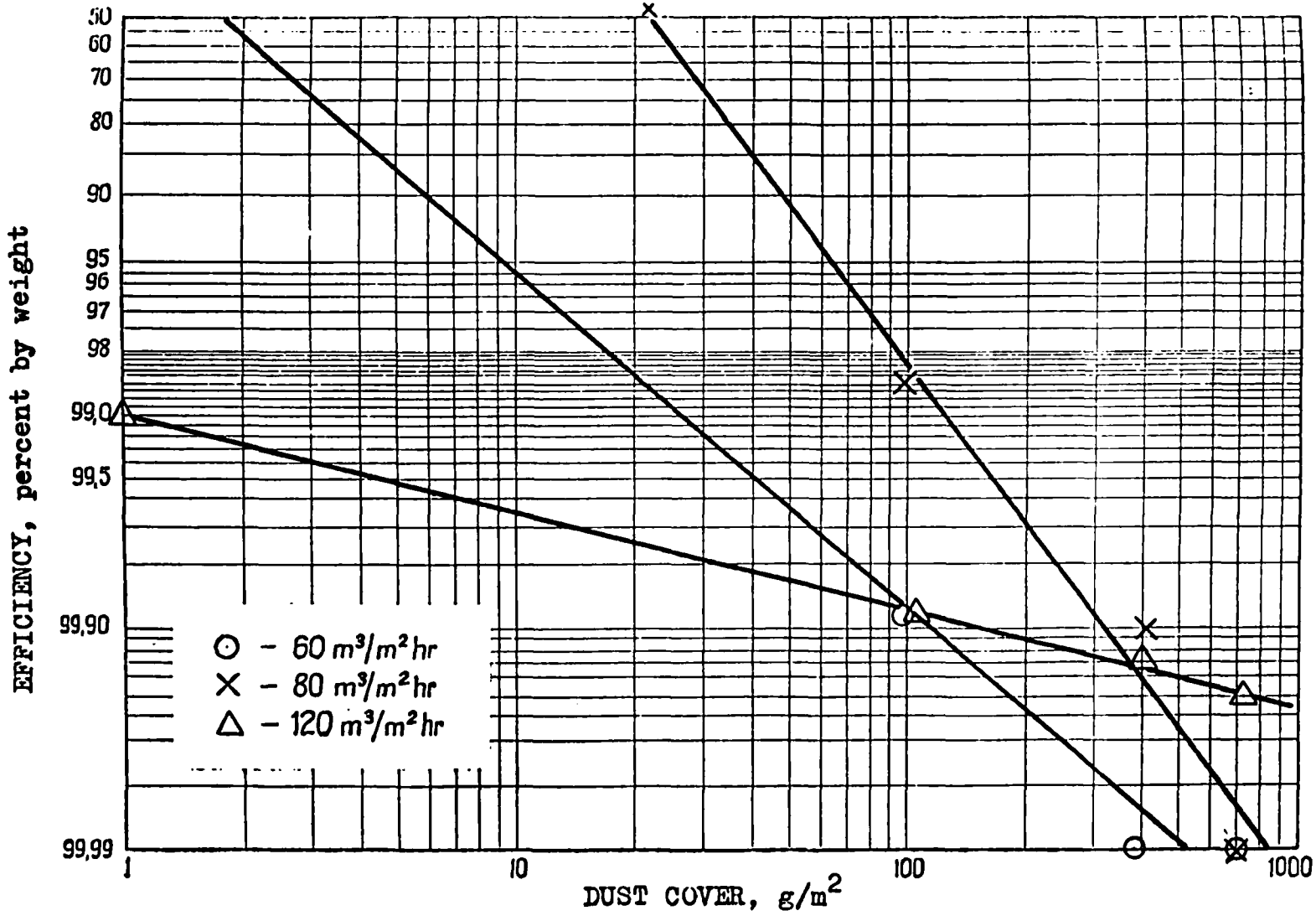

Figure A-48. Theoretical Laboratory Efficiency for Cement Dust and Fabric PT-15 (unseparated dust).

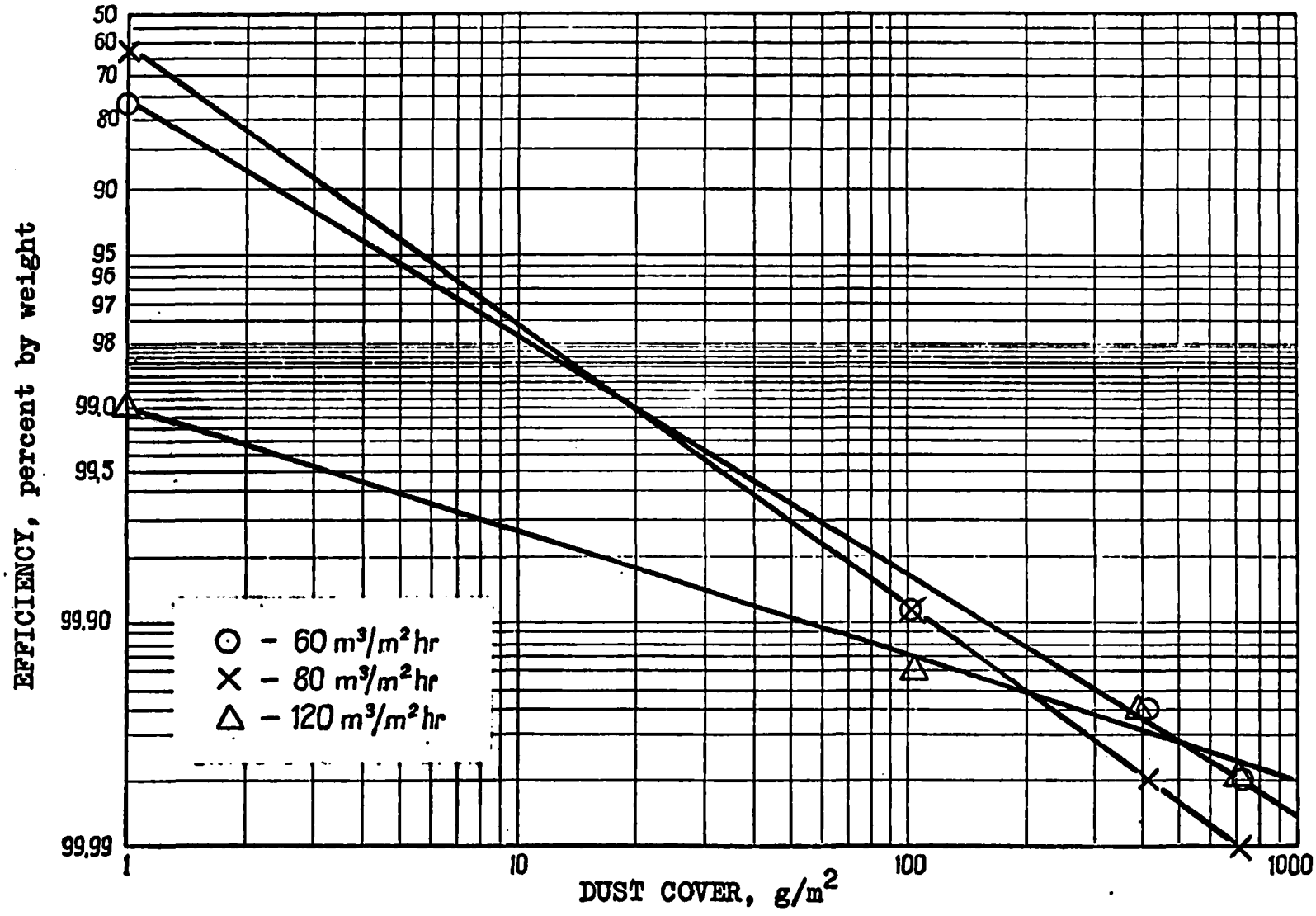

Figure A-49. Theoretical Laboratory Efficiency for Coal Dust and Fabric PT-15 (separated dust).

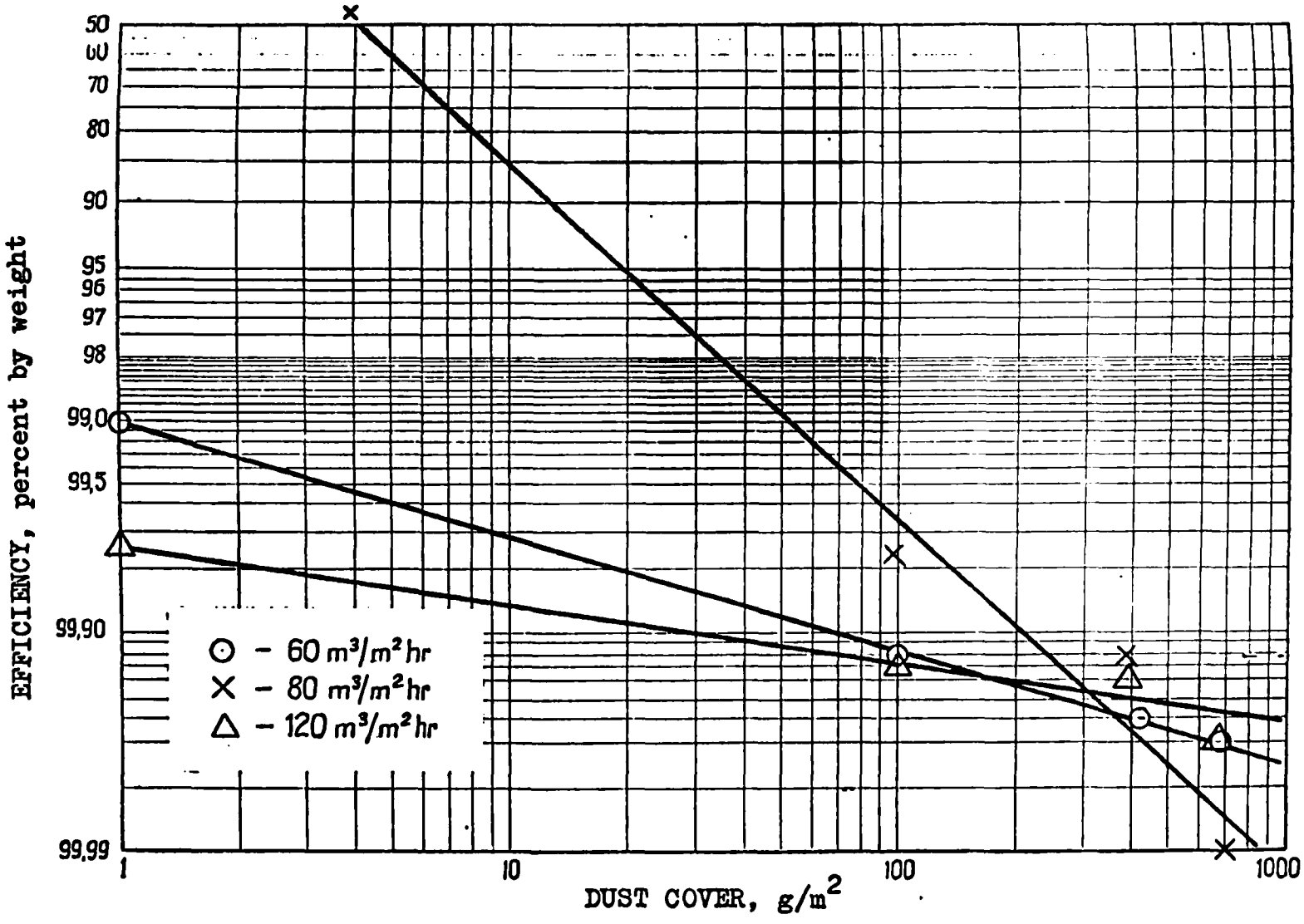

Figure A-50. Theoretical Laboratory Efficiency for Coal Dust and Fabric PT-15 (unseparated dust).

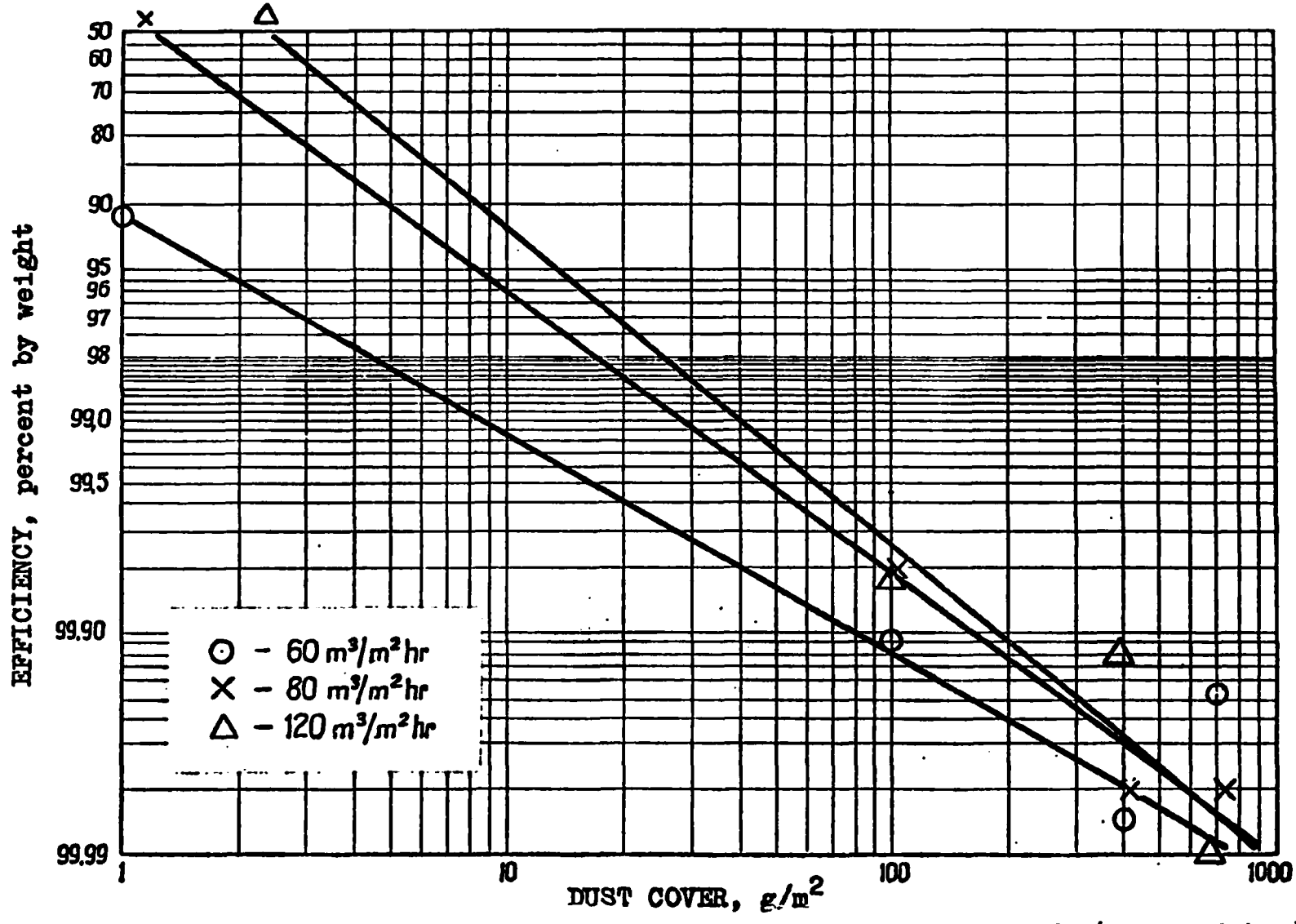

Figure A-51. Theoretical Laboratory Efficiency for Talc Dust and Fabric PT-15 (separated dust).

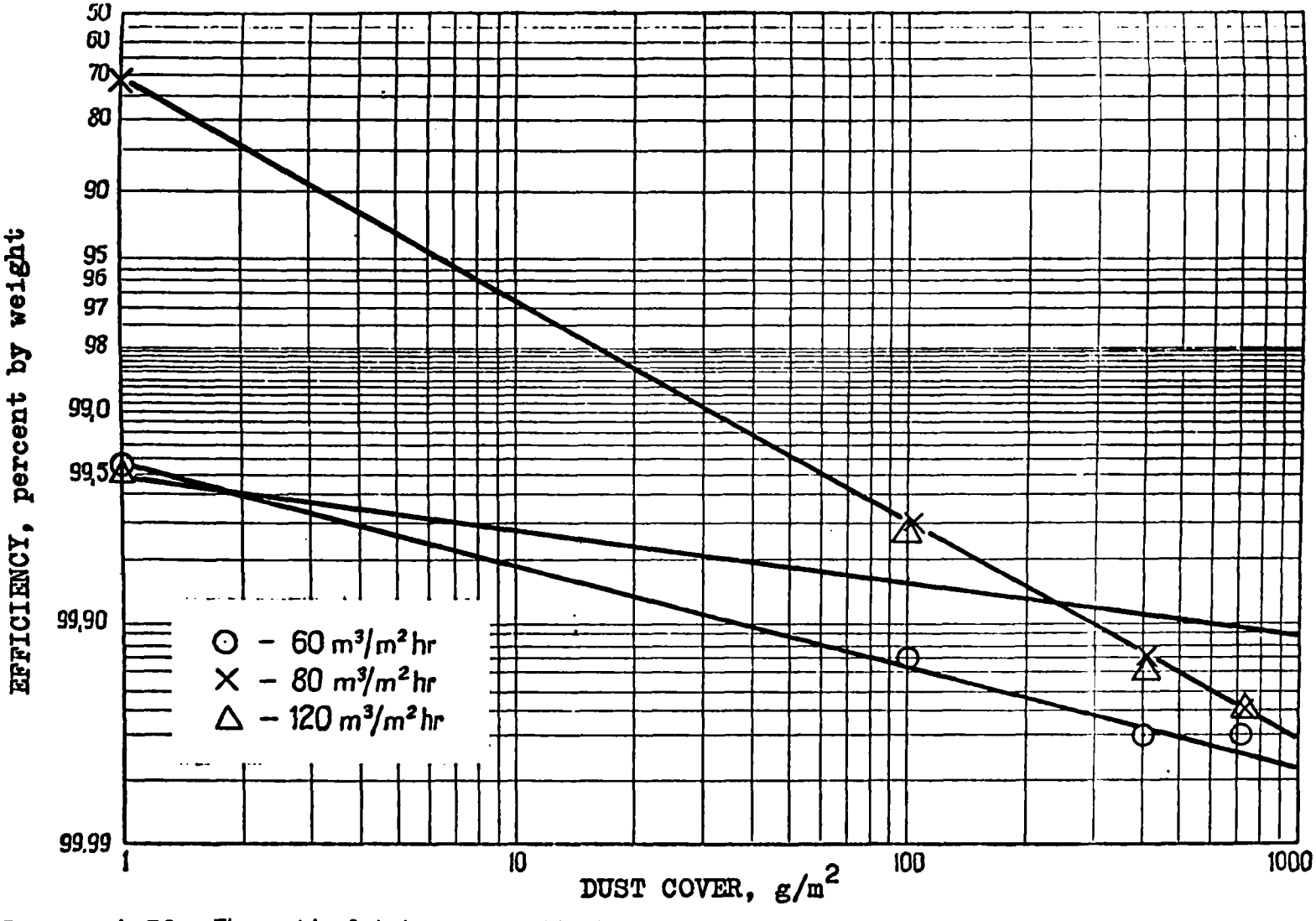

Figure A-52. Theoretical Laboratory Efficiency for Fly Ash Dust and Fabric PT-15 (separated dust).

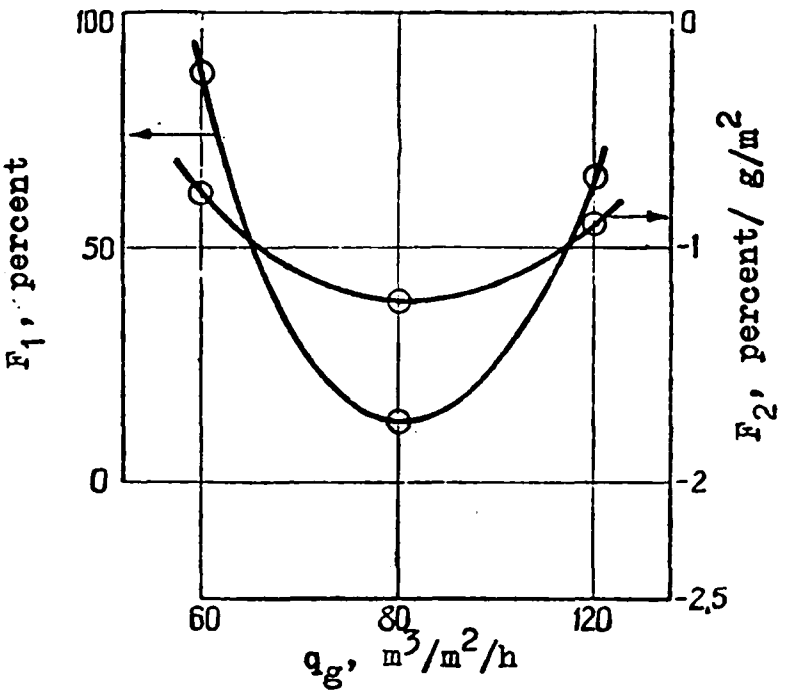

a. Fabric ET-4 and unseparated cement dust.

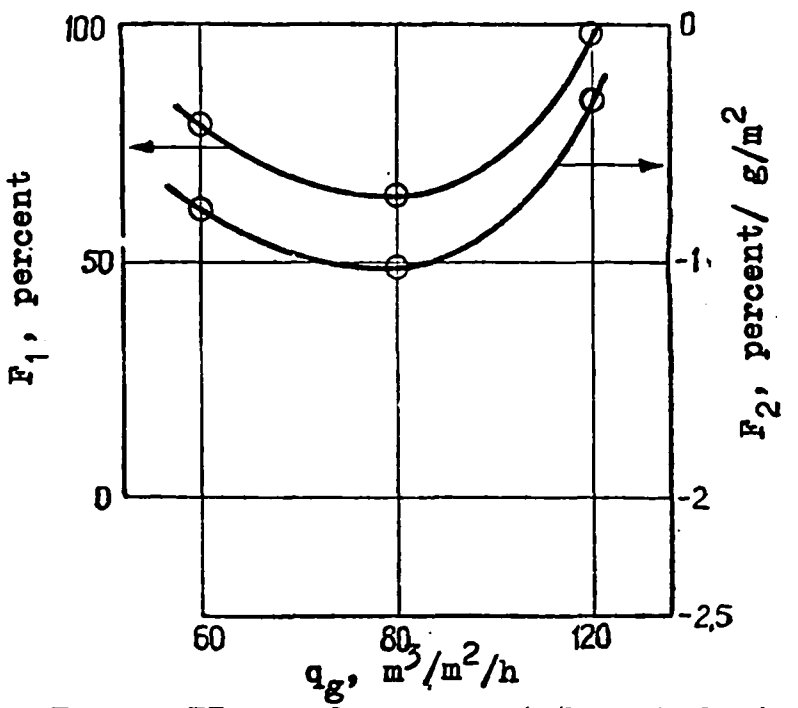

b. Fabric ET-4 and unseparated coal dust.

Figure A-53. Dependence of Function F_1 and F_2 on the Air-to-Cloth Ratio, q_g.

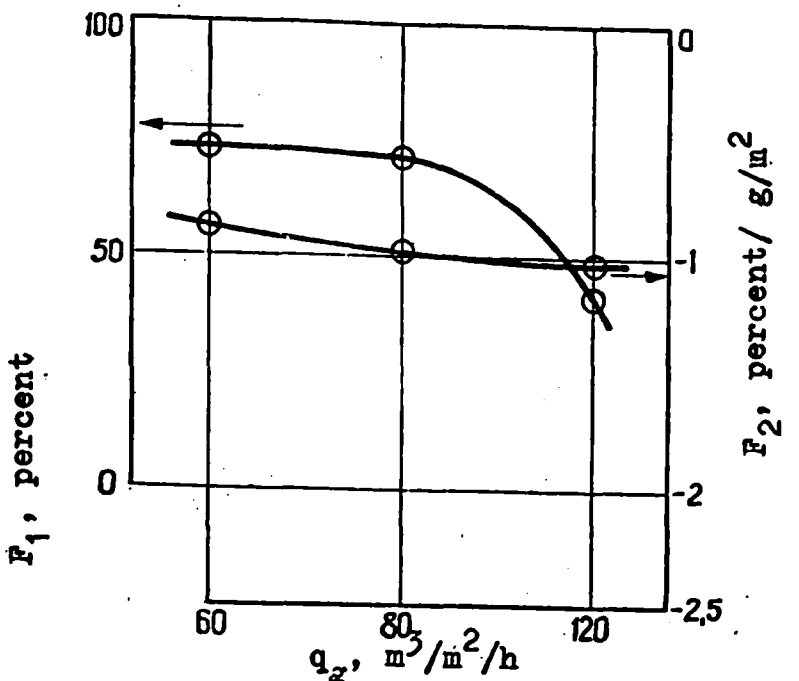

a. Fabric ET-4 and separated fly ash dust.

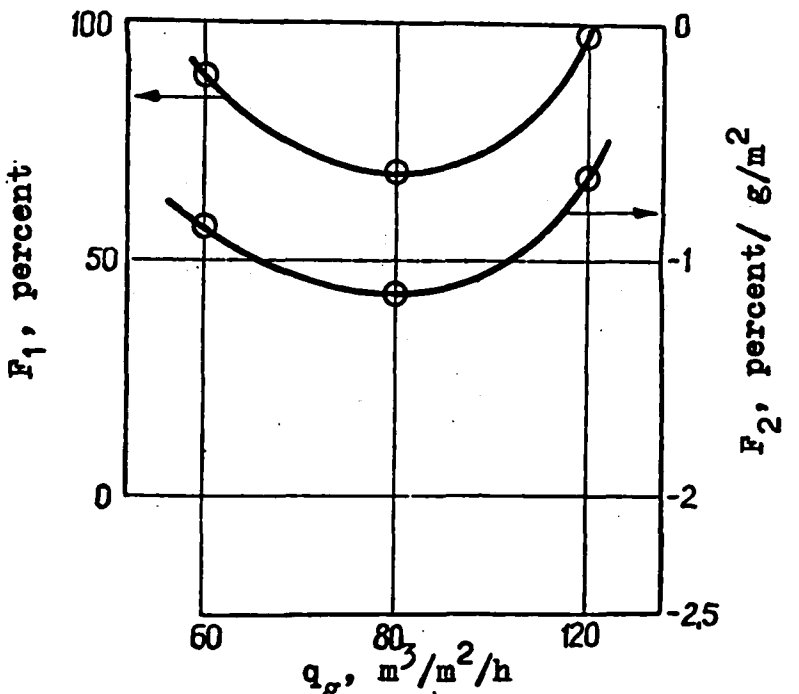

b. Fabric ET-30 and separated cement dust.

Figure A-54. Dependence of Function F_1 and F_2 On the Air-to-Cloth Ratio q_g.

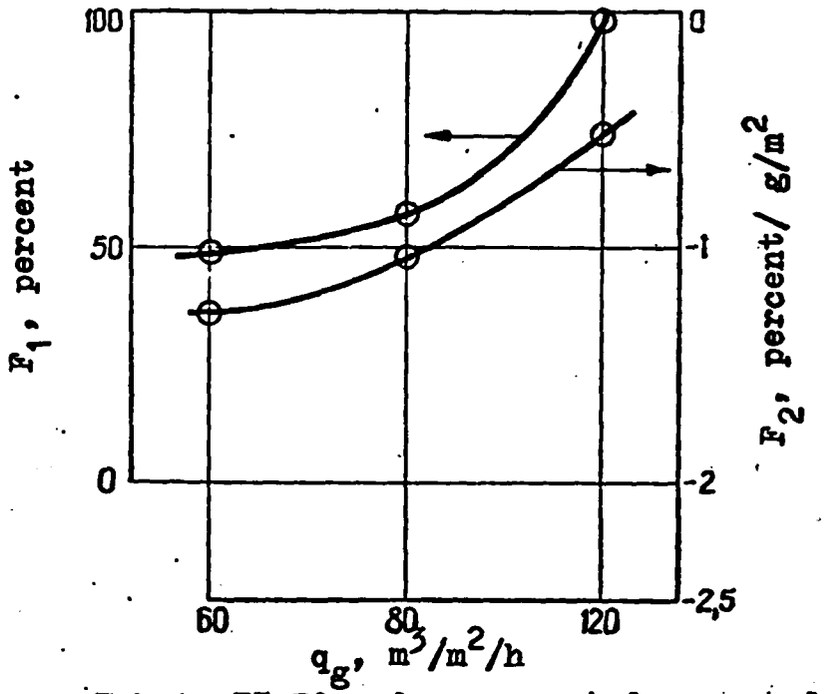

a. Fabric ET-30 and unseparated cement dust.

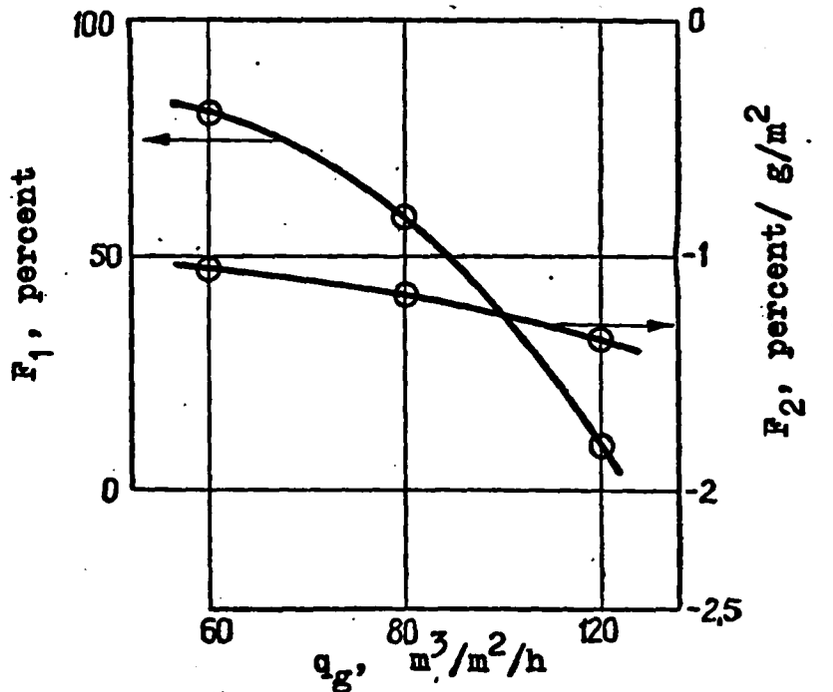

b. Fabric ET-30 and separated coal dust

Figure A-55. Dependence of Function F_1 and F_2 On the Air-to-Cloth Ratio, q_g.

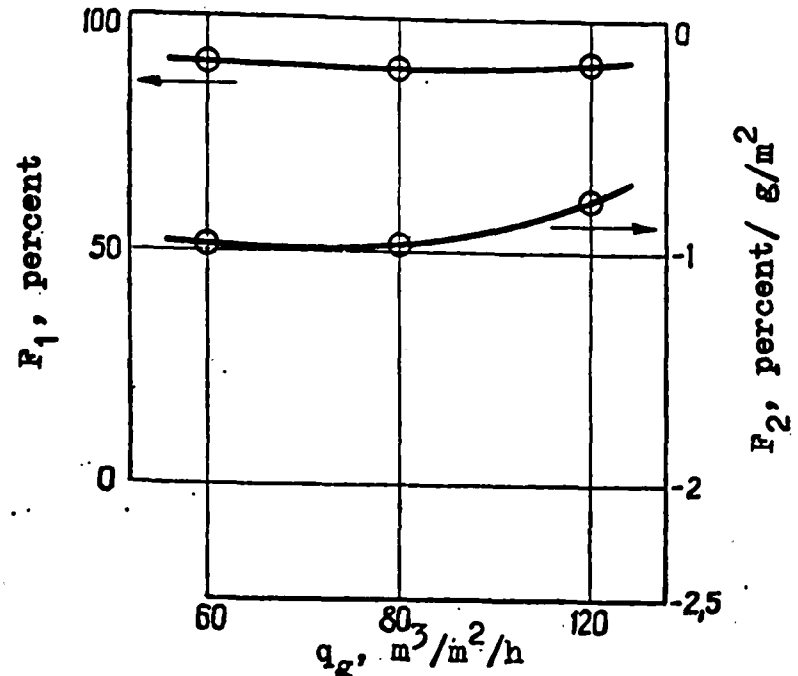

a. Fabric ET-30 and unseparated coal dust.

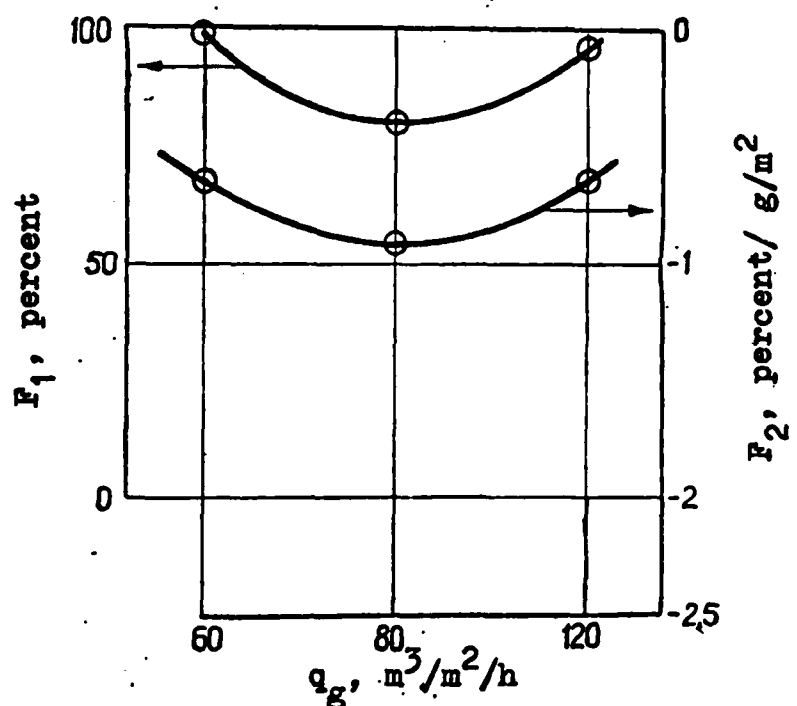

b. Fabric ET-30 and separated talc dust.

Figure A-56. Dependence of Function F_1 and F_2 On the Air-to-Cloth Ratio, q_g.

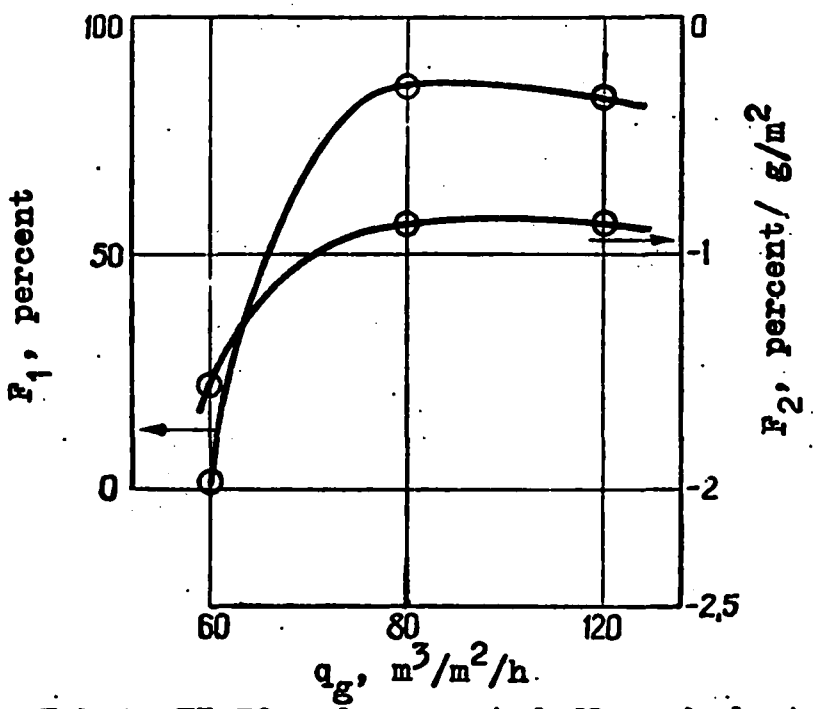

a. Fabric ET-30 and separated fly ash dust.

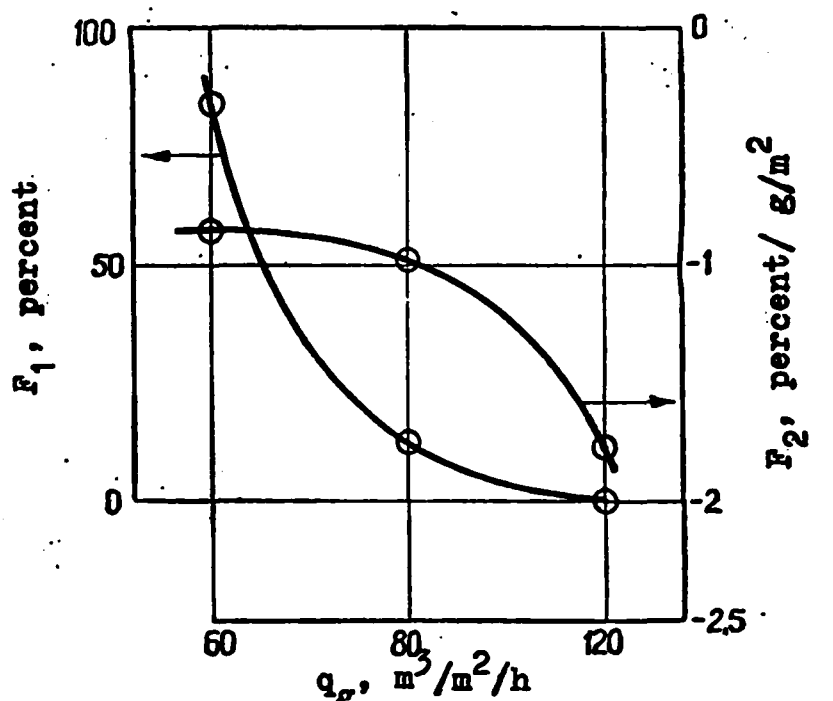

b. Fabric F-tor 5 and separated cement dust

Figure A-57. Dependence of Function F_1 and F_2 On the Air-to-Cloth Ratio q_g.

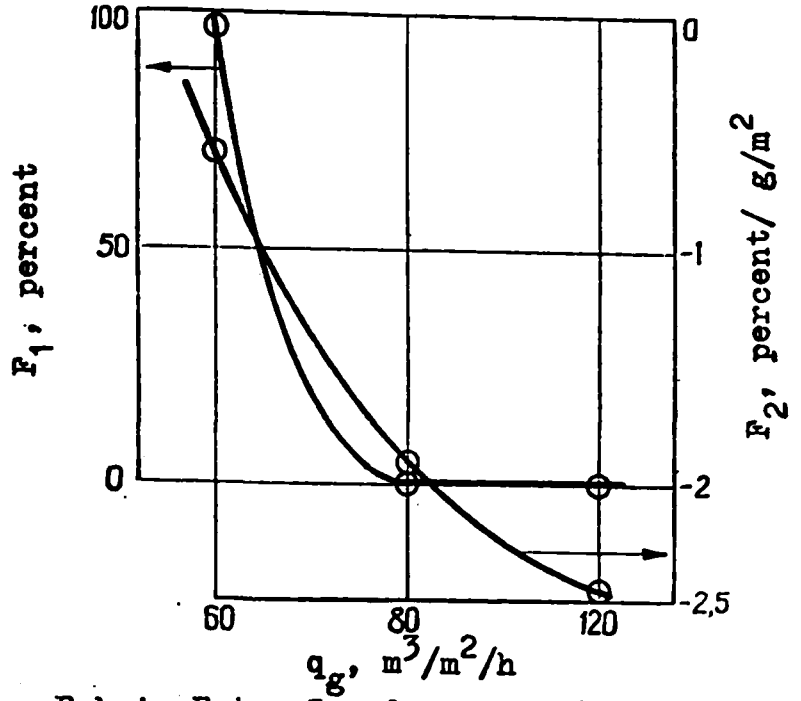

a. Fabric F-tor 5 and unseparated cement dust.

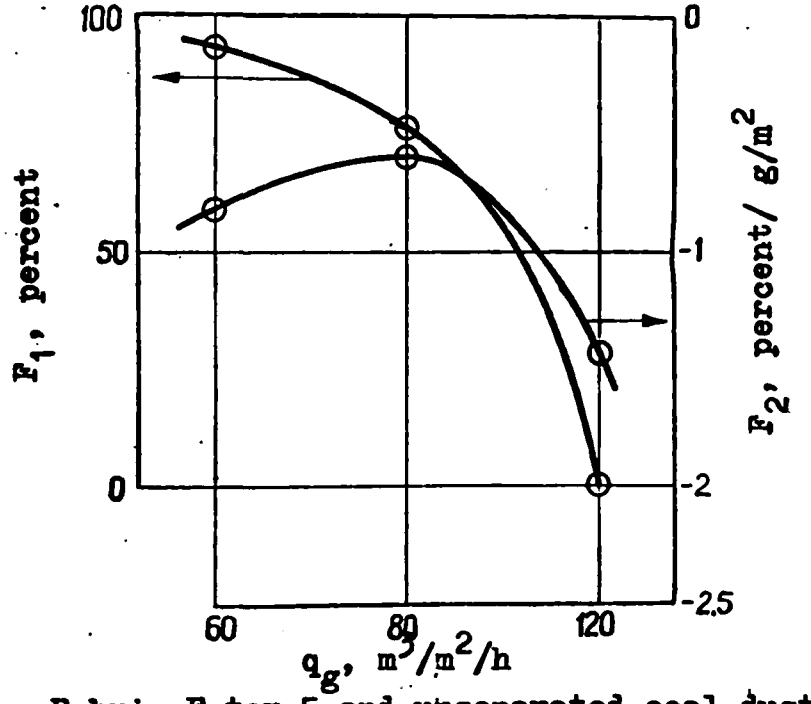

b. Fabric F-tor 5 and unseparated coal dust.

Figure A-58. Dependence of Function F_1 and F_2 On the Air-to-Cloth Ratio, q_g.

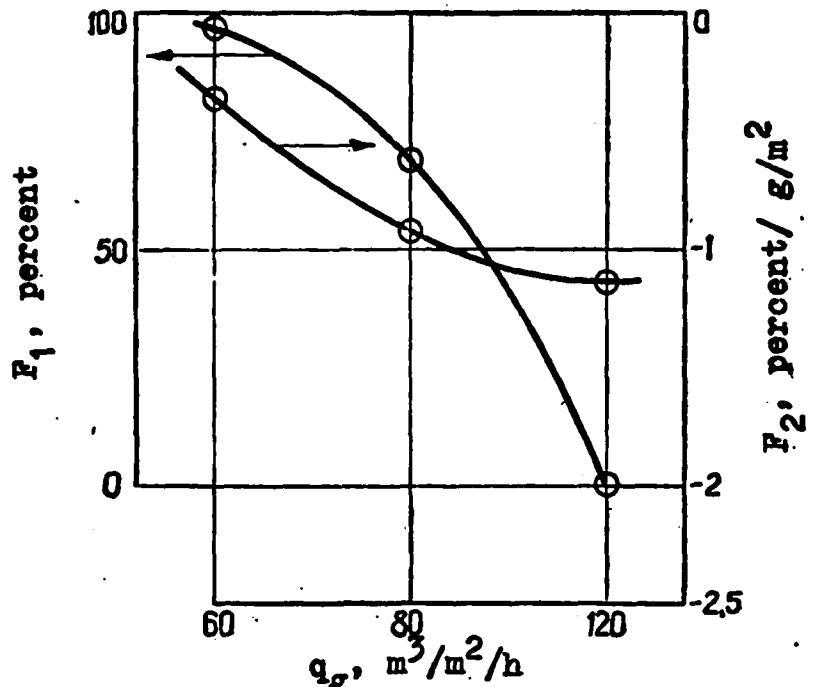

a. Fabric F-tor 5 and talc dust (separated).

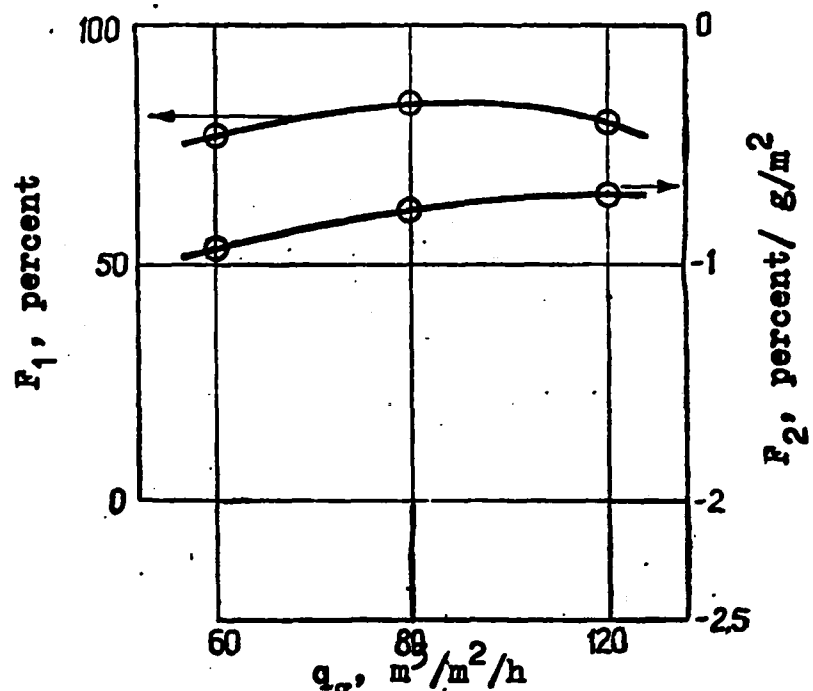

b. Fabric F-tor 5 and fly ash dust (separated).

Figure A-59. Dependence of Function F_1 and F_2 On the Air-to-Cloth Ratio, q_g.

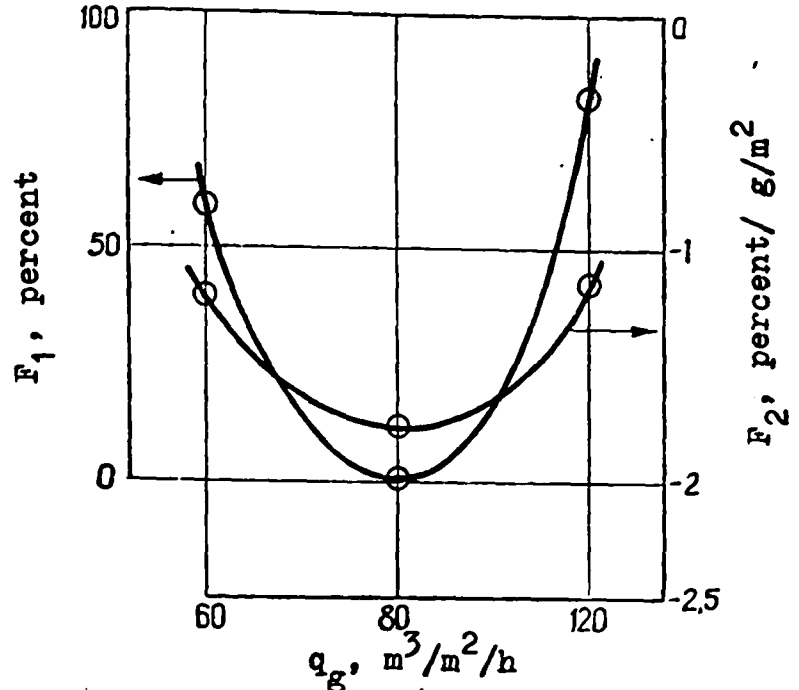

a. Fabric PT-15 and separated cement dust.

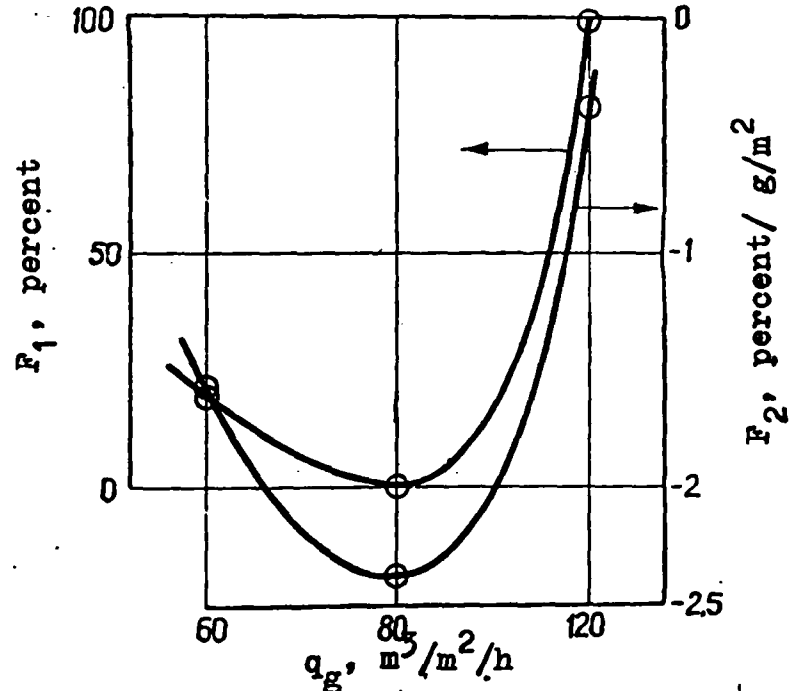

b. Fabric PT-15 and unseparated cement dust.

Figure A-60. Dependence of Function F_1 and F_2 On the Air-to-Cloth Ratio, q_g.

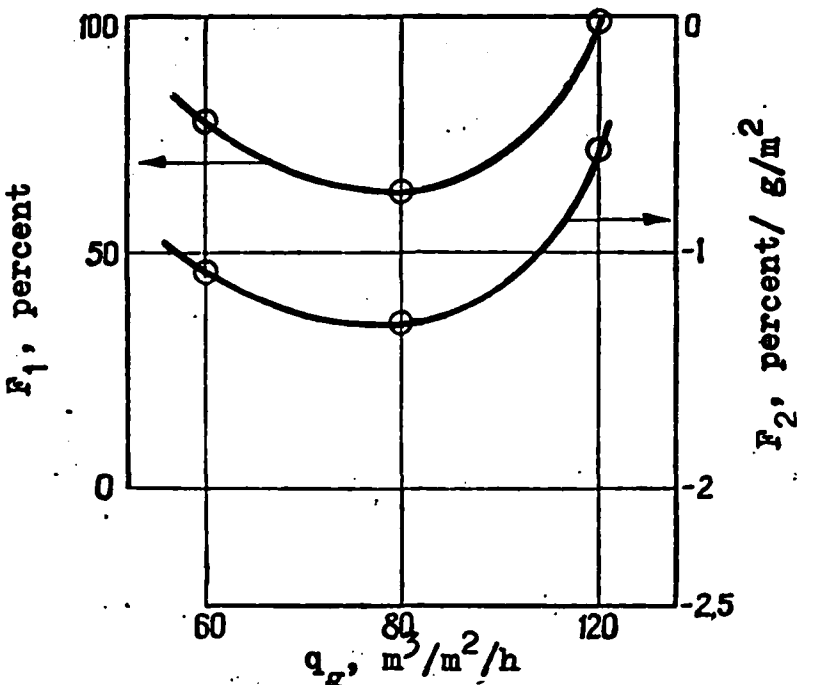

a. Fabric PT-15 and separated coal dust.

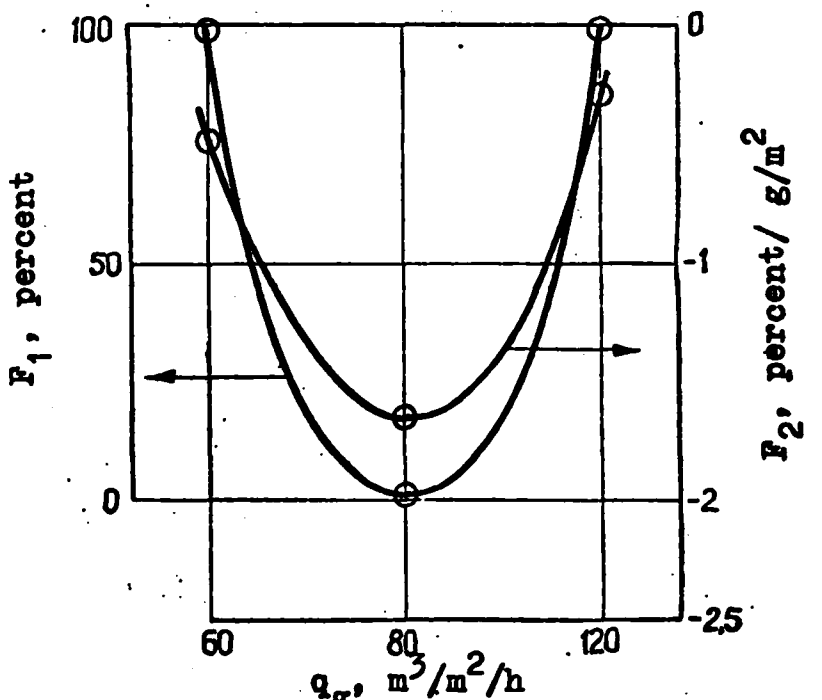

b. Fabric PT-15 and unseparated coal dust.

Figure A-61. Dependence of Function F_1 and F_2 On-the-Air to Cloth Ratio, q_g.

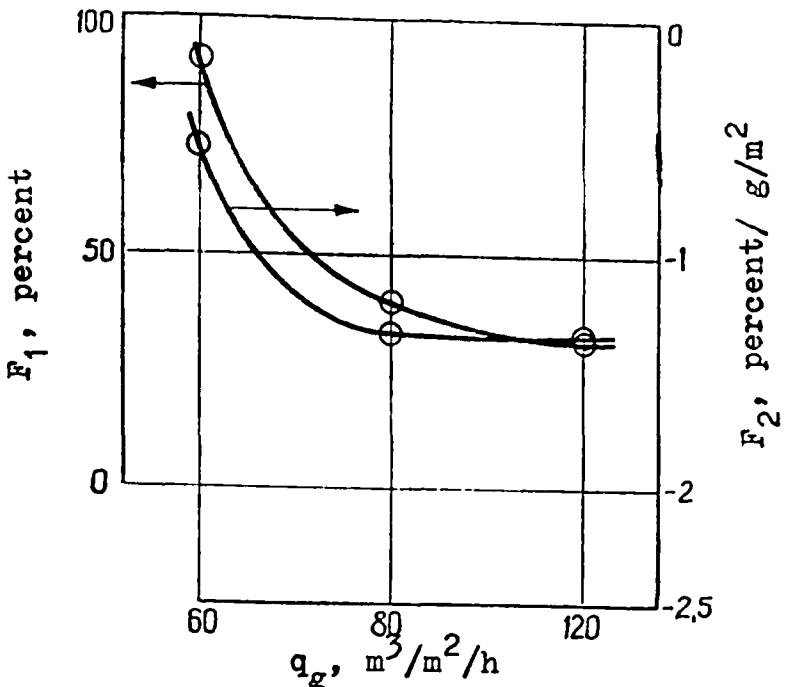

a. Fabric PT-15 and separated talc dust.

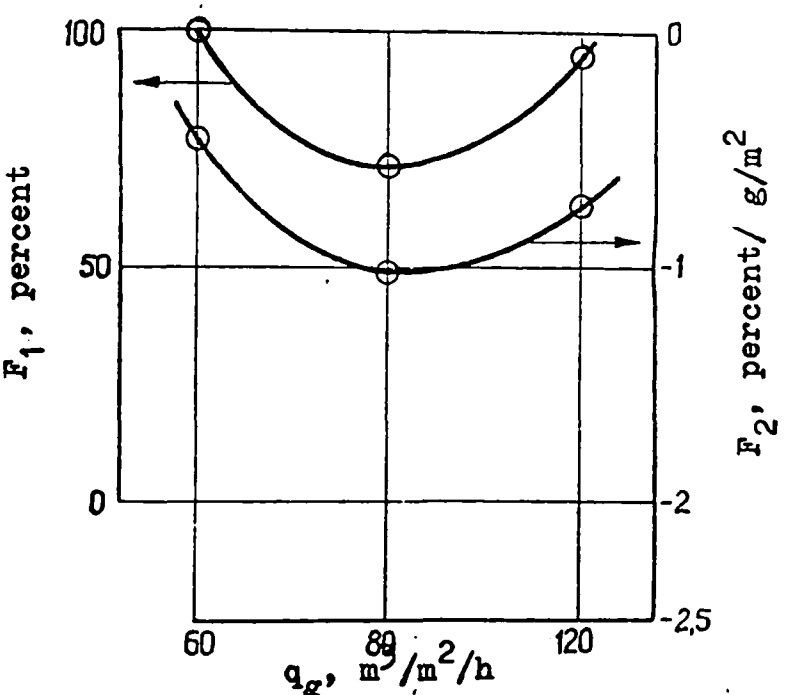

b. Fabric PT-15 and separated fly ash dust.

Figure A-62. Dependence of Function F_1 and F_2 On the Air-to-Cloth Ratio, q_g.

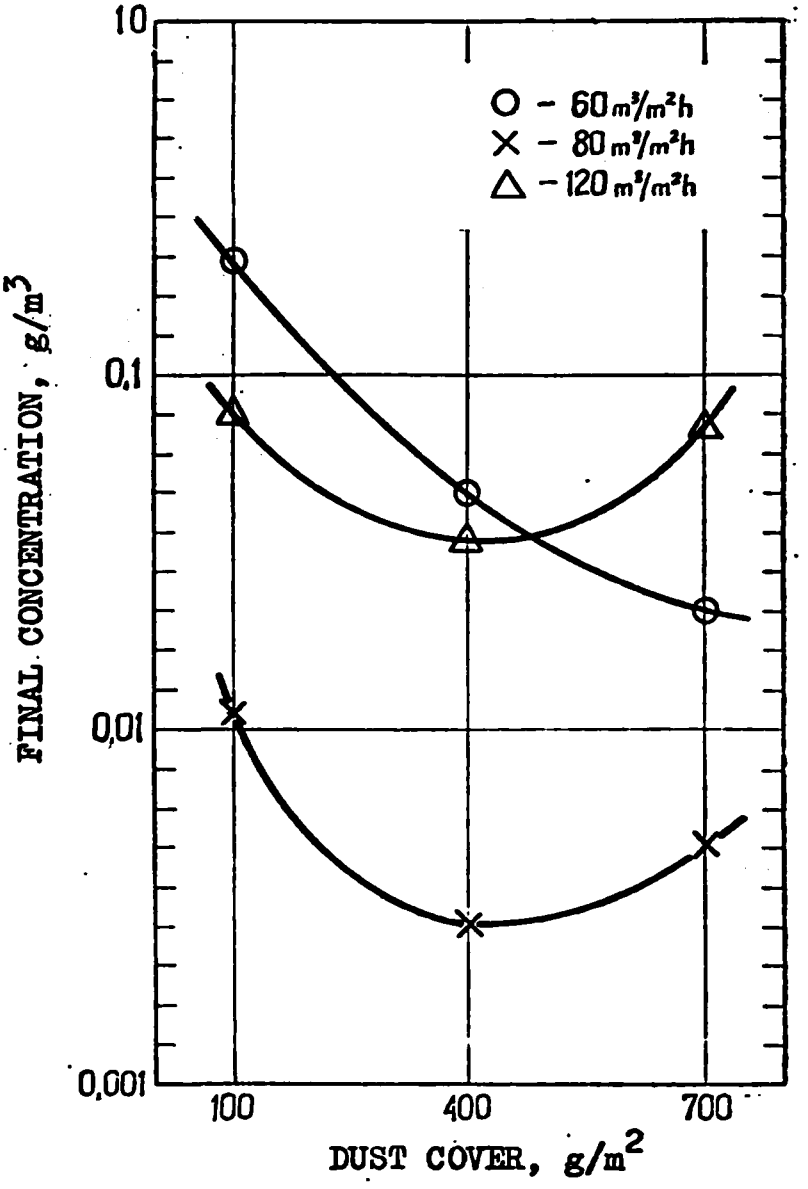

Figure A-63. Variation of Final Concentration for Fabric ET-4 and Separated Cement Dust.

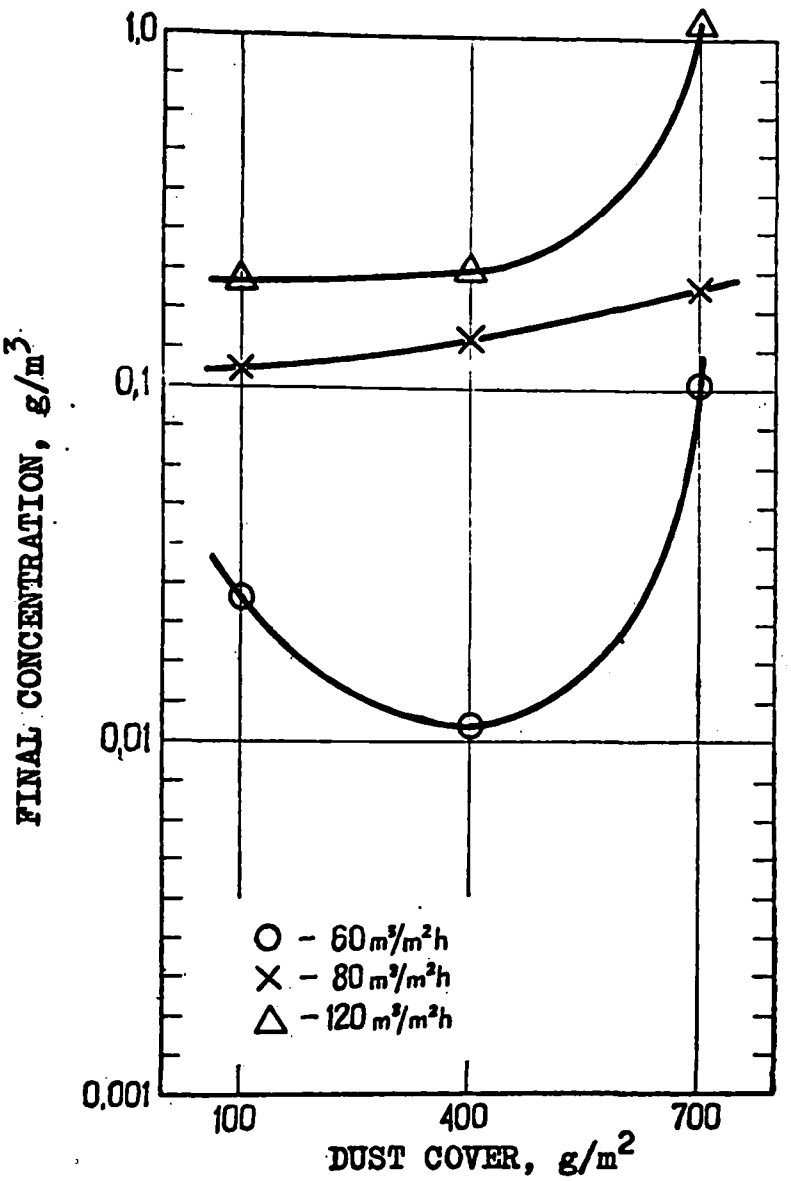

Figure A-64. Variation of Final Concentration for Fabric ET-4 and Separated Coal Dust.

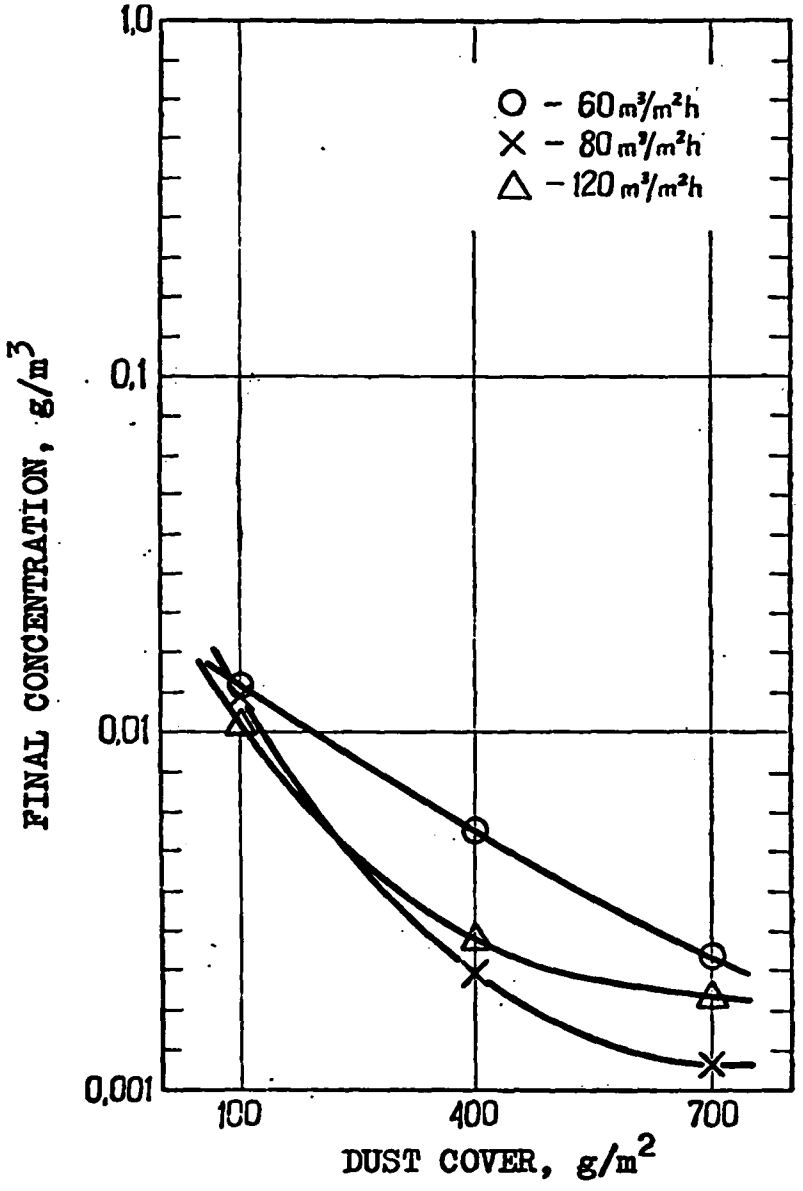

Figure A-65. Variation of Final Concentration for Fabric ET-30 and Separated Cement Dust.

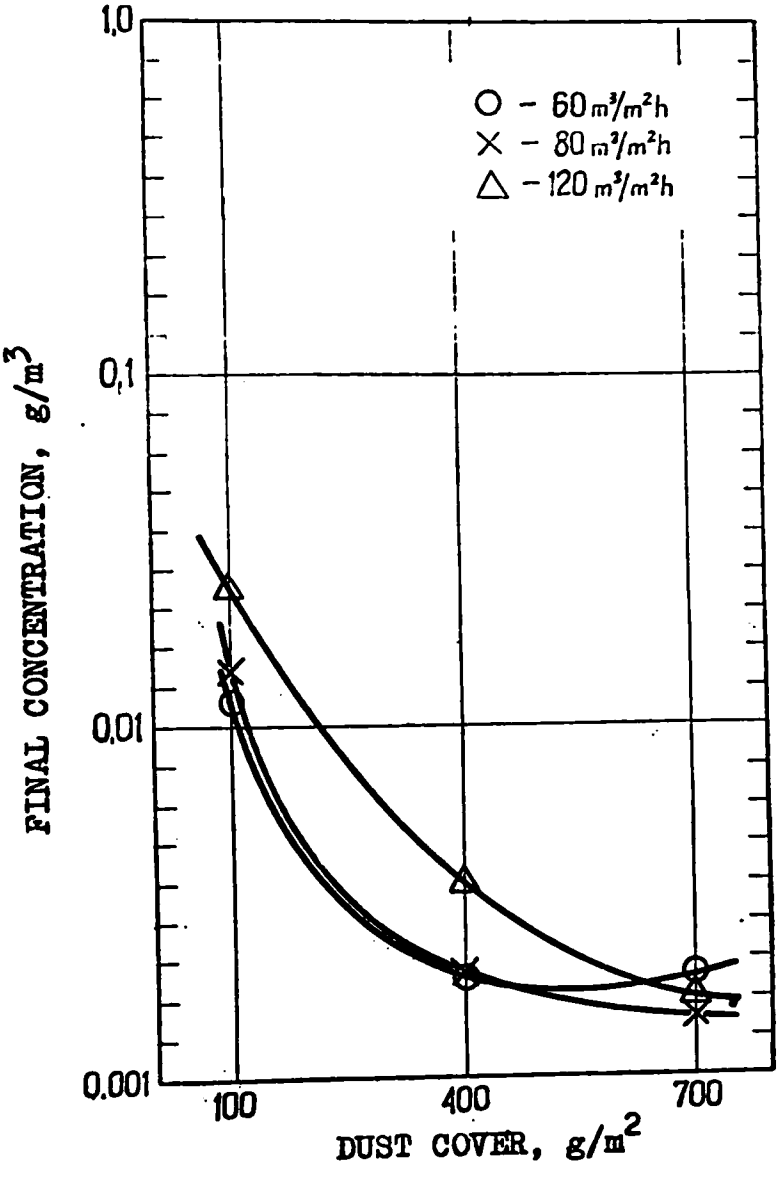

Figure A-66. Variation of Final Concentration for Fabric ET-30 and Separated Coal Dust.

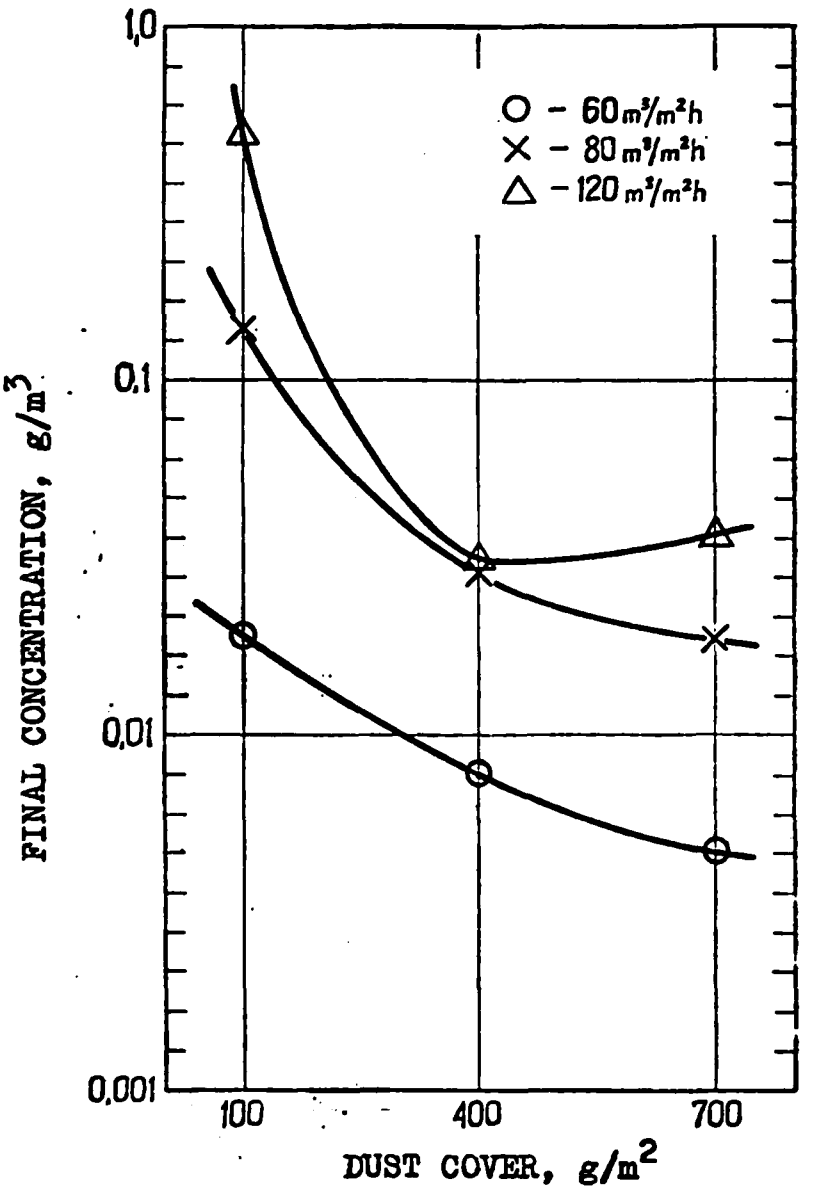

Figure A-67. Variation of Final Concentration for Fabric F-tor 5 and Separated Cement Dust.

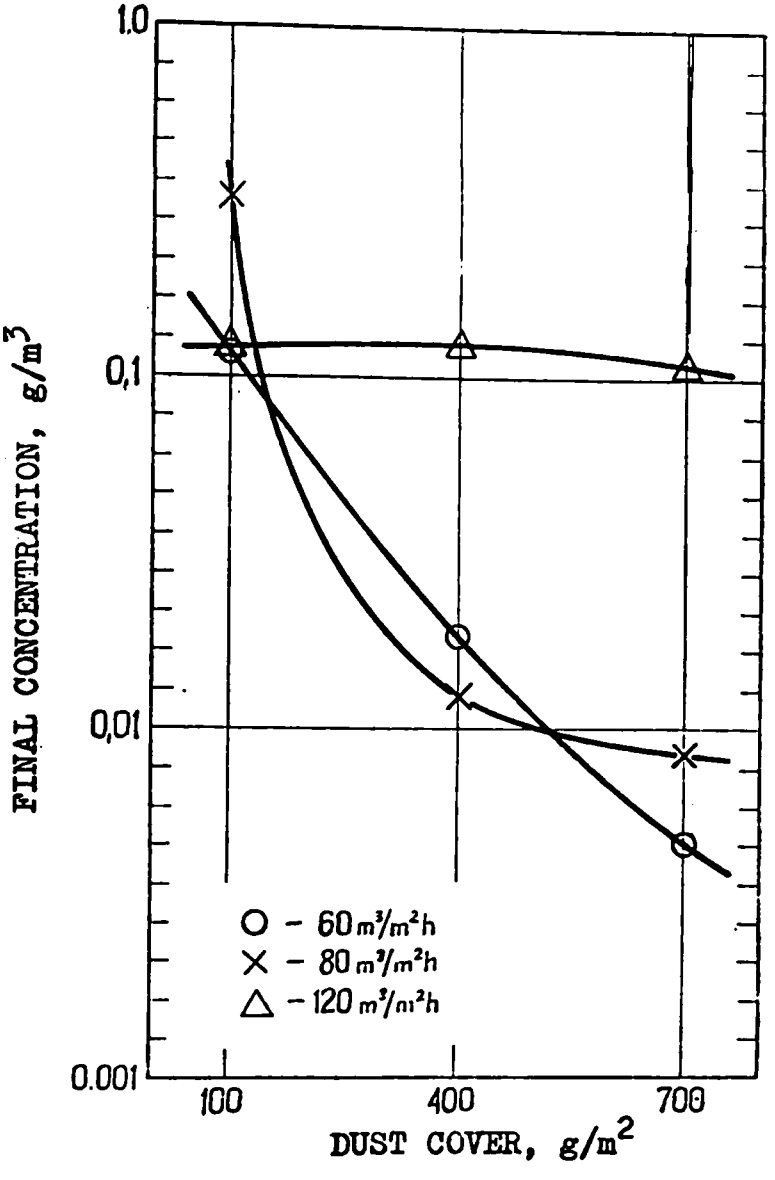

Figure A-68. Variation of Final Concentration for Fabric F-tor 5 and Separated Coal Dust.

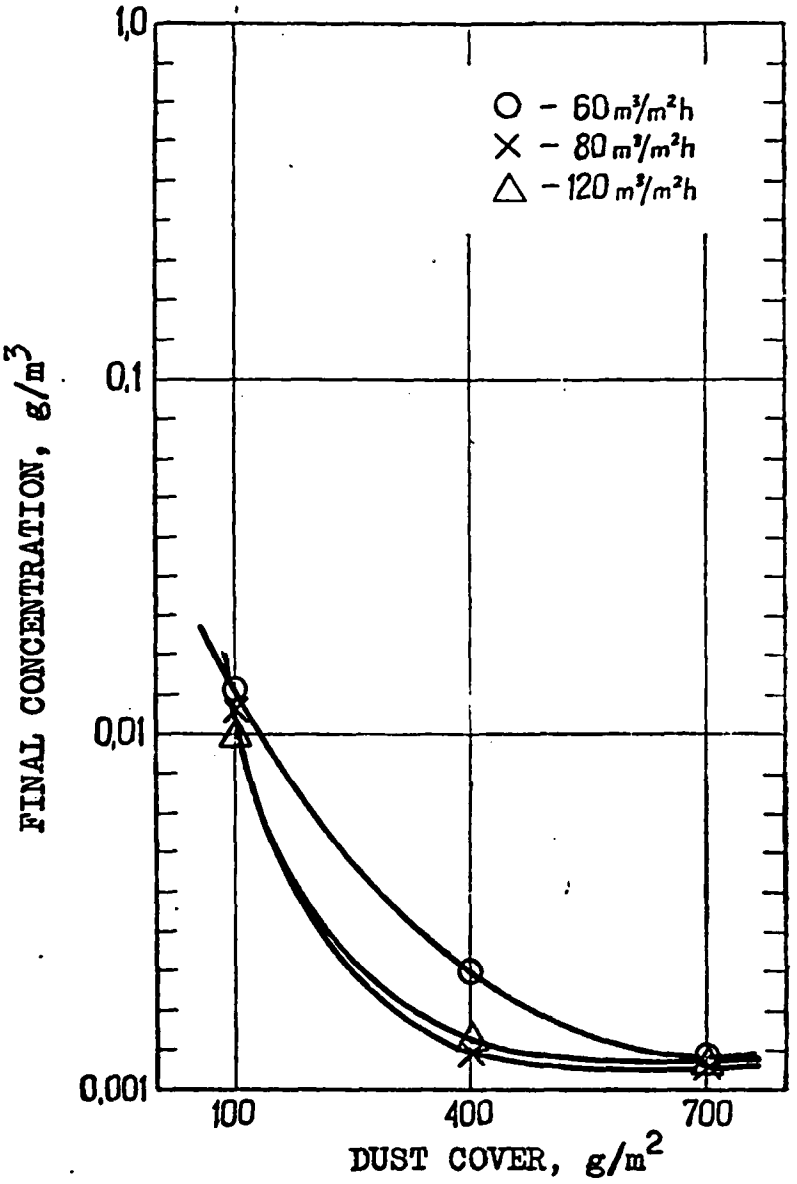

Figure A-69. Variation of Final Concentration for Fabric PT-15 and Separated Cement Dust.

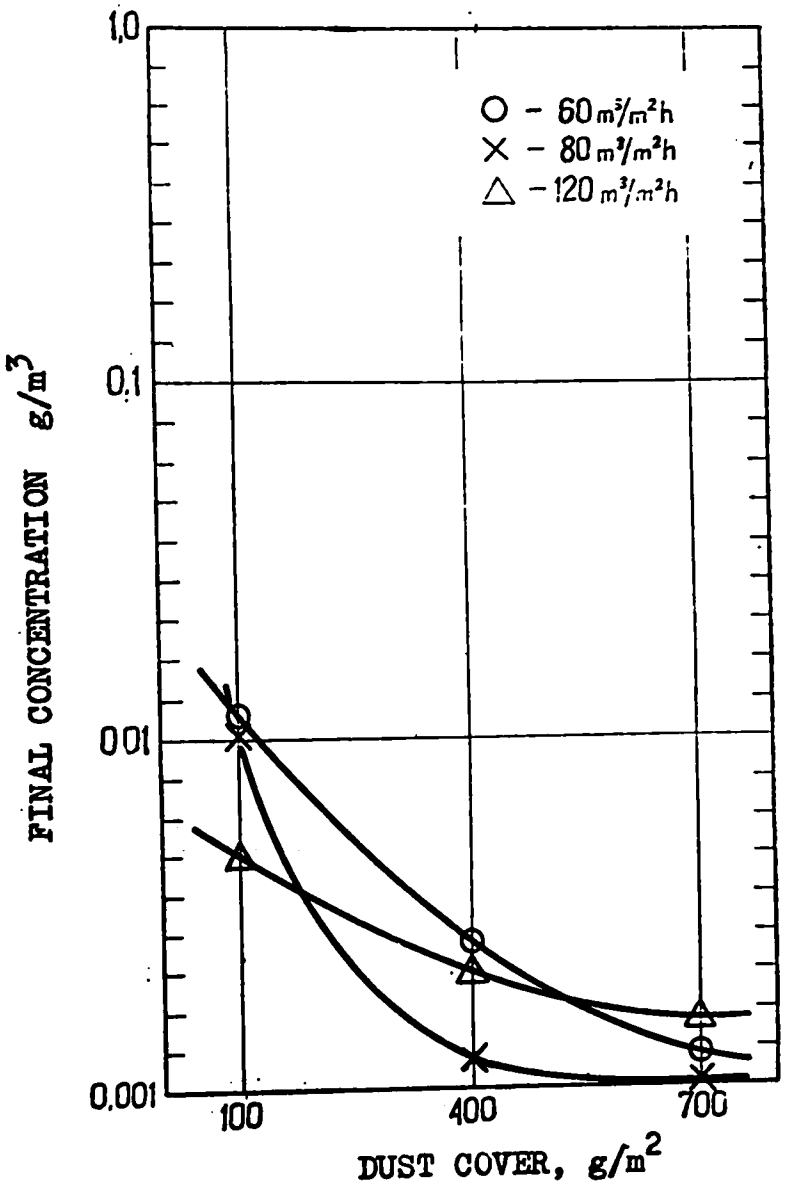

Figure A-70. Variation of Final Concentration for Fabric PT-15 and Separated Coal Dust.

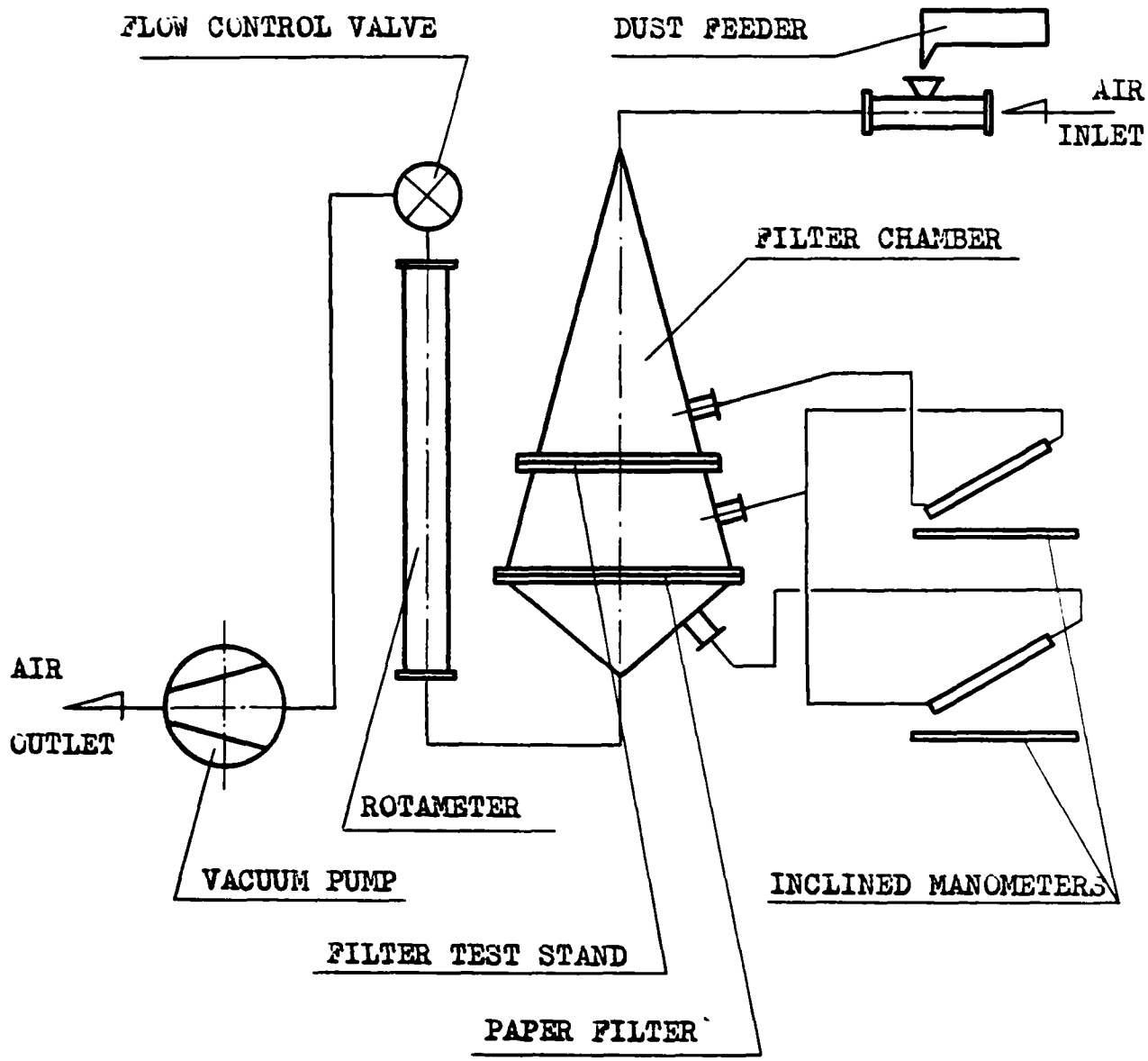

Figure A-71. Diagram of the Laboratory Test Stand.

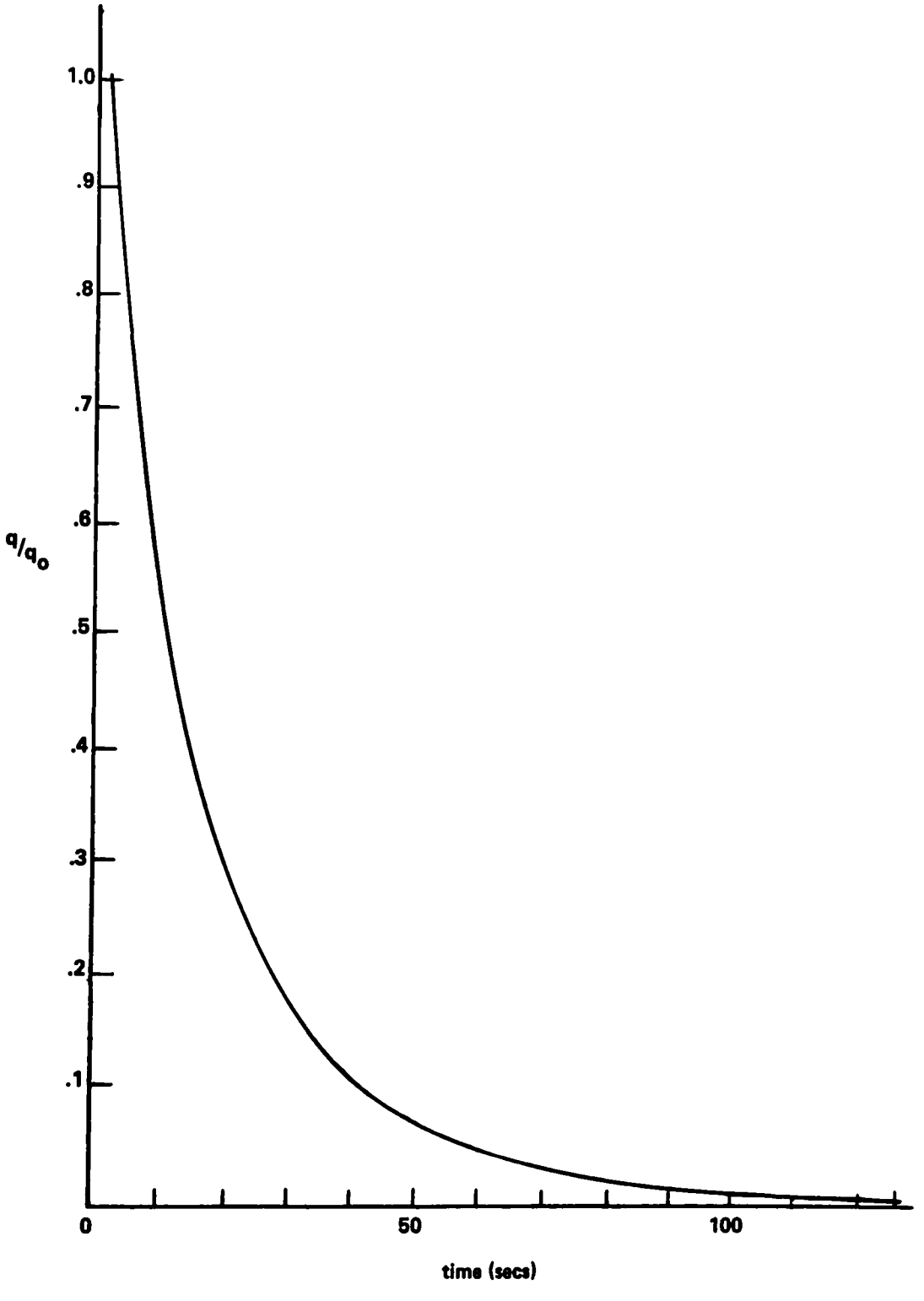

Figure A-72. Loss of Charge for Fabric F-tor 5.

APPENDIX B

GLOSSARY OF TERMS

Because of the different terms used in the fabric filtration literature concerning dust filtration through filtration media and because of the many parameters, stages, etc., which are characteristic of the dust filtration process, we propose to standardize the terminolgy for dust filtration. The proposed terms have physical sense according to the processes and phenomena occuring during the dust filtration process (which is quite different from air filtration).

FILTRATION - Process for the removal of solid particles from an aerosol stream by a porous medium.

AIR FILTRATION - Filtration process for atmospheric aerosols.

DUST FILTRATION - Filtration process for industrial aerosols.

DUST FILTRATION TYPE I - The initial phase of the complete dust filtration process when the fabric first begins operation as a filtration medium. This phase ends when the pressure drop reaches a predetermined level.

DUST FILTRATION TYPE II- The second phase continues until the fabric is fully filled with dust. This phase ends when the structure reaches the state of balance.

DUST FILTRATION TYPE III - This phase occurs when a stable level of filling of the fabric by dust has been reached and when the pressure drop returns to a constant level after regenerations. This type operation is typical for industrial dust collectors.

GAS LOADING OF FILTRATION AREA - Mean calculated value of gas quantity, in cubic meters, passing through a square meter of filtration medium per hour (the air-to-cloth ratio).

PERMEABILITY - Gas loading of the filtration areas at a definite pressure drop.

American Standard pressure drop: 0.5 inch of water,
Polish Standard pressure drop: 20 mm of water.

DUST LOADING OF FILTRATION AREA - Mean calculated value of dust quantity on the filter medium per square meter of filtration medium per hour.

FILTRATION VELOCITY - The true velocity of aerosol, in meters per second (minute), passing through the filter medium (measured in true conditions).

FILL OF STRUCTURE - (Dust fill). The dust accumulated during the filtration process, in g/m^2, which is retained after regeneration (without dust cake).

COVERED WITH DUST STRUCTURE - (Dust cover). The retained dust accumulated during the filtration process, in g/m^2, including the dust cake prior to regeneration.

DEGREE OF FILLING(β) - The ratio of the dust fill for a given regeneration schedule to that of the completely filled structure, in percent.

The full glossary of terms will be enclosed in the final report.

APPENDIX C

METRIC CONVERSIONS

To convert from	To	Multiply by
ft	meters	0.305
ft^2	$meters^2$	0.0929
ft^3	$meters^3$	0.0283
ft/min	centimeters/sec	0.508
ft^3/min	$centimeters^3$/sec	471.9
in	centimeters	2.54
in^2	$centimeters^2$	6.45

TECHNICAL REPORT DATA
(Please read Instructions on the reverse before completing)

1. REPORT NO.	2.	3. RECIPIENT'S ACCESSION NO.
EPA-600/7-79-031		

4. TITLE AND SUBTITLE	5. REPORT DATE
Filtration Parameters for Dust Cleaning Fabrics	January 1979
	6. PERFORMING ORGANIZATION CODE

7. AUTHOR(S)	8. PERFORMING ORGANIZATION REPORT NO.
J. R. Koscianowski, Lidia Koscianowska, and Eugeniusz Szczepankiewicz	

9. PERFORMING ORGANIZATION NAME AND ADDRESS	10. PROGRAM ELEMENT NO.
Institute of Industry of Cement Building Materials 45-641 Opole Oswiecimska Str. 21, Poland	EHE624
	11. CONTRACT/GRANT NO. Public Law 480 (Project P-5-533-3)

12. SPONSORING AGENCY NAME AND ADDRESS	13. TYPE OF REPORT AND PERIOD COVERED
EPA, Office of Research and Development Industrial Environmental Research Laboratory Research Triangle Park, NC 27711	Final; 6/73 - 12/78
	14. SPONSORING AGENCY CODE EPA/600/13

15. SUPPLEMENTARY NOTES IERL-RTP project officer is James H. Turner, MD-61, 919/541-2925. Report EPA-600/2-76-074 contains complementary information.

16. ABSTRACT The report describes laboratory and pilot scale testing of bag filter fabrics. Filtration performance data and mathematical modeling parameters are given for four Polish fabrics tested with cement dust, coal dust, flyash, and talc. Conclusions include: (1) The process of clean air flow, as well as the dust filtration process, are stochastic processes of the normal type. (2) For filtration Type I (laboratory scale), dust collection efficiency is an exponential function depending on air-to-cloth ration, dust covering, and type of filtration structure. (3) For filtration Type I, resistance increases parabolically with time or dust covering. Outlet concentration as a function of dust covering is also parabolic. Structurally, the fabrics are heterogeneous anistropic media. (4) Free area is presently the best structural parameter for characterizing structure of staple fiber fabrics. (5) Electrostatic properties of dusts depend on their history; charge decays with time. Dust cake formation can be influenced by specific electrostatic properties of the fabric and dust.

17. KEY WORDS AND DOCUMENT ANALYSIS

a. DESCRIPTORS		b. IDENTIFIERS/OPEN ENDED TERMS	c. COSATI Field/Group	
Pollution	Coal Dust	Pollution Control	13B	21D
Dust Filters	Fly Ash	Stationary Sources	13K	21B
Fabrics	Talc	Fabric Filters	11E	08G
Mathematical Models		Particulate	12A	
Dust	Electrostatics	Polish Fabrics	11G	20C
Cements			11B,13C	

18. DISTRIBUTION STATEMENT	19. SECURITY CLASS *(This Report)*	21. NO. OF PAGES
Unlimited	Unclassified	225
	20. SECURITY CLASS *(This page)* Unclassified	22. PRICE

EPA Form 2220-1 (9-73)

☆U.S. GOVERNMENT PRINTING OFFICE: 1979-640-013 4173REGION NO. 4